

University of Alberta

ENZYME ASSAY BY CAPILLARY ELECTROPHORESIS
WITH LASER-INDUCED FLUORESCENCE DETECTION

BY

YANNI ZHANG



A thesis submitted to the Faculty of Graduate Studies and Research in partial
fulfillment of the requirements for the degree of Doctor of Philosophy

Department of Chemistry

Edmonton, Alberta

Fall, 1996



National Library
of Canada

Bibliothèque nationale
du Canada

Acquisitions and
Bibliographic Services Branch

Direction des acquisitions et
des services bibliographiques

395 Wellington Street
Ottawa, Ontario
K1A 0N4

395, rue Wellington
Ottawa (Ontario)
K1A 0N4

Your file *Votre référence*

Our file *Notre référence*

The author has granted an irrevocable non-exclusive licence allowing the National Library of Canada to reproduce, loan, distribute or sell copies of his/her thesis by any means and in any form or format, making this thesis available to interested persons.

L'auteur a accordé une licence irrévocable et non exclusive permettant à la Bibliothèque nationale du Canada de reproduire, prêter, distribuer ou vendre des copies de sa thèse de quelque manière et sous quelque forme que ce soit pour mettre des exemplaires de cette thèse à la disposition des personnes intéressées.

The author retains ownership of the copyright in his/her thesis. Neither the thesis nor substantial extracts from it may be printed or otherwise reproduced without his/her permission.

L'auteur conserve la propriété du droit d'auteur qui protège sa thèse. Ni la thèse ni des extraits substantiels de celle-ci ne doivent être imprimés ou autrement reproduits sans son autorisation.

ISBN 0-612-18139-1

Canada

University of Alberta

Library Release Form

Name of Author: YANNI ZHANG

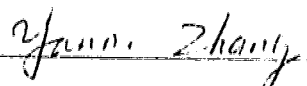
Title of Thesis: ENZYME ASSAY BY CAPILLARY ELECTROPHORESIS
WITH LASER-INDUCED FLUORESCENCE DETECTION

Degree: DOCTOR OF PHILOSOPHY

Year this Degree Granted: 1996

Permission is hereby granted to the University of Alberta Library to reproduce single copies of this thesis and to lend or sell such copies for private, scholarly, or scientific research purposes only.

The author reserves all other publication and other rights in association with the copyright in the thesis, and except as hereinbefore provided, neither the thesis nor any substantial portion thereof may be printed or otherwise reproduced in any material form whatever without the author's prior written permission.



Apt# 810, 8515-112 Street


Edmonton, Alberta, T6G 1K7

July 25, 1996

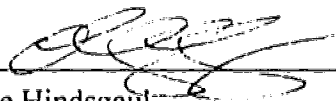
University of Alberta

Faculty of Graduate Studies and Research

The undersigned certify that they have read, and recommend to the Faculty of Graduate Studies and Research for acceptance, a thesis entitled Enzyme Assay by Capillary Electrophoresis with Laser-Induced Fluorescence Detection submitted by Yanni Zhang in partial fulfillment of the requirements for the degree of Doctor of Philosophy.



Dr. Norman J. Dovichi



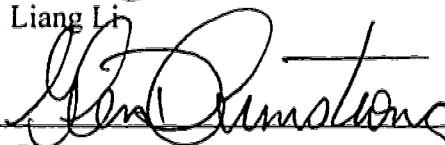
Dr. Ole Hindsgaul



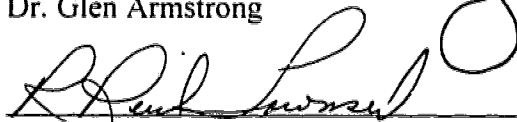
Dr. Monica M. Palcic



Dr. Liang Li



Dr. Glen Armstrong



Dr. R. Reid Townsend
(External Examiner)

July 24, 1996

Abstract

Capillary electrophoresis is a fast and effective separation method for many biological important molecules, and laser-induced fluorescence detection (LIF) provides high sensitivity and low detection limits. Recently, CE-LIF has been extended to the study of oligosaccharides. Problems associated with the study of carbohydrates include the lack of a native fluorophore. Also, the molecules generally do not have a net charge. High separation efficiency is required to isolate structurally very similar isomers.

In Chapter 2, a sample with a concentration as low as 1.0×10^{-9} M 1-glucosamine was fluorescently tagged with CBQCA. The five CBQCA labeled basic monosaccharides that are commonly found in mammalian cells were baseline separated by use of a 20 mM phosphate-50 mM phenylboronate-20 mM borate buffer.

CE-LIF was also applied extensively in *in vitro* and *in vivo* glycosyltransferases and glycosidases studies in different cells.

In chapter 3, CE-LIF was used to monitor biosynthetic transformations of a labeled derivative of *N*-acetylglucosamine in crude microsomal extracts. All of the standards were kinetically competent substrates for the enzymes present in HT-29 cells and could be baseline separated in a single run requiring 11 minutes. The action of competing enzymes acting on the common LacNAc sequence could thus be monitored in a single run with sensitivity routinely as low as a few thousand molecules.

In Chapter 4, *in vivo* biotransformations of a labeled derivative of Le^c in A431 cells were monitored by CE-LIF. The localization of the fluorescently tagged substrate in Golgi was confirmed using laser scanning confocal microscopy. The biosynthetic products were identified by hydrolytic enzymes and mass spectrometry. One unknown peak formed was proven not to be a sialyl acid, a sulfate, or a phosphate sugar.

In Chapter 5, the biosynthesis of the Le^x (Gal β (1 \rightarrow 4)[Fuc α (1 \rightarrow 3)]GalNAc β -determinant in two strains of *Helicobacter pylori* has been investigated. With CE-LIF, the formation of Le^x in this bacteria cells, especially in strain UA861, was proven. The

formation of a disaccharide ($\text{Gal}\alpha(1\rightarrow6)\text{GlcNAc}$) from UA 861 incubated with GlcNAc and UDP-Gal was first observed by CE-LIF and confirmed by the methylation analysis method. The biosynthetic pathway for Le^x is identical to that found in humans.

In Chapter 6, the characterization of the isolated glucosidase I and II activities from yeast cells with a trisaccharide and a disaccharide as a substrate, respectively, were also investigated. The CE-LIF is also used to monitor enzymatic products formed after incubating yeast cells with a trisaccharides *in vivo*.

Acknowledgment

I was impressed by the famous instrument set up in Dr. Norm Dovichi's laboratory after a visit in January 1992, and I decided to join his group. I gained tremendous experience during my study with him. I would like to thank Norm for his patience, understanding, guidance and advice.

I also want to thank all my co-workers and previous members of the Northern Light Laser Lab for their support and help, especially, to Dr. Edgar Arriaga for introducing me to laser-induced fluorescence detection.

I would like to express my sincere appreciation to all who have taught me and my Ph.D final exam committee members. Special thanks go to Dr. Monica M. Palcic and Dr. Ole Hindsgaul for their teaching and excellent guidance in my enzyme related carbohydrate studies. I also want to express my thanks to Catharine A. Compton for her enthusiastic support and teaching me about cell culture

I would like to thank the Alberta Heritage Foundation for Medical Research for granting me a full-time scholarship for one year (1993/94), the Department of chemistry for a one year TA scholarship (1994/95), and a Dissertation Fellowship from Graduate Study at University of Alberta (1995/96).

Finally, I would like to thank my parents, Yufang Zhang and Peiji Li for taking care of my son Jiahua Zhang for five years, providing selfless support during my graduate studies in Canada. Thanks also go to my dear husband, Zhongsheng Zhang for his support, care and patience. Without their support, I would not have been able to finish my Ph.D study.

Table of Contents

1. Introduction	1
1.1 Introduction	2
1.2 Capillary Electrophoresis	3
1.2.1 Capillary Zone Electrophoresis (CZE)	3
1.2.2 Capillary Gel Electrophoresis (CGE)	4
1.2.3 Micellar Electrokinetic Capillary Chromatography (MECC)	4
1.2.4 Capillary Isoelectric Focusing (CIEF)	4
1.2.5 Capillary Isotachopheresis (CITP)	4
1.3 Principles of Capillary Zone Electrophoresis	6
1.3.1 Electroosmotic Flow and Zeta Potential	7
1.3.2 Electrophoretic Mobility	9
1.3.3 Separation Efficiency	10
1.3.4 Resolution	10
1.4 Principle of MECC	11
1.4.1 The Formation of Micelles	11
1.4.2 Several Important Parameters in MECC	12
1.4.3 Selectivity Manipulation	15
1.5 Sample Injection	16
1.5.1 Electrokinetic Injection	16
1.5.2 Hydrodynamic Injection	17
1.6 Detection Methods	17
1.6.1 On-Column Detection	17
1.6.2 Post-Column Detection	18
1.7 Post-Column Laser-Induced Fluorescence Detection (LIF)	18
1.8 Fluorescence Derivatization	19

1.8.1 CBQCA Labeling of Aminated Sugars	20
1.8.2 TRSE Labeling of Aminated Sugars	21
1.9 Instrumentation	22
1.9.1 Laser	22
1.9.2 Sheath Flow Cuvette	25
1.9.3 Optical Collection System	27
1.9.4 Fluorophors Used for Alignment	30
1.10 The Limit of Detection	31
1.11 Introduction to Mammalian Cell Surface Carbohydrate	33
1.11.1 Basic Introduction to Mammalian Monosaccharides	33
1.11.2 Glycosyltransferases	35
1.11.3 Glycans	35
1.12 References	38
2. Nanomolar Determination of Aminated Sugars by Capillary Electrophoresis	42
2.1 Introduction	43
2.2 Experimental Section	46
2.2.1 Instrumentation	46
2.2.2 Preparation of Sugar Derivatives	48
2.2.3 CBQCA Labeling Reaction	48
2.2.4 Separation	50
2.3 Results And Discussion	51
2.3.1 Selection of Labeling Reaction Conditions	51
2.3.2 Concentration Limit for Labeling of 1-glucosamine	54
2.3.3 The Possible Labeling Mechanism	60
2.3.4 Limit of Detection (LOD)	60
2.3.5 Reaction Yield for Different Aminated Sugars	62
2.3.6 Separation of CBQCA Derivatives of Five Aminated Sugars	65

2.4 Conclusions	67
2.5 References	68
3. Monitoring Biosynthetic Transformations of <i>N</i> -Acetyllactosamine Using Fluorescently Labeled Oligosaccharides and Capillary Electrophoretic Separation	70
3.1 Introduction	71
3.2 Experimental Section	74
3.2.1 Materials	74
3.3 Methods	75
3.3.1 General Procedure Used for the Preparation of Ethylenediamine Monoamides (Dr. Ole Hindgaul's group)	75
3.3.2 General Procedure Used for the Fluorescence Labeling (Dr. Ole Hindgaul's group)	75
3.3.3 Preparation of Enzyme Extracts from HT-29 Cells (Dr. Monica M. Palcic's group)	76
3.3.4 Fucosyltransferase (FucT) Assays (Dr. Monica Palcic's group)	79
3.3.5 Fucosyltransferase and Fucosidase Incubations for Analysis by Capillary Electrophoresis	80
3.3.6 Instrumentation of Capillary Electrophoresis with Laser-induced Fluorescence Detection	81
3.4 Results And Discussion	84
3.4.1 Standards of Substrate and Possible Biosynthetic and Hydrolysis Products	84
3.4.2 Electropherograms and Discussion	84
3.5 Conclusions	96
3.6 References	97
4. Le ^c Uptake by A431 Cells	99
4.1 Introduction	100

4.2 Materials and Methods	102
4.2.1 Cell Culture	106
4.2.2 Preparation of A431 Crude Cell Extracts and Incubation with Le ^c -O-TMR	107
4.2.2.1 Crude cell extract preparation	107
4.2.2.2 Incubation of A431 crude cell extracts with Le ^c -TMR or LacNAc-TMR and GDP fucose	107
4.2.2.3 Incubation of A431 cell extracts with Le ^c -TMR without a donor GDP Fucose	108
4.2.2.4 Cell extract incubation with Le ^c and PAPS (a sulfate donor)	108
4.2.3 Le ^c -TMR Uptake by A431 Cells	109
4.2.4 HT-29 Cells	109
4.2.5 Products Identification Approach with Hydrolysis Enzymes	110
4.2.5.1 Fucosidase assays	110
4.2.5.2 Neuraminidase assay	110
4.2.5.3 Phosphatase assay	110
4.2.5.4 Sulfatase digestion assay	111
4.2.6 Sample Preparation For MALDI-MS	111
4.2.7 Laser Scanning Confocal Microscopy	112
4.2.8 CE Separation Conditions	112
4.3 Results and Discussion	113
4.3.1 A431 cell Extract Analysis by CE-LIF	113
4.3.1.1 Standards of substrate and possible biosynthetic and hydrolysis products	113
4.3.1.2 A431 Cell extracts incubation with substrates and GDP-fucose	113

4.3.2 A431 Cell Uptake	115
4.3.2.1 A431 cell uptake of Le ^c monitored by confocal microscopy	115
4.3.2.2 Le ^c -TMR uptake by A431 cells	116
4.3.3 Identification of Novel Peaks	119
4.3.3.1 Neuraminidase substrate specificity	120
4.3.3.2 Peak identifications using hydrolysis enzymes	120
4.3.4 A431 Cell Extracts Incubation with Le ^c without Adding a Donor and Peak Identification	121
4.3.4.1 A431 cell extract incubation with Le ^c without adding a donor	121
4.3.4.2 A novel peak identification	122
4.3.4.3 Mass spectrometry	122
4.3.5 LacNAC-TMR Uptake by HT-29 Cells	122
4.3.6 Comparison of Le ^c Uptake by A431 Cells and LacNAc Uptake by HT-29 cells	123
4.3.7 Separation of Mixture Containing Thirteen TMR Labeled Compounds	124
4.4 Conclusion	124
4.5 References	126
5. The Biosynthesis of Le ^x In <i>Helicobacter Pylori</i>	155
5.1 Introduction	156
5.2 Experimental Section	157
5.2.1 Materials	157
5.2.2 Cell Growth	158
5.2.3 Enzyme Extract Preparation and Activity Screening	159
5.2.4 Capillary Electrophoresis	160

5.2.5 Preparative Synthesis and Methylation Analysis	160
5.3 Results and Discussion	161
5.3.1 Fucosyltransferase and Galactosyltransferase Activities	161
5.3.2 Detection Le ^N and a New Product by CE-LIF	163
5.3.3 Identification of the New Product	163
5.3.4 Biosynthesis Pathway of Le ^N in <i>Helicobacter Pylori</i>	166
5.4 Conclusions	167
5.5 References	169
6. Enzymatic Hydrolysis Study of a Tetramethylrhodamine Labeled Trisaccharide in Yeast Cell	171
6.1 Introduction	172
6.2 Experimental Section	173
6.2.1 Materials	173
6.2.2 Incubation of Isolated Glucosidase I and II with Trisaccharide and Disaccharide (Dr. Christine Scaman in Dr. Monica Palcic' group)	173
6.2.3 Incubation of Yeast Cells (Dr. Christine Scaman in Dr. Monica Palcic' group)	174
6.2.4 Time Course Study of Trisaccharide Hydrolysis by Glucosidase I	175
6.2.5 Absorption Measurement for the Tetramethylrhodamine Labeled Compounds	175
6.2.6 Capillary Electrophoresis	175
6.3 Results and Discussion	176
6.4 Conclusion	181
6.5 References	185
7. Conclusion	186
7.2 References	191

List of Tables

Table 1.1 Critical micelle concentration, aggregation number (n), and Kraft point (Kp) of selected ionic surfactants	12
Table 1.2 Some parameters of CBQCA and TRSE	20
Table 1.3 The properties of Helium-Neon laser	23
Table 1.4 The Argon Ion laser properties	24
Table 1.5 Collection efficiency of microscope objective (n = 1)	27
Table 1.6 Water Raman band for different lasers	28
Table 1.7 R1477 side-on type photomultiplier tubes (25 °C)	29
Table 1.8 Some parameters of fluorescein and rhodamine	30
Table 1.9 Multiplier constants for LOD	32
Table 2.1 Effect of pH on CBQ-Glc-NH ₂ derivative signal	54
Table 2.2 Concentration range for labeling reaction	58
Table 2.3 Calibration curve data	58
Table 2.4 Numbers of theoretical plates for CBQ labeled sugars	63
Table 2.5 The number of theoretical plate of CBQ labeled 1-glucosamine in different running buffer	63
Table 3.1 ¹ H NMR (chemical shifts and coupling constants), mass spectral (MS), and R _f data (on silica gel TLC) for the aminated precursors	77
Table 3.2 ¹ H NMR (chemical shifts and coupling constants), mass spectral (MS), and R _f data (on silica gel TLC) for tetramethylrhodamine-labeled structures 1-6	78
Table 3.3 Optimization substrate concentration	87
Table 3.4 Different substrates incubated with HT-29 microsomal extracts Le ^Y Degradation	94
Table 3.5 H type II incubation with microsomal enzyme and GDP-fucose	95
Table 4.1 Hydrolysis enzymes	128

Table 4.2 Buffers for glycosidase assays	130
Table 4.3 The specificity of α -fucosidases and neuraminidase	131
Table 5.1 Cellular distribution of galactosyltransferase and fucosyltransferase activities in <i>H. pylori</i> extracts	162
Table 6.1 Trisaccharides incubation with glucosidase I	179
Table 6.2 Trisaccharide and Disaccharide incubated with glucosidase II	181
Table 6.3 Percentage of tri and disaccharide incubation with glucosidase II	181

List of Figures

Figure 1.1 Simple diagram of a capillary electrophoresis separation system	6
Figure 1.2 Electroosmotic flow and ζ potential	8
Figure 1.3 Schematic separation by MECC	13
Figure 1.4 Aminated Sugar Labeling by CBQCA	21
Figure 1.5 TRSE Labeling Aminated Sugar	21
Figure 1.6 Schematic diagram of sheath flow cuvette	26
Figure 2.1 Structure of CBQCA. 3-(4-carboxybenzoyl)-quinoline-2-carboxyaldehyde	45
Figure 2.2 Schematic diagram of capillary electrophoresis system and detector	47
Figure 2.3 Structures of five aminated monosaccharides	49
Figure 2.4 Glucose was reduced to 1-glucosamine. 1-glucosamine was reacted with CBQCA and potassium cyanide to form a fluorescence derivative product	52
Figure 2.5 Electropherogram of 10^{-4} M CBQCA	53
Figure 2.6 Electropherogram of CBQCA labeled glucosamine. 10^{-4} M glucosamine was reacted with 4 mM CBQCA and 2 mM KCN for 4 h at 50° C	53
Figure 2.7 Electropherograms of fluorescently labeled samples containing 10^{-9} M 1-glucosamine	55
Figure 2.8 Concentration range of 1-glucosamine for the labeling reaction	57
Figure 2.9 Log-Log calibration curve for CBQ labeled synthetic 1-glucosamine (Glc-NH ₂)	59
Figure 2.10 Mechanisms for CBQ labeling reaction of amino acids and CBQ direct reaction with cyanide	61
Figure 2.11 Comparison of the electropherograms for five aminated monosaccharides labeled under identical conditions	64
Figure 2.12 Separation of five CBQCA derivatives of monosaccharides	66

Figure 3.1 Instrument set up	82
Figure 3.2 Capillary zone electropherogram of baseline separation of five standard tetramethylrhodamine-labeled oligosaccharides 1-5 and the linker arm 6.	86
Figure 3.3 Capillary electropherograms of 50, 187, and 343 μM LacNAc-O-TMR after incubation with HT-29 microsomal extract and GDP fucose for 24 h	88
Figure 3.4 Capillary zone electropherograms of 50 μM LacNAc-O—TMR after incubation with HT-29 microsomal extract and GDP fucose	89
Figure 3.5 Capillary zone electropherogram of almond meal fucosidase incubated with Le^{N} for 24 h	90
Figure 3.6 Capillary zone electropherograms of degradation controls	92
Figure 3.7 The percentage change of Le^{Y} , Le^{N} , H type II, LacNAc and GlcNAc hydrolyzed by microsomal enzymes to incubation time (h)	93
Figure 3.8 Capillary electropherograms of 150 μM H type II and Le^{N} -O-TMR after incubation with HT-29 microsomal extracts and GDP-fucose, respectively	93
Figure 4.1 Electropherograms of A431 crude cell extracts incubated with substrate Le^{C} -O-TMR and donor GDP fucose (50 μM each)	132
Figure 4.2 Electropherograms of LacNAc-TMR incubated with A431 cell extracts and GDP fucose (50 μM each)	133
Figure 4.3 Photo from Laser scanning confocal microscopy	134
Figure 4.4 Electropherograms of A431 cells growing up in culture medium containing 25 μM Le^{C} for 20 h	135
Figure 4.5 Electropherograms of Le^{C} uptake by 3×10^6 A431 cells for 18 h	136
Figure 4.6 Electropherograms of A431 (3×10^6) cells incubated with substrate Le^{C} (15 μM) for 19 h	137
Figure 4.7 Electropherograms of 25 μM Le^{C} uptake by A431 cells (6×10^6) for 19h	138
Figure 4.8 Electropherograms of the 19.5 h of 25 μM Le^{C} uptake by A431 cells (6×10^6)	

	139
Figure 4.9 Electropherograms of hydrolysis 2.3sialyl Le ^c by neuraminidase	140
Figure 4.10 Electropherogram of an α -fucosidase and a neuraminidase digestion of post-trypsin PBS wash	141
Figure 4.11 Electropherograms of α -fucosidase treatment of the pellet from 25 μ M Le ^c uptake by A431 cells for 20 h	142
Figure 4.12 The electropherograms of α -fucosidase and neuraminidase treatment pellet of 15 μ M Le ^c uptake by A431 cells for 19 h	143
Figure 4.13 Electropherograms of neuraminidase treatment of 25 μ M Le ^c uptake for 19.5 h by A-431 cell pellet	144
Figure 4.14 Electropherograms of A431 cell extract incubated with Le ^c without adding donor GDP fucose (Mixture A)	145
Figure 4.15 Electropherograms of A431 cell extract and Lec incubated with PAPS (a sulfate donor) or without a PAPS	146
Figure 4.16 Electropherograms of Mixture A hydrolyzed by phosphatases	147
Figure 4.17 Electropherograms of the mixture A digested by three sulfatases	148
Figure 4.18 Mass Spectrum of A431 cell extract incubated with Le ^c for 65 h	149
Figure 4.19 Electropherograms of 25 μ M LacNAc uptake by HT-29 cells (6×10^6) for 20 h	150
Figure 4.20 Electropherograms of 25 μ M LacNAc uptake by HT-29 cells for 22 h	151
Figure 4.21 Electropherograms of pellet from 25 μ M LacNAc uptake by A431 cells for 20 h further treated with a fucosidase and a neuraminidase, respectively	152
Figure 4.22 Electropherograms of LacNAc uptake by HT-29 cells and Le ^c uptake by A431 cells	153
Figure 4.23 Electropherograms of the same sample run in different time	153
Figure 4.24 Electropherograms of the separation of 13 TMR labeled compounds by	

different buffer compositions	154
Figure 4.25 Electropherograms of the separations of six LacNAc series standards by 10 mM PBsBS and 10 mM PBpBS	154
Figure 5.1 Analysis of reaction mixture from <i>Helicobacter pylori</i> UA861 and UA802 incubations by capillary zone electrophoresis with laser induced fluorescence detection	164
Figure 5.2 Schematic diagram of biosynthesis of Le ^N in <i>Helicobacter pylori</i>	168
Figure 6.1 Electropherogram of three fluorescently labeled saccharide and one linker arm	178
Figure 6.2 Capillary electropherograms of trisaccharide hydrolyzed by glucosidase I	180
Figure 6.3 Electropherograms of the time course study of glucosidase I incubated with a trisaccharide	180
Figure 6.4 Time course study of glucosidase I hydrolysis of trisaccharide and the formation of disaccharide with incubation time	182
Figure 6.5 Capillary electropherograms of mixtures after glucosidase I hydrolysis was further incubated with glucosidase II	184
Figure 6.6 Electropherogram of trisaccharide (14) incubated with yeast cells for 48 h	184

List of Schemes

Scheme 3.1 The general reaction catalyzed by glycosyltransferase	72
Scheme 3.2 Some potential biosynthetic transformations of LacNAc-O-TMR	85
Scheme 4.1 Structures of LacNAc series standards	103
Scheme 4.2 Structures of Le ^c series standards	104
Scheme 4.3 Structures of sialyl standards	105
Scheme 4.4 Some potential biosynthetic transformations of Le ^c -O-TMR incubation with A431 crude cell extract and GDP-fucose	114
Scheme 4.5 Some potential biosynthetic transformations of Le ^c -O-TMR uptake by A431 cells	117
Scheme 6.1 Schematic diagram of hydrolytic pathways in yeast cells	177

List of Nomenclature of Sugars, Abbreviations, and Symbols

LacNAc	$\beta\text{Gal}(1\rightarrow4)\beta\text{GlcNAc-O-TMR}$. 1
H I	$\alpha\text{Fuc}(1\rightarrow2)\beta\text{Gal}(1\rightarrow4)\beta\text{GlcNAc-O-TMR}$. H type I. 2
Le ^λ	$\beta\text{Gal}(1\rightarrow4)[\alpha\text{Fuc}(1\rightarrow3)]\beta\text{GlcNAc-O-TMR}$. Lewis X. 3
Le ^Y	$\alpha\text{Fuc}(1\rightarrow2)\beta\text{Gal}(1\rightarrow4)[\alpha\text{Fuc}(1\rightarrow3)]\beta\text{GlcNAc-O-TMR}$. Lewis Y. 4
GlcNAc	$\beta\text{GlcNAc-O-TMR}$. 5
HO-TMR	H-O(CH ₂) ₈ CONHCH ₂ CH ₂ NH-tetramethylrhodamine. Linker arm. 6
Le ^c	$\beta\text{Gal}(1\rightarrow3)\beta\text{GlcNAc-O-TMR}$. Lewis C. 7
H I	$\alpha\text{Fuc}(1\rightarrow2)\beta\text{Gal}(1\rightarrow3)\beta\text{GlcNAc-O-TMR}$. H type I. 8
Le ^a	$\beta\text{Gal}(1\rightarrow3)[\alpha\text{Fuc}(1\rightarrow4)]\beta\text{GlcNAc-O-TMR}$. Lewis A. 9
Le ^b	$\alpha\text{Fuc}(1\rightarrow2)\beta\text{Gal}(1\rightarrow3)[\alpha\text{Fuc}(1\rightarrow4)]\beta\text{GlcNAc-O-TMR}$. Lewis B. 10
2.3-sialyl Le ^c	$\alpha\text{NeuAc}2\rightarrow3\beta\text{Gal}(1\rightarrow3)\beta\text{GlcNAc-O-TMR}$. 11
2.6-sialyl LacNAc	$\alpha\text{NeuAc}2\rightarrow6\beta\text{Gal}(1\rightarrow4)\beta\text{GlcNAc-O-TMR}$. 12
2.3-sialyl LacNAc	$\alpha\text{NeuAc}2\rightarrow3\beta\text{Gal}(1\rightarrow3)\beta\text{GlcNAc-O-TMR}$. 13
TriGlc	$\alpha\text{-D-Glc}(1\rightarrow2)\alpha\text{-D-Glc}(1\rightarrow3)\alpha\text{-D-Glc-O-TMR}$. T. 14
DiGlc	$\alpha\text{-D-Glc}(1\rightarrow3)\alpha\text{-D-Glc-TMR}$. D. 15
Glc	$\alpha\text{-D-Glc-TMR}$. M. 16 (chapter 6)
Glc	1-amino-1-deoxy-D-glucitol (chapter 2). 1-glucosamine
Gal	1-amino-1-deoxy-D-galacitol. 1-galactosamine
2-Glc	2-amino-2-deoxy-D-glucitol. 2-glucosamine
Man	1-amino-1-deoxy-D-glucitol mannitol. 1-mannosamine
Fuc	1-amino-1-deoxy-D-glucitol fucitol. 1-fucosamine
NeuAc	N ⁵ -acetyl-neuraminic acid
NANA	sialic acid
UDP	uridine diphosphate
GDP	guanosine diphosphate
CMP	cytidine monophosphate

ANS	5-aminonaphthalene-2-sulfonate
ANTS	7-amino-1,3-naphthalenedisulfonate
AP	2-aminopyridine
B	borate
Bp	phenyl borate
BSA	bovine serum albumin
CBQCA	3-(4-carboxybenzoyl)-2-quinolinecarboxyaldehyde
CE	capillary electrophoresis
CGE	capillary gel electrophoresis
C_{LOD}	concentration detection limit
CMC	critical micelle concentration
CITP	capillary isotachopheresis
CIEF	capillary isoelectric focusing
CM	culture medium
C_s	analyte concentration
CZE	capillary zone electrophoresis
D	diffusion coefficient
DEA	Diethanol Amine
DMEM	Dulbecco's Modified Eagle's Medium
DMF	Dimethyl formamide
DMSO	dimethyl sulfoxide
E	electric field
EDTA	ethylenediaminetetraacetic acid
E_{inj}	potential of injection
EOF	electroosmotic flow
EPF	electrophoretic flow
E_{sep}	potential of separation

FCS	fetal calf serum
g	gravitational force constant
HEPES	N-(2-hydroxyethyl)piperazine-N'-ethanesulfonic acid
h_n	largest noise fluctuation
h_s	peak height
HPLC	high performance liquid chromatography
<i>H. Pylori</i>	<i>Helicobacter pylori</i>
h_s	analyte peak height
k'	capacity factor
K_{LOD}	multiplier constants for LOD
L_c	capillary length (cm)
LC	liquid chromatography
LIF	laser-induced fluorescence detection
LOD	limit of detection
MALDI	matrix assisted laser desorption ionization
MECC	micellar electrokinetic capillary chromatography
MeOH	methanol
MS	mass spectrometry
n	refractive index
N	separation efficiency
N.A.	numerical aperture
NDA	2,3-naphthalenedicarboxaldehyde
NMR	nuclear magnetic resonance
OPA	o-phthalaldehyde
P	phosphate
PAGE	polyacrylamide gel electrophoresis
PAPS	adenosine 3'-phosphate 5'-phosphosulfate lithium salt $C_{10}H_{15}N_5O_{13}P_2S$

PBS	phosphate buffered saline
pI	isoelectric point
PMT	photomultiplier tube
q	charge on the ion
r	ion radius
SDS	sodium dodecyl sulphate
t_{inj}	injection time of the analyte
t_{mc}	migration time of micelle
t_{mig}	migration time of the analyte
t_o	migration time of micelle insolubilized solute
t_r	migration time of the analyte
TE	trypsin and EDTA
TLC	thin-layer chromatography
Triton X-100	t-octylphenoxypolyethoxyethanol
TRIS	tris(hydroxymethyl)aminomethane
TRSE	5-carboxytetramethylrhodamine succinimidyl ester
V	high voltage
V_c	volume of capillary
V_{inj}	injection volume
$W_{1/2}$	full peak-width in terms of time at half peak height
Δh	height difference between collection and injection reservoirs
ϵ	dielectric constant
ζ	wall zeta potential
γ	capillary radius
η	viscosity of the medium
μ_{eo}	electroosmotic mobility

μ_{ep}	electrophoretic mobility
v_{eo}	electroosmotic flow rate
v_{ep}	migration velocity of the solution
ρ	buffer density
σ^2	variance

CHAPTER 1
INTRODUCTION

1.1 INTRODUCTION

Separation by electrophoresis is based on differential migration of analyte under the influence of an electric field. This technique is widely used for the resolution of a mixture of biological molecules such as peptides, proteins, nucleic acids as well as carbohydrates. However, bands of separated molecules are easily disrupted and broadened by heating effects and diffusion. In most biochemical laboratories, electrophoresis is normally carried out in a buffer utilizing a supporting medium such as paper, cellulose acetate, starch, agarose, and polyacrylamide. These media not only function to restrict diffusion of bands, but can also act, in the case of polyacrylamide gels, as molecular sieves.

In 1937, the idea of using moving boundary electrophoresis to separate human serum was proposed by Tiselius (1). Thirty years later, Hjerten (2) provided the earliest demonstration of the use of high electric field strength in free solution electrophoresis in a 3 mm i.d. capillary. Virtanen (3) described the advantages of using smaller diameter columns in 1974. He reported the potentiometric detection of electrophoretically separated solutes in 200-500 μm i.d. glass tubes. His work dealt with zone electrophoresis and discussed many of the unique advantages of using small-diameter tubes. Mikkers et al. used this technique with 200 μm i.d. PTFE capillaries (4). The timely advance to smaller capillaries was made by Jorgenson and Lukacs (5, 6).

Capillary electrophoresis is a modern analytical technique in which free solution electrophoresis can give high resolution by decreasing zone broadening. The narrow diameter of the silica capillary allows the application of high voltages and ensures rapid heat dissipation. The use of high voltage leads to extremely efficient separations with a dramatic decrease in analysis time compared to conventional electrophoresis. This technique can be utilized to analyze a wide variety of charged and uncharged species. Sizes range from small analytes, such as metal ions, to large molecules, such as complex

oligosaccharides and nucleic acids. The ultra low injection volume permits sampling from picoliter environments, which is especially useful in the study of biological cells.

Comparison of Capillary Electrophoresis and Conventional Electrophoresis

Methods

Conventional electrophoresis in most biochemical laboratories is normally carried out in a buffer containing supporting media. It is limited by the temperature rise induced by the heat generated by applying voltage between two electrodes. Joule heating (the heating of a conducting medium as current flows through it) results in temperature gradients and convection that cause zone broadening, affect electrophoretic mobilities and can even lead to evaporation or boiling of solvent, which decreases the resolution.

The use of capillary tubes effectively increases heat dissipation. Small inner diameter capillaries (10 to 75 μm i.d.) have large surface area and provide more efficient heat dissipation compared to conventional electrophoresis tubes. Very high voltage can be applied and fast and efficient separations can be achieved. Another advantage is the decrease in band broadening because of the minimized convection in narrow capillary tubes.

Capillary electrophoresis is ideally suited to aqueous solutions, especially those of biological significance due to small volume, fast analysis and high resolution. The electroosmotic flow towards the cathode propels all components (anion, neutral species, and cations) towards the same end of the capillary. This property makes it possible to adapt the detectors that are well developed from column liquid chromatography.

1.2 CAPILLARY ELECTROPHORESIS

1.2.1 Capillary Zone Electrophoresis (CZE)

Capillary zone electrophoresis, or free solution capillary electrophoresis, is the most commonly used technique in CE. The capillary is filled with an aqueous buffer

solution. The separation depends on the different electrophoretic mobilities of the ionic species. The electrophoretic mobility is mainly based on differences in solute size and charge at a given pH. When a positive high voltage is applied at the injection end, cations migrate first, followed by neutral molecules, and finally anions. Because neutral molecules do not carry charges (electrophoretic mobility is zero), CZE is primarily restricted to separation of ionic analytes, with virtually no limitation in molecular size.

1.2.2 Capillary Gel Electrophoresis (CGE)

Larger biological molecules cannot be separated readily in free solution. Early work on RNA separations used cellulose fibers of 10 μm i.d and 25 mm length (7). The development of gel-filled capillaries and coated columns enhanced the scope and efficiency of capillary electrophoretic techniques (8, 9). Gel-filled capillaries for separation of oligonucleotides (10-12) and proteins (8, 9) have been reported. Generally, the capillary is filled with an anticonvection medium (e.g. polyacrylamide) which block the saline group from deprotonation and the electroosmotic flow is suppressed. The separation is based on differences in solute size as analytes migrate through the pores of the gel-filled column (molecular sieving effect). Elution time increases relative to molecular weight.

1.2.3 Micellar Electrokinetic Capillary Chromatography (MECC)

MECC, which involves adding a surfactant to the electrophoretic buffer to form micelles, is an important technique developed by Terabe and co-workers (13) to separate neutral species. Above the critical micelle concentration (CMC), surfactant molecules aggregate to form spherical shaped micelles having a hydrophobic interior and charged exterior. These micelles provide a pseudo-phase into which analyte can partition, providing a means of retention. This technique not only extends to the separation of neutral analytes, but also improves separation of ionic species.

1.2.4 Capillary Isoelectric Focusing (CIEF)

The separation is carried out in a pH gradient and based on the isoelectric points or pI values of the solutes. Zwitterionic chemicals are used as carrier ampholytes to provide a pH gradient where the pH is low at the anode and high at the cathode. Zwitterionic compounds with different pIs, such as proteins, peptides, amino acids and various drugs, can be resolved by isoelectric focusing. These solutes migrate until they align themselves at their pI point where the zwitterion possesses no net overall charge and will therefore concentrate at this point as migration ceases. After isoelectric focusing separation, a salt can be added into either the cathodic buffer or the anodic buffer. A high voltage is reapplied, the anions or cations of the added salts compete with $\text{OH}^- / \text{H}_3\text{O}^+$ migration, resulting in a pH gradient change and migration of both ampholytes and sample components toward the end of the capillary within the buffer reservoir with added salt.

1.2.5 Capillary Isotachopheresis (CITP)

Typically in conventional isotachopheretic separations, electroosmotic flow is eliminated or minimized. The capillary is filled with two different electrolytes, a leading electrolyte with higher electrophoretic mobility (in one reservoir) and a terminating electrolyte (in another reservoir) with lower electrophoretic mobility than any of the sample components. Sample components in a low concentration condense between leading and terminating constituents, and separation is based on the individual electrophoretic mobilities of the sample components. Only ionic species can be separated in a single run. This technique can be used as a preconcentration step for other capillary electrophoresis analysis.

1.3 PRINCIPLES OF CAPILLARY ZONE ELECTROPHORESIS

The general components of a CE instrument are shown in Figure 1.1. A buffer-filled silica capillary is placed between two buffer reservoirs, and a high voltage is applied through two electrodes immersed in the reservoirs. The injection end of the system is confined in a Plexiglas box equipped with a safety interlock. The detector can be on-column or post-column at the end of the capillary. The principles of CE are described in greater detail below.

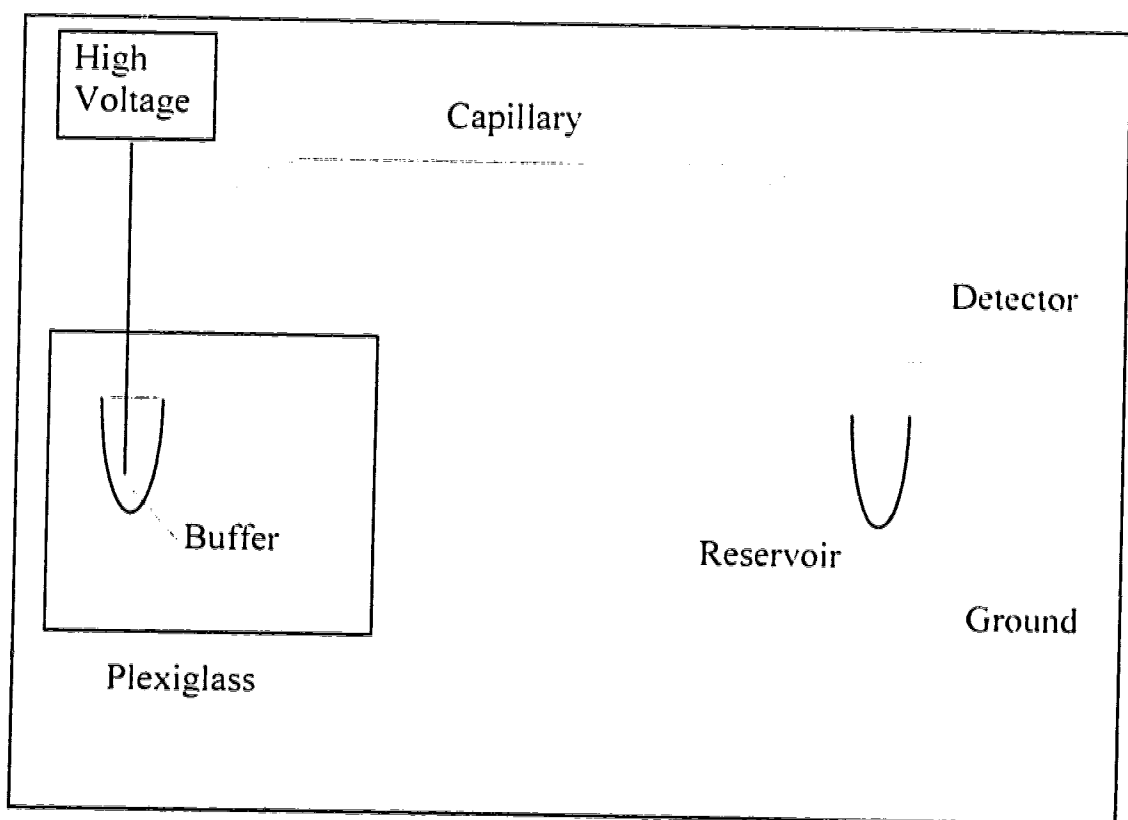


Figure 1.1 Simple diagram of a capillary electrophoresis separation system.

1.3.1 Electroosmotic Flow and Zeta Potential

The electroosmotic flow, which is generated by applying high voltage to the buffer solution inside the capillary, plays a fundamental role in capillary electrophoresis. Figure 1.2.

The silica capillary wall consists of -SiOH groups. When the capillary wall is in contact with an ionic solution, the neutral -SiOH groups will be dissociated to anionic SiO^- depending on the buffer pH. Counterions to these anions are in the stagnant layer adjacent to the capillary walls. This cationic nature extends into the diffuse layer, which is mobile. The potential created across the layers at the silica/water interface is termed the zeta potential (ζ), and is given by:

$$\zeta = \frac{4\pi\eta\mu_{eo}}{\epsilon} \quad (1.1)$$

where η is the viscosity, ϵ is the dielectric constant of the solution, and μ_{eo} is electroosmotic mobility.

This bulk movement of buffer is caused by the small zeta potential at the silica/water interface, which induces a minute excess of cationic charge at the surface of the silica (Figure 1.2b). This charge, due to the presence of dissociated -SiOH groups on the surface of the capillary, is dependent on the pH of the buffer solution. The degree of dissociation of the silanol groups ($-\text{SiOH} \leftrightarrow -\text{SiO}^- + \text{H}^+$) alters the ζ potential.

Close to the silica surface, an excess of cationic species in bulk solution migrates toward the cathode, producing a net flow from anode to cathode. The flow of the bulk solution induced by a minute excess of anionic charge is called electroosmosis (Fig1.2b), and can be calculated by:

$$v_{eo} = \mu_{eo} \times E \quad (1.2)$$

where v_{eo} is the electroosmotic flow rate and E is the electric field.

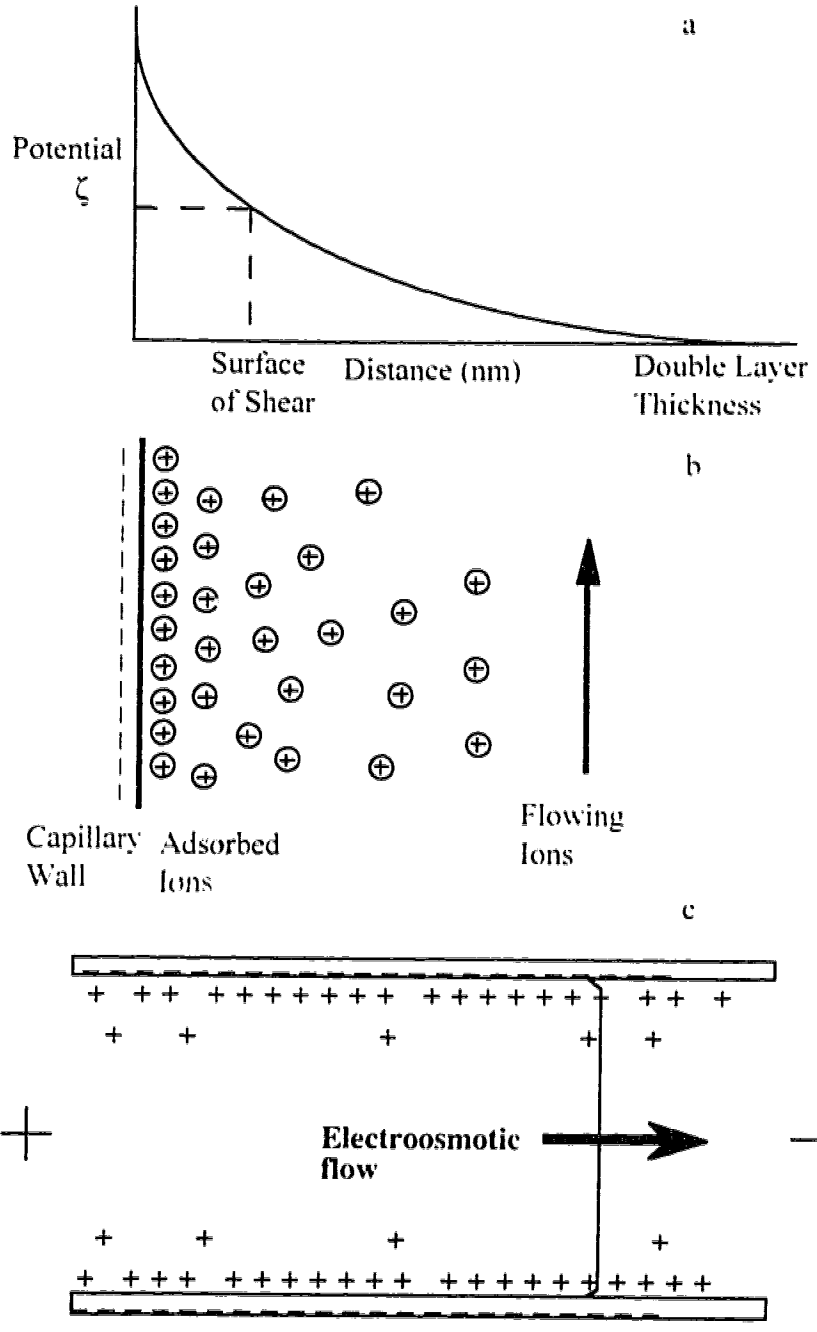


Figure 1.2 Electroosmotic flow and ζ potential.

The double layer thickness ranges from 3 to 300 nm for electrolyte concentration of 10^{-2} to 10^{-6} M (14). The thin double layer leads to flow that originates at the walls of the capillary, resulting in a flat flow profile (Figure 1.2c) (15) when the capillary radius is greater than seven times the double-layer thickness (16).

1.3.2 Electrophoretic Mobility

The electrophoretic mobility describes the migration of charged species in the buffer solution under the electric field. The migration velocity (v_{ep}) is given by (17):

$$v_{ep} = \mu_{ep}E = \mu_{ep} \frac{V}{L_c} \quad (1.3)$$

V is the high voltage, L_c (cm) is the capillary length, and μ_{ep} , the electrophoretic mobility, is given by:

$$\mu_{ep} = \frac{v_{ep}}{E} = \frac{q}{6\pi\eta r} \quad (1.4)$$

where r is the ion radius and q is the charge on the ion. From equation 1.4, we know that the electrophoretic flow depends on both the charge and the size of a solute.

The migration time is determined by both electrophoretic and electroosmotic mobilities. The total velocity of a solute is :

$$v_{total} = (\mu_{ep} + \mu_{eo}) \frac{V}{L_c} \quad (1.5)$$

and the time needed for the solute to migrate from injection end to detection end is:

$$t = \frac{L_c^2}{(\mu_{ep} + \mu_{eo})V} \quad (1.6)$$

The migration time is proportional to the square of the capillary length under the constant applied voltage and inversely proportional to the sum of electrophoretic and electroosmotic mobilities.

It can be noted from Equation 1.5 that if the rate of electroosmotic flow is greater in magnitude than the electrophoretic mobility of all analyte, all ions and nonionic species in the buffer will be carried by the electroosmotic flow and elute at one end of the capillary. Electroosmotic flow affects the total time solutes spend in the capillary; however, separation is based on differential electrophoretic migration of each ionic species. Therefore neutral species are not separated by zone electrophoresis alone.

1.3.3 Separation Efficiency

The lack of any stationary phase and the flat flow profile result in longitudinal diffusion being the major source of band broadening. Using Einstein's law of diffusion, the statistical equivalence of variance (σ^2), the maximum separation efficiency (N), is given by:

$$N = \frac{L_c^2}{\sigma^2} = \frac{(\mu_{ep} + \mu_{eo})}{2D} \quad (1.7)$$

where D is the diffusion coefficient. N is independent of the capillary length.

Generally, the number of theoretical plates can be calculated by:

$$N = 5.54 \left(\frac{t_r}{W_{1/2}} \right)^2 \quad (1.8)$$

where t_r is the migration time for a certain solute and $W_{1/2}$ is the full peak width at half height.

1.3.4 Resolution

The resolution, R, of two peaks in electrophoresis can be given by the equation:

$$R = \frac{1}{4} N^{1/2} \frac{\Delta v}{\bar{v}} \quad (1.9)$$

where N is the average number of theoretical plates. Δv is the difference in zone velocities of two components, and \bar{v} is the average zone velocity. Using equations 1.5 and 1.7 and substituting into equation 1.9, the resolution can be expressed as:

$$R = \frac{\sqrt{2}}{8} (\mu_{ep,1} - \mu_{ep,2}) \left[\frac{V}{D(\bar{\mu}_{ep} + \bar{\mu}_{eo})} \right]^{1/2} \quad (1.10)$$

Resolution can be estimated experimentally by the same equation used in chromatography:

$$R = \frac{t_{r,1} - t_{r,2}}{\frac{1}{2}(W_1 + W_2)} \quad (1.11)$$

where $t_{r,1}$ and $t_{r,2}$ are the migration times of component 1 and component 2, respectively. w_1 and w_2 are the full peak-widths at baseline (in unit of time) of peak 1 and peak 2.

1.4 PRINCIPLE OF MECC

Although CZE has a high separation power, it is not applicable to the separation of uncharged compounds, because neutral compounds have no electrophoretic mobility. This problem can be overcome by forming ionic micelles in the running buffer.

1.4.1 The Formation of Micelles

MECC is most commonly performed with anionic surfactants, especially sodium dodecyl sulfate (SDS). When the concentration of the sodium dodecyl sulfate $\text{CH}_3(\text{CH}_2)_{11}\text{OSO}_3\text{Na}$ is above the critical micelle concentration (Table 1.1), micelles will form that consist of about 60 molecules. The hydrophobic tail groups (non-polar hydrocarbon chain) tend to orient toward the center and the negatively charged head groups point into the solution. The SDS micelle, therefore, migrates toward the positive

electrode by electrophoresis. The electroosmotic flow is in the direction of the negative electrode, and it is stronger than the electrophoretic migration of the SDS micelle under conditions of pH above 5. The neutral molecules will partition between the two phases, and they can be separated based on differences in their solubility in the micellar phase (Figure 1.3). The lower the solubility, the less the solute will partition in the micellar phase, and the faster the solute moves.

Table 1.1 Critical micelle concentration (CMC), aggregation number (n), and Kraft point (Kp) of selected ionic surfactants (18)

Surfactant	CMC ^a , mM	n	Kp (°C) ^b
SDS	8.1	62	16

^a 25 °C

^b micelle can be formed when the temperature is above the Kraft point.

1.4.2 Several Important Parameters in MECC

The Capacity Factor (k').

k' is defined as the ratio of the number of the analyte molecules incorporated into the micelle, n_{mc} , over that in the aqueous phase, n_{aq} , in Eq. 1.12:

$$k' = \frac{n_{mc}}{n_{aq}} \quad (1.12)$$

Micellar Electrokinetic Capillary Chromatography

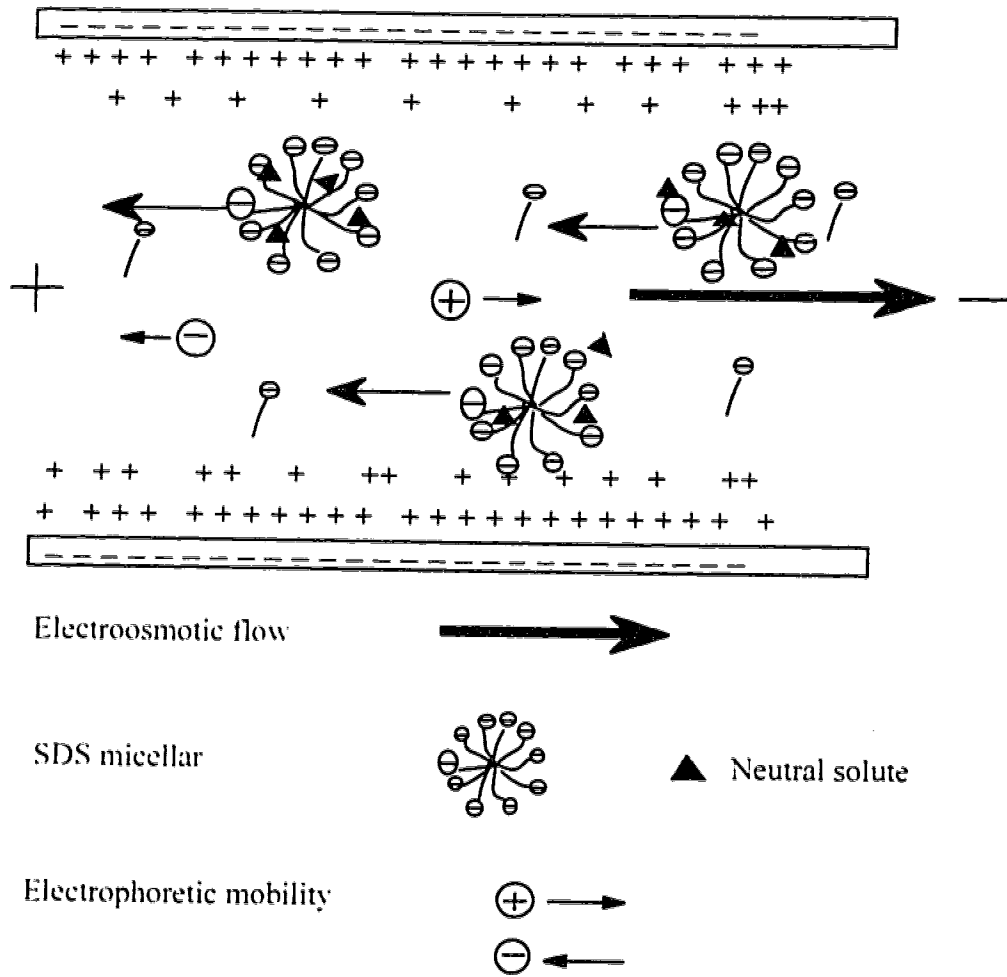


Figure 1.3 Schematic separation by MECC.

The capacity factor for the best resolution per unit time ranges from 1.2 to 2. The relation between the migration time and the capacity factor is given by (13):

$$t_r = \frac{1+k'}{1+(\frac{t_0}{t_{mc}})k'} t_0 \quad (1.13)$$

where t_r , t_0 , and t_{mc} are the migration times of the analyte, the micelle insolubilized solute, and the micelle, respectively. When the analyte does not interact with the micelle, then t_r is equal to t_0 . When the analyte is totally incorporated into the micelle, then the analyte migration time equals the micelle migration time. So the migration time window of the neutral analyte is limited between the insolubilized solute and micelle phase migration times.

The t_0 can be determined by use of methanol (or acetone or formamide) as a marker that is electrically neutral and negligibly incorporation into the micelle. A marker selected for measuring a micelle migration time, t_{mc} , must be totally incorporated into the micelle. An organic dye, Sudan III or Yellow OB (19) can be used for t_{mc} measurement. The capacity factor can be calculated from t_r , t_0 , and t_{mc} by using Eq. 1.13.

Resolution

The resolution, R , of two adjacent peaks whose capacity factors are k'_1 and k'_2 is expressed as (19):

$$R = \frac{\sqrt{N}}{4} \left(\frac{\alpha-1}{\alpha} \right) \left(\frac{k'_2}{1+k'_2} \right) \left(\frac{1-t_0/t_{mc}}{1+(t_0/t_{mc})k'_1} \right) \quad (1.14)$$

where N is the theoretical plate number and α is the separation factor (k'_2/k'_1).

The resolution can be affected by the selectivity, α , which is determined by the kind of surfactant used in MECC and by the pH of the buffer solution. The pH determines whether the solute will be a neutral molecule and α is determined by the

solute partition in the micelle phase. Very hydrophilic solutes and highly hydrophobic solutes are difficult to separate by using MECC.

Details for optimizing those parameter are discussed in depth by several authors (20, 21, 22). MECC also can be used to separate ionic species. MECC has been used successfully for separation of amino acids, proteins and carbohydrates (23-27).

1.4.3 Selectivity Manipulation

The micellar structure is affected by type of surfactants. Surfactants (cationic or anionic) have a hydrophobic and a hydrophilic group within each molecule and the different types of surfactants can provide moderate changes in the separation selectivity (19). The hydrophilic, or ionic group, is generally more important in determining selectivity than is the hydrophobic group because many compounds are adsorbed on the surface of the micelle or at least interact considerably with the surface of the micelle. In the case of ionic analytes, hydrophobicity and charge affect the partition coefficient. The force between ionic species and micelles can be electrostatic attraction or repulsion. The analyte having the opposite charge to that of a micelle will strongly interact with the micelles through electrostatic force, and the analyte having the same charge will interact weakly owing to the electrostatic repulsion. The micelle used in MECC can be modified by forming a mixed micelle with ionic or nonionic surfactants that are usually larger and have a lower charge density on the surface. The selectivity of a mixed micelle shows difference from that of the original ionic micelle (28).

The pH of a buffer also influences the micelle structure. The aqueous solution can be modified by changing the pH of the buffer. The pH changes the charge on the analyte and its electrophoretic mobility, so the partition coefficients of the ionizable analytes can be changed. Several solvent additives (urea, cyclodextrins, and organic solvents) can be added to change the partition coefficient of the analytes.

An increase in temperature causes a decrease in partition coefficient and viscosity, which results in shorter migration time. Temperature affects selectivity to some extent in MECC (29), but it seriously affects the migration time. Therefore, it is essential to the reproducibility of results to keep temperature constant.

1.5 SAMPLE INJECTION

To avoid excessive band broadening, only a minute amount of sample can be loaded onto the capillary. Sample is injected onto the capillary column in a minimal volume (<0.1% capillary volume, in nanoliter to picoliter range, allowing less than 5% broadening by injection) (30) to get high separation efficiency and short analysis times. Two sample injection methods have been used.

1.5.1 Electrokinetic Injection

Electrokinetic injection is also known as electromigration injection. The capillary tip is dipped momentarily into the sample, potential is applied for a few seconds, and the capillary is removed to the separation buffer. The number of moles of analyte that is injected into the capillary depends on the electrophoretic mobility of the analyte. Analytes with higher electrophoretic mobilities travel faster and thus are injected to a greater extent than slower moving analytes (31). The injection volume (V_{inj}) of an individual component can be calculated by the following equation:

$$V_{inj} = V_c \left(\frac{t_{inj}}{t_{mig}} \right) \left(\frac{E_{inj}}{E_{sep}} \right) \quad (1.15)$$

where V_c is the volume of the capillary, E_{inj} and E_{sep} are the potentials of injection and separation respectively, and t_{inj} and t_{mig} are the injection time and migration time of the

analyte. This calculation assumes that the conductivity of the sample is the same as that of the separation buffer (32).

1.5.2 Hydrodynamic Injection

This injection method is based on a pressure difference between a sample reservoir and a waste reservoir. The pressure difference induced between the two reservoirs drives analyte onto the capillary. This method is also known as hydrostatic or siphoning injection. The siphoning injection can be performed manually or automatically (33). The injection volume produced in hydrostatic injection is given by

$$V_{inj} = \frac{\rho g \pi r^4 \Delta h_{inj}}{8 \eta L} \quad (1.16)$$

where ρ is the buffer density, g is the gravitational force constant, r is the capillary radius, Δh is the height difference between collection and injection reservoirs, η is the buffer viscosity, and L is the total capillary length. The injection is based on bulk flow of the buffer, so the injected volume is basically the same for all components in the bulk sample solution.

1.6 DETECTION METHODS

The small capillary dimensions and zone volumes present a challenge to achieve sensitive detection. On-column UV adsorption and fluorescence detection have been the most commonly used detection techniques for CE applications.

1.6.1 On-Column Detection

A small section of the polyimide coating is burned off the capillary to form a window. The on-column detection methods include UV absorbance, fluorescence and refractive index measurements. Most commercial CE instruments are equipped with a UV detector. The detection limit for on-column detection with thermo-optical absorbance

can reach 0.2 femtomoles (23) and fluorescence detection is in the attomole (1×10^{-18} mole) range (180 ± 100 attomol/cell for aspartic acid and 5.1 ± 1.5 femtomol/cell for taurine) (5, 6, 34, 35). The best detection limit for on-column fluorescence detection has been reported to be 1.4 zeptomole (1×10^{-21} moles) for Lissamine 20 (36). Several modified on-column detection methods have also been reported (37). Other detection methods used in on-column detection include electrochemical (conductivity and amperometric) and radioactive detection. Fluorescence detection is the most sensitive method.

1.6.2 Post-Column Detection

Chemiluminescence is a post detection method in which optical excitation is not used (40, 41, 42). Amperometric detection is used as a post-column detection method for carbohydrate separation (43). Both on-line CE-MS (44) and off-line CE-MS (MALDI time-of-flight) (45) have been used to identify separated proteins and peptides. Post-column laser-induced fluorescence detection will be discussed in more detail.

1.7 POST-COLUMN LASER-INDUCED FLUORESCENCE DETECTION (LIF)

Lasers are superior excitation sources for use with small-diameter capillaries. The high spatial coherence of a laser can be focused on a narrow bore capillary. The laser monochromaticity reduces stray light levels, which increase the detection sensitivity dramatically. When coupled with an efficient collection and detection optical system, minute amounts of analyte can be detected.

Initially, the laser-induced fluorescence detection was on-column. Zare and coworkers were the first to report the use of laser induced fluorescence detection in capillary electrophoresis (46, 47). Their detection limit was on the order of two femtomole (10^{-15} mole) for dansylated amino acids. Several other papers also described

on-column fluorescence detection. Hernandez and co-workers (48) developed an elegant fluorescence detector based on an epiillumination design. Jorgenson's group (49) worked on amino acid separation and Novotny's group used fluorescence for detecting primary amine and amino sugars (50). The best detection limits were in the low attomole range. Generally, fluorogenic reagents were used for pre-column labeling in order to permit LIF detection. This level was reached by minimizing solvent impurities and selecting a collection wavelength range to minimize Raman and Rayleigh scatter from water (51). Fluorescence reflection and refraction at the capillary wall cause high background signals for on-column detection. This prevented further improvement of detection limits using this combination of technologies.

Dovich's group reported that stray light can be minimized by using of a sheath-flow cuvette (38, 52). This sheath flow cuvette was designed to limit the extra band broadening for post column detection and decreased the reflection by using high quality quartz as a detection window. The detection limits were improved from sub-attomole (10^{-18} mole) in 1988 (38) to a few molecules of sulforhodamine 101 in 1994 with a low-cost green He-Ne laser used as an excitation source (39).

1.8 FLUORESCENCE DERIVATIZATION

Since most analytes do not fluoresce, pre- or post-column derivatization of the sample with some type of fluorophore allows the extension of fluorescence detection to many analytes. The selection of dye must match the available laser wavelength. Fluorescent labeling becomes important to "visualize" the otherwise spectroscopically invisible molecules. Post-column derivitization requires a fast labeling reaction and a carefully designed chamber to carry the reaction after analytes are separated by CE.

Pre-column labeling is the most commonly used method with fluorescence detection. The labeled product can be purified through other methods.

Amino sugars can be labeled by CBQCA and TRSE using post-column derivatization methods. The properties of these derivatives are listed in Table 1.2.

Table 1.2 Some parameters of CBQCA and TRSE

Dye	CBQCA glycine derivative	TRSE labeled aminated sugar
Maximum absorbance	466 nm	552 nm
Laser for excitation	488 nm (Ar ⁺ ion)	535.5 nm (green He-Ne)
Maximum emission	544 nm	570 nm
Spectral filter	535DF35, 635DF55	580DF40
(M ⁻¹ cm ⁻¹)	—	8.0 × 10 ⁴
Labeling reaction pH	9	9

1.8.1 CBQCA Labeling of Aminated Sugars

3-(4-Carboxybenzoyl)-2-quinolinecarboxaldehyde (CBQCA or CBQ) is a fluorogenic reagent that reacts specifically with hydrophilic peptides and amino sugars to form charged conjugates (50). This reagent does not fluoresce unless it has reacted with a primary amine and cyanide (see Figure 1.4). Non-amino carbohydrates are reductively aminated (53) before labeling. CBQCA stock solution (10 mM) is prepared in MeOH and sonicated 30 min to ensure complete solubilization. Derivatization of amino sugars is performed by mixing an aliquot of the amino sugar with 10-20 µl of 10 mM KCN solution and 5-10 µl of CBQCA solution. The mixture reacts at room temperature for more than one hour. A pH range of 7 to 9 is optimal for an amino sugar reacting with CBQ. Aqueous solutions of the labeled amino sugars are stable at least 10 h. The lyophilized products are stable for at least two weeks in the freezer.

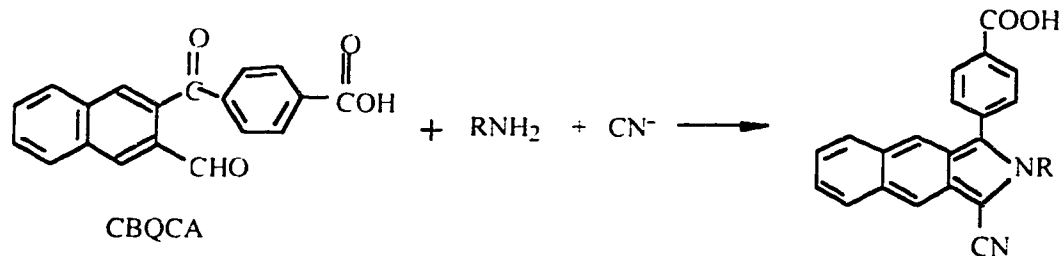


Figure 1.4 Aminated Sugar Labeling by CBQCA

1.8.2 TRSE Labeling of Aminated Sugars

5-Carboxytetramethylrhodamine succinimidyl ester (TRSE) is another fluorescent dye used for labeling primary amines (aminated sugars or amino acid) (see Figure 1.5). It is a good reagent for modifying aliphatic amines, since they form stable carboxamides and have reasonable reactivity. In general, TRSE does not react with aromatic amines, phenols or alcohols. The stock solution can be prepared in dimethylsulfoxide (DMSO). The labeling reaction pH is 7.5 to 8.5 (0.1 to 0.2 M sodium bicarbonate). The reaction is generally performed at room temperature and in the dark for one hour. During the labeling reaction, succinimidyl ester hydrolysis can compete as a side reaction, but this is usually slow at a pH below 9.

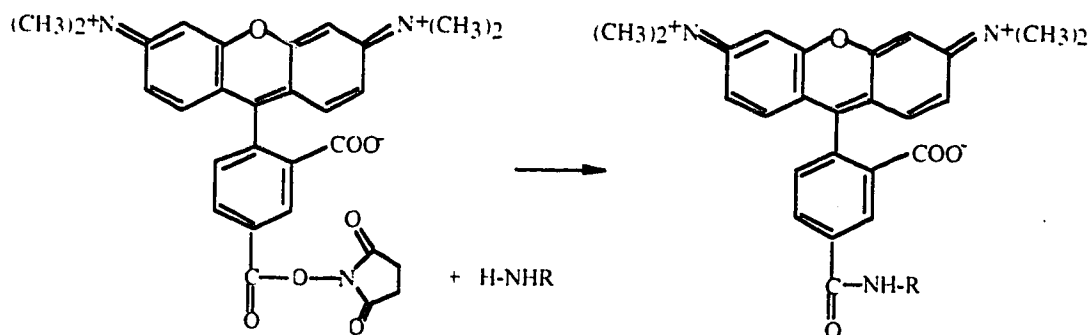


Figure 1.5 TRSE Labeling Aminated Sugar

1.9 INSTRUMENTATION

1.9.1 Laser

The spatial coherence of the laser facilitates focusing the entire beam to a small spot, which matches the size of the sample stream in the sheath flow cuvette. The laser beam provides high power and spectrally pure light.

A laser was selected using three criteria. First of all, the wavelength of a laser beam must match the absorbance spectrum of the analyte for analysis. For example, TRSE labeled aminated sugars have a maximum absorbance at 552 nm which is very close to the 543 nm He-Ne laser (see Table 1.3). Second, the background signal must be minimized. Raman scatter from the solvent is the major source of background signal for a well designed fluorescence detector. For water, there are two major Raman bands, one at 1650 cm^{-1} , and the other extending from 3100 to 3700 cm^{-1} . There are also two minor Raman bands at 1640 and 2200 cm^{-1} . So the excitation wavelength should be chosen so that the analyte emission wavelength occurs between the two main Raman bands. Another important parameter is the laser power and noise. A high stability laser is required to obtain shot-noise limited performance (see Table 1.4). Under shot noise conditions, the noise in the background increases with the square root of laser power while fluorescence signal gains linearly with the laser power. High power and irradiance ($>10^5\text{ Wcm}^{-2}$) are limited in use because optical saturation of the absorbance transition and photo degradation of the analyte molecules occur. Both saturation and photo degradation plus poor spatial beam quality limit the use of pulsed lasers for fluorescence excitation (52).

Since laser lines are monochromatic, background resulting from Rayleigh and Raman scattering is easily avoided by selection of the appropriate emission wavelengths. In general, lower background signals are observed for long-wavelength excitation. The decreased background signal is due in part to the decrease in scattered light intensity that

scales roughly as λ^{-4} . Also, there are relatively few impurity molecules that absorb long wavelength light to generate background fluorescence signals (54).

Table 1.3 The properties of a Helium-Neon laser

Green He-Ne Laser	543 nm
Model No.	LHGR-0100M (PMS)
Minimum output (mW)	1.0
Mode	Multi
Beam Diameter (mm)	0.9
Beam Diverge (mrad)	1.2
Power Supply (V)	115
Polarization Linear > 500:1	Random
Longitudinal Mode Spacing (MHz)	Multi-Mode
Operating Voltage (Vdc)	2460
Operating Current (mA)	5.5
Starting Voltage (KVdc)	< 10
*Measured Laser Power (mW)	2.2

From PMS Electro-Optics (PMS, Colorado, USA) data sheet.

*Measured by Power meter (model 835, Newport Optical)

Table 1.4 The properties of an Argon ion laser

Laser Wavelength (nm)	488.0
Output Power (TEM ₀₀) for INNOVA 90-4 Model	1300 mW
Bore Configuration	Tungsten disk with one piece ceramic envelope
Plasma Tube Cooling	Conductively water cooled
Cavity Configuration	Flat high reflector. long radius output coupler
Output Polarization	100:1 Electric Vector
Cavity Length	1093 mm
Excitation	Current Regulated DC
Input Voltage	208 ± 10% Vac 50 or 60 Hz 3 phase with ground
Maximum Input Current	45 Amperes
Cooling Water Flow Rates Incoming Temperature Pressure	8.5 liters/min (minimum) 30° C maximum Minimum 1.76 kg/cm ² Maximum 3.52 kg/cm ²
Beam Diameter ^a	1.5 mm at 1/e ² points
Beam Divergence ^a	0.5 mrad at 1/e ² points
Long Term Power stability ^b	Current Regulation ±3% Light Regulation ±0.5%
Optical Noise ^c	In current regulation 0.2% rms In light regulation 0.2% rms

^aBeam diameter and divergence measured at 514.5 nm at the output coupler.

Table 1.4 made from the manufacture data sheet (INNOVA 90 series. Coherent)

^b Maximum peak variation (over any 30 min period after 2-h warm-up).

^c Measurement is made with wide band photodiode driving resistive load. The noise voltage is measured with an rms voltmeter with 10 Hz-2 MHz bandwidth. Specification for 514.5 nm at specified output power.

1.9.2 Sheath Flow Cuvette

A flow cytometer cuvette (55, 56, 57, 58) is interfaced with capillary electrophoresis. The cuvette is made from high quality optically flat quartz and has 2 mm thick windows and a 200 μm wide hole in the center. The cuvette is held by a stainless steel holder at ground potential. A capillary with outer diameter less than 200 μm is inserted into the square flow chamber.

A sheath buffer is identical to separation buffer to eliminate their refractive index difference. Under the very low flow rate produced by electroosmosis, the sample stream travels as an 10 μm diameter stream through the center of the cuvette. The sheath flow at a high velocity can narrow the radius of the separated analyte dynamically and focus it as a narrow stream. The sheath can be formed by a high-precision syringe pump or generated through siphon by raising the sheath buffer level a few centimeters above the waste vial.

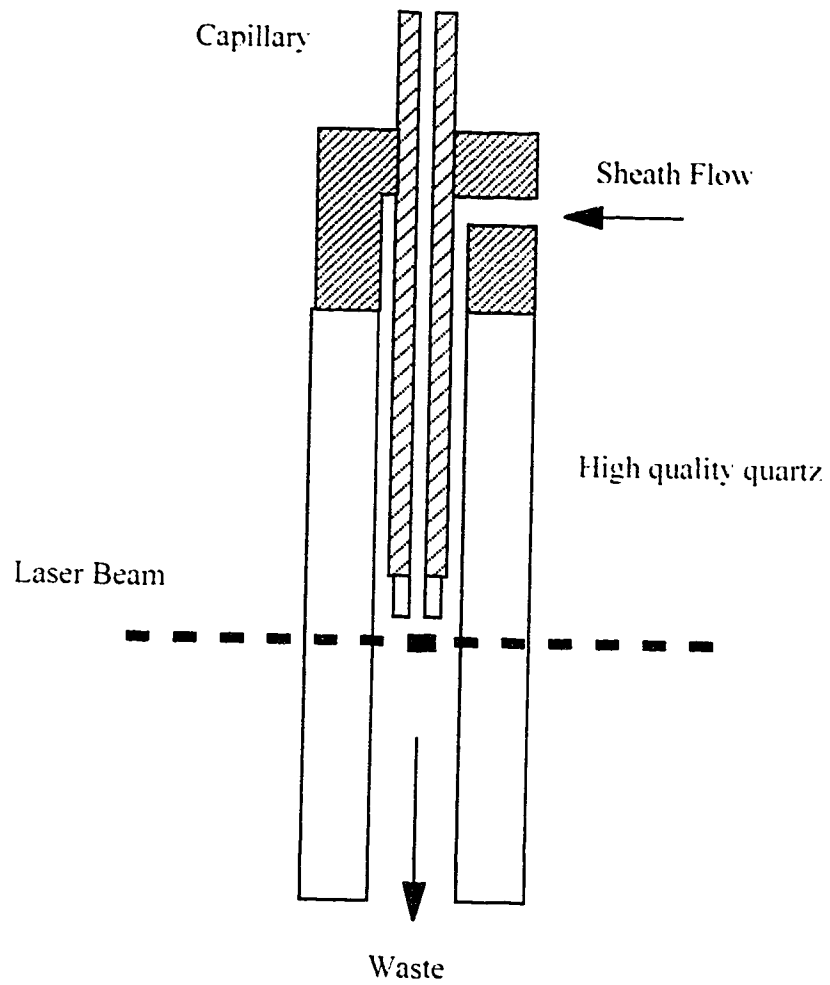


Figure 1.6 Schematic diagram of sheath flow cuvette.

1.9.3 Optical Collection System

Fluorescence is excited by a low-power laser beam focused to a 10 μm spot about 0.2 mm downstream from the capillary exit. The laser beam is directed by mirrors to the sheath flow cuvette at right angle. Fluorescence is collected at right angles to both the sample stream and the laser beam with a microscope objective. Either a pinhole with a fixed size or an iris with adjustable size may be used. The fluorescence generated from the illuminated sample stream can be collected with high efficiency and the scattered light reaching the detector can be minimized by using a pinhole and a spectral filter. The collection efficiency is related to the numerical aperture, N.A., and the refractive index of the surrounding medium, n .

$$\text{Collection efficiency} = \text{Sin}^2\left[\frac{\text{Arcsin}\left(\frac{\text{N.A.}}{n}\right)}{2}\right] \quad 1.17$$

Usually, the lens is surrounded by air and n is 1. A collection efficiency of 1 implies that the lens collects all of the photons emitted by the molecules. A lens with a numerical aperture of 1 will collect half of the light emitted by the sample. A high collection efficiency microscope objective is selected for this purpose.

Microscope Objective

Table 1.5 lists the collection efficiencies of microscope objective with different numerical apertures (52).

Table 1.5 Collection efficiency of microscope objective ($n = 1$)

N.A.	1.0	0.9	0.8	0.7	0.6	0.5	0.4	0.3	0.2	0.1
C.E.	0.500	0.280	0.200	0.140	0.100	0.067	0.042	0.023	0.010	0.003

N.A. is numerical aperture and C.E. is the collection efficiency.

Generally speaking, the microscope objective is positioned very close to the fluorescence area, but the cuvette window is 2 mm thick, which requires the working distance of the microscope objective to be greater than 2 mm. It is very hard to find a microscope objective with a high numerical aperture and a long working distance.

Pinhole

A pinhole or an iris, matched to the size of the sample image, is placed in the image plane of the microscope objective to isolate the illuminated sample regions while rejecting light scattered from the cuvette walls. The iris size can be adjusted from 0 to 1 mm.

Spectral Filter

Between a pinhole or iris and a PMT, a spectral filter is used to spectrally isolate fluorescence from the background scatter signal, and it rejects both Rayleigh scattered and the Stokes-shifted Raman scattered light (see Table 1.6) at the laser wavelength while providing high transmission (50%) (59).

Table 1.6 Water Raman band for different lasers

Laser, nm	Raman Bands, nm
488	495, 577-596
543.5	553, 657-680
514	522, 614-635
594	605, 732-761
612	623, 759-791

PMT

A photomultiplier tube (PMT) responds to the fluorescence signal with certain quantum efficiency (about 15% for R1477 tube at 550 nm in Table 1.7) and converts the photon signal into an electrical signal digitized by input/output board to a computer. A resistor-capacitor (RC) circuit is generally used to filter the signal.

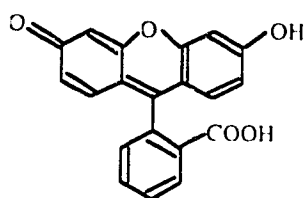
Table 1.7 R1477 side-on type photomultiplier tubes (25 °C)

R1477	High sensitivity
Spectral range (nm)	185-900
Spectral Response Peak Wavelength (nm)	450
Photo cathode Material	Multialkali
Window Material	UV glass
Outline No.	2
Dynode Structure/No. of Stages	CC/9
Socket	E678-11A
Maximum Anode to cathode Voltage (Vdc)	1250
Average Anode Current (mA)	0.1
Cathode luminous Sensitivity (min. $\mu\text{A}/\text{lm}$)	350
Cathode luminous Sensitivity (Typ. $\mu\text{A}/\text{lm}$)	375
Cathode Sensitivity ($\mu\text{A}/\text{lm-b}$)	10.0
Anode to cathode Supply Voltage (Vdc)	1000
Anode typical sensitivity (A/lm)	2000
Anode Dark Current (after 30 min) Max (nA)	50
Rise Time Typ. (ns)	2.2

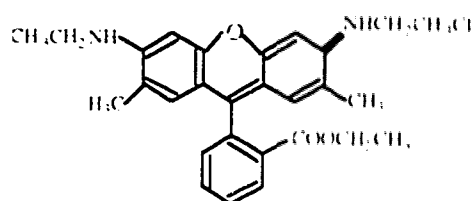
From manufacture (Hamamatsu, Japan) data sheet.

1.9.4 Fluorophors Used for Alignment

The fluorescent dyes commonly used for aligning a CE system are fluorescein and rhodamine, corresponding to the excitation source of 488 nm line of Argon ion and 543 nm He-Ne laser, respectively. Their properties are listed in the Table 1.8. The concentration is typically 1×10^{-9} to 1×10^{-10} M.



Fluorescein



Rhodamine

Table 1.8 Some parameters of fluorescein and rhodamine (59)

Dye	Fluorescein	Rhodamine (R6G)
Solvent	DMF	MeOH
AB (nm)	490	528
EM (nm)	514	550
ϵ ($M^{-1} \text{ cm}^{-1}$)	9×10^4	1.1×10^5
Laser for excitation	488 nm line of Argon ion	543.5 nm He-Ne

1.10 THE LIMIT OF DETECTION

The limit of detection is defined as the minimum analyte that produces a signal equal to three times the standard deviation of the gross blank signal. The background signal can be calculated by inspecting over a time period given by 10-100 times the full peak-width in terms of time ($W_{1/2}$) at one half peak height using Knoll's method (61).

$$C_{LOD} = K_{LOD} h_n \frac{C_s}{h_s} \quad (1.18)$$

where C_{LOD} is the concentration detection limit, h_s / C_s is the analyte peak height/unit amount of analyte, h_n is the largest noise fluctuation (either positive or negative) observed in the noise measurement interval, K_{LOD} is a constant and its values are listed in Table 1.9. This technique is based on the Tchebycheft inequality.

The equation assumes that the noise distribution is unimodal, that it is a monotonically decreasing function on both sides of its one mode, and that the system responds linearly (nearly Gaussian waveform) over the detection range.

The peak height (h_s) and the maximum deviation (h_n) are obtained from the electropherogram of a diluted sample (C_s). The detection limit generally is calculated in our experiment by the following equations:

$$\text{Capillary volume} \quad V_c = \pi r^2 L_c \quad (1.19)$$

$$\text{Injection volume} \quad V_{inj} = V_c \left(\frac{t_{inj}}{t_{mig}} \right) \left(\frac{E_{inj}}{E_{sep}} \right) \quad (1.20)$$

$$\text{Number of moles injected} \quad n_{inj} = C_s V_{inj} \quad (1.21)$$

Limit of Detection $n_{LOD} = K_{LOD} n_{inj} \frac{h_n}{h_s}$ (1.22)

K_{LOD} value (see Table 1.9) generally used for the calculation is 0.6536 because the baseline inspection is over 100 times the full peak width at one-half peak height. r is the capillary radius, L_c is the length of capillary, C_s is the analyte concentration.

Table 1.9 Multiplier constants for LOD

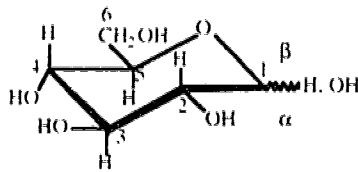
Peak width multiple	K_{LOD}
10	1.9718
20	1.4309
50	0.9194
100	0.6536

(Knoll, 1985 #59)

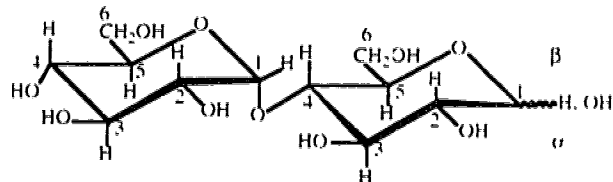
1.11 INTRODUCTION TO MAMMALIAN CELL SURFACE CARBOHYDRATES

1.11.1 Basic Introduction to Mammalian Monosaccharides

There are an enormous variety of monosaccharides in nature, the most common sugar being D-glucose (Glc). In an oligosaccharide, the cyclic monosaccharides are normally joined together by covalent bonds in which the hydroxyl of carbon atom 1 is reacted with any available hydroxyl other than C1 of a second monosaccharide with the elimination of a water molecule. Since the configuration at C1 can vary, an α - or β -glycosidic linkage can be formed. In an alpha linkage, the hydrogen is pointing up, and in beta linkage it is pointing down.



Structure of glucose



Structure of a disaccharide (Glc α 1 \rightarrow 4Glc)

Mammalian oligosaccharide chains commonly are composed of nine unmodified monosaccharide building blocks (62, 63). The most common sugars are glucose (Glc), galactose (Gal), mannose (Man), *N*-Acetylglucosamine (2-Glc), *N*-acetylgalactosamine (2-Glc), fucose (Fuc), sialic acids, xylose, and glucuronic acids (Figure 1.7). All of the monosaccharides have the D configuration except fucose is the L configuration.

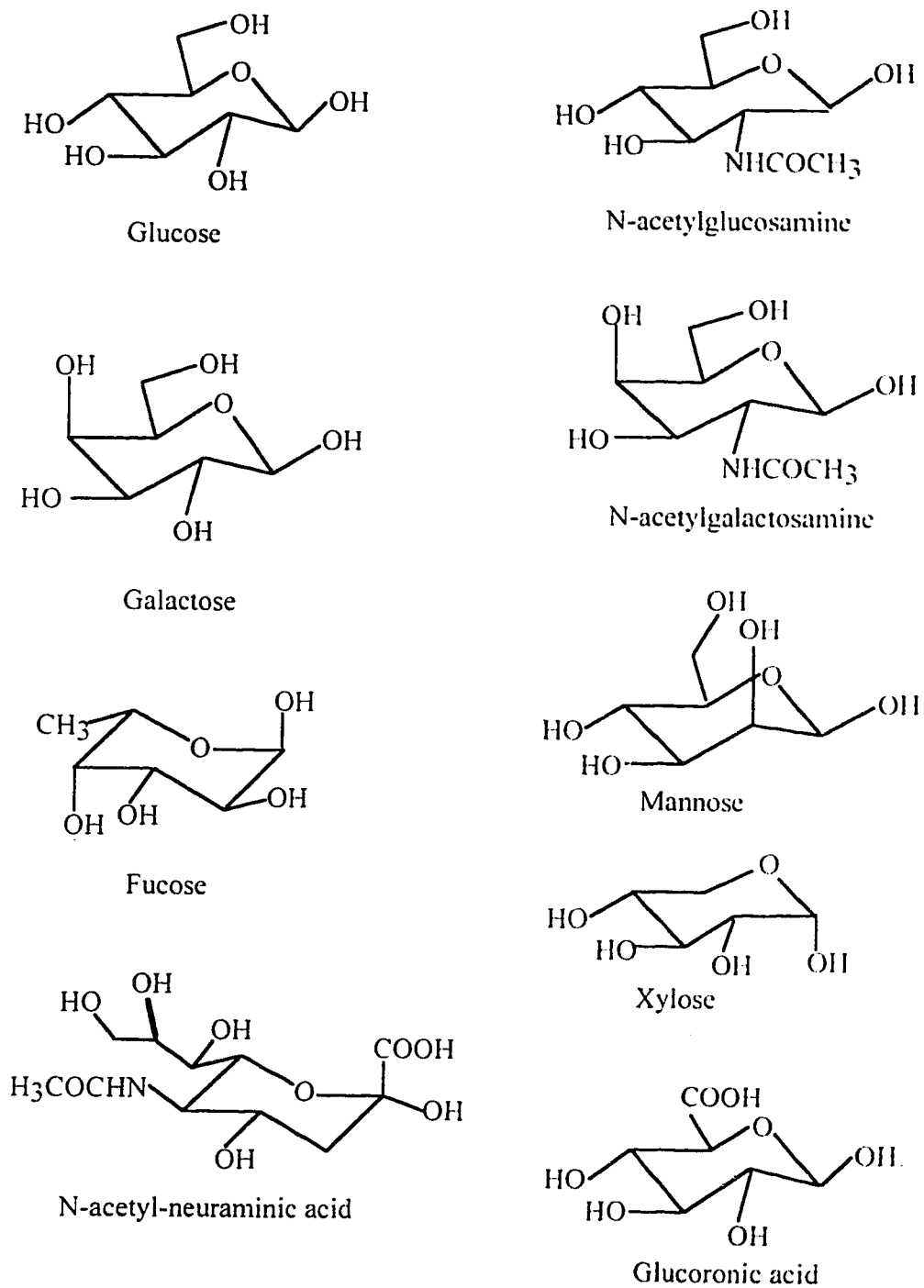
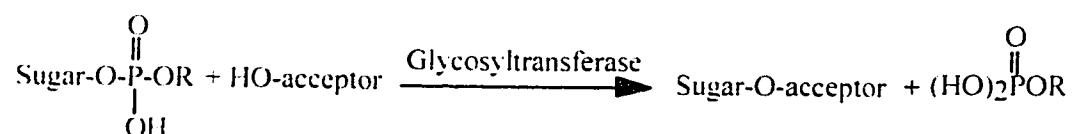


Figure 1.7 The nine monosaccharide building blocks commonly found in mammalian cells.

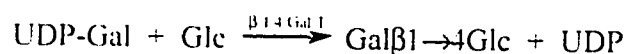
1.11.2 Glycosyltransferases

Glycosyltransferases catalyze the transfer of a single monosaccharide from a nucleotide donor to the hydroxyl group of an acceptor saccharide, either a glycoprotein, glycolipid, or polysaccharide.



The nucleotide donors corresponding to the above monosaccharides are UDP-Glc, UDP-Gal, GDP-Man, UDP-GlcNAc, UDP-GalNAc, GDP-Fuc, and CMP-NeuAc (62).

The biosynthesis of lactose is a simple illustration of these transfer reactions.



Sialic acid, fucose, *N*-acetylglucosamine and galactose residues with distinct linkages can be added to a disaccharide (eg. Gal β 1 \rightarrow 4Glc), in a controlled manner by glycosyltransferases and sugar nucleotides to form branched oligosaccharides.

1.11.3 Glycans

In the past decade, the structural analysis of carbohydrates attached to glycoproteins has resulted in the accumulation of a vast amount of information concerning the chemical structures of carbohydrates. In particular, carbohydrates attached to asparagine residues of proteins, *N*-glycans, serine or threonine residues of proteins, *O*-glycans, needed to be extensively characterized (64).

N-Glycan

N-Glycans linked to asparagine residues can be classified into three types. The first is called high mannose type which contains only mannose and *N*-acetylglucosamine residues. The second is a complex type having a common pentasaccharide structure, $\text{Man}\alpha 1 \rightarrow 6(\text{Man}\alpha 1 \rightarrow 3)\text{Man}\beta 1 \rightarrow 4\text{GlcNAc}\beta 1 \rightarrow 4\text{GlcNAc}$, which is called the trimannosyl core with additional sugar residues such as galactose, fucose and sialic acid. The third is called the hybrid type which is characterized by structural features of both the high mannose and complex types.

Some variation of complex-type *N*-Glycans has been observed in the structure of the outer chains themselves. Two isomeric backbone structures are formed by galactosylation: one is the $\text{Gal}\beta 1 \rightarrow 3\text{GlcNAc}$ group (Type 1 chain) and another is the $\text{Gal}\beta 1 \rightarrow 4\text{GlcNAc}$ group (Type 2 chain). Sialic acid residues occur as $\text{Sia}\alpha (2 \rightarrow 6)\text{Gal}$, $\text{Sia}\alpha (2 \rightarrow 3)\text{Gal}$, and $\text{Sia}\alpha (2 \rightarrow 6)\text{GlcNAc}$. Addition of α -fucosyl residues to the Gal and/or the GlcNAc residue of both H type 1 and H type 2 chains by different linkages produces the following blood group-related antigenic structures: $\text{Fuc}\alpha 1 \rightarrow 2\text{Gal}\beta 1 \rightarrow 3$ or 4GlcNAc (H type I or H type 2), $\text{Gal}\beta (1 \rightarrow 3)(\text{Fuc}\alpha 1 \rightarrow 4)\text{GlcNAc}$ (Lewis A), $\text{Fuc}\alpha 1 \rightarrow 2\text{Gal}\beta 1 \rightarrow 3(\text{Fuc}\alpha 1 \rightarrow 4)\text{GlcNAc}$ (Lewis B), $\text{Gal}\beta 1 \rightarrow 3(\text{Fuc}\alpha 1 \rightarrow 3)\text{GlcNAc}$ (Lewis X), and $\text{Fuc}\alpha 1 \rightarrow 2\text{Gal}\beta 1 \rightarrow 4(\text{Fuc}\alpha 1 \rightarrow 3)\text{GlcNAc}$ (Lewis Y). By combination of fucosylation and sialylation, $\text{Sia}\alpha 2 \rightarrow 3\text{Gal}\beta 1 \rightarrow 3(\text{Fuc}\alpha 1 \rightarrow 4)\text{GlcNAc}$ (2,3 sialyl Le^a) and $\text{Sia}\alpha 2 \rightarrow 3\text{Gal}\beta 1 \rightarrow 4(\text{Fuc}\alpha 1 \rightarrow 3)\text{GlcNAc}$ (2,3 sialyl Le^x) are also formed. Some of these antigen structures have been noticed as tumor markers.

***O*-Glycans**

O-Glycans with reducing terminal *N*-acetylgalactosamine residues, which are limited to serine and threonine residues, are found in mucinous glycoproteins. The glycans are easily released from the peptide moiety by reductive β -elimination in alkaline borohydride solution. *O*-Glycans can be categorized into at least four groups according to their core structures: $\text{Gal}\beta 1 \rightarrow 3\text{GalNAc}$ (core 1), $\text{GlcNAc}\beta 1 \rightarrow 6(\text{Gal}\beta 1 \rightarrow 3)\text{GalNAc}$ (core

2). GlcNAc β 1 \rightarrow 3GalNAc (core 3), and GlcNAc β 1 \rightarrow 6(Gal β 1 \rightarrow 3)GalNAc β 1 \rightarrow 3GalNAc (core 4). Those core structures can be elongated by the stepwise addition of galactose and *N*-acetylglucosamine residues. The structural variation formed on the Gal β 1 \rightarrow 4GlcNAc and Gal β 1 \rightarrow 3GlcNAc groups of *O*-glycans is quite similar to that found in the outer chain moieties of *N*-glycans (64)

In the process of terminal glycosylation of complex-type glycans, sugar residues are sequentially added from nucleotide sugars to acceptor substrates. Glycosyltransferases catalyzing these reactions have strict specificities for donor and acceptor substrates. Competition also occurs between glycosyltransferases which add different sugars to a common acceptor substrate.

In glycosyltransferase studies, it is very difficult to isolate enough natural oligosaccharide and also time-consuming to synthesize complicated glycans as substrate molecules. It was found that fragments of complex oligosaccharides possess biological activity sufficient to study glycosyltransferase activities (65).

1.12 REFERENCES

- (1) Tiselius, A. *Transaction of the Faraday Society* **1937**, 33, 524-531.
- (2) Hjerten, S. *Chromatography Review* **1967**, 9, 122-219.
- (3) Virtanen, R. *Acta Polytech. Scand.* **1974**, 123, 1-67.
- (4) Mikkers, F. E. P.; Everaerts, F. M.; Verheggen, Th. P. E. M. *J. Chromatogr.* **1979**, 169, 11-20.
- (5) Jorgenson, J. W.; Lukacs, K. D. *Anal. Chem.* **1981**, 53, 1298-1302.
- (6) Jorgenson, J. W.; Lukacs, K. D. *Science* **1983**, 222, 266-272.
- (7) Edstrom, J. E. *Nature* **1953**, 172, 809.
- (8) Hjerten, S. *J. Chromatogr.* **1983**, 270, 1-6
- (9) Cohen, A. and Karger, B. L. *J. Chromatogr.* **1987**, 397, 409-417.
- (10) Cohen, A. S.; Najarian, D. R.; Paulus, A.; Guttman, A.; Smith, J. A.; Karger, B. L. *Proc. Natl. Acad. Sci. U.S.A* **1988**, 85, 9660-9663.
- (11) Swerdlow, H.; Zhang, J. Z.; Chen, D.Y.; Harke, H. R.; Grey, R.; Wu, S. and Dovichi, N. J. *Anal. Chem.* **1991**, 63, 2835-2841.
- (12) Chen, D. Y.; Harke, H. R.; Dovichi, N. J. *Nucleic Acids Research* **1992**, 20, 4873-4880.
- (13) Terabe, S.; Otsuka, K.; Ichikawa, K.; Tsuchiya, A. and Ando, T. *Anal. Chem.* **1984**, 56, 111-113.
- (14) Ewing, A. G.; Wallingford, R. A. and Olefirowicz, T. M. *Anal. Chem.* **1989**, 61(4), 292A-303A.
- (15) Kuhr, W. G. *Capillary Electrophoresis: Theory and Practice*, (Patrick Camilleri, Eds), CRC Press, Boca Raton, **1993**, pp.79, pp. 65-116.
- (16) Stevens, T. S.; Cortes, H. J. *Anal. Chem.* **1983**, 55, 1365-70.
- (17) Hirokawa, T.; Tsuyoshi, T. and Kiso, Y. *J. Chromatogr.* **1987**, 408, 27.
- (18) Terabe, S. *Micellar Electrokinetic Chromatography*, Beckman Instruments, Inc., CA, pp. 4-19, 20-37.

- (19) Otsuka, K.; Terabe, S. and Ando, T. *J. Chromatogr.* **1985**, 332, 219-226.
- (20) Foley, J. P. *Anal. Chem.* **1990**, 62, 1302-1308.
- (21) Sepaniak, M. J. and Cole, R. O. *Anal. Chem.* **1987**, 59, 472-476.
- (22) Khaledi, M. G.; Smith, S. C. and Strasters, J. K. *Anal. Chem.* **1991**, 63, 1820-1830.
- (23) Waldron, K. C. and Dovichi, N. J. *Anal. Chem.* **1992**, 64, 1396-1399.
- (24) Zhao, J. Y.; Chen, D. Y. and Dovichi, N. J. *J. Chromatogr.* **1992**, 608, 117-120.
- (25) Zhao, J. Y.; Diedrich, P.; Zhang, Y.; Hindsgaul, O. and Dovichi, N. J. *J. Chromatogr.* **1994**, 657, 307-313.
- (26) Zhang, Y.; Le, X.; Dovichi, N. J.; Compston, C. A.; Palcic, M. M.; Diedrich, P. and Hindsgaul, O. *Anal. Biochem.* **1995**, 227, 368-376.
- (27) Zhang, Y.; Arriaga, E.; Diedrich, P.; Hindsgaul, O.; Dovichi, N. J. *J. Chromatogr. A.* **1995**, 716, 221-229.
- (28) Dossi, G.; Celentano, F.; Gianazza, E. and Righetti, P. G. *J. Biochem. Biophys. Methods.* **1983**, 8, 123-142.
- (29) Terabe, S.; Katsura, T.; Okada, Y.; Ishihama, Y. and Otsuka, K. *J. Microcol. Sep.* **1993**, 5, 23.
- (30) Huang, X.; Coleman, W. F. and Zare, R. N. *J. Chromatogr.* **1989**, 480, 95-110.
- (31) Jorgenson, J. W. and Lukacs, K. D. *Science* **1983**, 222, 266-272.
- (32) Huang, X.; Gordon, M. J. and Zare, R. N. *Anal. Chem.* **1988**, 60, 375-377.
- (33) Honda, S.; Iwase, S. and Fujiwara, S. *J. Chromatogr.* **1987**, 404, 313-320.
- (34) Kuhr, W. G. and Yeung, E. S. *Anal. Chem.* **1988**, 60, 2642-2644.
- (35) Gilman, S. D. and Ewing, A. G. *Anal. Chem.* **1995**, 67, 58-64.
- (36) Lim, H. B.; Lee, J. J.; Lee, K. J. *Electrophoresis*, **1995**, 16(4), 674-8.
- (37) Monnig, C. A. and Kennedy, R. T. *Anal. Chem.* **1994**, 66, 280R-314R.
- (38) Cheng, Y. F. and Dovichi, N. J. *Science* **1988**, 242, 562-564.
- (39) Chen, D. Y. and Dovichi, N. J. *J. Chromatogr. B* **1994**, 657, 265-269.

- (40) Dadoo, R.; Colon, L. A. and Zare, R. N. L. *High Resolut. Chromatogr.* **1992**, 15, 133-135.
- (41) Ruberto, M. A. and Grayeski, M. L. *Anal. Chem.* **1992**, 64, 2758-2762.
- (42) Zhao, J-Y.; Labbe, J. and Dovichi, N. J. *J. Microcol. Sep.* **1993**, 5, 331-339.
- (43) Lu, W. and Cassidy, R. M. *Anal. Chem.*, **1993**, 65, 2878-2881.
- (44) Garcia, F. and Henion, J. D. *Anal. Chem.* **1992**, 64, 985-990.
- (45) Keough, T.; Takigiku, R.; Lacey, M. P. and Purdon, M. *Anal. Chem.* **1992**, 64, 1594-600.
- (46) Gassman, E.; Kuo J. and Zare, R. *Science* **1985**, 230, 813-815.
- (47) Pentoney, S.; Huang, X.; Burgi, D. and Zare, R. *Anal. Chem.*, **1988**, 60, 2625-2630.
- (48) Hernandez, L.; Escalona, J.; Joshi, N. and Guzman, N. *J. Chromatogr.* **1991**, 559, 183-196.
- (49) Nickerson, B. and Jorgenson, J. *J. Chromatogr.*, **1989**, 480, 157-168.
- (50) Liu, J.; Shirotu, O. and Novotny, M. *Anal. Chem.*, **1991**, 63, 413-417.
- (51) Parker, C.A. *Photoluminescence of Solutions*. New York: Elsevier, **1968**, Section 5C.
- (52) Wu, S. and Dovichi, N. J. *J. Chromatogr.* **1989**, 480, 141-155.
- (53) Liu, J.; Shiota, O.; Wiesler, D. and Novotny, M. *Proc. Natl. Acad. Sci.* **1991**, 88, 2302-2306.
- (54) Dovichi, N. J. in *Capillary Electrophoresis: Theory and Practice* (P. Camilleri, Eds.), CRC Press, Inc. **1993**, pp. 52-64.
- (55) Nguyen, D.C.; Keller, R.A.; Jett, J.H. and Martin, J.C. *Anal. Chem.* **1987**, 59, 2158-2160.
- (56) Melamed, M.R.; Mullaney, P.F. and L. Mendelsohn, M. *Flow Cytometry and Sorting*. New York: Wiley, **1979**.
- (57) Pinkel, D. *Anal. Chem.* **1982**, 54, 503A-508A.

- (58) Dovichi, N. J.; Martin, J. C.; Jett, J. H. and Keller, R. A. *Science*. **1983**, 219, 845-847.
- (59) Welraffen, G. E. and Blatz, L. A. *J. Chem. Phys.*, **1973**, 59, 2646-2650.
- (60) Haugland, R. P. *Molecular Probes: Handbook of Fluorescent Probes and Research Chemicals*. Eds by K. D. Larison. Molecular Probes, Inc., Eugene, OR. **1994**.
- (61) Knoll, J. E. *J. Chromatogr. Science* **1985**, 23, 422-424.
- (62) Hughes, R.C. *Outline Studies in biology. Glycoproteins*. Chapman and Hall, USA. **1983**, pp. 7-10, pp.15-35.
- (63) Kleene, R. and Berger, E. G. *Biochimica et Biophysica Acta* **1993**, 1154, 283-325.
- (64) Kobata, A. and Takasaki, S. *Cell Surface Carbohydrates and Cell Development*. (Eds by Minoru Fukuda). CRC Press. **1992**, pp. 1-25.
- (65) Palcic, M. M. *Methods in Enzymology*. **1994**, 230, 300-319.

CHAPTER 2

NANOMOLAR DETERMINATION OF AMINATED SUGARS BY CAPILLARY ELECTROPHORESIS

*A version of this chapter has been published.

Zhang, Y., Arriaga, E., Diedrich, P., Hindsgaul, O., Dovichi, N. *J. Chromatogr. A*, 1995, **716**, 221-229.

2.1 INTRODUCTION

Some oligosaccharides are ligands that mediate specific biological recognition. Generally, oligosaccharides attached to proteins or lipids play a major role in cell-cell and cell-molecule recognition events. The structural complexity of carbohydrates complicates the establishment of a relationship between their structures and their biological functions. Determination of the structure of the oligosaccharide moieties in biomolecules such as glycoproteins, proteoglycans, and polysaccharides requires a technology that allows identification of the individual monosaccharides and determines how they are linked to each other. Selective enzymatic cleavage of complex carbohydrates can be used to determine how monosaccharides are interconnected to form carbohydrates. This requires techniques to separate monomers and isomers that are involved. In addition, a separation/identification technique for monosaccharides that is compatible with the enzymatic cleavage is required.

Analytical methods for monosaccharides, such as high-performance liquid chromatography, gas chromatography, and thin layer chromatography (1) usually require large amounts of samples. Ideally, determination of carbohydrate structure requires the handling and analysis of samples in very small volumes. Small volume analysis is impractical for general carbohydrate analytical methods, eg, methylation analysis and enzymatic degradation in association with nuclear magnetic resonance spectroscopy (2). Because carbohydrates have very low UV absorbance, directed UV absorbance detection is limited to the nanomole (10^{-9} mole) range (3-6). For example, if complex carbohydrates or monosaccharides from a single cell are to be analyzed, a technique that provides high sensitivity and low detection limits such as capillary electrophoresis with laser-induced fluorescence detection (CE-LIF) is required.

CE-LIF is a useful technique for trace analysis of biological molecules such as DNA, proteins, peptides, and carbohydrates (7-8). However, CE-LIF analyses of oligosaccharides encounter more obstacles than analyses of other biomolecules since

oligosaccharides do not have a net charge (except for acidic oligosaccharides). Thus, direct separation of oligosaccharides by CE is not possible. The use of borate as a complexing agent in the separation buffer facilitates the formation of carbohydrate-borate complexes which are charged; thus, electrophoretic separation is possible (3, 9-17).

Another difficulty in analyzing carbohydrates by CE-LIF is the lack of a native fluorophore in the molecule, making it necessary to attach a fluorescent tag to the molecule. Some procedures for fluorescent labeling of oligosaccharides use direct attachment of an amine-containing fluorescent tag to the reducing hydroxyl of the oligosaccharide. Reagents such as 2-aminopyridine (AP), 5-aminonaphthalene-2-sulfonate (ANS), and 7-amino-1,3-naphthalenedisulfonate (ANTS) can be conjugated to the anomeric carbon of the oligosaccharide via reductive amination using sodium cyanoborohydride (18-21). ANTS is an attractive reagent since it fluoresces at longer wavelengths than AP and ANS and it provides the labeled oligosaccharide with three negative charges that contribute to labeled-oligosaccharide electrophoretic mobility. AP and ANS provide no and one negative charge to the labeled oligosaccharide, respectively. Other procedures require reduction of the hydroxyl group at the anomeric carbon to form a primary amine, followed by labeling with an amine-reactive probe. Liu *et al.* added a primary amino group to the anomeric carbon by reacting the oligosaccharide in the presence of sodium cyanoborohydride and excess of ammonium (22).

In general, fluorescent labeling reactions for oligosaccharides require extremely high concentrations of the oligosaccharide and the labeling reagent. Zhao *et al.*, despite attaining the lowest limit of detection for an aminated sugar monomer ever reported (60 molecules), still needed to use 1 mM 5-carboxytetramethylrhodamine succinimidyl ester to label a solution that was 20 mM in aminated sugar (17). Since the level of some carbohydrates found in biological samples is submicromolar, the labeling scheme should be effective at those levels. In addition, high concentrations of fluorescent labeling reagents (10^{-3} to 10^{-4} M CBQCA) can result in overlapping reagent peaks in the

electropherograms. Thus, techniques that allow labeling of carbohydrates at submicromolar levels and do not result in electropherograms containing reagent peaks are required to handle many biological samples.

Novotny *et al.* introduced the use of 3-(p-carboxybenzoyl)quinoline-2-carboxyaldehyde (CBQCA), a fluorogenic reagent to label monosaccharides as well as polysaccharides that have been previously aminated (22,23,24). This approach offers the advantage that the reagent does not fluoresce unless it reacts with an amine group. Thus, electropherograms are free of reagent peaks that in other cases may overlap with the oligosaccharide derivative peaks. Using CBQCA for labeling aminated sugars, excitation with the 457-nm argon-ion laser line, and on-column detection, Liu *et al.* have achieved a limit of detection (LOD) in the subattomole range (12).

In this chapter, we studied CBQCA labeling of monosaccharides and showed labeling capabilities down to 10^{-9} M 1-glucosamine. The CBQCA derivative of 1-glucosamine is then detected by CE-LIF. The highly sensitive detection scheme is based on selection of an alternative excitation line and prevention of the water Raman scattering from reaching the detector. CE separation of five aminated monosaccharides based on formation of charged complexes with borate and phenyl boronate is presented to illustrate the compatibilities of the labeling technique. CE separation and LIF detection. Figure 2.1 shows the structure of CBQCA. The maximum absorption of the CBQ-glycine derivative is 466 nm and the maximum emission wavelength is 554 nm in methanol.

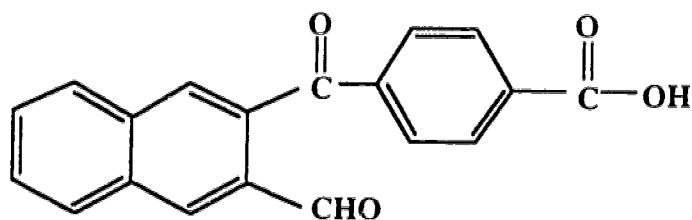


Figure 2.1 Structure of CBQCA, 3-(p-carboxybenzoyl)quinoline-2-carboxyaldehyde.

2.2 EXPERIMENTAL SECTION

2.2.1 Instrumentation

The CE-LIF instrument is described in Figure 2.2. Non-coated capillaries (180 μm o.d., 50 μm i.d. or 142 μm o.d., 10 μm i.d.) were used for the separation. A CZE1000R high voltage power supply (Spellman, Plainview, NY) with maximum output of 29 kV provided positive high voltage at the injection end (cathodic mode). Usually, CBQCA derivatives of aminated sugars (maximum excitation at 456 nm) are excited with the 442-nm He-Cd laser line or the 457-nm argon-ion laser line and the emission detected at 552 nm (12,13). In our experiment, fluorescence excitation was provided by the 488-nm argon-ion line from a multiple-wavelength argon-ion laser (INNOVA 99-4, Coherent, Palo Alto, CA) set at 30 mW. The laser power was actually 4.4 mW after passing through a neutral density filter. The laser beam was focused by a 6.3 \times microscope objective (Melles Griot, Nepean) about 20 μm from the tip of the capillary. The fluorescence was collected at 90° from the direction of excitation by a 60 \times (N. A. 0.70) microscope objective. A dichroic beamsplitter, 590DRLP $\tilde{\omega}$ 45 (Omega Optical, Brattleboro, VT) reflected light with wavelengths shorter than 590 nm (reflected channel) and transmitted light with wavelengths longer than 590 nm (transmitted channel). Reflected light was sent through a 535DF35 bandpass filter (transmission range 517.5 to 552.5 nm; Omega Optical) before reaching the reflected channel photomultiplier tube R1477 (Hamamatsu). For the transmitted channel, light was transmitted through a 635DF55 bandpass filter (transmission range 607.5 to 662.5 nm; Omega Optical) before reaching the R1477 photomultiplier tube. The PMT outputs were digitized using a NB-MIO-16X-18 input/output board (National Instruments, Austin, TX). The digitized signals were summed by an Igor program to obtain a combined signal that includes fluorescence in the 517.5-552.5 nm and 607.5-662.5 nm ranges and excludes light from 552.5 to 607.5 nm. Since the water Raman band is in the range 577-596 nm, it is effectively blocked by this detector configuration, resulting in lower background and lower limits of detection.

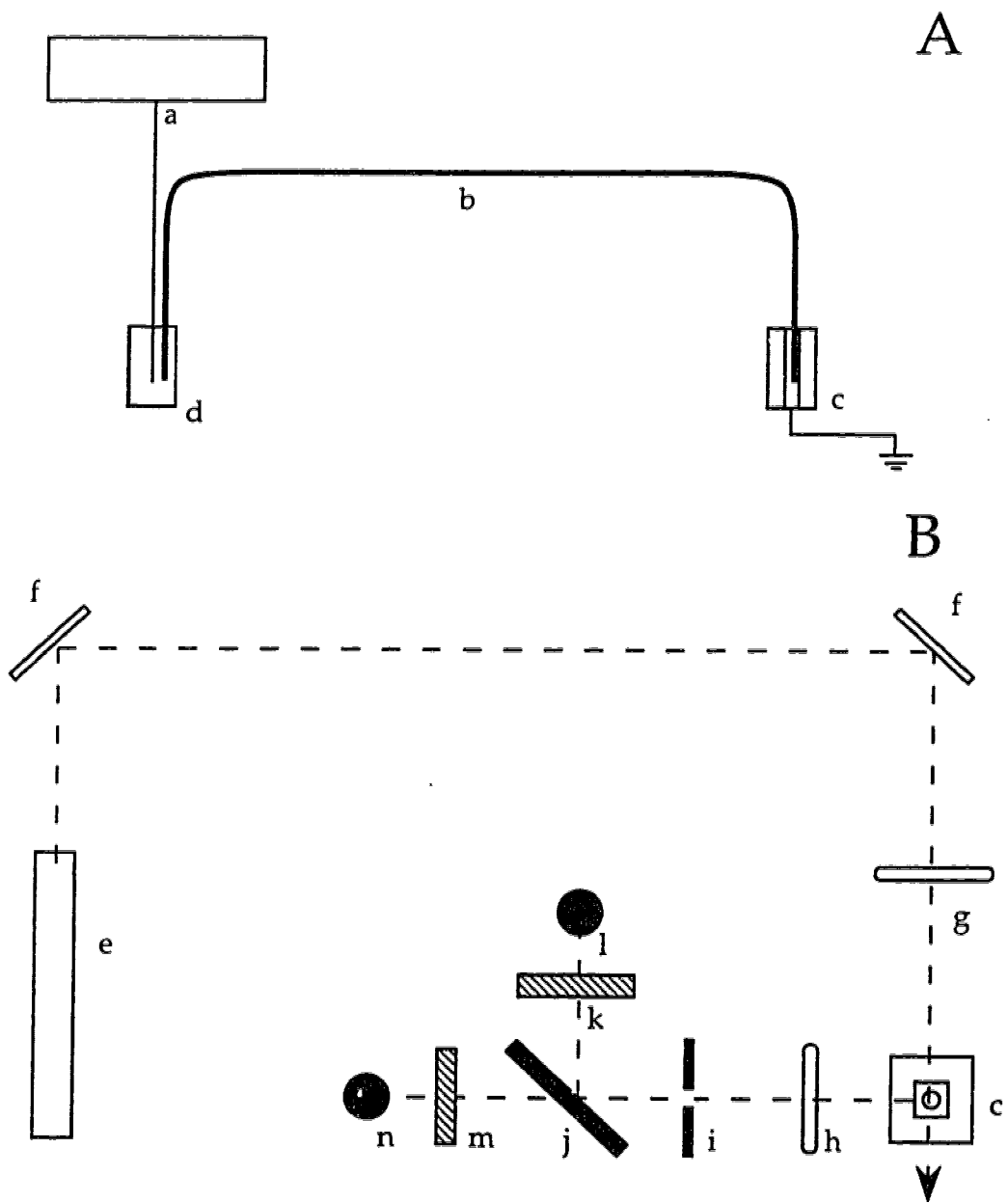


Figure 2.2 Schematic diagram of capillary electrophoresis system and detector. (A) Electrophoresis system: (a) high-voltage power supply, (d) sample or running buffer vial, (b) capillary, (c) virtual grounded sheath flow cuvette. (B) Detector: (e) multi-wavelength argon-ion laser, (f) mirrors, (g) focusing objective, (c) sheath flow cuvette, (h) collecting objective, (i) adjustable slit, (j) dichroic beam splitter@590 nm, (k) 535DF45 interference filter for reflected channel, (m) 630DF55 interference filter for transmitted channel, (l,n) photomultiplier tubes.

2.2.2 Preparation of Sugar Derivatives

Glucose, galactose, mannose and fucose were reductively aminated to produce their 1-amino-1-deoxy-D-itol. 2-amino-2-deoxy-D-glucitol was synthesized by reduction of glucosamine. Their synthesis has been described elsewhere (17). In this chapter the sugar monomers will be referred to as 1-glucosamine, 1-galactosamine, 1-mannosamine, 1-fucosamine, and 2-glucosamine. Figure 2.3 shows five monomer structures.

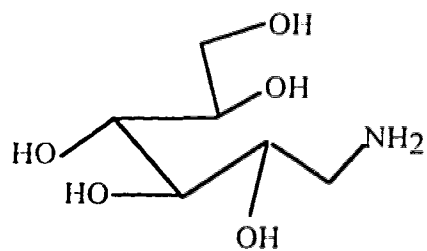
2.2.3 CBQCA Labeling Reaction

CBQ

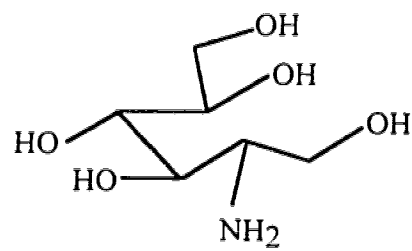
CBQ(3-(p-carboxybenzoyl)quinoline-2-carboxyaldehyde or CBQCA) reacts specifically with primary amines to form charged conjugates that can be analyzed by electrophoretic or chromatographic methods. CBQ also reacts with hydrophilic peptides and amino sugars.

Stock Solution

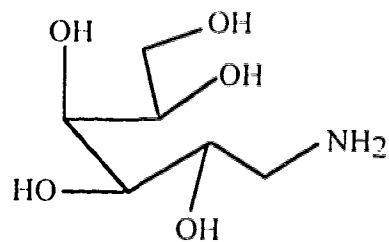
Stock solutions (1.0×10^{-2} M) of synthetic aminosugar derivatives (provided by Dr. Ole Hindsgaul) were prepared in 0.185 M sodium bicarbonate (BDH) and stored at 4 °C. Dilutions for labeling reactions were done in HPLC-grade water (Fisher Scientific). Dilutions for electrokinetic injections were done in 10 mM sodium borate (Fisher Scientific) and 10 mM sodium dodecyl sulfate (BDH) buffer (BS buffer). A 10 mM stock solution of CBQCA (Molecular Probes) was prepared in methanol and stored at -20 °C. Potassium cyanide (Molecular Probes) was dissolved in HPLC-grade water to obtain a 0.20 M stock solution and stored at 4 °C.



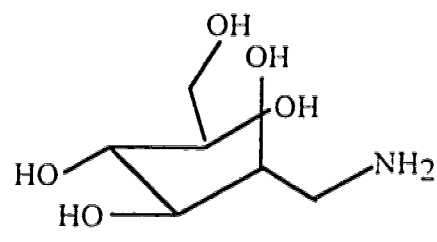
1-amino-1-deoxy-D-glucitol
(1-glucosamine)



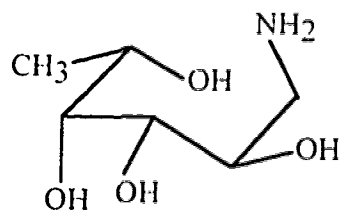
2-amino-2-deoxy-D-glucitol
(2-glucosamine)



1-amino-1-deoxy-D-galactitol
(1-galactosamine)



1-amino-1-deoxy-D-mannitol
(1-mannosamine)



1-amino-1-deoxy-L-fucitol
1-fucosamine

Figure 2.3 Structures of five aminated monosaccharides.

Labeling Reactions

The labeling reaction was performed by mixing 5-10 μL of a dilution of the aminated sugar in HPLC-grade water, 10 μL of the CBQCA stock solution, and an aliquot of methanol (or phosphate buffer) to make up 23 μL . Then 2 μL of 50 mM cyanide was added to the mixture. Finally, 25 μL of the reaction mixture contained 4 mM CBQCA, 4 mM cyanide, and 10^{-4} to 10^{-9} M aminated sugar. After vigorously shaking the mixture using vortex shaker, it was incubated in the dark for 2 to 10 hours. The mixture was shaken every half hour. A blank was prepared by replacing the aminated sugar aliquot with water. The reaction mixtures could be stored at $-20\text{ }^{\circ}\text{C}$ for one week without noticeable degradation.

The effect of pH on the labeling reaction was assayed by using 100 mM phosphate buffer instead of methanol to make the reaction volume 25 μL . The reaction mixture contained 4 mM CBQCA and 2 mM cyanide and the reaction was carried out for 4 hours.

2.2.4 Separation

Prior to electrokinetic injection, CBQCA derivatives of aminated sugars were diluted to 2.0×10^{-7} M in BS buffer. This assumes that the yield of the labeling reaction was 100%. For concentrations below or equal to 2.0×10^{-7} M, no dilution was performed prior to injection.

Separation buffers were prepared from stock solutions of 0.556 M sodium dodecyl sulfate, 0.20 M sodium phosphate dibasic acid (Fisher), 0.20 M sodium borate, and 0.10 M phenyl boronic acid (Sigma, Saint Louis, MO). The pH was adjusted with 1.1 M sodium hydroxide (BDH). Although several buffers were investigated for use in the separation, the buffer selected for the separation contained 50 mM phenyl boronic acid, 20 mM sodium phosphate and 20 mM borate (pH 9).

2.3 RESULTS AND DISCUSSION

2.3.1 Selection of Labeling Reaction Conditions

The labeling reaction (see Figure 2.4) was optimized by using 1-glucosamine. The conditions required to maximize the reaction yield depended on the concentration of 1-glucosamine. For samples with high concentrations of 1-glucosamine (e.g. 10^{-4} M), the labeling reaction gave its highest yield when 6 mM CBQCA and 8 mM cyanide were used. On the other hand, samples with low 1-glucosamine concentrations (e.g., 10^{-9} M) could not be detected by CE-LIF when these concentrations of CBQCA and cyanide were used. Samples with low concentrations of 1-glucosamine were labeled by 4 mM CBQCA and 2 to 4 mM potassium cyanide in methanol (data not shown here).

Figure 2.5 presents the electropherograms of CBQCA diluted from 10 mM stock solution in methanol by the 10 mM borate and 10 mM SDS (pH 9). Only two small peaks were detected even with high concentration of 10^{-4} M CBQ dye because it was a fluorogenic reagent.

Figure 2.6 shows the electropherogram of a solution made from a 200 times dilution from 10^{-4} M 1-glucosamine labeled by 4 mM CBQ and 2 mM KCN at pH 7.1 for 4 h and at 50 °C. The capillary is 49.6 cm long and 10 μ m inner diameter. The sharp peak represents less than 5×10^{-7} M CBQ labeled glucosamine.

pH effect

The pH of the labeling reaction has been known to affect the efficiency of the CBQCA labeling reaction of different amine-containing molecules. Amino acids and small peptides give their highest reaction yield when the labeling reaction is carried out at pH 8.5 to 9.5, while reaction yields for larger peptides are pH insensitive (23) and sugar reaction yields are highest at pH 7.0 (13).

The yield for a 5 h labeling reaction of 10^{-4} M 1-glucosamine with CBQCA varied with pH. For pH's 7.1, 8.0, and 9.0 (Table 2.1) the relative yield was 0.7 ± 0.1 , 1.0 ± 0.1 ,

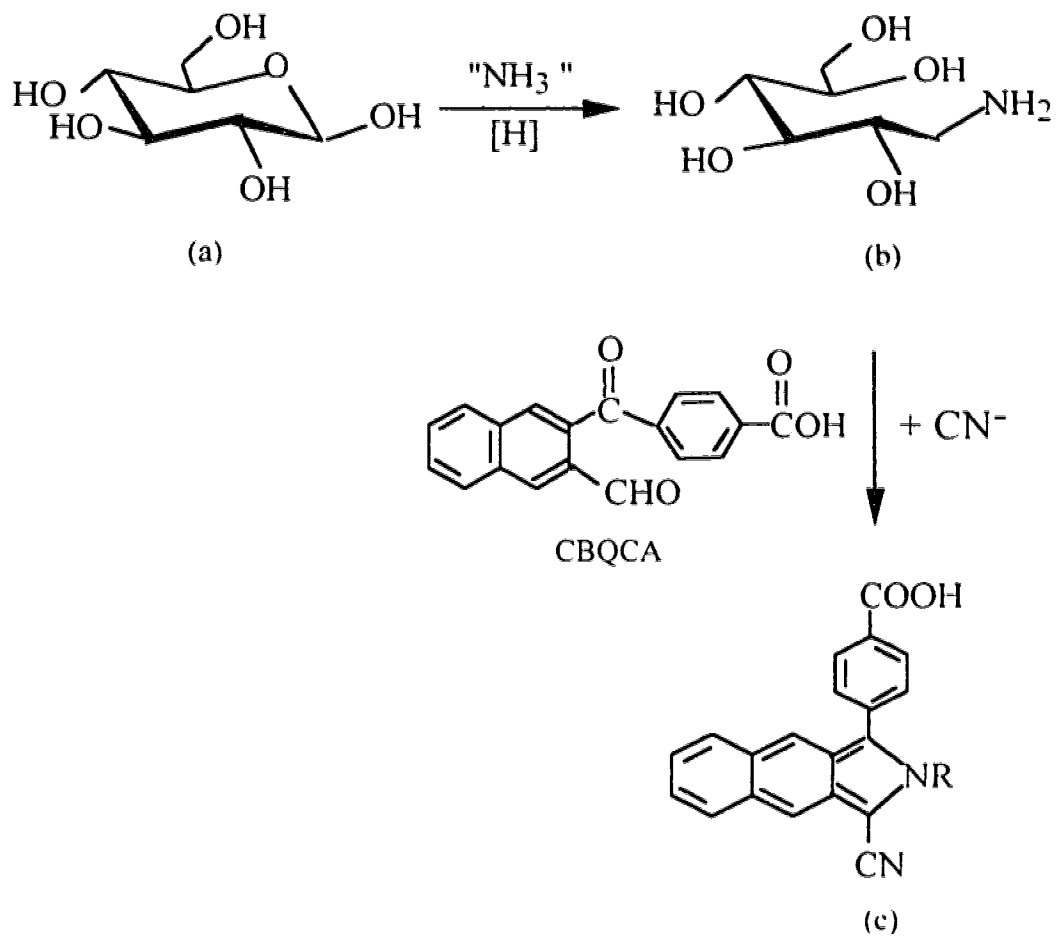


Figure 2.4 Glucose (a) was reduced to 1-amino-1-deoxy-glucitol (1-glucosamine). (b) 1-glucosamine was reacted with CBQCA and potassium cyanide to form a fluorescence derivative product (c).

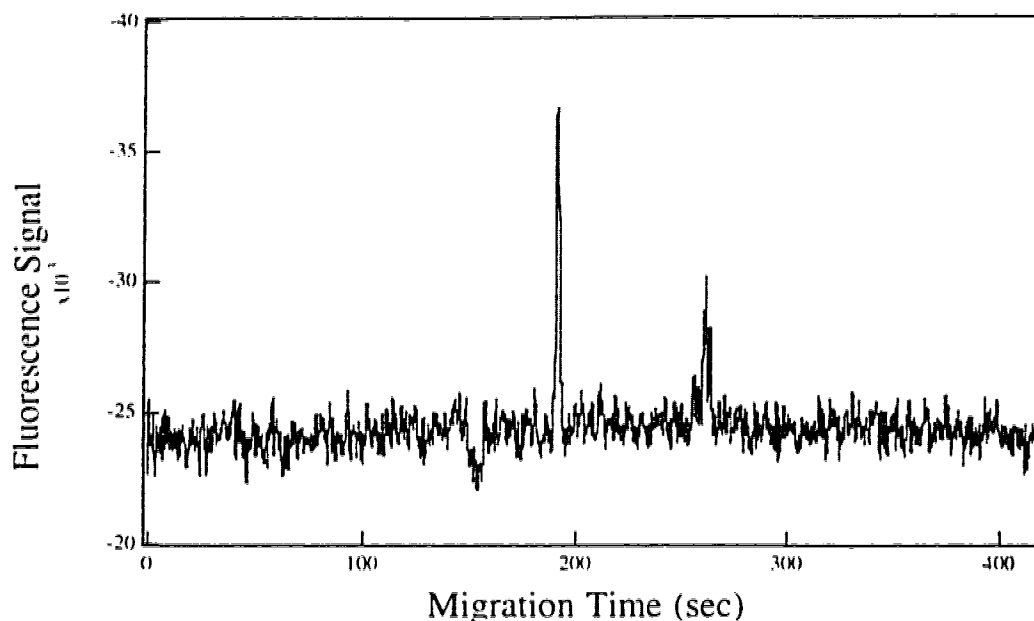


Figure 2.5 Electropherogram of 10^{-4} M CBQCA.

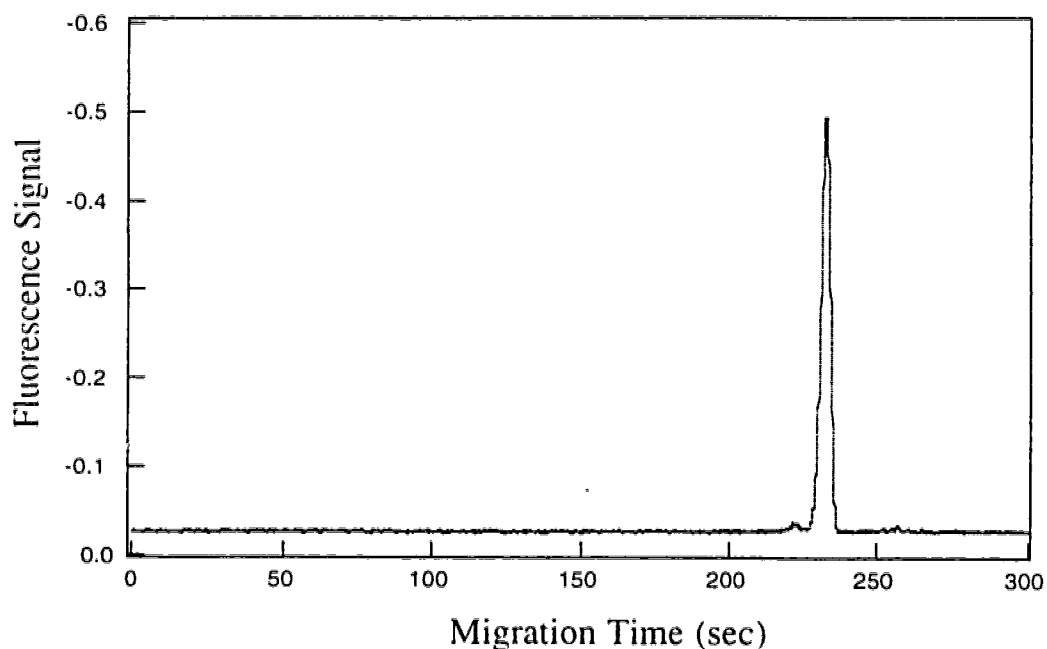


Figure 2.6 Electropherogram of CBQCA labeled glucosamine. 10^{-4} M glucosamine was reacted with 4 mM CBQCA and 2 mM KCN for 4 h at 50 °C. The CBQ labeled glucosamine injected was less than 5×10^{-7} M. The Argon-ion laser power is 4.4 mW. Separation: 10 mM borate-10 mM SDS, pH 9.3 buffer, 400 V/cm; 10 μ m i.d., 49.6 cm long capillary. Sample was injected at 2500 v for 5 sec.

and 0.95 ± 0.1 . If no phosphate buffer was used to regulate the pH in the sample, the reaction yield was about 40 times lower. Despite the low reaction yield when the reaction mixture lacks phosphate buffer, samples with low concentrations of 1-glucosamine (e.g. 10^{-9} M) were labeled without addition of such buffer. Since samples containing low concentrations of 1-glucosamine cannot be diluted prior to injection, the presence of phosphate buffer results in unstable baseline around the elution time of the CBQCA derivative of 1-glucosamine as well as tailing of the peak. To compensate for the slow kinetics when no phosphate buffer is used, the reaction time was extended to 10 h.

Table 2.1 Effect of pH on CBQ-Glc-NH₂ derivative signal

Buffer	Peak height (average \pm S.D.)
phosphate, pH 9	0.38 ± 0.08
phosphate, pH 8	0.40 ± 0.07
phosphate, pH 7	0.28 ± 0.002
methanol	0.018 ± 0.005

2.3.2 Concentration Limit for Labeling of 1-Glucosamine

10^{-9} M 1-glucosamine Labeled by CBQCA

Figure 2.7A shows an electropherogram of a sample containing 1.0×10^{-9} M 1-glucosamine that has been labeled with CBQCA and detected by CE-LIF. The capillary is 41.5 cm long and 50 μ m i.d. The blank peaks attributed to secondary reactions between CBQCA and cyanide (Figure 2.7B) are much bigger than the peak of the CBQCA derivative of 1-glucosamine. It has been observed that cyanide can induce condensation of two aromatic aldehydes to form an α -hydroxyketone; many condensation products are possible (25). Formation of cyanohydrins is another possible explanation for the secondary

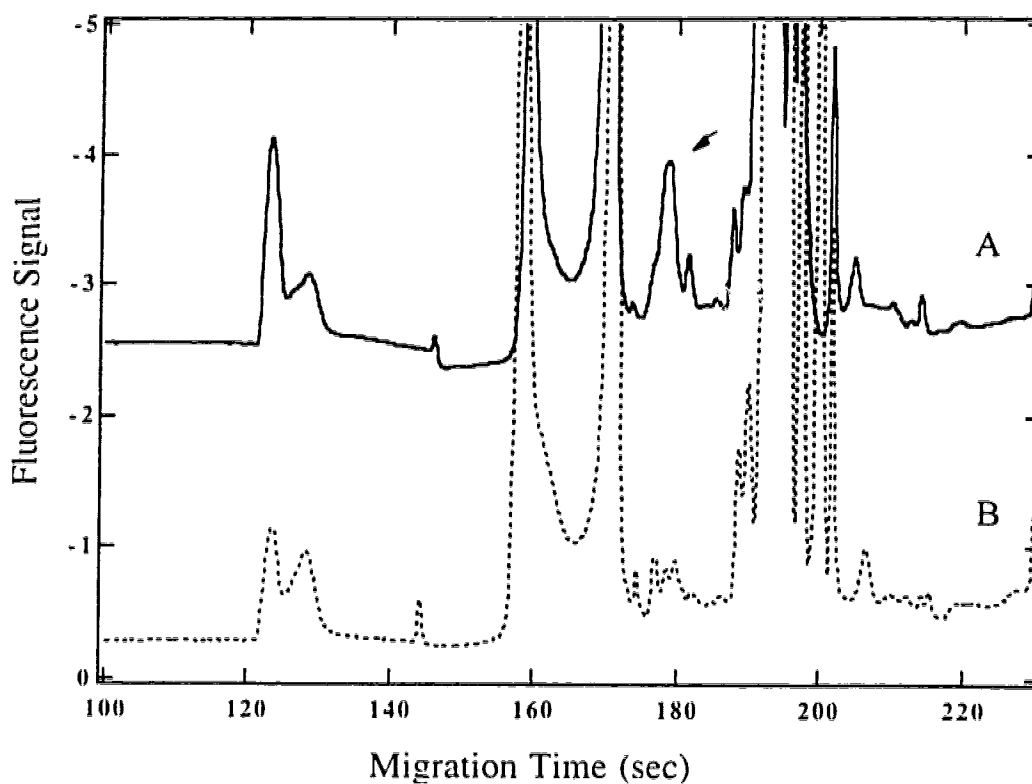


Figure 2.7 Electropherograms of fluorescently labeled samples containing (A) 10^{-9} M 1-glucosamine and (B) a reaction blank. Reaction conditions: (A) 10^{-9} M 1-glucosamine -4 mM CBQCA- 4 mM KCN for 10 h at room temperature. (B) 4 mM CBQCA- 4 mM KCN for 10 h at room temperature. Separation conditions: 41.5 cm x 50 μ m I.D. capillary; running buffer 10 mM borate -10 mM SDS; 400 v/cm. Injection conditions: 2500 v for 5 s. The Argon-ion laser power is 30 mW.

peaks that appear in the electropherograms (26). However, the peak of CBQCA derivative elutes in a region (170 to 190 seconds) where the electropherogram baseline is relatively flat. If the concentrations of CBQCA or cyanide used in the labeling reaction are higher than 4 mM, the baseline is quite irregular in the elution region of the CBQCA derivative, making its detection impossible. Another fluorogenic reagent for labeling primary amine with similar structure as CBQCA but has different side group could be a good alternative to obtain less side reaction electropherogram (27).

Labeling Reaction Concentrations

Samples containing 1.0×10^{-4} to 1.0×10^{-9} M 1-glucosamine were labeled using 4 mM CBQCA and 4 mM cyanide since these reagent concentrations allowed the analysis of 1-glucosamine over the whole concentration range. Figure 2.8 shows a plot of signal intensity corrected for dilution versus concentration of 1-glucosamine (Data listed in Table 2.2) in the sample prior to derivatization. The lack of linearity at the low end of the concentration range is attributed to the presence of methanol in the sample buffer. As the 1-glucosamine concentration was decreased, less dilution was required prior to injection resulting in higher concentration of methanol in the injected dilution. The presence of methanol resulted in an increased local electric field during injection and a resultant increase in the amount of sample injected.

Calibration Curve

Table 2.3 lists the data of CBQCA labeled 10^{-4} M glucosamine diluted to different concentrations in running buffer. The labeling reaction was carried out at room temperature for 10 h without phosphate buffer in the reaction mixture. The calibration curve is shown in Figure 2.9. The linear range is at least three order of magnitude.

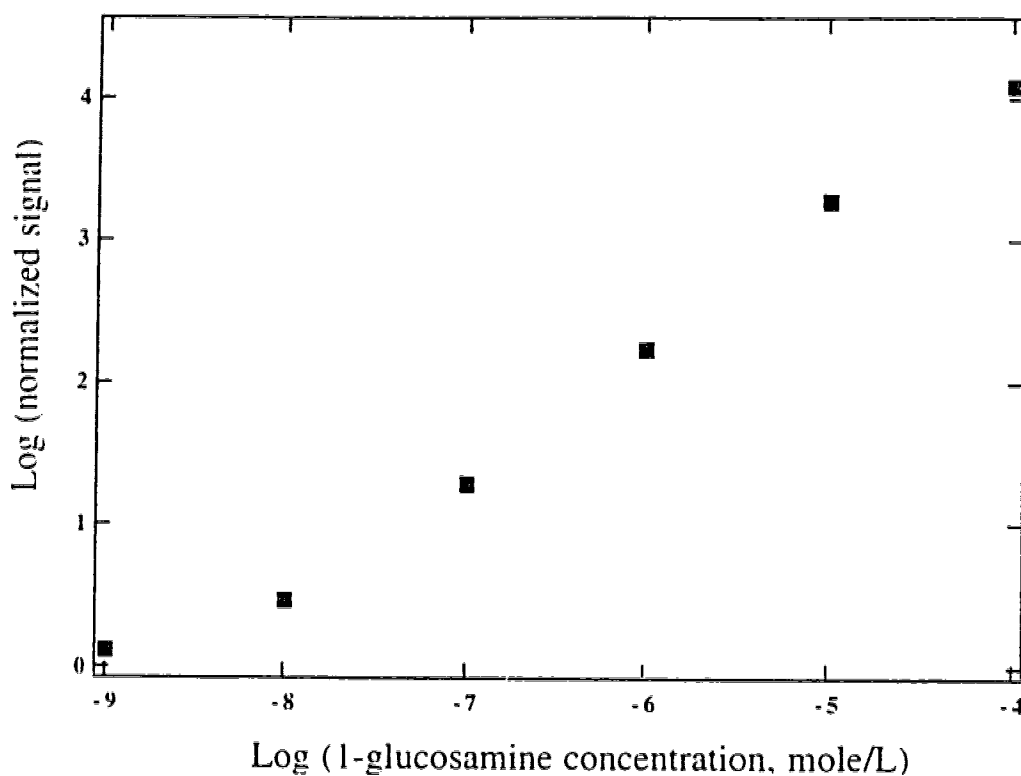


Figure 2.8 Concentration range of 1-glucosamine for an effective labeling reaction. Reaction conditions: 10^{-9} to 10^{-4} M 1-glucosamine, 4 mM CBQCA, 4 mM KCN for 5 h at room temperature. Separation conditions as in Figure 2.7. Injection conditions: prior to injection samples were diluted down to 1.0×10^{-8} M (labeled and unlabeled) 1-glucosamine except for labeling reaction samples containing 10^{-9} to 10^{-8} M 1-glucosamine.

Table 2.2 Concentration range for labeling reaction

[1-Glc-NH ₂] ^a , M	LOG [1-Glc-NH ₂]	Signal	LOG Signal*
10 ⁻⁴	-4.0	1.25	4.10
10 ⁻⁵	-5.0	1.89	3.28
10 ⁻⁶	-6.0	1.78	2.25
10 ⁻⁷	-7.0	1.94	1.29
10 ⁻⁸	-8.0	3.03	0.48
10 ⁻⁹	-9.0	1.32	0.12

^aAll samples were diluted to 10⁻⁸ M before CE analysis except 10⁻⁸ M and 10⁻⁹ M sample was injected without any dilution.

*Signal corrected by the dilution factor.

Table 2.3 Calibration curve data

[sugar], M	log ([sugar], M)	sugar peak height	Log (sugar peak height)
8.0 x 10 ⁻⁸	-7.0	9.8	0.99
2.0 x 10 ⁻⁸	-8.0	1.3	0.12
1.0 x 10 ⁻⁹	-9.0	0.13	-0.90
1.0 x 10 ⁻¹⁰	-10.0	0.013	-1.88

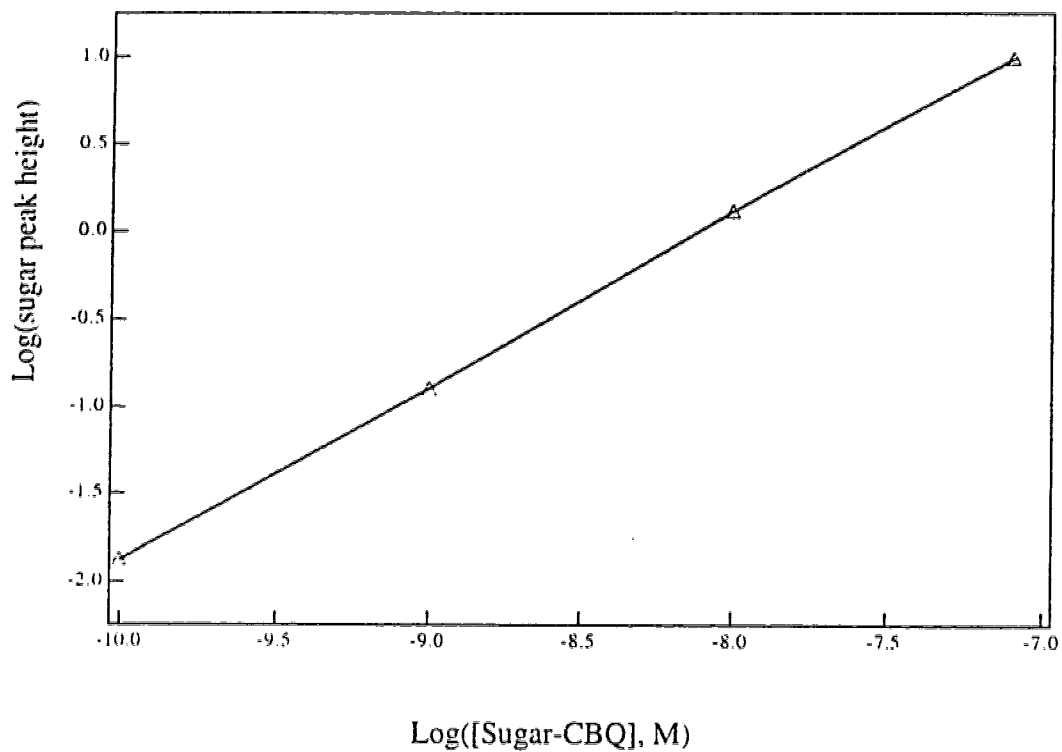


Figure 2.9 Log-Log calibration curve for CBQ labeled synthetic 1-glucosamine (Glc-NH₂).

2.3.3 The Possible Labeling Mechanism

The labeling reaction mechanism has been proposed by others (23). The reaction starts with the nucleophilic attack of cyanide on CBQCA and then the amine group is incorporated and participates in the formation of a quinoline ring: the resulting derivative has highly fluorescent properties as compared to the unreacted CBQCA reagent.

Understanding the mechanism for the labeling reaction of sugar with CBQ could suggest ways of improving the reaction yield and eliminate secondary reactions. In Figure 2.10, a mechanism is proposed for CBQ labeling reaction of glucosamine based on labeling reaction mechanisms of *o*-phthalaldehyde (OPA) and 2,3-naphthalenedicarboxaldehyde (NDA) (28-30). First, CBQ (I) and the aminated sugar react to form an imine intermediate (II). In principle, the reaction is first order with respect to CBQ and aminosugar. Second, the imine intermediate is attacked by a nucleophile, CN^- in this case. Elimination of water leads to the formation of an isoindole ring (III) responsible for the fluorescent properties of the derivative. If the reaction is considered first order with respect to CBQ, high concentrations of CBQ should increase the rate of formation of the imine intermediate, which would increase its concentration. It is found that the fluorescent signal increases with CBQ concentration up to 6mM CBQ; higher concentrations of CBQ resulted in weaker fluorescence. If the nucleophilic attack by cyanide shows first order kinetics, then the formation of the next two intermediates would be favored by increasing the concentration of cyanide. Using 8 mM CN^- the fluorescence signal reaches a plateau and higher concentrations do not improve the yield.

2.3.4 Limit of Detector. (LOD) for Labeled Sugar

The LOD (three times the standard deviation of the background) is calculated from the injected volume (31) and the total concentration of aminated sugar. The LOD for 1-glucosamine is 75 zeptomoles and 4.5×10^{-11} M 1-glucosamine (based on a labeling reaction of 10^{-4} M and diluted to 5×10^{-7} M prior to injection, Figure 2.6). This is a

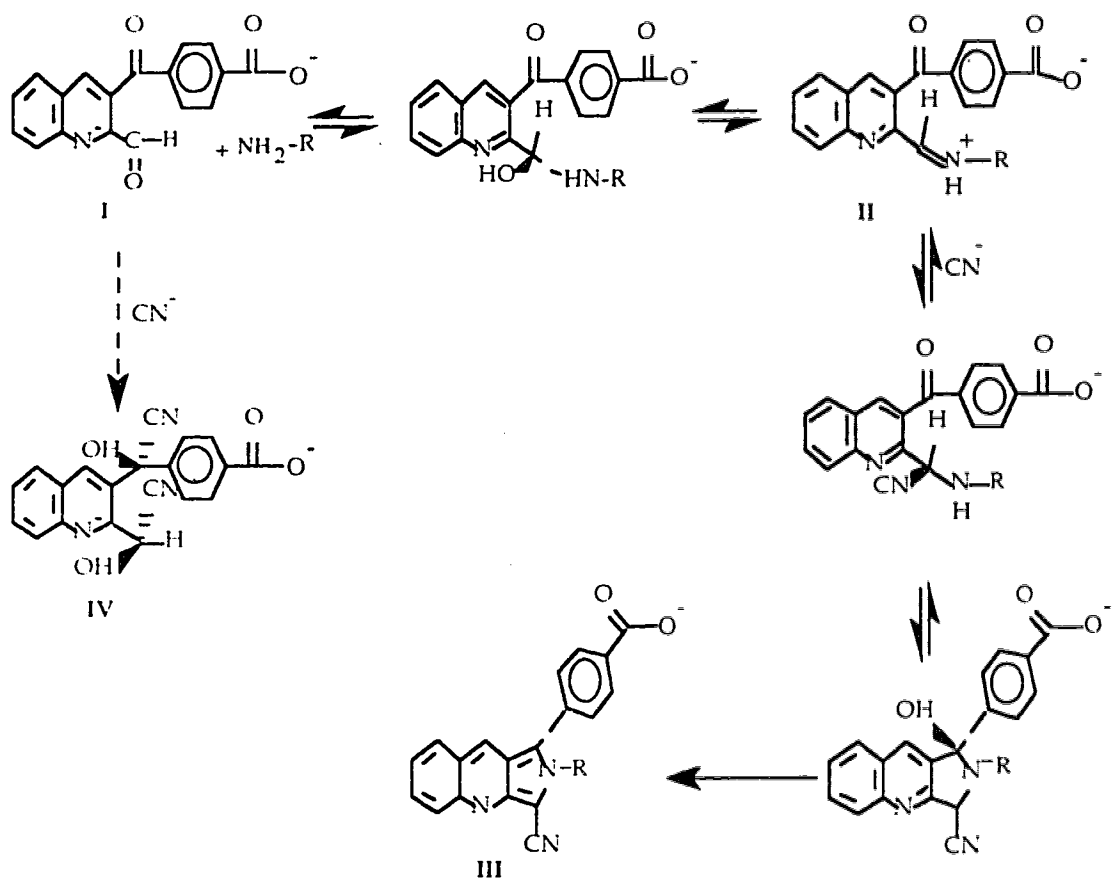


Figure 2.10 Mechanisms for CBQ labeling reaction of amino acids and CBQ direct reaction with cyanide. CBQ (**I**) forms the imine intermediate (**II**); the formation of the intermediate is favoured by slightly acidic conditions; (**II**) reacts with cyanide (basic conditions) to form the CBQ derivative (**III**). Direct reaction of CBQ with cyanide would favour the formation of a cyanohydrin (**IV**); different degrees of substitutions and orientations could be expected.

conservative estimate, since it assumes 100% labeling of the aminated sugar. This LOD is more than one order of magnitude lower than those reported by Novotny's group for the labeling of monosaccharides with CBQCA (2.3 attomole for 1-mannosamine, 1.3 attomole for 1-glucosamine, 0.5 attomole for 1-galactosamine, 12.240 attomoles for 1-galactosamine) (13). The improvement in the LOD reported here is attributed to the use of a sheath flow cuvette with low light scattering as a post-column detector which results in low background and the elimination of the main water Raman band from the background by using two filters. Novotny's group used the 457-nm argon-ion line for better excitation since it has better overlap with the absorption profile of the derivative. However the water Raman band coincides with the maximum fluorescence, making it impossible to eliminate Raman scattering as a source of background.

2.3.5. Reaction Yield for Different Aminated Sugars

As expected, the yield of the CBQCA labeling reaction for the five aminated sugars studied here is not the same. Figure 2.11 shows the electropherograms of the CBQCA derivative of the five different aminated sugars labeled, injected, and separated under identical conditions. The relative yields were calculated by the relative areas under the peak for each aminated sugar. The highest yield was observed for 1-fucosamine. The lowest yield was observed for 1-mannosamine (26%). The yields for 1-galactosamine, 2-glucosamine, and 1-glucosamine were 91%, 84%, and 66% respectively. These results suggest that LOD's for the other aminated sugars will be of the same order of magnitude as for 1-glucosamine. The theoretical plate ranges from 3.5×10^5 to 8.3×10^5 for CBQ labeled monosaccharide by using PBpBS buffer (Table 2.4). Buffer without adding phenyl borate gave poor resolutions (Table 2.5).

Table 2.4 Numbers of theoretical plates for CBQ labeled sugars

Glc-NH ₂ -CBQ	7.0×10^5
2-Glc-NH ₂ -CBQ	8.3×10^5
Gal-NH ₂ -CBQ	4.1×10^5
Man-NH ₂ -CBQ	7.4×10^5
Fuc-NH ₂ -CBQ	3.5×10^5
CBQ	7.0×10^4

Except for CBQ, which was run in BS buffer, all labeled sugars were run in PBpBS buffer.

Table 2.5 The number of theoretical plate of CBQ labeled 1-glucosamine in different running buffers

Running Buffer ^a	Peak Height (v)	T _r (sec)	Peak Width (sec)	N ^b
BS	0.1483	251.1	3.2	3.3×10^4
PB	0.1026	297.9	2.6	7.3×10^4
PBS	0.036	318.0	2.6	8.3×10^4
PBpBS	0.1044	408.9	1.2	5.5×10^5

^a B, borate; S, SDS; P, phosphate; Bp, phenyl borate. The concentration of all buffer components was 10 mM.

^b The number of theoretical plate.

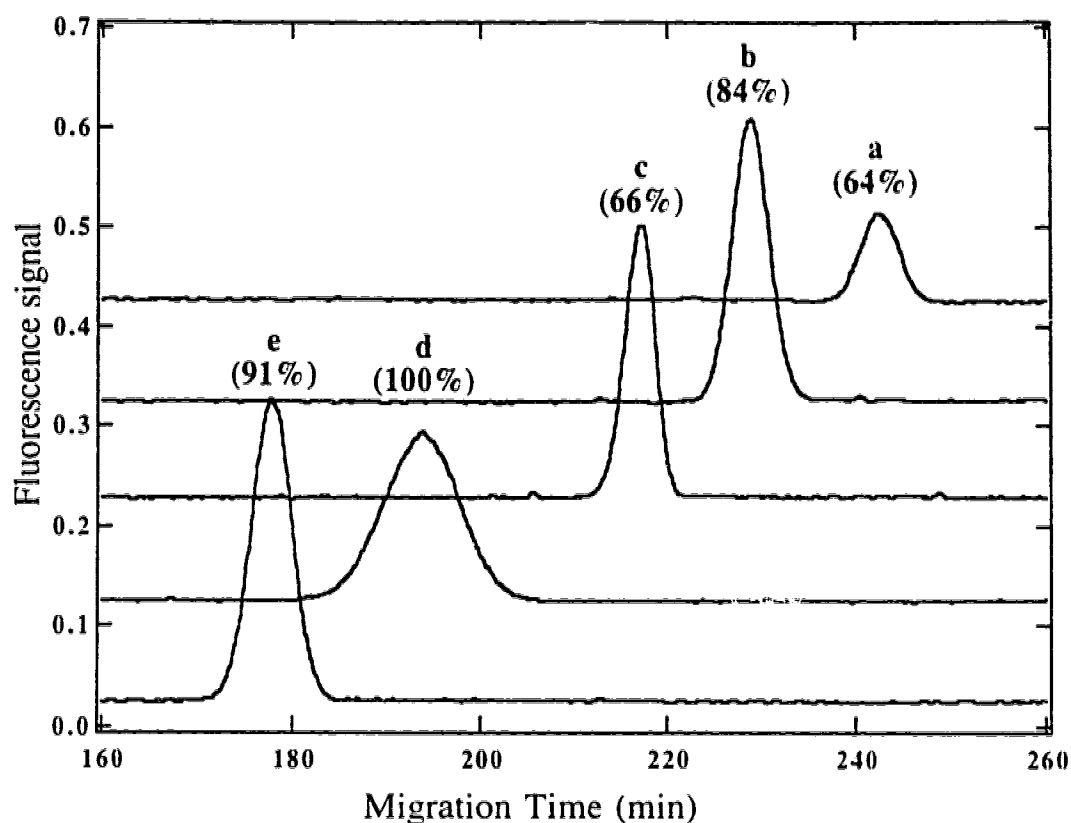


Figure 2.11 Comparison of the electropherograms for five aminated monosaccharides labeled under identical conditions. 1-mannosamine (a), 2-glucosamine (b), 1-glucosamine (c), 1-fucosamine (d), 1-galactosamine (e). The axis time does not represent the migration time since peak positions have been offset. Relative area under the peak is indicated within parenthesis. Reaction conditions: monosaccharides (10^{-4} M) were labeled individually; 4 mM CBQCA, 2 mM KCN, pH 7.1, during 2 h at 50 °C. Separation conditions as in Figure 2.6. Injection conditions: samples were diluted down to 1.0×10^{-6} M (labeled and unlabeled) aminated monosaccharide prior to injection (1000 V for 5 sec).

2.3.6. Separation of CBQCA Derivatives of Five Aminated Sugars

After the five aminated sugars (1-glucosamine, 1-mannosamine, 1-fucosamine, 1-galactosamine, and 2-glucosamine) were converted to CBQCA derivatives, they were expected to have similar electrophoretic mobilities since they had similar molecular weight, and the same net charge. They cannot be resolved in a conventional electrophoretic separation based on mass-to-charge ratio. However, if borate (or phenyl boronate) is added to the running buffer, the derivatives can be separated since borate (and phenyl boronate) complexes with the CBQCA. Borate complexation is due to the interaction of hydroxyl groups in the sugar moiety with tetrahydroxyborate ions $B[OH]_4^-$, one of the borate species presented in pH's from 8 to 12 (3, 9). The charge of the complex is proportional to its formation constant. For example, favorable configurations (with high formation constants) such as the cis-oriented pair of hydroxyl groups at C2 and C4 and the cis-1, 2-diol configuration of the monosaccharide will have greater charge. Differences in mass-to-charge ratio for the various complexes allow for their electrophoretic separation.

The use of borate in the running buffer for the separation of monosaccharides or their derivatives has been reported by several authors (3,12,13,16). However, based on their electropherograms, complete separation of the five aminated sugars used in our experiments with use of borate should not be possible. Evidence that phenyl boronate in the running buffer allows for better separations of monosaccharides has been published by Zhao et al. for the derivatives of aminated sugars labeled with 5-carboxytetramethylrhodamine succinimidyl ester (17). They reported the separation of the derivatives of 1-glucosamine, 2-glucosamine, 1-mannosamine, 1-galactosamine, 2-galactosamine, and 1-fucosamine.

In our experiments, the separation of the CBQCA derivatives of 1-glucosamine, 2-glucosamine, 1-mannosamine, 1-galactosamine, and 1-fucosamine was possible when the running buffer was composed of 50 mM phenyl boronate, 20 mM phosphate, and 20 mM borate. Figure 2.12 shows the separation of the CBQCA derivatives of the five aminated

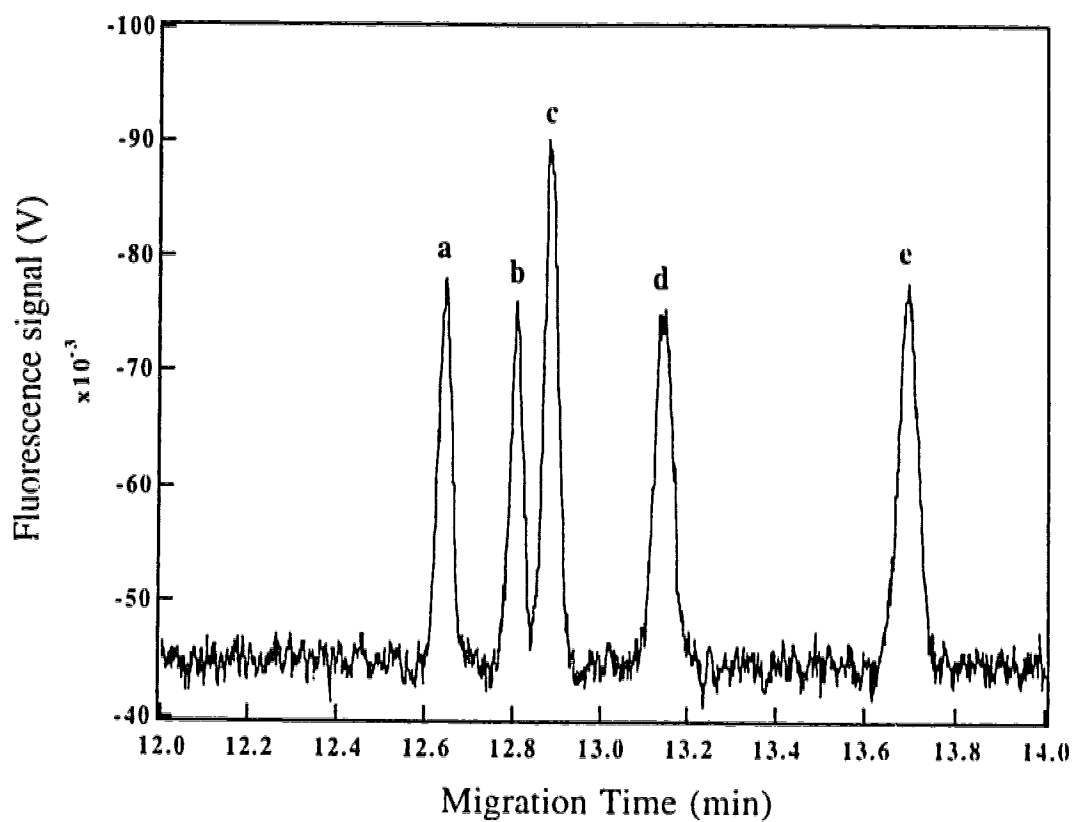


Figure 2.12 Separation of five CBQCA derivatives of monosaccharides. (a)1-mannosamine, (b) 2-glucosamine, (c)1-glucosamine, (d)1-fucosamine. (e)1-galactosamine. Reaction conditions: monosaccharides (1×10^{-4} M) were labeled individually, 4 mM CBQCA-4 mM KCN during 5 h at room temperature. Separation conditions: 10 μ m i.d., 72.5-cm long capillary; running buffer 20 mM phosphate + 50 mM phenyl boronate + 20 mM borate; 400 V/cm. Injection conditions: Samples were diluted down to 2.0×10^{-7} M (labeled and unlabeled) aminated monosaccharide prior to injection (2.5 kV for 5 sec).

sugars. In separations using 30 mM (or lower) phenyl boronate, the CBQCA derivatives for 1-glucosamine and 2-glucosamine were not resolved. Use of higher concentrations of borate (in the absence of phenyl boronate) did not allow for complete separation of the five aminated sugars. At present, no information for the interaction of boronate with carbohydrates is available. Complex stability is expected to be somewhat different for boronate complexation than it is for borate since the bulky phenyl group would introduce some steric hindrance. The interaction of the hydroxyl groups in the sugar moiety with trihydroxyboronate $B(Ph)[OH]_3$ would increase the mass of the monosaccharide but it would not affect the charge of the monosaccharide. Competitive equilibrium between boronate and borate for the monosaccharide would increase the structural differences among the different monosaccharide complexes resulting in a better separation. Competitive borate and phenyl boronate complexation may prove to be useful for separation of other monosaccharides and oligosaccharides.

2.4 CONCLUSIONS

Samples with concentrations as low as 1.0×10^{-9} M 1-glucosamine or other aminated monosaccharides can be fluorescently tagged using CBQCA as a fluorogenic reagent. The LOD in our experiment for CBQ-labeled 1-glucosamine is 75 zeptomole. This is possible as a result of selection of labeling conditions that favor the formation of the CBQCA sugar derivative over the secondary fluorescent products. In addition, the availability of a detector that has low light scattering characteristics (sheath flow cuvette) and the elimination of the main water Raman band from the background allows limits of detection for aminated sugars at the zeptomole level. The separation of five basic aminated sugars using a mixture of phenyl boronate and borate in the separation buffer was also demonstrated. These results illustrate a promising methodology for the separation and identification of very low levels of monosaccharides.

2.5 REFERENCES

- (1) Churms, S. C. *J. Chromatogr.* **1990**, *500*, 555-583.
- (2) Sweeley, C. C.; Nunez, H. A. *Ann. Rev. Biochem.* **1986**, *54*, 765-801.
- (3) Hoffstetter-Kuhn; Paulus, A.; Gassmann, E.; Widmer, H. M. *Anal. Chem.* **1991**, *63*, 1541-1547.
- (4) Bornhop, D. J., Nolan, T. G., Dovichi, N. J., *J. Chromatogr.* **1987**, *384*, 181-187.
- (5) Garner, T. W.; Yeung, E. S. *J. Chromatogr.* **1990**, *515*, 639-644.
- (6) Vorndran, A. E., Oefner, P. J., Scherz, H., Bonn, G. K. *Chromatographia* **1992**, *33*, 163-168.
- (7) Monnig, C. A.; Kennedy, R. T. *Anal. Chem.* **1994**, *66*, 280R-314R.
- (8) Kuhr, W. G.; Monnig, C. A. *Anal. Chem.* **1992**, *64*, 389R-407R.
- (9) Stefansson, M.; Westerlund, D. *J. Chromatogr.* **1993**, *632*, 195-200.
- (10) Honda, S.; Iwase, S.; Makino, A.; Fujiwara, S. *Anal. Biochem.* **1989**, *176*, 72-77.
- (11) Honda, S.; Makino, A.; Susuki, S.; Kakehi, K. *Anal. Biochem.* **1990**, *191*, 228-234.
- (12) Liu, J.; Shirota, O.; Wiesler, D.; Novotny, M. *Proceedings of the National Academy of Sciences USA* **1991**, *88*, 2302-2306.
- (13) Liu, J.; Osamu, S.; Novotny, M. *Anal. Chem.* **1991**, *63*, 413-417.
- (14) Liu, J.; Shirota, O.; Novotny, M. V. *Anal. Chem.* **1992**, *64*, 973-975.
- (15) Nashabeh, W.; El Rassi, Z. *J. Chromatogr.* **1990**, *514*, 57-61.
- (16) Nashabeh, W.; El Rassi, Z. *J. Chromatogr.* **1991**, *536*, 31-42.
- (17) Zhao, J. Y.; Diedrich, P.; Zhang, Y.; Hindsgaul, O.; Dovichi, N. J. *J. Chromatogr. B* **1994**, *657*, 307-313.
- (18) Jackson, P. *Biochem. J.* **1990**, *270*, 705-713.
- (19) Jackson, P.; Williams, G. R. *Electrophoresis* **1991**, *12*, 94-96.
- (20) Stefansson, M.; Novotny, M. *Anal. Chem.* **1994**, *66*, 134-1140.
- (21) Stefansson, M.; Novotny, M. *Carbohydrate Research* **1994**, *258*, 1-9.
- (22) Liu, J.; Shirota, O.; Novotny, M. *J. Chromatogr.* **1991**, *559*, 223-235.

- (23) Liu, J.; Hsieh, Y.-o.; Wiesler, D.; Novotny, M. *Anal. Chem.* **1991**, *63*, 408-412.
- (24) Sudor, J.; Novotny, M. *Proceedings of the National Academy of Sciences USA* **1993**, *90*, 9451-9455.
- (25) Kwakman, P. J. M.; Koelewijn, H.; Kool, I.; Brinkman, U. A. T.; De Jong, G. J. *J. Chromatogr.* **1990**, *511*, 155-166.
- (26) Arriagar, E. A.; Zhang, Y.; Dovichi, N. J. *Analytica Chimica Acta* **1995**, *299*, 319-326.
- (27) Pinto, D. M.; Arriaga, E. A.; Sia, S.; Li, Z.; Dovichi, N. J. *Electrophoresis* **1995**, *16*, 534-540.
- (28) Sternson, L. A.; Stobaugh, R. S.; Repta, A. J. *Anal. Chem.*, **1985**, *144*, 233-246.
- (29) Matuszewski, B. K.; Givens, R. S.; Srinivasachar, K.; Carlson, R. G.; and Higuchi, T. *Anal. Chem.* **1987**, *59*, 1102-1105.
- (30) Montigny, P. D.; Stobaugh, R. S.; Carlson, R. G.; Srinivasschar, K.; Sternson, L. A.; and Higuchi, T. *Anal. Chem.*, **1987**, *59*, 1096-1101.
- (31) Huang, X.; Gordon, M.; Zare, R. *Anal. Chem.* **1988**, *60*, 375-377.

CHAPTER 3

MONITORING BIOSYNTHETIC TRANSFORMATIONS OF *N*- ACETYLLACTOSAMINE USING FLUORESCENTLY LABELED OLIGOSACCHARIDES AND CAPILLARY ELECTROPHORETIC SEPARATION

A version of this chapter has been published.

Zhang, Y., Le, X., Dovichi, N., Compston C. A., Palcic, M. M., Diedrich, P., and Hindsgaul, O. *Anal. Biochem.* **1995**, 227, 368-376.

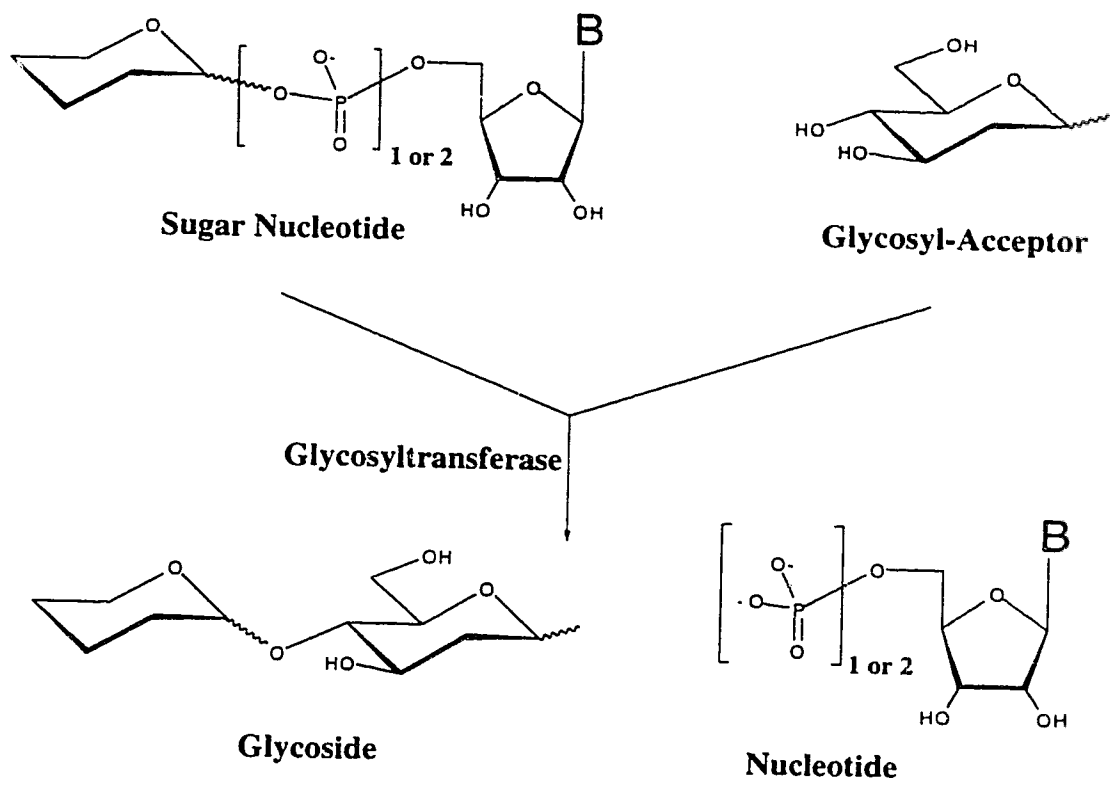
Acknowledgments: The HT-29 microsomes were a generous gift from Dr. S. Laferte, University of Saskatchewan.

3.1 INTRODUCTION

Complex cell surface oligosaccharides are implicated in numerous biological phenomena, one of the most interesting being the regulated control of cell-cell adhesion (1-4). Many cell surfaces are covered with glycoproteins and glycolipids that are frequently large, heavily glycosylated molecules ideally placed to mediate initial contacts between cells. The terminal carbohydrate sequences of these protein and lipid-conjugated oligosaccharide chains are biosynthesized by Golgi-localized glycosyltransferases that catalyze the addition of single sugar residues from their UDP-, GDP-, or CMP- derived sugar nucleotide donors (Scheme 3.1). The activity of individual enzymes within the cell can control the distribution of oligosaccharide structures presented as potential ligands at the cell surface (4). Sensitive methods for monitoring the specific activities of glycosyltransferase in cell extracts, and within cells, are therefore required for understanding the control of cell surface glycosylation.

The most commonly used assays for glycosyltransferases are radiochemical assays, which quantitate the transfer of tracer-labeled (^3H or ^{14}C) sugars from their sugar nucleotides (5). The sensitivity of the method normally requires about a picomole of product to be formed. Ideally, product identity should be confirmed using an additional parameter such as affinity to an immobilized lectin (6), sensitivity to enzymatic degradation or coelution of the labeled enzyme product with an authentic standard in HPLC (7) BioGel chromatography (8).

Affinity-based methods using either antibodies or lectins to detect and quantitate products have recently become increasingly popular because they may be done rapidly in an ELISA format and provide simultaneous evidence for the identity of the product (9). Typically, an acceptor conjugate is incubated with the enzyme source and the sugar nucleotide and then the immobilized or captured product is identified and quantitated either stoichiometrically or in an enzyme-amplified fashion. The sensitivity of these



Scheme 3.1 The general reaction catalyzed by glycosyltransferase.

methods lies in the femtomole range. The other product of the transferase reaction, the UDP, GDP, or CMP released on glycosylation, can also be quantitated in a coupled enzyme assay (10). Coupled assays require on the order of 0.5 nmol of product to be formed.

Electrophoresis has emerged as a highly promising technique for the analysis of mono- and oligosaccharides. The approaches developed for overcoming the lack of chromophoric and fluorophoric functions in most carbohydrates involve the use of indirect photometric detection, amperometry, mass spectrometry, and precolumn derivatization with various tags (12). Capillary electrophoretic separation of fluorescently labeled oligosaccharides is emerging as a powerful tool for carbohydrate analysis (11, 12) and this technology has also produced the most sensitive glycosyltransferase assays reported to date. Capillary electrophoresis offers excellent separation efficiency. Also, the small dimensions of the capillary tubes facilitate the analysis of extremely small amounts of samples.

With laser-induced fluorescence and sheath flow cuvette developed by Dovichi's group, detection of a few thousand molecules of product (zeptomole, 10^{-21}) is routine in capillary electrophoresis while sensitivity down to a few molecules has been achieved (13-18). The high separation efficiency also has made it possible to separate oligosaccharides with different molecular weights and the same molecular weight (same atoms) with different linkages (isomers). For this promising ultrasensitive method of analysis to gain wide acceptance, it is essential that standards be available to confirm the structures of products produced in an enzymatic reaction. The availability of standards is particularly important when assays are performed in crude cell extracts where several enzymes are often competing for the same fluorescently labeled substrate leading to isomeric products.

In this chapter, the $\beta\text{Gal}(1\rightarrow4)\beta\text{GlcNAc-O}(\text{CH}_2)_8\text{CONHCH}_2\text{CH}_2\text{NH}_2$ and its coupling with a commercial *N*-hydroxysuccinimide ester of tetramethylrhodamine to

produce LacNAc-O—TMR: where "—TMR" denotes the linker arm attached to tetramethylrhodamine were synthesized (i.e. $-(\text{CH}_2)_8\text{CONHCH}_2\text{CH}_2\text{NH}-$ tetramethylrhodamine ester, see Scheme 3.2). As well, the products that would form on exposure of LacNAc-O—TMR to cellular glycosidases and the products that could form by mono- and difucosylation of LacNAc-O—TMR were prepared and characterized. All six molecules could be baseline resolved in capillary electrophoresis in 11 minutes and were shown to be useful in the detection of specific enzyme activities in crude microsomal preparations.

3.2 EXPERIMENTAL SECTION

3.2.1 Materials

8-Methoxycarboxyloctanol and its glycosides: $\beta\text{GlcNAc-O}(\text{CH}_2)_8\text{COOMe}$, $\beta\text{Gal}(1\rightarrow4)\beta\text{GlcNAc-O}(\text{CH}_2)_8\text{COOMe}$, $\alpha\text{Fuc}(1\rightarrow2)\beta\text{Gal}(1\rightarrow4)\beta\text{GlcNAc-O}(\text{CH}_2)_8\text{COOMe}$, $\beta\text{Gal}(1\rightarrow4)[\alpha\text{Fuc}(1\rightarrow3)]\beta\text{GlcNAc-O}(\text{CH}_2)_8\text{COOMe}$, $\alpha\text{Fuc}(1\rightarrow2)\beta\text{Gal}(1\rightarrow4)[\alpha\text{Fuc}(1\rightarrow3)]\beta\text{GlcNAc-O}(\text{CH}_2)_8\text{COOMe}$, were available from Dr. Ole Hindsgaul's group (19-21). The *N*-hydroxysuccinimide ester of tetramethylrhodamine was from Molecular Probes. The following analyte stock solutions of fluorescent derivatives were prepared (the structures of **1-6** are shown in Scheme 3.2): 1 mM **1**, 1.5 mM **2**, 1 mM **3**, 0.78 mM **4**, 1.2 mM **5** and 1 mM **6**. Preparative TLC plates (2.0 mm, 20 x 20 cm, PLK-5F) were from Whatman. Stock buffer solutions were prepared in deionized water (Barnstead NANO pure system) and filtered with 0.2 μm pore size disposable filter (Nalgene). Aqueous stock solutions included 0.2 M Na_2HPO_4 (Fisher), 0.2 M borate (Fisher), 0.5 M sodium dodecyl sulfate (BDH) and 0.1 M phenyl boronic acid (Sigma). The electrophoresis buffer was prepared by mixing these stock solutions to final concentrations of 10 mM Na_2HPO_4 , 10 mM borate, 10 mM phenyl boronic acid, and 10 mM SDS (pH 9). A standard containing 5×10^{-9} M of each analyte was prepared in running buffer. Triton X-100, benzamidine, bovine serum albumin and almond meal

fucosidase were from Sigma. Sep Pak Plus C-18 cartridges were from Waters. HPLC grade methanol was from Baxter. Ecolite (+) liquid scintillation cocktail was from ICN and GDP-³H-fucose (6.45 Ci/mmol) was from Dupont. Protein concentrations were estimated with a Bio-Rad Bradford assay kit using bovine serum albumin as a protein standard. GDP-fucose was prepared as previously described (22). All other chemicals were of reagent grade.

3.3 Methods

3.3.1 General Procedure Used for the Preparation of Ethylenediamine

Monoamides (Dr. Ole Hindgaul's group)

8-Methoxycarboxyloctanol or its glycoside (5 mg) was dissolved in neat anhydrous ethylenediamine (2 mL) and heated at 70 °C for 50 h in a screw-capped tube with a Teflon lined cap. The tube was cooled in an ice bath and water (5 mL) was added. The cooled solution was then passed through a Sep-Pak cartridge which was washed with water (30 mL). The aqueous flow-through was loaded onto a fresh Sep-Pak which was also washed with water (30 mL). Product was eluted from each Sep-Pak by washing with MeOH (30 mL), the eluates were combined and the MeOH was evaporated. The residue was dissolved in water (10 mL) and reisolated on a fresh Sep-Pak from which it was eluted with MeOH. The residue after evaporation was dissolved in water (8 mL) and passed through a 0.2-µm filter and lyophilized. Recoveries were in the range 80-90%.

3.3.2 General Procedure Used for the Fluorescence Labeling (Dr. Ole Hindgaul's group)

Labeling of the amines described above was performed as described by the manufacturer. Briefly, tetramethylrhodamine *N*-hydroxysuccinimide ester (5 mg) was dissolved in DMF (0.25 mL) and added to the amine (3-4 mg) in 0.185 M NaHCO₃ (pH 8.5, 0.25 mL). After 4 h, the reaction mixture was diluted with water (4 mL) and applied

to a column of DEAE-A25 (Cl⁻ form, 0.8 × 5 cm) and water was passed through the column until the eluate was colorless (30-40 mL). The brilliant red product was isolated from the washes by Sep-Pak adsorption as described above. The residue in MeOH was applied to a preparative silica gel plate which was developed using the solvent listed in Table 3.2. The red band containing product was scraped from the plate and extracted with MeOH (4 × 50 mL) by stirring for 10 min until the silica gel was colorless. The labeled compounds were then recovered on a Sep-Pak as described above. Final purification was performed by passage through Bio-Gel P2 (2.5 × 40 cm) using 10% aq EtOH as solvent. Evaporation of the first red fraction, reisolation on a Sep-Pak, Millipore-filtration, and lyophilization produced dark red fluffy powders which were stored at -20 °C protected from light. Yields were in the 70% range.

The NMR (Bruker AM, 360 MHz in D₂O), MS (Fast atom bombardment using Xe as the gas and 5:1 1,4-dithiothreitol:1,4-dithioerythritol as the matrix on a Kratos AEI MS-9 instrument), and *R_f* data for the compounds synthesized as described above are listed in Tables 3.1 and 3.2. The solvent systems used for TLC were designated as follows: (A)- 60:35:2 CH₂Cl₂:MeOH:H₂O; (B)- 60:35:6 CH₂Cl₂:MeOH:H₂O; (C)- 10:9:1 CHCl₃:MeOH:H₂O; (D)- 8:3:1 CHCl₃:MeOH:H₂O.

3.3.3 Preparation of Enzyme Extracts from HT-29 Cells (Dr. Monica Palcic' group)

HT-29 cells were grown to confluency in Dulbecco's minimal essential medium supplemented with 10% fetal calf serum on four 20 × 150 mm dishes. Cells were washed with phosphate buffered saline, harvested by scraping with a rubber policeman, centrifuged at 500g for 5 min to give a 2 mL cell pellet which was stored frozen at -20 °C. Microsomes were prepared by resuspending the cell pellet in 4 vol of 25 mM Tris-HCl, pH 7.4, containing 8.6% sucrose, 1 mM EDTA, 1 mM phenylmethylsulfonyl fluoride, 1 mM benzamide, and 0.02% sodium azide, homogenizing with a Polytron homogenizer (3 × 10 sec bursts) and centrifugation of the homogenate at 8500g for 6 min

Table 3.1
¹H NMR (Chemical Shifts and Coupling Constants), Mass Spectral (MS), and Rf Data (on Silica Gel TLC) for the Aminated Precursors

Compound	NAc	-CH ₂ C(O)NH ₂	-CH ₂ NH ₂	-C(O)NHCH ₂ -	Characteristic Data	MS M + H ⁺	Rf solvent
LacNAc-O(CH ₂) ₈ CONH(CH ₂) ₂ NH ₂	2.02	2.25 (7.5 Hz)	2.81 (6.5 Hz)	3.29 (6.5 Hz)	βGlcNAc 4.51 (8.0 Hz) βGal 4.47 (7.5 Hz)	582.4	0.06 (A)
H type 2-O(CH ₂) ₈ CONH(CH ₂) ₂ NH ₂	2.04	2.25 (7.5 Hz)	2.86 (6.5 Hz)	3.32 (6.5 Hz)	βGlcNAc 4.53 (8.0 Hz) βGal 4.48 (8.5 Hz) αFuc 5.30 (3.0 Hz) H5 Fuc 4.22 (6.5 Hz) CH ₃ Fuc 1.22 6.5 Hz)	728.8	0.03 (A)
Lewis X-O(CH ₂) ₈ CONH(CH ₂) ₂ NH ₂	2.01	2.25 (7.5 Hz)	2.77 (6.5 Hz)	3.29 (6.5 Hz)	βGlcNAc 4.52 (8.0 Hz) βGal 4.45 (7.5 Hz) αFuc 5.11 (4.0 Hz) H5 Fuc 4.84 (6.5 Hz) CH ₃ Fuc 1.17 (6.5 Hz)	728.65	0.05 (B)
Lewis Y-O(CH ₂) ₈ CONH(CH ₂) ₂ NH ₂	2.00	2.25 (7.5 Hz)	2.73 (6.5 Hz)	3.25 (6.5 Hz)	βGlcNAc 4.51 (~8.0 Hz) βGal 4.51 (~8.0 Hz) αFuc ^{'''} 5.28 (2.0 Hz) αFuc' 5.10 (4.0 Hz) H5 Fuc' 4.88 (6.5 Hz) H5 Fuc ^{'''} 4.26 (6.5 Hz) CH ₃ Fuc ^{'''} 1.27 (6.5 Hz) CH ₃ Fuc' 1.24 (6.5 Hz)	874.5	0.04 (B)
βGlcNAcO(CH ₂) ₈ CONH(CH ₂) ₂ NH ₂	1.93	2.25 (7.5 Hz)	2.80 (6.5 Hz)	3.29 (6.5 Hz)	βGlcNAc 4.53 (8.5 Hz)	420.4	0.21 (A)
HO(CH ₂) ₈ CONH(CH ₂) ₂ NH ₂		2.28(7.5Hz)	2.95 (6.5 Hz)	3.37 (6.5 Hz)	---	ND	ND

Note: ND, not determined.

Table 3.2
¹H NMR (Chemical Shifts and Coupling Constants), Mass Spectral (MS), and R_f Data (on Silica Gel TLC) for
 Tetramethylrhodamine-Labeled Structures 1-6

Compound	<u>CH₂C(O)NH</u>	NAc	Methyls	Characteristic data ^a	MS (M + H ⁺)	R _f (solvent)
LeuNAc-O-TMR (1)	2.35 (7.5 Hz)	2.04	3.22	βGlcNAc 4.53 (8.0 Hz) βGal 4.50 (7.5 Hz)	994.7	0.33 (B)
H type 2-O-TMR (2)	2.32 (7.5 Hz)	2.00	3.22	βGlcNAc 4.57 (7.5 Hz) βGal 4.47 (8.0 Hz) αFuc ^{'''} 5.36 (3.0 Hz) H5 Fuc ^{'''} 4.25 (6.5 Hz) CH ₃ Fuc ^{'''} 1.25 (6.5 Hz)	1140.6	0.33 (D)
Le X-O-TMR (3)	2.33 (7.2 Hz)	2.01	3.22	βGlcNAc 4.41 (8.0 Hz) βGal 4.40 (8.0 Hz) αFuc 5.06 (3.5 Hz) H5 Fuc 4.87 (6.5 Hz) CH ₃ Fuc 1.14 (6.5 Hz)	1140.4	0.36 (C)
Le Y-O-TMR (4)	2.34 (7.2 Hz)	2.03	3.22	βGlcNAc 4.56 (7.8 Hz) βGal ^{'''} 4.52 (8.4 Hz) αFuc ^{'''} 5.34 (3.3 Hz) αFuc ^{''} 5.15 (3.9 Hz) H5 Fuc ^{''} 4.94 (6.5 Hz) H5 Fuc ^{'''} 4.30 (6.5 Hz) CH ₃ Fuc ^{'''} 1.31 (6.5 Hz) CH ₃ Fuc ^{''} 1.30 (6.5 Hz)	1287.2	0.17 (C)
βGlcNAc-O-TMR (5)	2.35 (7.5 Hz)	2.04	3.22	βGlcNAc 4.46 (8.0 Hz)	832.7	0.47 (B)
H-O-TMR (6)	2.28 (7.5 Hz)	-	3.18	-	629.4	ND

Note. ND, not determined.

^aAll TMR derivatives showed similar additional signals for the aromatic protons at 8.38, 8.10, 7.58, 7.25, 6.93, and 6.57.

at 4 °C. The supernatant from the low speed spin was centrifuged at 100,000g for 1 h at 4 °C to give a microsomal pellet. The pellet was resuspended in 0.25 M sucrose and 10 mM EDTA, pH 7.4, giving 400 µL of microsomes (2.1 mg protein) which were stored frozen at -70 °C. The microsomes were resuspended in 800 µL of 50 mM Hepes buffer, pH 7.0, containing 25% glycerol, 1 mM EDTA, 0.2% Triton X-100 and homogenized by 20 strokes every 15 min over a 1.5 h period in a Wheaton glass homogenizer. The homogenate was centrifuged at 41,000g for 30 min to give the enzyme extract in the supernatant.

3.3.4 Fucosyltransferase (FucT) Assays (Dr. Monica Palcic's group)

Enzyme assays were carried out in a total volume of 40 µL, containing 20 mM Hepes buffer, pH 7.0, 20 mM MnCl₂, 0.2% bovine serum albumin, 50 µM GDP-fucose, 43,000 dpm GDP-³H-fucose, 450 µM or 3 mM acceptor and 14 µL of enzyme extract. Reaction mixtures were incubated at 37 °C for 120 min and then diluted with water and applied to a C-18 reverse phase cartridge (23). The cartridge was washed with 50 mL of water to remove unreacted donor and then product was eluted dropwise with 3.5 mL of MeOH directly into a scintillation vial. Product formation was quantitated by liquid scintillation counting after the addition of 10 mL of Ecolite (+) cocktail. The protein content in the extract was 1.2 mg/mL with the following FucT activities: 25 µunits/mL of α(1→2)FucT using 3 mM phenyl-β-D-galactopyranoside as an acceptor, 200 µunits/mL of α(1→3)FucT using 450 µM αFuc(1→2)βGal(1→4)βGlcNAcO(CH₂)₈COOMe and 13 µunits/mL of α(1→4)fucosyltransferase using 450 µM αFuc(1→2)βGal(1→3) βGlcNAcO-(CH₂)₈ COOMe as an acceptor. When βGal(1→4)βGlcNAcO(CH₂)₈COOMe was used as an acceptor at concentrations of 450 and 50 µM, 135 and 77 µunits/mL, respectively of combined α(1→3) and α(1→2)FucT activity were measured, while for LacNAc-O-TMR the activities were 100 and 68 µunits/mL for the same concentrations.

Enzyme activity was constant in the extracts for one week at 4 °C after which there was a slow loss of activity.

3.3.5 Fucosyltransferase and Fucosidase Incubations for Analysis by Capillary Electrophoresis

Reaction mixtures were prepared by lyophilizing 0.8, 3.0, and 5.5 μL of 1 mM (final concentration: 50, 187, and 343 μM) LacNAc-O-TMR in a 0.5 mL microfuge tube and then adding 14 μL of enzyme extract, 1 μL of 1 mM GDP-fucose, and 1 μL of concentrated assay buffer (200 mM Hepes, pH 7.0, containing 200 mM MnCl_2 and 2 % bovine serum albumin). Mixtures were incubated at 37 °C with removal of 2- μL aliquots after 24 h of incubation.

The following components were added after each removal from the incubation containing 50 mM LacNAc-O-TMR from above: at 24 h, 5 μL of enzyme extract, 0.5 μL of 1 mM GDP-fucose, and 0.5 μL of concentrated assay buffer; at 48 h, 2.5 μL of enzyme extract, 0.5 μL of 1 mM GDP-fucose and 0.5 μL concentrated assay buffer. Mixtures were incubated at 37° C with removal 2- μL aliquots after 48 and 72 h.

All aliquots were diluted with 5 mL water and applied to conditioned Sep-Pak cartridges that were washed with 30 mL of water. Sep-Pak cartridges were conditioned by washing with MeOH then water (30 mL each). Unreacted acceptors and products were eluted with 3.5 mL HPLC grade MeOH, diluted 1:2 with 10 mM phosphate, 10 mM borate, 10 mM SDS and 10 mM phenylboronic acid (CE running buffer) and analyzed by capillary electrophoresis.

For the fucosidase treatment, a 674 μL sample from the 3.5 mL methanol eluent of the 72 h incubations (50 mM LacNAc) was lyophilized to dryness. This product was incubated with 5.3 μunits of almond meal fucosidase in 27 μL of 0.1 M citrate-0.2 M phosphate buffer, pH 5.5 from 2 to 24 h at 37 °C. A 5 μL aliquot was removed, diluted with 5 mL of water at 2, 4, 7.5, 12, 24 h, applied to a Sep-Pak cartridge, washed with 50

mL of water and then eluted with 3.5 mL of HPLC grade methanol. The methanol eluates were lyophilized to dryness, 50 μ L of methanol were added, samples were diluted 1:1 with CE running buffer and 16-17 μ L was injected into the capillary column.

Degradation controls were prepared by lyophilizing 1 μ L of stock solutions (final concentration Le^N (4) 97.5 μ M; Le^X (3) 125 μ M; H type II (2) 187 μ M, LacNAc (1) 187 μ M and GlcNAc (5) 155 μ M) and then adding 7 μ L microsomal cell extracts. Mixtures were incubated at 37 °C with removal of 1 μ L aliquots after 24, 48, 72, 144 h. The mixtures were purified by Sep Pak as described above and the unreacted substrates and hydrolytic products were eluted with 3.5 mL methanol.

Other two substrates incubated separately with microsomal extracts and GDP-fucose were H type II and Le^X in a total volume 16 μ L and 150 μ M final concentration. After 24 and 48 h, aliquots of 2 μ L were removed, purified by Sep Pak cartridge, and diluted 1:2 ratio in a running buffer prior to CE analysis.

The standards were stable in running buffer at room temperature for several months. All samples processed by Sep-Pak and eluted with methanol were stable at room temperature or 4 °C for more than four months.

3.3.6 Instrumentation of Capillary Electrophoresis with Laser-induced Fluorescence Detection

A locally constructed capillary electrophoresis system similar to Chapter 2.2 was used for the laser-induced fluorescence detection. Basically, a 2.2 mW Helium-Neon laser beam (543 nm) was focused into a post-column sheath flow cuvette detector (Figure 3.1a). Fluorescence was collected at right angles with a high-numerical-aperture microscope objective (60 \times 0.7 numerical aperture, Universe Kogaku, NY), imaged onto a hand adjusted iris matched in size to the illuminated sample stream, spectrally filtered with a bandpass filter 580DF40 (Omega Optical, Brattleboro, VT), and detected with a Hamamatsu R1477 photomultiplier tube (Bridgewater, NJ). The signal was treated with a

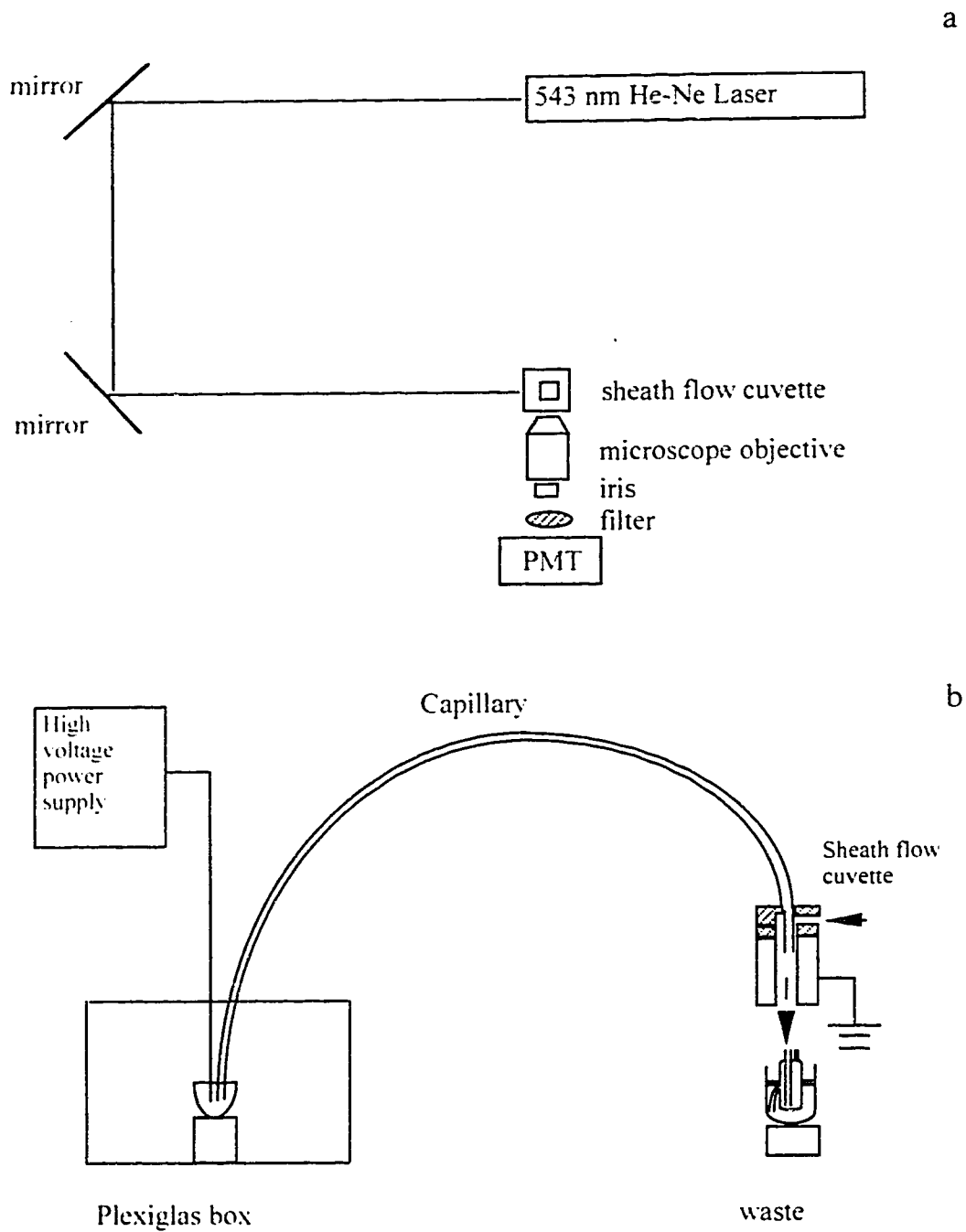
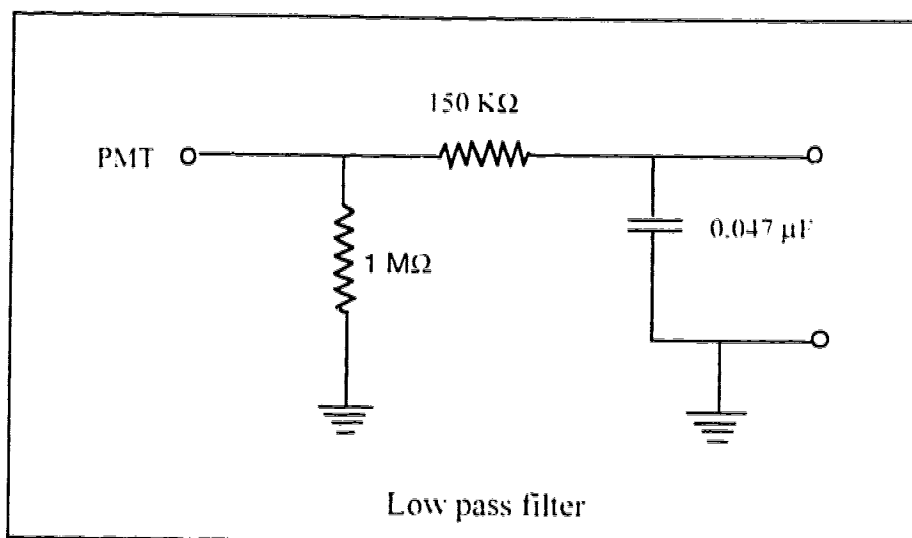


Figure 3.1 (a) Top view of instrument set up. (b) Capillary electrophoresis.

0.54 millisecond RC low pass filter shown below. Data were digitized by a National Instrument board (NB-MIO-16X I/O connector) to a Macintosh Centris 650 computer and collected by LabVIEW (National instruments, Austin, TX) software. All data were processed by Igor.



Separation was carried out in a 43 cm long, 10- μm inner diameter fused silica capillary (Polymicro, phoenix, AZ) at an electric field of 400 V/cm (Figure 3.1b). The aqueous electrophoresis buffer contained 10 mM phosphate, 10 mM borate, 10 mM sodium dodecylsulphate and 10 mM phenyl boronic acid (pH 9). The high voltage injection end of the capillary was held in a Plexiglas safety-interlock equipped box. The other end of the capillary was placed inside the sheath-flow cuvette detector. The stainless-steel detector body was held at ground potential. The sheath fluid was gravity fed from a 500 mL plastic bottle. The sheath buffer level was arranged to be 5 cm higher than the level in the waste reservoir. This arrangement maintained a smooth sheath flow through the cuvette. Electrokinetic injection of the sample was performed typically by applying a 1 kV potential for 5 sec. After injection, the sample was replaced with fresh running buffer. Separation was performed at room temperature in an unthermostated

room. The migration time for those runs was normalized to the migration time of a standard. To separate fluorescence labeled sugars, borate and phenylboronic acids were added to the buffer. Charge differences resulted from complexation between sugar and borate lead to separation of the analytes. The mixed borate-phenyl boronic acid buffer was required for baseline separations of the sugars: either component alone was unable to resolve the compounds. To confirm the identity of the enzyme products, standards of known concentration were added to the reaction mixture and co-migration of the product with the standards was verified. The whole system was constructed on an optical bread board (Newport, Irvine, CA).

3.4 RESULTS AND DISCUSSION

3.4.1 Standards of Substrate and Possible Biosynthetic and Hydrolysis Products

Scheme 3.2 summarizes the potential biosynthetic transformations for which standards were prepared and analyzed in the present work. Degradation of LacNAc-O—TMR (**1**) by β -galactosidase would produce β -GlcNAc-O—TMR (**5**) that, on further degradation by a hexosaminidase, would release the fluorescently tagged linking arm (HO—TMR, **6**). With GDP-fucose as the only added glycosyl donor, fucosylation could occur first by either an $\alpha(1\rightarrow2)$ FucT to yield the H-active trisaccharide (**2**) or an $\alpha(1\rightarrow3)$ FucT to produce the Le^X sequence (**3**). Trisaccharide (**2**) remains active as a substrate for the $\alpha(1\rightarrow3)$ FucT which converts it to the Le^Y sequence (**4**) as well as for fucosidase which hydrolyzes it to LacNAc (**1**). Structure (**3**), however, is not a substrate for the $\alpha(1\rightarrow2)$ FucT and can therefore not be converted to (**4**). These fucosyltransferase activities are known to be present in HT-29 cells (25-27).

3.4.2 Electropherograms and Discussion

Figure 3.2 shows the electrophoretic separation of the five fluorescently labeled sugar products and the linker arm. The peaks are baseline resolved. Each component in

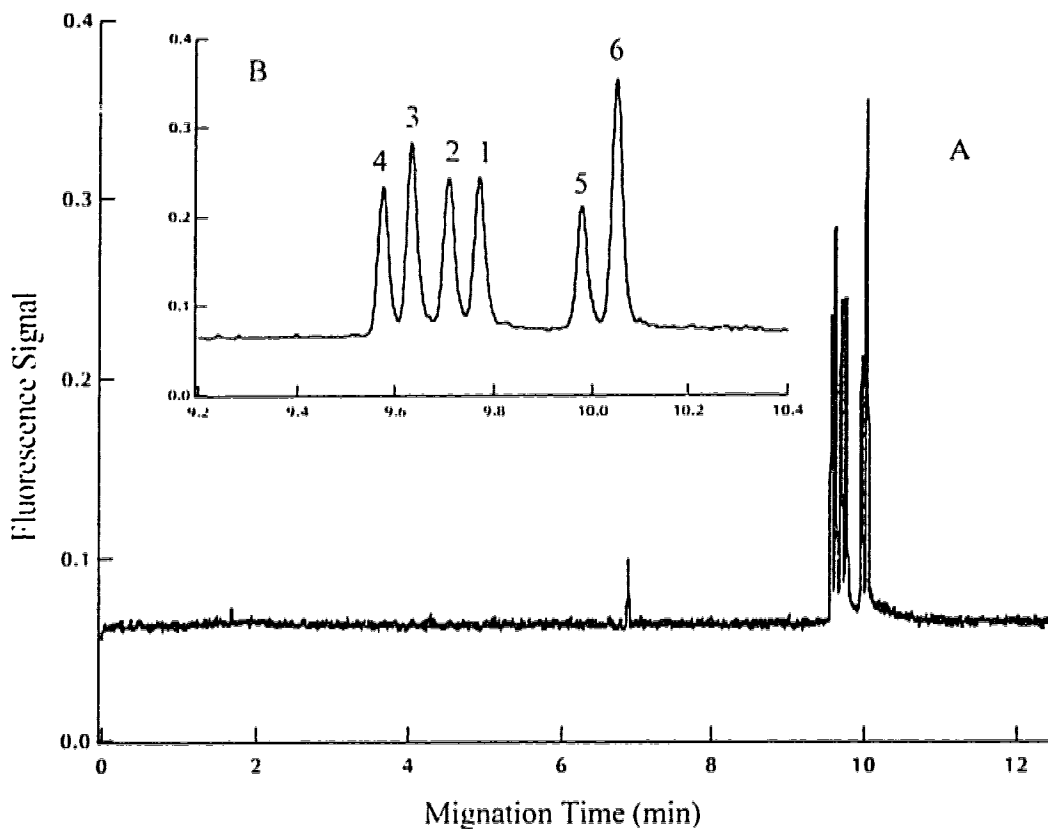


Figure 3.2 Capillary zone electropherogram of baseline separation of five standard tetramethylrhodamine-labeled oligosaccharides 1-5 and the linker arm 6. The mixture (5×10^{-9} M), was injected in a volume of 17 μ l (1 kV for 5 s) about 3×10^5 total molecules (0.5 attomoles). (A) A whole electropherogram. (B) Expansion of a narrow elution window. The detection limits calculated using Knoll's method (28) for each of TMR labeled standards were about 1200 molecules. The peaks in the electropherogram from left to right were 4, 3, 2, 1, 5 and 6.

- 1 LacNAc, β Gal(1 \rightarrow 4) β GlcNAc-O-TMR
- 2 H II, α Fuc(1 \rightarrow 2) β Gal(1 \rightarrow 4) β GlcNAc-O-TMR. H type II
- 3 Le^X, β Gal(1 \rightarrow 4)[α Fuc(1 \rightarrow 3)] β GlcNAc-O-TMR, Lewis X
- 4 Le^Y, α Fuc(1 \rightarrow 2) β Gal(1 \rightarrow 4)[α Fuc(1 \rightarrow 3)] β GlcNAc-O-TMR. Lewis Y
- 5 β GlcNAc-O-TMR. GlcNAc
- 6 H-O(CH₂)₈CONHCH₂CH₂NH-tetramethylrhodamine. the Linker arm

this standard mixture was 5×10^{-9} M in concentration. About 20 picoliters of this standard mixture was injected onto the column, corresponding to the introduction of 100 zeptomoles (1×10^{-19} mol or 60.000 analyte molecules). Detection limits are several orders of magnitude less than this amount. This high level of sensitivity and the excellent separation of the compounds allows the detection of small amounts of enzyme products in the presence of a large amount of substrate. The peaks eluted in the order **4**, **3**, **2**, **1**, **5** and **6**.

Substrate concentration was chosen by incubation of 50, 187, and 343 mM LacNAc-O-TMR with enzyme extract and donor GDP-fucose respectively (Figure 3.3). A 50 mM LacNAc incubation generated the highest percentage of biosynthetic product Le^X (**3**) over total TMR (Table 3.3).

Table 3.3 Optimization substrate concentration

[LacNAc] (μ M)	Percentage of products and substrate (%)			
	Le ^X	LacNAc	GlcNAc	H-O-TMR
50	29.0	60.5	5.3	5.3
187	14.4	78.0	3.6	4.0
343	11.0	76.2	7.3	5.5

Figure 3.4 presents electropherograms of 50 μ M LacNAc-O—TMR (**1**) after incubation with HT-29 microsomal extract and GDP fucose. The electropherograms shown in panels A, B and C were obtained after 24, 48, and 72 h incubations, respectively. After 24 h, the major peak (**1**) is unreacted substrate but with 30% conversion to the Le^X trisaccharide (**3**). Minor amounts of β GlcNAc-O—TMR (**5**) and labeled linker arm (**6**) are noted. After 48 hours, more Le^X-O—TMR has been formed, also with very small amounts of Le^Y (**4**) and H type 2 (**2**). The electropherogram is

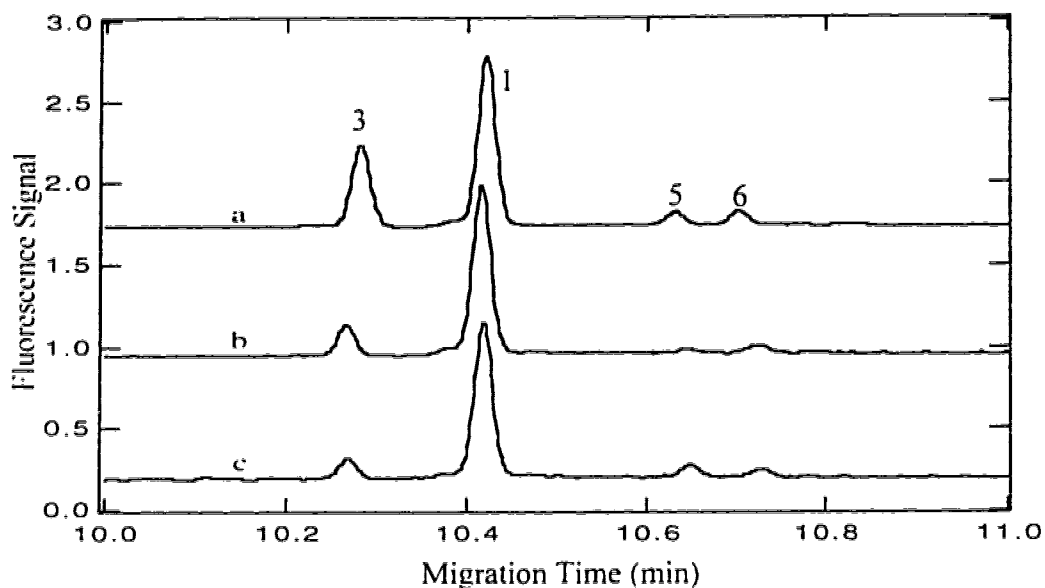


Figure 3.3 Capiillary electropherograms of (a) 50, (b) 187 and (c) 343 μM LacNAc-O-TMR after incubation with HT-29 microsomal extract and GDP fucose for 24 h. Aliquots of 2 μl mixture were processed by Sep-Pak and eluted with 3.5 ml methanol, then diluted by 1:2 ratio into running buffer. Total TMR labeled compounds injected in each case were about 1×10^{-8} M.

- 1 LacNAc, $\beta\text{Gal}(1 \rightarrow 4) \beta\text{GlcNAc-O-TMR}$
- 3 Le^X, $\beta\text{Gal}(1 \rightarrow 4)[\alpha\text{Fuc}(1 \rightarrow 3)] \beta\text{GlcNAc-O-TMR}$, Lewis X
- 5 $\beta\text{GlcNAc-O-TMR}$, GlcNAc
- 6 $\text{H-O}(\text{CH}_2)_8\text{CONHCH}_2\text{CH}_2\text{NH-tetramethylrhodamine}$, the Linker arm

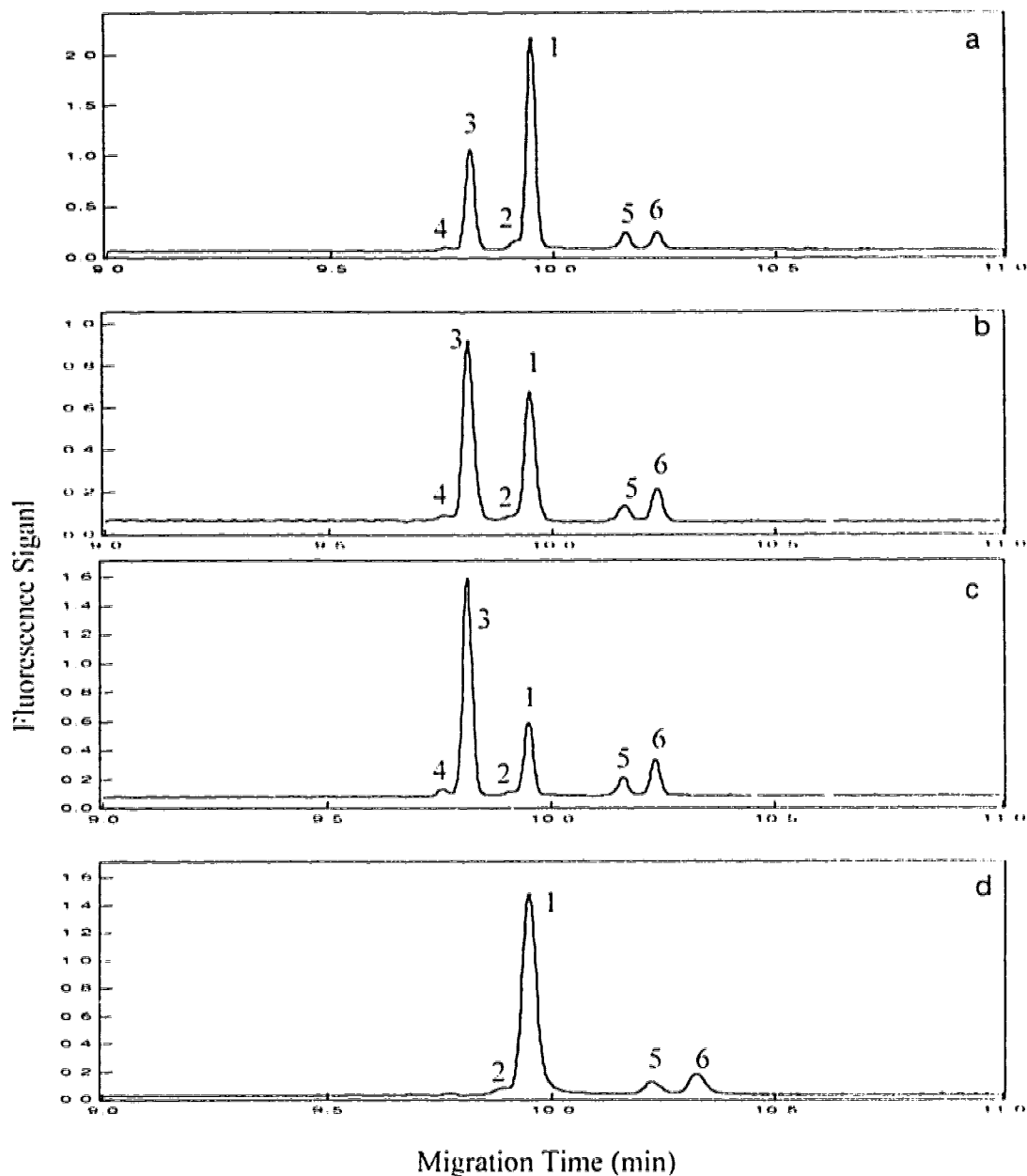


Figure 3.4 Capillary zone electropherograms of 50 μM LacNAc-O—TMR after incubation with HT-29 microsomal extract and GDP fucose. 2 μl aliquots were processed by Sep-Pak and eluted with 3.5 ml methanol, diluted 1: 2 ratio into running buffer, were injected on the electrophoresis column at 1 kV for 5 s. (A) 24 h, (B) 48 h, (C) 72 h incubation. (D) Reinjection of the fucosidase treatment of (C). The capillary was 43.5 cm long for (A), (B), and (C), but was 41.9 cm long for (D). The volumes injected were 16 μl and total concentrations of labeled compounds injected in each case were 1.4×10^{-8} M for (A), 1×10^{-8} M for (B), 8.4×10^{-9} M for (C) and 2.1×10^{-8} M for (D) (Around 0.5 to 1 attomoles TMR compounds were injected).

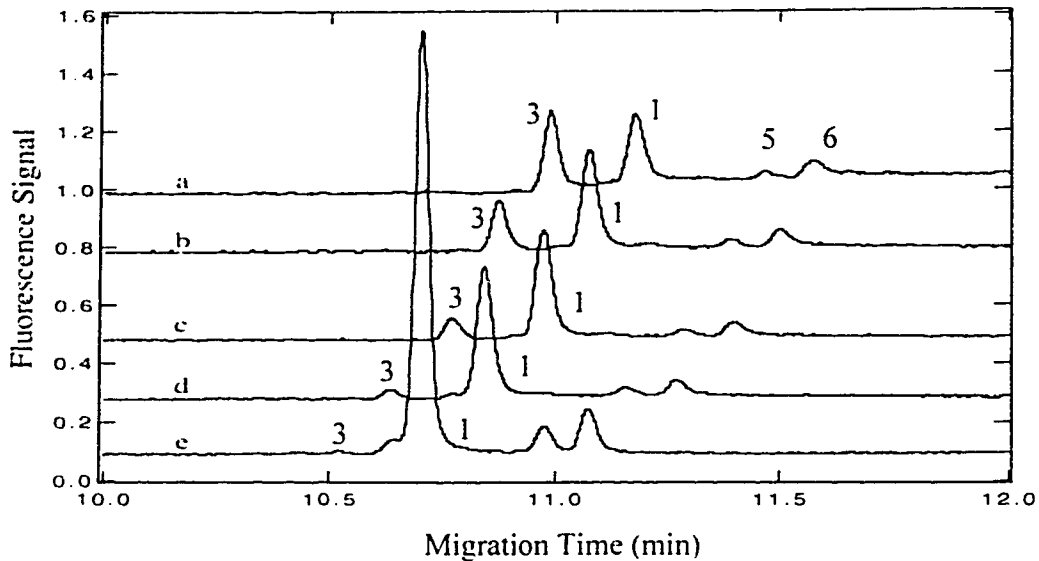


Figure 3.5 Capillary zone electropherogram of almond meal fucosidase incubated with Le^x for (a) 2, (b) 4, (c) 7.5, (d) 12, and (e) 24 h. The total TMR labeled compounds injected were 1×10^{-8} M for (a)-(d) except 2.1×10^{-8} M for (e). Electropherograms were offset in both Y and X axis for presentation. The last two peaks in each electropherogram were GlcNAc (5) and the linker arm (6). Substrate LacNAc (1) is next to GlcNAc and Le^x (3) is the first peak in (a)-(d). Other conditions are the same as Figure 3.3D.

- 1 LacNAc, β Gal(1 \rightarrow 4) β GlcNAc-O-TMR
- 3 Le^x, β Gal(1 \rightarrow 4)[α Fuc(1 \rightarrow 3)] β GlcNAc-O-TMR, Lewis X
- 5 β GlcNAc-OTMR, GlcNAc
- 6 H-O(CH₂)₈CONHCH₂CH₂NH-tetramethylrhodamine, the Linker arm

similar after 72 h but with increased formation of products. To confirm the formation of Le^X-O—TMR, the 72-hour incubation product was treated with fucosidase from 2 to 24 h (Figure 3.5); as expected the peak assigned to Le^X-O—TMR disappeared after 24 h digestion, reforming the LacNAc-O—TMR substrate (Figure 3.4 panel D).

Figure 3.6 is electropherograms of 24 and 48 h degradation control of Le^Y, Le^X, H type II, LacNAc and GlcNAc by microsomal enzyme. The Le^Y and Le^X-O—TMR structures were independently found to be stable under the incubation conditions: less than 8% was degraded to form **2** and **6** after 24 h incubation with the microsomal extract of HT-29 cells without added donor (Table 3.4). However, under the same conditions, over 30% of H type **2** (**2**) had degraded to LacNAc-O—TMR and **6** while 12% LacNAc-O—TMR degraded to **5** and **6**. The percentage change of each substrate and hydrolytic products with incubation time are plotted in Figure 3.7 and the corresponding data listed in Table 3.4. Le^Y and Le^X are very stable, however nearly 30% LacNAc is hydrolyzed (122 h) and 67% H type II is degraded, and almost all GlcNAc is converted to the linker arm (H-O-TMR) in 144 h.

Electropherograms of Figure 3.8 confirmed that Le^X-O—TMR was not a substrate for α 1,2Fuc T to produce any Le^Y-O—TMR (Figure 3.8c), i.e. the pathway described in Scheme 3.2 remains valid with the fluorescently labeled derivatives. Whereas H type II is a substrate for α 1,3FucT activity to form Le^Y (Figure 3.8a and b), and meanwhile the fucosidase from the cell extracts competes for H type I. After 48 h, more than half of H type II was converted to Le^Y and 20.9% hydrolyzed to LacNAc (Table 3.5).

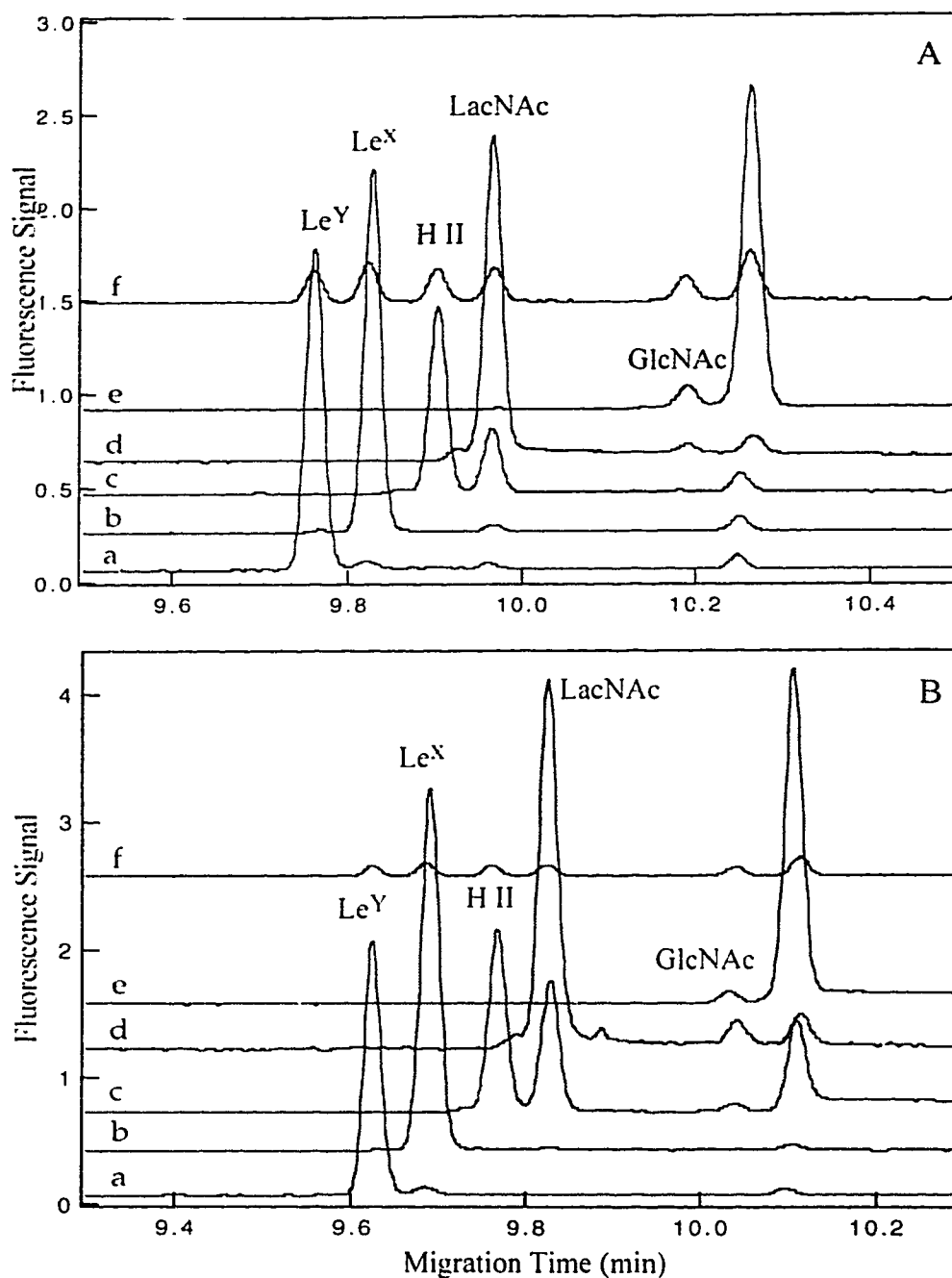


Figure 3.6 Capillary zone electropherograms of degradation controls: (a) Le^Y, (b) Le^X, (c) H type II, (d) LacNAc and (e) GlcNAc incubated with HT-29 microsomal extracts and GDP-fucose for 24 h (A) and 48 h (B). (f) LacNAc standard mixture. 1 μ l of each reaction mixture was placed in a C-18 reverse phase Sep Pak Plus cartridge and eluted with 3.5 ml methanol. Total concentrations of each labeled compounds injected in each case were about $3-5 \times 10^{-8}$ M.

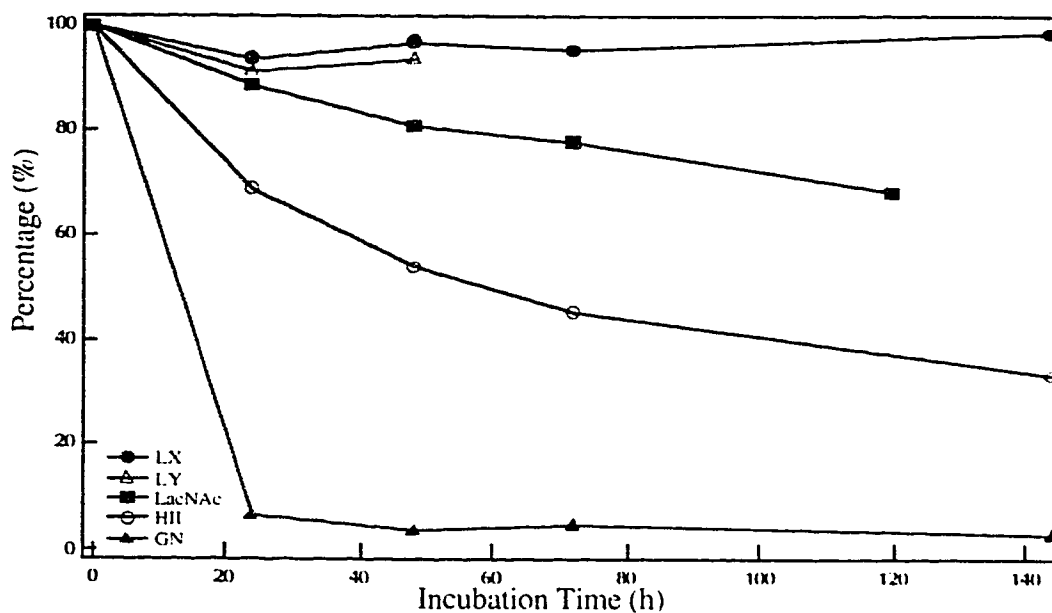


Figure 3.7 The percentage change of Le^Y, Le^X, H type II, LacNAc and Gn hydrolyzed by microsomal enzymes to incubation time (h).

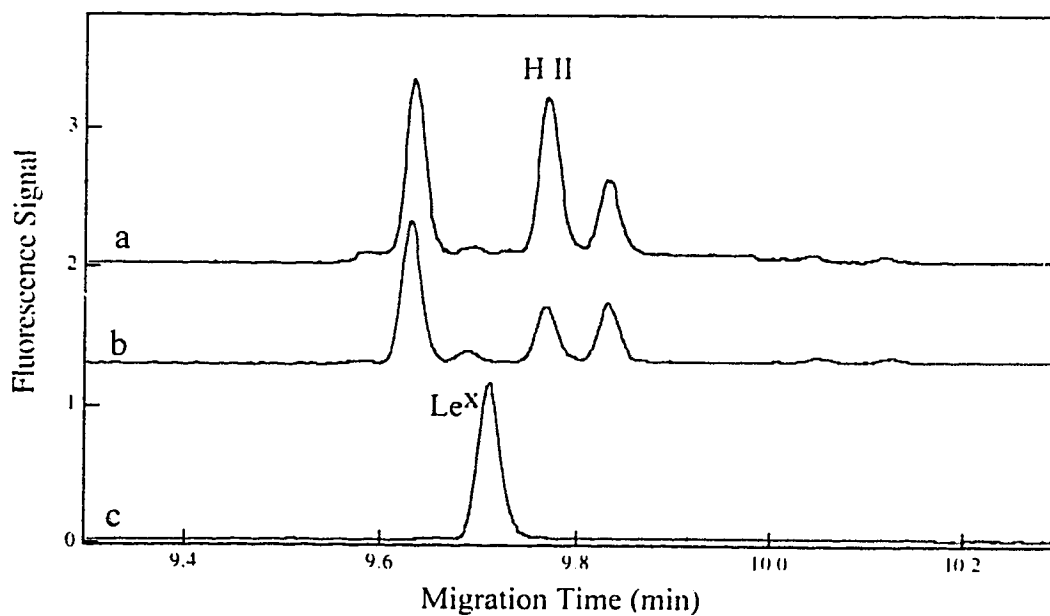


Figure 3.8 Capillary electropherograms of H type II 150 μ M and Le^X-O-TMR after incubation with HT-29 microsomal extracts and GDP-fucose, respectively. (a) H II, 24 h, (b) H II, 48 h, and (c) Le^X, 48 h. The total concentration of labeled compounds injected in each case was $1-2 \times 10^{-8}$.

Table 3.4 Different substrates incubated with HT-29 microsomal extracts

Le^Y Degradation

	Percentage of Substrate and Degradation Products(%)					
Time (h)	Le ^Y	Le ^X	H type II	LacNAc	GlcNAc	HO-TMR
24	91	3		2		4
48	94	3				3
72	*					
144	*					

* no degradation products monitored

Le^X Degradation

	Percentage of Substrate and Degradation Products(%)				
Time(h)	Le ^X	H type II	LacNAc	GlcNAc	HO-TMR
24	94		2		4
48	97		1		2
72	95	5			
144	99		1		

H type II Degradation

	Percentage of Substrate and Degradation Products(%)			
Time (h)	H type II	LacNAc	GlcNAc	HO-TMR
24	69	24		8
48	54	41	1	4
72	46	47	4	3
144	33	57	5	7

LacNAc Degradation

Time (h)	Percentage of substrate and Degradation Products(%)		
	LacNAc	GlcNAc	HO-TMR
24	89	5	7
48	81	10	10
72	78	11	11
144	68	12	20

GlcNAc Degradation

Time (h)	Percentage of substrate and degradation Product(s%)	
	GlcNAc	HO-TMR
24	7	93
48	4	96
72	5	95
144	3	97

Table 3.5 H type II incubation with microsomal enzyme and GDP-fucose

Time (h)	Le ^y	Le ^x	H type II ⁱⁱ	LacNAc
24	44	1	37	17
48	53	5	21	21

^a Substrate

*GlcNAc and HO-TMR less than 1 % are not counted here.

Fucosyltransferase activity has previously been assayed by capillary electrophoresis using enzymatically galactosylated chitobiose as the acceptor which had been chemically conjugated to 7-amino-1,3-naphthalenedisulfonic acid to allow fluorescence detection down to 80 fmol of product (29). In the present work, using TMR as the fluorophore with laser-induced fluorescence detection, the sensitivity is greater by six orders of magnitude for microsomal enzyme assay.

3.5 CONCLUSIONS

The importance of having reference standards of potential biosynthetic products formed from LacNAc sequences is clearly demonstrated in this work using a microsomal preparation of HT-29 cells. In conventional radioactive assays using LacNAc as the acceptor and ^3H or ^{14}C -labeled GDP-fucose as the donor, the identity of the major fucosylated product, the Le^x structure, would not have been established. Furthermore, the degradation pathways we observed for both substrate and product would not have been seen. Such degradation pathways will be more dominant when whole cell extracts, or intact cells (chapter 4), are used as the enzyme source with the outcome that erroneous conclusions about the enzyme activities present may be reached. While the present study was restricted to the assay of fucosyltransferases it should be readily adaptable for other glycosyltransferases, especially sialyltransferases and glucosaminyltransferases, acting on LacNAc sequences, since the required fluorescently labeled reference standards can be prepared from 1-4 using either cloned or isolated enzymes (3, 4, 26, 27) of known specificities.

3.6 REFERENCES

- (1) Varki, A. *Glycobiology* **1993**, 3, 97-130.
- (2) Fukuda, M. in *Molecular Glycobiology: Frontiers in Molecular Biology Series* (M. Fukuda and O. Hindsgaul, Eds.), Oxford University Press, Oxford, UK, **1994**, pp 1-52.
- (3) Lowe, J. B., in *Molecular Glycobiology: Frontiers in Molecular Biology Series* (M. Fukuda and O. Hindsgaul, Eds.), Oxford University Press, Oxford, UK., **1994**, pp 163-205.
- (4) H. Schachter, in *Molecular Glycobiology: Frontiers in Molecular Biology Series* (M. Fukuda and O. Hindsgaul, Eds.), Oxford University Press, Oxford, UK., **1994**, pp 88-162.
- (5) Sadler, J. E., Beyer, T. A., Oppenheimer, C. L., Paulsen, J. C., Prieels, J.-P., Rearick, J. I., and Hill, R. L. *Methods Enzymol.* **1982**, 83, 458-514.
- (6) Cummings, R. D. *Methods Enzymol.* **1994**, 230, 66-86.
- (7) Baenziger, J. U. *Methods Enzymol.* **1994**, 230, 237-249.
- (8) Kobata, A. *Methods Enzymol.* **1994**, 230, 200-208.
- (9) Keshvara, L. M., Gosselin, S., and Palcic, M. M. *Glycobiology* **1993**, 3, 416-418.
- (10) Gosselin, S., Alhussaini, M., Streiff, M. B., Takabayashi, K., and Palcic, M. M. *Anal. Biochem.* **1994**, 220, 92-97.
- (11) Olechno, J. D. and Ulfelder, K. J. *CRC Handbook of Capillary Electrophoresis: A Practical Approach*, CRC Press, **1994**, pp 255-286.
- (12) Oefner, P. E. and Chiesa, C. *Glycobiology*, **1994**, 4, 397-412.
- (13) Cheng, Y. F., and Dovichi, N. J. *Science* **1988**, 242, 562-564 .
- (14) Wu, S. and Dovichi, N. J. *J. Chromatog.* **1989**, 480, 141-155.
- (15) Zhao, J. Y., Dovichi, N. J., Hindsgaul, O., Gosselin, S., and Palcic, M. M. (*Glycobiology* **1994**, 4, 239-242.

- (16) Zhao, J. Y., Diedrich, P., Zhang, Y., Hindsgaul, O., and Dovichi, N. J. (*) Journal of Chromatography* **1994**, 657, 307-313.
- (17) Chen, D. Y. and Dovichi, N. J. *J. Chromatog. B* **1994**, 657, 265-269.
- (18) Chen, D. Y., Adelhelm, K., Cheng, X. L., and Dovichi, N. J. *The Analyst* **1994**, 119, 349-352.
- (19) Lemieux, R. U., Bundle, D. R., and Baker, D. A. *J. Amer. Chem. Soc.* **1975**, 97, 4076-4083.
- (20) Hindsgaul, O., Norberg, T., LePendu, J., and Lemieux, R. U. (*) Carbohydr. Res.* **1982**, 190, 109-142.
- (21) Khare, D. P., Hindsgaul, O., and Lemieux, R. U. *Carbohydr. Res.* **1985**, 136, 285-308.
- (22) Gokhale, U. B., Hindsgaul, O., and Palcic, M. M. *Can. J. Chem.* **1990**, 68, 1063-1071.
- (23) Palcic, M. M., Heerze, L. D., Pierce, M., and Hindsgaul, O. *Glycoconjugate J.* **1988**, 5, 49-63.
- (24) Zhao, J. Y., Chen, D. Y., and Dovichi, N. J. *J. Chromatog.* **1992**, 608, 117-120.
- (25) Stroup, G. B., Anumula, K. R., Kline, T. F., and Caltabiano, M. M. *Cancer Research* **1990**, 50, 6787-6792.
- (26) Macher, B. M., Holmes, E. H., Swiedler, S. J., Stults, C. L. M., and Srnka, C. A. *Glycobiology* **1991**, 1, 577-584.
- (27) Lowe, J. B. *Seminars Cell Biol.* **1991**, 2, 289-307.
- (28) Knoll, J. E., *J. Chrom. Sci.*, **1985**, 23, 422-425.
- (29) Lee, K. B., Desai, U. R., Palcic, M. M., Hindsgaul, O., and Linhardt, R. J. *Anal. Biochem.* **1992**, 205, 108-114.

CHAPTER 4

Le^c UPTAKE BY A431 CELLS

Acknowledge: Thanks to Dr. Rakesh Bhatnager for technical assistance on confocal laser scanning microscopy study.

4.1 INTRODUCTION

In the previous chapter, the enzymes from HT-29 microsome cell extracts were studied using CE-LIF with a sheath flow cuvette as a post-column detector. In this chapter we will further utilize capillary electrophoresis to analyze the contents of A431 cells grown in the presence of Le^f substrates.

Capillary electrophoresis has been applied recently to separate nucleotides (1), derivatized amino acids (2), recombinant human interferon-glycoforms (3) from different cell types, and as well as the surface glycoproteins in ovine lentiviruses (a group of viruses that infect sheep and goats) (4). However there is little information on the separation and detection of oligosaccharides by CE from cancer cells, especially from *in vivo* cell uptake experiments.

The human epidermoid carcinoma A431 cell line was earlier shown to express blood group Le^a and Le^b structures on the carbohydrate chains of the epidermal growth factor receptor which occurs on its cell surface (5). Since aberrant expression of cell surface glycoconjugates is thought to be a reflection of alteration in glycosyltransferase activities, it is important to investigate the enzymes involved in their biosynthesis (6).

The assay of glycosyltransferases in cells involves transfer of a radiolabeled monosaccharide residue from the sugar-nucleotide to a suitable acceptor oligosaccharide (7, 8). Generally, these radioactive techniques require picomoles of product to be formed for quantitation. Enzyme-linked immunosorbent assays (ELISAs) for glycosyltransferases have recently been used and while more complex in their requirement for reagents, they have added advantages in that the glycosylation products formed are structurally characterized by their binding with a specific antibody or lectin (9, 10, 11). The sensitivity is also tremendously increased with detection of a product in the femtomole range. Very recently, fluorescently labeled oligosaccharides have been used as glycosyltransferase-acceptors and the products separated by either chromatography or electrophoresis (12, 13). The detection of an attomole of a labeled

oligosaccharide has been reported (14). The sensitivity achieved in a *in vitro* glycosyltransferase assay was from the femtomole range in 1992 (13) to 100 molecules in 1994 reported by Dovichi's group (15).

All methods mentioned above have in common that a sugar-nucleotide is added to the cell extract (*in vitro*) and the enzymatic reaction products can usually be predicted. However, in *in vivo* cell uptake experiments, all sugar-nucleotides must be produced by the cells (endogenous) and the biosynthetic products are a complicated mixture. The development of a fluorescence-based glycosyltransferase assay can be used to quantitate less than 1000 molecules of products formed, which is the most sensitive of any non-amplified assay for enzyme activity. This assay involves the preparation of structurally well-characterized specific acceptors for glycosyltransferases that are covalently attached to fluorescent dyes selected for their favorable excitation and emission properties as well as cell membrane permeability.

In this chapter, the *in vivo* uptake of Le^c and LacNAc substrates by A431 cells was achieved by growing the cells with TMR labeled substrates. After approximately 20 h of growth, the excess Le^c-TMR was removed by washing the cells with isotonic buffer. Confocal microscopy was used to monitor the fluorescence in the cells. Then a portion of the labeled cells was lysed and products from the lysate were purified and concentrated, then analyzed by LIF-CE.

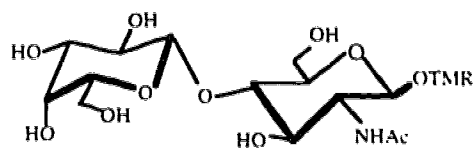
The behavior of the fluorescent oligosaccharides towards commercial exo-glycosidases and several other hydrolytic enzymes was evaluated as an additional means for the structural characterization of peaks on the electropherograms.

4.2 MATERIALS AND METHODS

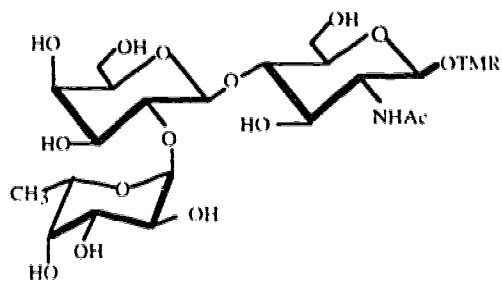
Materials

8-methoxycarbonyloctanoltetramethylrhodamine HO(CH₂)₈CO-TMR (H-O-TMR, **6**) and its glycosides. βGlcNAc-O-TMR (GlcNAc, **5**), βGal(1→3)βGlcNAc-O-TMR (Le^c, **7**) were chemically synthesized and provided by Dr. Ole Hindsgaul (16) The potential biosynthetic products αFuc(1→2)βGal(1→3)βGlcNAc-O-TMR (H I, **8**), βGal(1→3)[αFuc(1→4)]βGlcNAc-O-TMR (Le^a, **9**), αFuc(1→2)βGal(1→3)[αFuc(1→4)]βGlcNAc-O-TMR (Le^b, **10**), αNeuAc2→3βGal(1→3)βGlcNAc-O-TMR (2.3-sialyl Le^c, **11**), αNeuAc2→6βGal(1→4)βGlcNAc-O-TMR (2.6-sialyl LacNAc, **12**), and αNeuAc2→3βGal(1→3)βGlcNAc-O-TMR (2.3-sialyl LacNAc, **13**) were enzymatically synthesized and provided by Dr. Monica M. Palcic (Scheme 4.1 to 4.3).

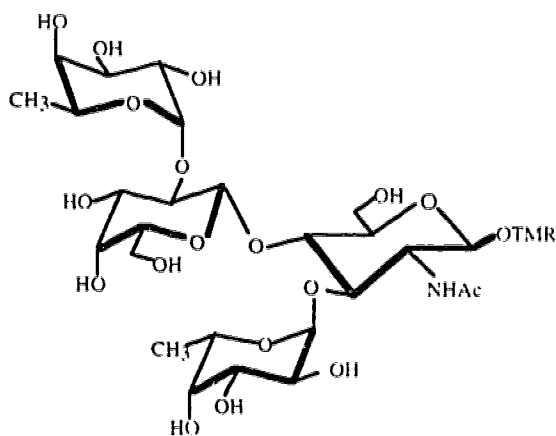
Cell culture flasks (T 25 cm²) were purchased from Falcon. Fetal calf serum (FCS) and Dulbecco's Modified Eagle's Medium (DMEM) with high glucose and 10X TE (0.5% trypsin and 5.3 mM EDTA 4Na) were obtained from Gibco (Gibco BRL). Phosphate buffered saline (PBS) was prepared from NaCl, 8 g; KCl, 0.2 g; Na₂HPO₄, 1.84 g; Na₂HPO₄•12H₂O, 1.5g, at pH 7.5. TE (1X) was made by diluting TE (10X, kept under -20° C) solution with PBS buffer and filtering through a 0.22 μm filter (Nalgene). Lyophilization was done on Virtis Vacuum Concentrator (Virtis Sentry 5L, The Virtis Company, Inc. Gardiner, N.Y., 12525) and Speed Vac (SC100, Savant). Polypropylene disposable sterile cryogenic vials were purchased from Corning. The cell incubator and hood were from Forma Scientific. An aspirator pump (Neuberger Vacuum Pump) was used. The cell counting device was 10 hemocytometer Deck glassier (Germany). Reagents purchased from Sigma were: 3'-phosphate adenosine 5'-phosphosulfate C₁₀H₁₅N₅O₁₃P₂S (PAPS), dimethyl sulfoxide (DMSO), HEPES (N-(2-hydroxyethyl)piperazine-N'-ethanesulfonic acid, pKa 7.55), Triton X-100 (t-octylphenoxypolyethoxyethanol), DEA (Diethanol Amine), cacodylic acid sodium salt (CH₃)₂AsO₂Na, dimethylarsinic acid sodium salt). Potassium phosphate (KH₂PO₄) was



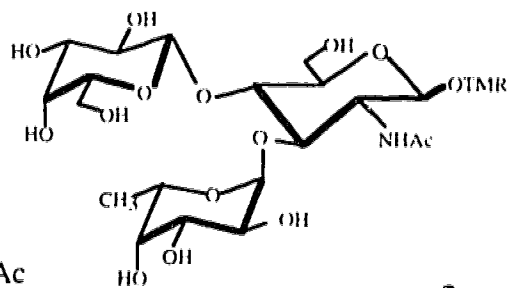
LacNAc (1)
 β Gal(1→4) β GlcNAc



H type II or H II (2)
 α Fuc(1→2) β Gal(1→4) β GlcNAc

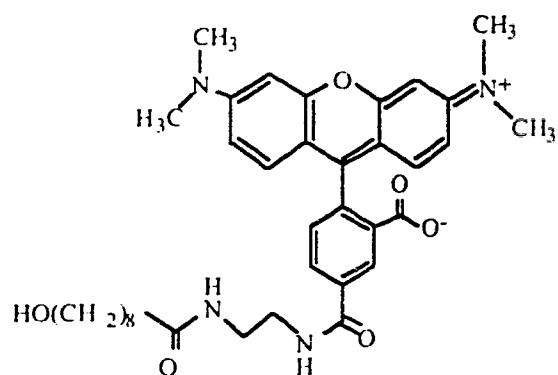


Lewis Y or Le^Y (4)
 α Fuc(1→2) β Gal(1→4)[α Fuc(1→4)] β GlcNAc

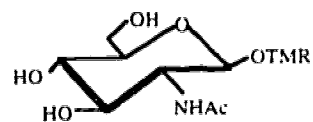


Lewis X or Le^X (3)
 β Gal(1→4)[α Fuc(1→3)] β GlcNAc

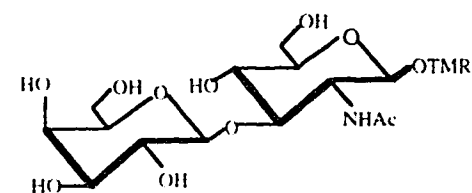
Scheme 4.1 Structures of LacNAc series standards.



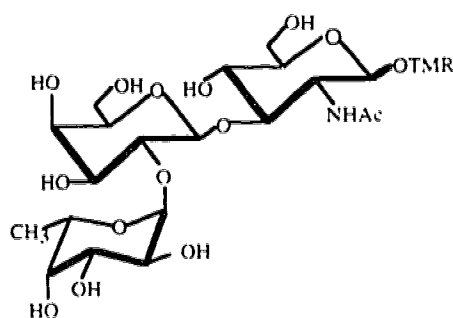
H-OTMR (6)



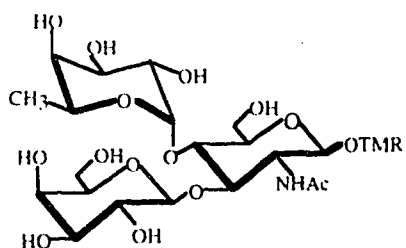
GlcNAc (5)
N-acetyl-β-D-Glucosaminide-O-TMR



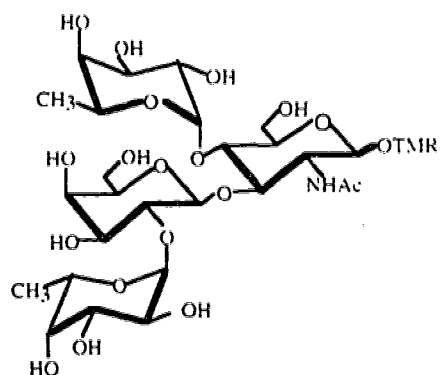
Lewis C or Le^c (7)
βGal(1→3)βGlcNAc



H type I or (H I) (8)
αFuc(1→2)βGal(1→3)βGlcNAc

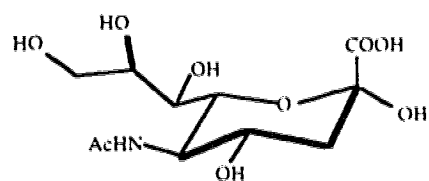


Lewis A or Le^a (9)
βGal(1→3)[αFuc(1→4)]βGlcNAc



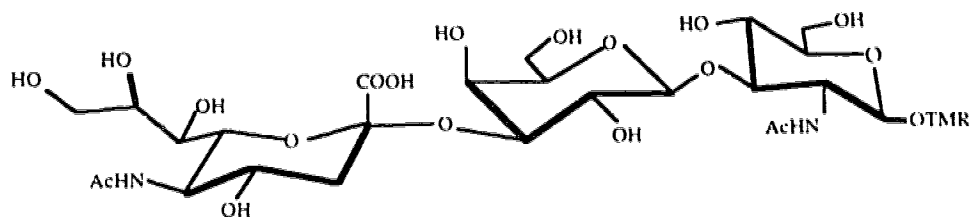
Lewis B or Le^b (10)
αFuc(1→2)βGal(1→3)[αFuc(1→4)]βGlcNAc

Scheme 4.2 Structures of Le^c series standards.



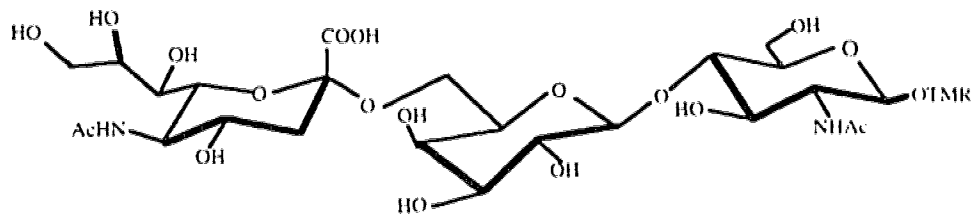
Sialic Acid

α NANA



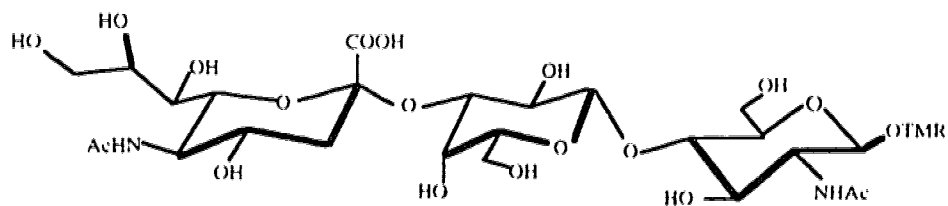
2,3-Sialyl Le^c (11)

α NANA(2→3) β Gal(1→3) β GlcNAc



2,6-Sialyl LacNAc

α NANA(2→6) β Gal(1→4) β GlcNAc (12)



2,3-Sialyl LacNAc

α NANA(2→3) β Gal(1→4) β GlcNAc (13)

Scheme 4.3 Structures of sialyl standards.

from BDH. 3-aminophenylboronic acid (monohydrate, 98%) was from Aldrich. TRIS (tris(hydroxymethyl)aminomethane) was from Fisher. All solutions were filtered through a 0.2 μm filter (Corning Glass Works, Corning, NY) to remove particulates. The glycosidase properties and the buffer used for assays are listed in Table 4.1 and Table 4.2. C-18 Sep Pak cartridges were purchased from Millipore (MA, USA). A water jacketed incubator (NUAIR) was used.

Methods

4.2.1 Cell Culture

The culture medium (CM) for the human A431 epidermoid carcinoma and HT-29 colon adenocarcinoma cells was prepared by mixing 450 ml DMEM (Dulbecco's Modified Eagle's Medium) containing high glucose (90%) and L-glutamine, and 110 mg/ml sodium pyruvate with 50 ml of inactivated FCS (fetal bovine serum) and 2 mL gentamycin (10 mg/mL stock). the solution was filter sterilized, transferred aseptically to 50 mL Falcon tubes and stored at 4 °C. FCS was inactivated by heating at 56 °C for 15 minute to destroy complement that could kill cells.

A431 cells (passage #?) were obtained from the American Type Culture Collection (ATCC, Rockville, MD) and cultured in the medium (90% DMEM and 10% FCS) described above at 37 °C in water saturated 5% CO₂ atmosphere (pH 7.2 to 7.4). CM was removed by pipette and replaced with the same amount of fresh CM (6 mL) every 24 h. A 72 h cell incubation gave 60-70% confluence. Then the CM was removed to get rid of FCS which contains a trypsin inhibitor. Cells were washed twice with 6 mL PBS buffer. Then 2 mL TE (1X) (0.05% trypsin and 0.53 mM EDTA) was added to the flask in the incubator for 10 min to detach the adherent cells from the plastic container. Trypsin was inactivated by the addition of about 4 mL of the CM. A small part of the cell suspension (100 μL) was used for counting or viability testing by mixing with 200 μL

trypan blue (0.4% in PBS, Sigma) with a haemocytometer. Meanwhile, most of the cell suspension was pelleted by centrifugation (< 1000 g) for 10 min and the medium was removed. The cell pellet was resuspended in 1 mL of CM. Continuous cultures were maintained every 4 days by seeding $2-4 \times 10^4$ cell/cm² (or 1×10^5 cells/mL) to 6 mL CM to a new culture flask. The remaining cells (2×10^6 cells) were pelleted. One milliliter frozen medium containing 700 μ L DMEM, 200 μ L FCS and 100 μ L DMSO was added to the pellet and the pellet was kept at -70 °C (17).

4.2.2 Preparation A431 Crude Cell Extracts and Incubation with Le^c-O-TMR

4.2.2.1 Crude cell extract preparation

One milliliter of cell extraction buffer containing 50 mM HEPES, 25% glycerol and 1 mM EDTA (pH 7.0) was added to the thawed cell pellet (1.2×10^8 cells) and the suspension was transferred to a Wheaton homogenizer. An additional 1 mL of buffer was added to rinse the tube and combined with the first wash. Then, 38 μ L of 16% Triton X-100 solution was added to the cell suspension to give a final Triton X-100 concentration of 0.2%. Cells were kept on ice and disrupted by 20 strokes of the homogenizer every 15 min for 1.5 h. The solution was transferred to a centrifuge tube and was centrifuged using a JA-20 rotor at 41,400 g (18,500 rpm) for 30 min. The supernant was removed and stored in a conical tube.

4.2.2.2 Incubation of A431 crude cell extracts with Le^c-TMR or LacNAc-TMR and GDP fucose

Assay buffer, 4 μ L, containing 200 mM HEPES, 200 μ M MnCl₂ and 2% bovine serum albumin, 31.8 μ L of A431 cell extract (2×10^6 cells or 1.2×10^8 cells / 2mL), 2.2 μ L of 0.9 mM substrate Le^c-TMR (or 2 μ L of 1 mM LacNAc-TMR) and 2 μ L of 1 mM GDP-fucose donor were added to a 0.5 mL microfuge tube. The final concentrations of Le^c-TMR, LacNAc-TMR, and GDP-fucose was 50 μ M. The mixtures were vortexed.

centrifuged in a microcentrifuge, wrapped in aluminum foil and transferred to 50 mL Falcon tubes. The mixtures were rotated end over end overnight at room temperature. At 17 and 41 h, 20 μ L of each incubation mixture was removed and loaded onto a C-18 Sep Pak cartridge. Each C-18 Sep Pak cartridge was washed with 10 mL HPLC methanol and 20 mL Milli Q water before use. The loaded cartridge was washed with 30 mL of Milli Q water, then fluorescent products were eluted with 3.5 mL HPLC grade methanol. For CE analysis 5 μ L of methanol eluent was diluted to 50 μ L buffer by adding 20 μ L methanol and 25 μ L PBpBS. The total TMR concentration was 2.8×10^{-8} M in each injected sample.

4.2.2.3 Incubation of A431 cell extracts with Le^c-TMR without donor GDP Fucose

The incubation mixture contained 200 μ L of A431 cell extract (1.4×10^7 cells or 6.7×10^7 cells/mL), 5.1 μ L of 1 mM Le^c-TMR (final concentration 25 μ M) and 1 μ L of 1 M MnCl₂ (to remove EDTA). The mixture was incubated at 37 °C for 21 and 65 h. After incubation, each sample was purified on a Sep Pak cartridge as described above. The 3.5 mL of MeOH eluent was lyophilized. The dried mixtures were redissolved in 513 μ L of MeOH. Mixtures were diluted to 10^{-7} M with running buffer prior to CE analysis.

4.2.2.4 Cell extract incubation with Le^c and PAPS (a sulfate donor)

The mixture containing 200 μ L enzyme extract of A431 cells (2.6×10^7 cells or 6.5×10^7 cells/0.5 mL), 5.2 μ L 1 mM of Le^c-TMR, 1 μ L of 1M MnCl₂, and 1 μ L of 2 mM PAPS donor were incubated at 37 °C for 65 h. At 24 and 48 h, 1 mL of 2 mM PAPS was added. A control experiment was done in an analogous fashion with cell extract and Le^c by adding 3 μ L of HPLC water instead of PAPS. Products were isolated as described above.

4.2.3 Le^c-TMR Uptake by A431 Cells

Cells that reached 60-70% confluence (a total of 3×10^6 cells per T 25 cm² culture flask) were washed with 6 mL PBS buffer. Fresh CM containing Le^c-TMR (typically 25 μ M) was added to the cell culture flask. Incubation was continued for 18-20 h at 37 °C and in 5% CO₂ atmosphere. CM containing Le^c-TMR was removed and saved for CE analysis. A total volume of 250 mL PBS was used to wash away the excess Le^c-TMR from the cells. The final PBS wash (10 mL) was also saved for CE analysis (PBS wash pretrypsin). Then 2 mL trypsin-EDTA (0.05% trypsin and 0.53 mM EDTA) was added to the flask and incubated for 10 min at 37 °C. Most of cells were detached from the bottom of the flask and the flask was rotated gently back and forth to detach the remaining cells from the flask wall. Trypsin was inactivated by the addition of about 2 mL of the CM. The flask content was transferred to a round centrifuge tube and spun down at 1000 g for 10 min. The supernatant was saved for CE analysis (this is referred to as PBS wash after Trypsin) and the pellet was used for confocal microscopy and CE analysis.

A portion (2/3) of the pellet was lysed by adding 500 μ L Milli Q water and vortexed until the pellet disappeared (i.e. lysed). The lysate was loaded to a Sep Pak Plus C-18 Cartridge, then washed with 30 mL of Milli Q water. Sugar-TMR compounds were finally eluted in 3.5 mL methanol. This sample and several other samples (saved from the last PBS wash, trypsin wash and culture medium with Le^c-TMR) were diluted in running buffer prior to CE injections.

4.2.4 HT-29 Cells (Colon. Adenocarcinoma. Human. from ATCC)

Cell culture and subculture were the same as described for the A431 cells. Generally, 70-80% confluence was reached in 72 h of growth at 37 °C in 5% CO₂ atmosphere.

HT-29 cell uptake of LacNAc-TMR: Two T × 25 cm² flasks of HT-29 cells (6-8 × 10⁶ cells, 80% confluence) were incubated with 25 μM LacNAc-O-TMR for 20 to 22 h at 37 °C in water saturated 5% CO₂ incubator. Cell wash and sample collection steps were the same as in A431 cell uptake experiments.

4.2.5 Product Identification Approach with Hydrolysis Enzymes

The substrate specificities of fucosidases and neuraminidase are listed in Table 4.3 and the assays are described as follows.

4.2.5.1 Fucosidase assays

4 μL pH 5.5 buffer and 1 μL of 15.6 μU/μL α-fucosidase from human placenta were added to 5 μL (Le^c uptake by A431 cell mixture) pellet in methanol. The mixture was incubated for 94 h at 37 °C. 4 μL methanol was added prior to CE analysis.

4.2.5.2 Neuraminidase assay

Typically, 1 to 5 μL of sample containing either lysate from Le^c growth with A431 cells or incubation with cell extract and GDP-fucose was lyophilized. Then 4 μL of 150 mM citrate (pH 5) buffer and 1 μL of 9 μU/μL or 900 μU/μL neuraminidase were added and incubated at 37 °C for 46 h. The mixture was loaded on a Sep Pak cartridge and purified by the same steps described in 4.2.2.2. The sample eluted from the Sep Pak cartridge was dried. 5 μL MeOH was added to the dried sample prior to the CE analysis.

4.2.5.3 Phosphatase assay

Alkaline phosphatase assay: 2 μL of mixture A (cell extract 65 h incubation with Le^c without adding donor), 0.1 μL of alkaline phosphatase (1 mU/ μL), and 5 μL 50 mM Tris buffer (pH 8.5) were added together, vortexed and incubated for 68 h at 37 °C in an Isotemp Incubator (Fisher). The mixture was purified on a C-18 cartridge as described

in 4.2.2.2. lyophilized and then resuspend in 100 μ L PBpBS buffer before making a CE injection. A total of 2×10^{-7} M TMR was injected.

Phospholipase A₂ assay: A 7 μ L volume of mixture A was lyophilized. 5 μ L of 50 mM Tris-HCl (pH 8.6) or 250 mM DEA (pH 9.5) and 1 μ L (2 U/ μ L) phospholipase A₂ were added and the solution was vortexed. Incubation proceeded for 66 h at room temperature in the dark (inside drawer). The purification steps were the same as before (4.2.2.2). Samples were lyophilized and diluted in 100 μ L P_{1.75}BpBS buffer. A total of 2×10^{-7} M TMR was injected on CE.

4.2.5.4. Sulfatase digestion assays

2 μ L of mixture A (10 μ M total TMR, 4.2.2.3) was lyophilized. Then 3.5 μ L 150 mM citrate (pH 5.0) and 2.5 μ L (1 μ unit) sulfatase from limpet or sulfatase from abalone entrails were added. The mixture was incubated at 37 °C for 65 h. Using the same clearing up procedures, the sample was lyophilized and redissolved in 50 μ L PBpBS buffer and a total 4×10^{-7} M TMR was injected onto a capillary column.

Sulfatase (Aerobacter aerogenes) assay 7 μ L mixture A (1.5 μ M total TMR) was dried. 5 μ L of 1 M sodium cacodylate buffer (pH. 7.1) and 1 μ L (19 μ unit/ μ L) sulfatase from aerobacter aerogenes were added and incubated for 66 h at 37 °C. The sample was purified on a Sep Pak cartridge, dried, and diluted in 100 μ L P_{1.75}BpBS buffer. The final injection concentration was 10^{-7} M total TMR.

4.2.6 Sample Preparation for MALDI-MS (by Randy Whittle from Dr. Liang Li's group)

A 1 mL of mixture A (4.2.2.3) was used for mass analysis. α -cyano-4 hydroxy-cinnamic acid (4-HCCA) (Aldrich) matrix solution of 0.12 M was prepared in 99% acetone and 1% H₂O. A 1 μ L aliquot of the matrix solution was placed on the sample probe. The mixture A, dissolved in methanol, was lyophilized and redissolved in 1:1

MeOH/H₂O. Then, 0.5 µL of this mixture was mixed with 33 mM 4-HCCA (in 33% CH₃CN/H₂O) in 1:1 ratio and deposited on top of the first matrix for MS analysis.

4.2.7 Laser Scanning Confocal Microscopy (Dr. Rakesh Bhatnagar from Biological Science Microscopy unit, University of Alberta)

A Molecular Dynamics, Multiprobe 2001 confocal laser scanning microscope (CLSM, Nikon TMD) was used. Samples were first examined with epifluorescence using a converted microscope (x100) with oil immersion (Resolve, high viscosity) objective (1.4 numerical aperture). Cell pellets were placed on a microscope slide and then covered with a coverslip. In some experiments fluorescent cells were fixed for 20 min at room temperature with Carlson-Millonig fixative (pH 7.2). The phase contrast mode was used to locate a cell and the fluorescence in the cell was monitored using the fluorescence mode. Then, confocal scanning microscopy was used to collect a series of pictures (20-30 sections) every 0.25 µm section thickness and images were collected and processed by Image space 3.1 software, on the Silicon Graphics Indigo workstation. The confocal microscope used an Argon/Krypton laser for excitation at 568 nm and an emission filter at 590 nm for collecting the rhodamine signal. Micrographs were taken using Fuji, super HG color negative film. Color prints were made using a Mitsubishi CP210 printer.

4.2.8 CE Separation Conditions

The CE-LIF system was the same as in Chapter 3. The capillary is about 10 µm i.d. x 40 cm long. The electrophoresis running buffer contained 10 mM Na₂HPO₄, 10 mM borate, 10 mM phenyl boronic acid, and 10 mM SDS (pH 9). Injection and separation electric fields were 1000 v for 5 sec and 400 v/cm respectively. A typical standard mixture contained 5 × 10⁻¹⁰ M each of Le^c, Le^a, Le^b, GlcNAc and the linker arm (HO-TMR), and 1 × 10⁻⁹ M of H type I.

4.3 RESULTS AND DISCUSSION

4.3.1 A431 Cell Extract Analysis by CE-LIF

4.3.1.1 Standards of substrate and possible biosynthetic and hydrolysis products

Scheme 4.4 summarizes the biosynthetic transformations for which standards were prepared and analyzed in this work. Degradation of Le^c-O-TMR (7) by β -galactosidase would produce β GlcNAc-O-TMR (5) that, on further degradation by a hexosaminidase, would liberate the fluorescently tagged linking arm (HO-TMR, 6). With GDP-fucose as the only supplementary glycosyl donor to the enzyme from crude cell extracts, fucosylation could occur first by either an addition of an $\alpha(1\rightarrow2)$ FucT to yield the H type I trisaccharide (8) or an $\alpha(1\rightarrow4)$ FucT to produce the Le^a sequence (9). Trisaccharide 2 remains active as a substrate for the $\alpha(1\rightarrow4)$ FucT which converts to the Le^b sequence (10). However, structure 9 is not a substrate for the $\alpha(1\rightarrow2)$ FucT and can therefore not be converted to 10. GDP-fucose that can be added to a crude cell extract (*in vitro*) gives a advantage since other enzymes do not have enough sugar nucleotide available to compete for the same substrate.

4.3.1.2 A431 cell extracts incubation with substrates and GDP-fucose

When an A431 cell extract was incubated with the Le^c substrate, Le^a and H type I were formed within 17 h. This results from the addition of a fucose to Le^c by an $\alpha1.4$ and $\alpha1.2$ Fuc T, respectively (**Figure 4.1**). After 41 h, further addition of a fucose to H I produced Le^b. From the Le^a and H type I peak heights, the $\alpha1.4$ and $\alpha1.2$ Fuc T activities in cell extracts were similar when Le^c was used as a substrate. For A431 cell extracts incubated with LacNAc (**Figure 4.2**), only H type II is observed along with an unconverted substrate. No Le^x was detected. Therefore, LacNAc was a poorer substrate for $\alpha1.2$ Fuc T and no $\alpha1.3$ Fuc T was detected even with the addition of GDP-fucose donor. Watkins' group (18) has also reported that Le^c was a better substrate than LacNAc

when Triton-solubilized A431 cell suspensions and GDP-fucose were incubated with these acceptors. The radiochemical methods they used could not differentiate between the two products (either Le^a and H type I or Le^x and H type II) using the same substrate (Le^c or LacNAc) with GDP fucose as a donor. Therefore their activity calculation ignored the contribution from the formation of H I and H II (α 1.2 Fuc T). However, in our experiments, no Le^x was formed after 41 h when LacNAc-O-TMR was incubated with an A431 cell extract. Watkins' group was able to purify an α 1.3/4 Fuc T activity from spent A431 cell culture medium and they also tested their substrates' specificity. They found that the best acceptor of the substrates tested was the Le^c disaccharide bearing the hydrophobic linker arm (-O-(CH₂)₈COOMe), and the corresponding LacNAc disaccharide was a very poor acceptor. The relative activity was 100/11 when Gal β (1 \rightarrow 3)GlcNAc and Gal β (1 \rightarrow 4)GlcNAc were used as substrates, but became 227/2 when the two substrates were attached to the hydrophobic linker. The presence of α 1.3 Fuc T activity was further confirmed using H II as a substrate and an α 1.3 fucosylated product (Le^b) was isolated. However no α 1.3 fucosyltransferase activity was detected in our CE experiments, this might be due to the TMR on our substrate, since the aglycon dramatically affects the α 1.3 fucosyltransferase activity.

4.3.2 A431 Cell Uptake

4.3.2.1 A431 cell uptake of Le^c monitored by confocal microscopy

Photographs of fluorescently labeled cells cultured for 18 h with 25 μ M Le^c in the medium are shown in **Figure 4.3** left panel. The small triangle finger-like bright area is believed to be the Golgi complex. The picture next to it is a phase contrast image of whole cells. The cell nucleus is the dark central area. More than half the cells contain Le^c-TMR, though some of the cells give relatively weak fluorescence signals. More than 95% of the cells are viable after incubation with Le^c-TMR. The *in vivo* biosynthetic

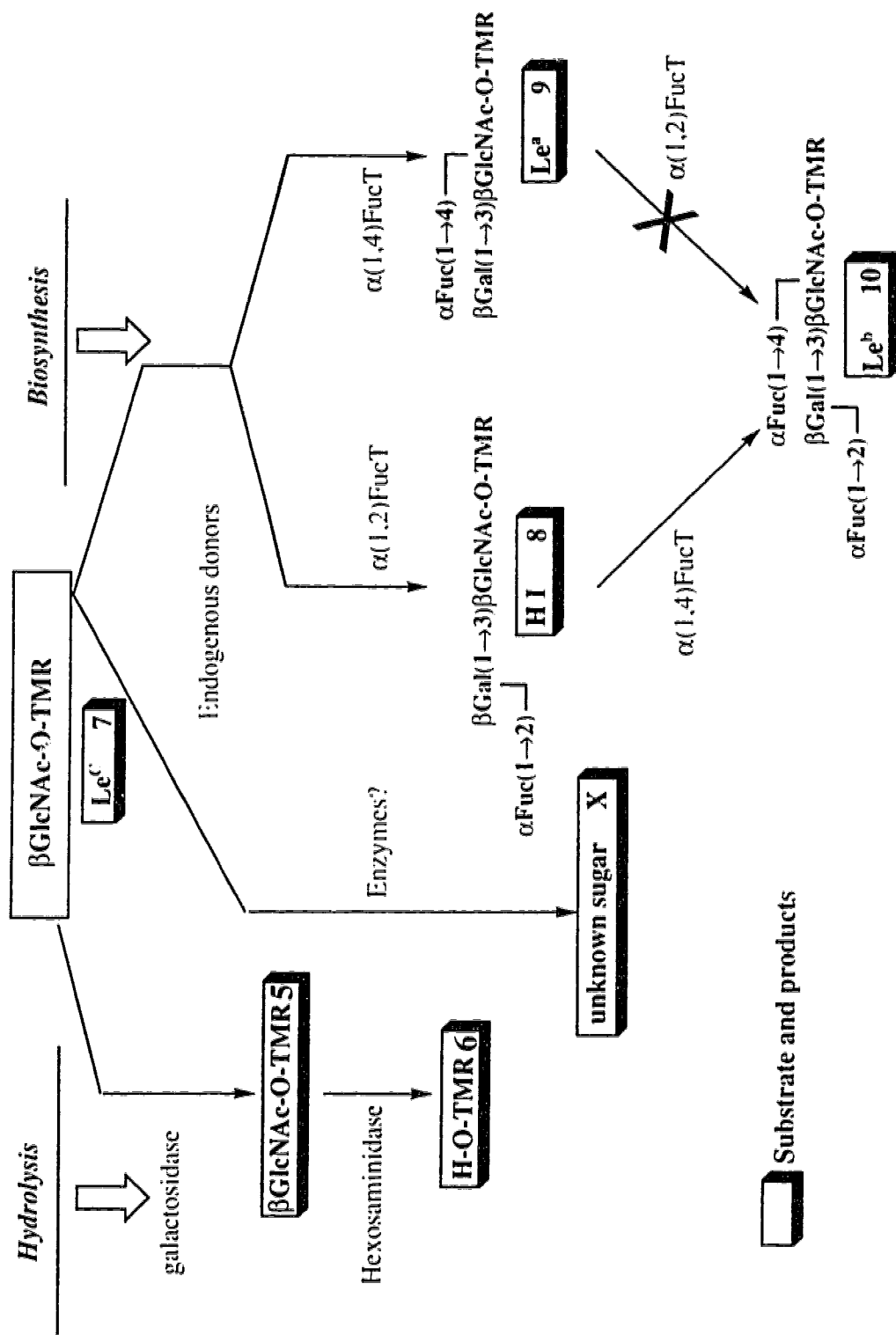
products formed inside the Golgi complex of A431 cells incubated with Le^c can be confirmed by CE analysis.

It has been found that the membrane solubility of a substrate is a key factor in the internalization of the compound, while its movement into the Golgi will be the limiting factor in the biosynthesis of oligosaccharides (19). However, our experimental results are insufficient to give a time course study of Le^c-TMR internalization and localization to the Golgi apparatus in A431 cells. A more detailed study of internalization and sorting using other fluorescent analogues of glycosylceramide to the Golgi apparatus has been reported by Pagano's group (20, 21), which can be valued as a useful model for our future cell uptake study with oligosaccharide substrates.

4.3.2.2 Le^c-TMR uptake by A431 cells

Scheme 4.4 is a summary of the biosynthetic transformation of Le^c taken up by A431 cells. One of the differences compared with **Scheme 4.1** is the potential formation of new products (unknown sugar X). These are formed because other glycosyltransferases can use Le^c or its biosynthetic products as substrates along with endogenous donors to synthesize novel products.

The electropherograms of **Figure 4.4** represent the contents of about 10 A431 cells after growth with 25 μM of Le^c for 20 h. The internalization and localization of Le^c-TMR in A431 cells was discussed in the previous paragraph. The biosynthetic products generated inside the Golgi complex by endogenous donors and glycosyltransferases reacted with a substrate are shown in trace **a** in **Figure 4.4**, where unreacted substrate Le^c remains as the biggest peak. Peaks in front of Le^c are H type I and Le^a respectively, but the H type I peak is bigger than that of curve **a** in **Figure 4.1**. A new peak containing about 18,000 TMR labeled molecules with an early migration time around 9.3 min is close to the standard of 2,3sialyl Le^c in **Figure 4.4d**. The hydrolytic products are



Scheme 4.5 Some potential biosynthetic transformations of Le^C-O-TMR uptake by A431 cells.

produced much more in cell uptake experiments than in cell extracts incubated with Le^c (**Figure 4.1**), since the Le^c can be degraded by lysosomal enzymes.

In cell extract incubation experiments, the additions of exogenous donors favor the expected biosynthetic pathways, and even though other enzymes are present, the corresponding donors are not present or are available in very low amounts. Therefore, in cell extract incubation with Le^c, only H type I, Le^a and Le^b can be synthesized with the addition of a GDP-fucose donor. However, in cell uptake studies, many transformations can occur. There will be competition among enzymes that utilize the same donor (i.e., GDP-fucose) or Le^c-TMR can also be a substrate for other glycosyltransferases (i.e., sialyltransferases) or modifying enzymes like, sulfotransferases and hydrolases since living cells can synthesize the sugar nucleotides they are needed. This depends on the substrate localization and enzyme availability inside the Golgi.

The PBS wash (curve **c**, **Figure 4.4**) and particularly the supernatant after trypsinization (curve **b**, **Figure 4.4**) show similar electropherograms to the lysed cell pellet. That proves the trypsinization step for the detachment cells from the flask wall can cause cell breakage.

Dennis and Zhuang have reported the biosynthesis of disialyl oligosaccharides secreted into the culture medium using aryl- α -D-GalNAc incubation with MDAY-D2 murine lymphoid tumor cells *in vivo* (19) and their absorbance detection is in the subpicomole range. However, we could not find any biosynthetic products (i.e. Le^a and H type I) in our cell culture medium after incubation with Le^c except very small amounts of hydrolytic products. The difference is probably due to the 250 times dilution of the culture medium prior to CE analysis, and also our substrate is labeled with the linker arm and the TRSE fluorescent dye. Also, the formation of biosynthetic products is much lower in our cell uptake experiments.

Attempts to identify the novel peak in the electropherogram required many repetitions of cell uptake experiments of which the results are shown in **Figure 4.5- 4.8** and a brief description follows in each cell uptake electropherogram.

The electropherogram of curve **d**, **Figure 4.5**, was from the lysed cell pellet after 18 h of A431 cells (3×10^6) growth with 25 μM Le^c -TMR. The biosynthetic products of the cells shown here are H I and a new peak with an early migration time around 9.4 min. No product is observed in the CM except a trace of hydrolysis products (curve **a**, **Figure 4.5**).

In a cell uptake experiment with 15 μM Le^c under the same conditions as above, more hydrolysis products are observed in the lysed cell pellet (curve **d**, **Figure 4.6**). The biosynthetic products are still H I, and both Le^a and a small amount Le^b were formed. The trypsin PBS wash (curve **c**, **Figure 4.6**) shows that the peaks are similar to those in curve **b**, **Figure 4.6**, but the linker arm-TMR produced is less than in the pellet, and an unidentified peak close to GlcNAc is larger (considering the baseline difference).

Le^c -TMR at 25 μM has been incubated with about 6×10^6 A431 cells for 19 h at the same cell incubation conditions. A new peak in **b**, **Figure 4.7** at a shorten migration time close to that of standard 2,3sialyl Le^c was produced. The profiles of electropherograms were similar to **Figure 4.4**.

Trace **c**, **Figure 4.8** shows two unknown peaks at a short migration time. Both Le^a and H I are formed in another repeated 25 μM Le^c uptake by A431 cells for 20 h.

There is no fluorescent peak shown in a control experiment under the same cell uptake conditions without adding a substrate.

Therefore, there is a variability from incubation to incubation using a similar cell uptake condition (cell subcultured for 72 h, 25 μM Le^c uptake by 18-20 h and the same wash steps). The electropherograms of different runs show somewhat different patterns. The relative amounts of biosynthetic, hydrolytic, and unknown products change from run to run. The reason for the variability is not understood.

4.3.3 Identification of Novel Peaks

Fucosidases and neuraminidase substrate specificity are listed in Table 4.3.

4.3.3.1 Neuraminidase substrate specificity

Electropherograms of **Figure 4.9** show a neuraminidase incubation with a synthetic 2.3sialyl Le^c. The 2.3 sialyl Le^c-TMR that was prepared in a borate buffer was not degraded by the neuraminidase after 165 h incubation (curve **a** to **c**, **Figure 4.9**). The lack of hydrolysis is attributed to the formation of sugar-borate complex that inhibited enzyme digestion. However, the 2.3sialyl Le^c prepared in water instead of a borate buffer can be digested within 65 h (curve **d**, **Figure 4.9**), so that pellets already dissolved in PBpBS buffer can not be used for treatments with glycosidases. Generally, samples eluted from a Sep Pak cartridge are lyophilized and redissolved in 10 μ L MeOH. For structure analysis, a portion of the sample (2 to 5 μ L) can be diluted in PBpBS buffer for CE analysis. An aliquot of the sample (several microliters in MeOH) was saved for further glycosidase digestion experiments.

4.3.3.2 Peak identification using hydrolysis enzymes

Mixture after cell uptake treated by a neuraminidase then with a fucosidase

The first peak close to the position of 2.3sialyl Le^c in **Figure 4.10** (post trypsin PBS wash, same as in **Figure 4.4**) cannot be removed by the neuraminidase digestion. The H I peak was eliminated by the neuraminidase treatment suggesting that the neuraminidase contains α 1.2 fucosidase activity (in **Figure 4.21** Neuraminidase can also remove LacNAc located in the same position as H I). This sample was purified by adsorption and elution from a Sep Pak cartridge. After further treatment with fucosidases (from human placenta), the Le^a was eliminated in trace **a** of **Figure 4.10**. Therefore, the formation of Le^a by A431 cells incubation with Le^c was confirmed.

Mixture after cell uptake treated by a fucosidase then with a neuraminidase

Cell uptake pellets (samples were the same as in **Figure 4.4a** and **Figure 4.6b**) were incubated with a fucosidase (human placenta). The Le^a disappeared and the peak height of H type I decreased (**Figure 4.11a** and **Figure 4.12c**). Therefore, the formation of H I and Le^a were confirmed. The sample after fucosidase treatment (**Figure 4.12c**) from above was lyophilized and further incubated with a neuraminidase. The peak on the H I position (not H I because it cannot be digested by the fucosidase) disappeared (**Figure 4.12d**), suggesting that this enzyme contained other hydrolytic enzyme activity.

The peak height of H type I formed from a Le^c cell uptake pellet was bigger than from A431 cell extracts incubated with Le^c and a donor GDP-fucose. When several cell pellet samples (Le^c uptake by A431 cell) were treated by a neuraminidase, H I peak can be completely removed (**Figure 4.12d** and **Figure 4.10** and **Figure 4.13b**) in each case. However, H I could only be partially removed by the fucosidase (from human placenta) digestion even after 94 h (**Figure 4.12c**). One possible explanation is that the cell could use β 1.4 Gal T to add a Gal to GlcNAc with an endogenous donor to form LacNAc that co-migrates with the H I.

Le^a, H I, and a smaller unknown peak in the position of standard 2.3 sialyl Le^c disappeared after incubation with a large amount of neuraminidase (900 μ units/ μ L, **Figure 4.13b**). However, it is hard to say that the small unknown peak is sialyl Le^c because this neuraminidase is not pure and also a small amount of unknown compound could be lost during Sep-Pak steps.

4.3.4 A431 Cell Extracts Incubation with Le^c without Adding a Donor and Peak Identification

4.3.4.1 A431 cell extract incubation with Le^c without adding a donor

Electropherograms in both **Figure 4.14** and **Figure 4.15** are from mixtures containing A431 cell extract incubation with Le^c-TMR for 21 and 65 h (**Mixture A**). An

unknown peak is shown in both electropherograms (12.5 min in Figure 4.14. 8.8 min in Figure 4.15). In **Figure 4.14**, a trisaccharide H type I, two hydrolytic products GlcNAc and the linker arm are produced. However, another trisaccharide Le^a and only one hydrolytic product were observed in **Figure 4.15**. The formation of H type I or Le^a must use an endogenous donor. Whether or not the unknown peak formed here is the same as the one found in Le^c uptake by A431 cell remains a question.

4.3.4.2 A novel peak identification

The peak at an early migration time (10.5 min) (**Figure 4.16c and d**) cannot be removed by alkaline phosphatase treatment at pH 8.6 and 9.5. Phospholipase cannot remove the unknown peak either (**Figure 4.16b**).

The unknown peak is probably not a sulfated sugar because it cannot be digested by three sulfatases (**Figure 4.17**). However, the substrate's specificity of these phosphatases and sulfatases are not known, since no standards are available. The sulfatases used in the hydrolysis may not act on the unknown sulfated products. When a cell extract, Le^c and a sulfate donor (PAPS) were incubated, the formation of the unknown peak does not increase compared to that without adding PAPs (**Figure 4.15**), suggesting that the unknown peak is not a sulfated sugar.

The relatively large scale cell extracts incubated with Le^c can provide enough sample for a MS analysis, which is the only way to identify the products because none of hydrolysis enzymes we tried can work on the mystery peak.

4.3.4.3 Mass spectrometry

Mixture A was analysed by mass spectrometry. Products of GlcNAc and Le^a and unreacted substrate Le^c were confirmed by their molecular weight. However, the unknown sugar X still was not identified (**Figure 4.18**).

identified

4.3.5 LacNAC-TMR Uptake by HT-29 Cells

Trisaccharide Le^X was formed (**Figure 4.19** and **Figure 4.20**) after 25 μ M LacNAC was incubated with by HT-29 cells for 20 h, and the identity of Le^X was confirmed by 36 h fucosidase (from almond meal) digestion (**Figure 4.21d**). The α 1.2 Fuc T activity was not detected because the incubation time was only 20 h in the cell uptake experiment instead of 72 h in the microsomal enzyme incubation (Chapter 3, **Figure 3.2c**). An unknown peak in front of GlcNAc peak was formed in **Figure 4.20**. The early migration peak (9.3 min) close to the 2,3sialyl LacNAC (**Figure 4.19**) was produced in a repeated LacNAC uptake by HT-29 cell experiment. The commercial neuraminidase preparation contained enzymes that hydrolyzed both Le^X and LacNAC. However, it did not contain anything that acted on the new peak (**Figure 4.21e**). Another unidentified peak positioned between GlcNAc and Gal α (1 \rightarrow 6)GlcNAc (in Chapter 5 Fig5.1, GlcNAc incubation with UA861) is also formed. No standards were available to confirm the identities of those peaks.

4.3.6 Comparison of Le^c Uptake by A431 Cells and LacNAC Uptake by HT-29 cells

Generally, in open tubular capillary electrophoresis, the more the negatively charged group on a molecule, the faster it moves. Upon comparison of electropherograms of LacNAC uptake by HT-29 cells with Le^c uptake by A431 cells (**Figure 4.22**), unknown peaks are eluted at an early migration time (13 min) far in front other peaks. What is a negative charge added on a sugar substrate? Is it a sialyl, a glucuronic, a sulfate or a phosphate group? What is the substrate-GlcNAc, an unknown compound between GlcNAc and Gal α (1 \rightarrow 6)GlcNAc, Le^c or LacNAC?

Product stability

Sample pellets from substrate uptake experiments were collected and stored in a refrigerator (4 $^{\circ}$ C). The cell uptake pellets were analyzed by CE after 130 days. This

indicated that the components in the pellet is stable at 4 °C for more than 130 days.

Sample solution diluted in CE running buffer was also stable at room temperature over 43 days in a dark room (**Figure 4.23**).

4.3.7 Separation of a Mixture Containing Thirteen TMR Labeled Compounds

Various studies have highlighted the use of anionic borate-sugar diol complexation to enhance the separation of mono- and oligosaccharides (22). The extent of this complexation is known to increase with pH and borate concentration. Therefore, the high-ionic-strength borate buffer is generally employed to obtain maximum resolution.

A comparison of the electropherograms of **a**, **b** and **c** in **Figure 4.24** reveals that when the concentrations of phenyl boric acid are increased from 20 mM, 30 mM and 40 mM, the migration times increased and one of the peak shows a shoulder. Ten peaks with one shoulder are observed for 13 compounds (**c** in **Figure 4.24**). If phenyl boric acid concentration is increased further, 13 sugars should be able to be separated.

From **Figure 4.25**, we can see that six standards for Le^c series do not reach baseline separation with 10 mM PBsBS. Since the migration time for all sugars is shorter in PBsBS than in PBpBS buffer, the resolution is getting worse due to the short migration time, because 3-aminophenylboronic acid probably carries more positive charge than phenyl boric acid at pH 9. The complex ability for both phenylboronate is similar because the peak shape and migration sequence remain the same.

4.4 CONCLUSION

CE-LIF is a highly sensitive method to detect very small amounts (10^{-21} mole) of enzymatic reaction products that have been taken up by cells from a strongly fluorescent substrate. The methods can detect the presence of α -2- and α -4 or α -2- and α -3-Fuc T activities. It can be developed to detect all glycosyltransferases activities in a cell. The separation efficiency is 10^6 theoretical plates and the products can be characterized with

synthetic sugar standards in a short analysis time. Single cell detection studies by other researchers is generally based on the selection of a cell containing relatively high amount analytes. for example, red blood cells (23) contains 300 million molecules (450 attomole) of hemoglobin in one human erythrocyte (24). In our experiments, the biosynthesis products (18,000 TMR labeled molecules) from 10 cells and also the substrate can be detected which is an unattainable level for other current instrumentation. If this method could be used to detect rare mutated cells (1/1000 normal cells), it could be used in the medical, biological, and pharmaceutical fields.

The experimental results showed that the low molecular weight substrate permitted the separation and analysis of pure products and the subsequent results demonstrated more than one enzyme activity in a crude cell extract (25). CE-LIF can also provide a method for enzyme assays in which levels of a particular transferase are correlated with a physiological or pathological state (26).

It is useful to apply a C-18 Sep Pak cartridge that is good to eliminate other impurities from cells. However, disadvantages also exist. If the cell were directly injected into the capillary, the other contents (proteins) from the cell could cause adsorption and the separation efficiency of CE systems would decrease. Lee and Yeung have reported the lower separation efficiencies for components directly extracted from single cells compared to those standards obtained from commercial source (27).

4.5 REFERENCE

- (1) O'Neil, K.; Shao, X. W.; Zhao, Z. X.; Malik, A. and Lee, M. L. *Anal. Biochem.* **1994**, 222, 186-189.
- (2) Gilman, S. D. and Ewing, A. G. *Anal. Chem.*, **1995**, 67, 58-64.
- (3) James, D. C.; Freedman, R. B. and Jenkins, N. *Anal. Biochem.*, **1994**, 222, 315-322.
- (4) Schmerr, M. J. and Goodwin, K. R. *J. Chromatogr. A*, **1993**, 652, 199-205.
- (5) Childs, R. A.; Gregoriou, M.; Scudder, P.; Thorpe, S. J.; Rees, A. R.; Feiz, T. *EMBO J* **1984**, 3, 2227-33.
- (6) Stroup, G. B.; Anumula, K.R.; Kline, T. F. and Caltabiano, M.M. *Cancer Research*, **1990**, 50, 6787-6792.
- (7) Schachter, H. *Current Opinion in Structural Biology* **1991**, 1, 755-765.
- (8) Palcic, M. M.; Heerze, L.D.; Pierce, M., and Hindsgaul O. *Glycoconj. J.* **1988**, 5, 49-63.
- (9) Stults, C. L.; Wilbur, B. J. and Macher, B. A. *Analyt. Biochem.*, **1988**, 174, 151-156.
- (10) Crawley, S.C.; Hindsgaul, O.; Alton, G.; Pierce, M. and Palcic, M. M. *Analyt. Biochem.*, **1990**, 185, 112-117.
- (11) Zatta, P. F.; Nyame, K.; Cormier, M. J.; Mattox, S. A. *Analyt. Biochem.*, **1991**, 194, 185-191.
- (12) Iwase, H.; Ishii, I.; Saito, T.; Ohara, S. and Hotta, K. *Analyt. Biochem.*, **1988**, 173, 317-320.
- (13) Lee, K. B.; Desai, U. R.; Palcic, M. M.; Hindsgaul, O. and Linhardt, R. J. *Analyt. Biochem.*, **1992**, 205, 108-114.
- (14) Liu, J.; Shirota, O.; Wiesler, D.; Novotny, M. *Proc. Natl. Acad. Sci.*, **1991**, 88, 2302-2306.

- (15) Zhao, J. Y.; Dovichi, N. J.; Hindsgaul, O.; Gosselin, S. and Palcic, M. M. *Glycobiology*. **1994**, 4, 239-242.
- (16) Zhang, Y.; Le, X.; Compton, C. A.; Palcic, M. M.; Diedrich, P. and Hindsgaul, O. *Anal. Biochem.* **1995**, 227, 368-376.
- (17) *Laboratory Equipment and planning, in Cell & Tissue Culture Laboratory Procedures.* (Doyle, A.; Griffiths, J. B. and Newell, D. G. Eds.), Wiley, UK, **1993**, pp???
- (18) Johnson, P. H.; Donald, A. S. R. and Watkins, W. M. *Glycoconjugate Journal* **1993**, 10, 152-164.
- (19) Dennis, J.W. and Zhuang, D. *Trends in Glycoscience and Glycotechnology*, **1993**, 5, 287-295.
- (20) Martin, O. C.; Comly, M. E.; Blanchette-Mackie, E. J.; Pentechev, P. G. and Pagano, R. E. *Proc. Natl. Acad. Sci. USA* **1993**, 90, 2661-2665.
- (21) Martin, O. C. and Pagano, R.E. *J. Cell Biol.* **1994**, 125, 769-781.
- (22) Honda, S.; Suzuki, S.; Nose, A.; Yamamoto, K. and Kakehi, K. *Carbohydr. Res.* **1991**, 215, 193-198.
- (23) Hogan, B. L. and Yeung, E. S. *Anal. Chem.* **1992**, 64, 2841-2845.
- (24) Curtis, H. *Biology*. Worth Publishers, Inc., New York, **1983**, pp. 70.
- (25) Schachter, H. *Trends in Glycoscience and Glycotechnology*, **1992**, 4, 241-250.
- (26) Palcic, M. M. *Methods in Enzymology*, **1994**, 230, 300-319.
- (27) Lee, T. and Yeung, E. S. *Anal. Chem.* **1992**, 64, 3045-3051.

Appendix Table 4.1 Hydrolysis enzymes

α -L-Fucosidase from	Activity	Catalog	Unit definition (one unit will)
1. Almond meal	20 μ units/vial. made of 20 μ U/10 μ L buffer. stored in 4 $^{\circ}$ C. Not assayed by Sigma	Sigma F-8899	liberate 1.0 μ mole of fucose from Lacto-N fucopentaose II per min at pH 5.0. 37 $^{\circ}$ C
2. Crude supernatant of a clonal CHO-derived cell line	stored in -20 $^{\circ}$ C	Ciba isolated by Dr. Benjamin R. Bowen	-
3. Bovine Epididymis	0.5 unit. Suspension in 2.5 M $(\text{NH}_4)_2\text{SO}_4$. pH 5.8. 2-3 units per mg protein at pH 6.5 at 25 $^{\circ}$ C.	Sigma F7753 Contains < 1.5% b-N acetylglucosaminidase. solution was 12.5 μ U/ μ L in pH 6.5.	hydrolyze 1.0 μ mole of p-nitrophenyl α -L-fucoside to p-nitrophenol and L-fucose per min at pH 6.5 at 25 $^{\circ}$ C.
4. Bovine kidney	0.5 unit. Suspension in 3.2 M $(\text{NH}_4)_2\text{SO}_4$. 10 mM NaH_2PO_4 . 10 mM citrate. pH 6.0. 5-15 units per mg protein (Biuret) at pH 5.5 at 25 $^{\circ}$ C. stock solution were diluted to 9.9 μ U/ μ L in pH 5.5 (0.1 M citrate and 0.2 M phosphate) buffer.	Sigma F5884 Contains less than 0.2% b-N-acetylglucosaminidase and 0.1 % β -galactosidase α -mannosidase activities. solution was 9.9 μ U/ μ L in pH 5.5.	hydrolyze 1.0 μ mole of p-nitrophenyl α -L-fucoside to p-nitrophenol and L-fucose per min at pH 5.5 at 25 $^{\circ}$ C.
5. Human Placenta	0.5 unit. Suspension in 80% ammonium sulfate and 0.1 M sodium phosphate/citrate buffer. pH 6.0. 2-4 units per mg protein at pH 5.6 at 37 $^{\circ}$ C.	Sigma F6151 Contains less than 2.5% β -N-acetylglucosaminidase and α -galactosidase and less than 5% β -mannosidase activities. Solution was 15.6 μ U/ μ L at pH 5.5.	hydrolyze 1.0 μ mole of p-nitrophenyl α -L-fucoside to p-nitrophenol and L-fucose per min at pH 5.6 and 37 $^{\circ}$ C.

Sulfatase	Activity	Catalog	Unit Definition
1.From <i>Aerobacter aerogenes</i> Type VI. Partially purified enzyme in 50% glycerol-0.01 M Tris solution. pH 7.5	3.5units/mg protein (Biuret). 19 U/mL. stored in -20°C. No detectable b-Glucuronidase activity at pH 7.	Sigma S-1629	one unit will hydrolyze 1.0 μ mole of p-nitrophenyl sulfate to p-nitrophenol and free sulfate per minute at pH 7.2, 37 °C.
2.From Limpets (<i>Patella vulgata</i>). Type V. Lyophilized, essentially salt-free powder	9.9 units/mg solid. Solution contained 1 μ unit /2.5 μ L. stored in 4°C. < 2 sigma units per mg solid of -Glucuronidase activity.	Sigma S-8629	one unit will hydrolyze 1.0 μ mole of p-nitrocatechol sulfate per hour at pH 5.0, 37 °C.
3.From Abalone entrails Lyophilized powder	27 units/mg. 1 μ unit /2.5 μ L. stored in 4°C. <3 Sigma units per mg solid of b-glucuronidase Activity	Sigma S-9754	One unit will hydrolyze 1.0 μ mole p-nitrocatechol sulfate per hour at pH 5.0 and in 37 °C.

Neuraminidase	Activity	Catalog	Unit definition
Neuraminidase TypeV from <i>clostridium perfringens</i> prepared by salt fractionation. Dialyzed and lyophilized powder	0.3 mg. about 3 units/mg. total 0.9 unit. diluted in 1000 μ L buffer (150 mM citrate.pH 5) and stored at 4 °C in fridge. Diluted solution contained 9 μ U/ μ L	Sigma. N2876 0.5-6 units per mg solid using NAN-lactose and 0.1-3 units per mg solid using mucin. may contain protease and NAN-aldolase	one unit will liberate 1.0 μ mole of N-acetylneuraminic acid per min. at pH 5.0 at 37 °C using NAN-lactose or bovine submaxillary mucin. unless otherwise specified.

Phosphatase	Activity	Catalog	Definition
Phosphatase, alkaline, from bovine intestinal mucosa. Type VII-NTA	1000 DEA units, 2000-3000 DEA units(1000-1500 glycine units) per mg enzyme protein. 1mU/ μ L	Sigma, P-0530	One unit will hydrolyze 1.0 μ mole of p-nitrophenyl phosphate per min at 37 °C.
Phospholipase A ₂ from Naja naja venom, lyophilized powder	1300 units/mg, solution contained 2 units/ μ L in pH 8.6 50 mM Tris buffer	Sigma, P-6139	One unit will hydrolyze 1.0 μ mole of L- α -phosphatidylcholine to L- α -lysophosphatidylcholine and a fatty acid per min at pH 8.9 at 25 °C.

Diethanolamine (DEA) units are measured in a 1.0 M diethanolamine buffer, pH 9.8, containing 0.5 mM MgCl₂; substrate concentration 15.0 mM for most products. One glycine unit is equivalent to approx. 2 DEA units.

Table 4.2 Buffers for glycosidase assays

Buffer	pH
50 mM Tris·HCl(1x)	8.6
1 M Sodium Cacodylate	7.1
250 mM DEA	9.5
0.1 M Sodium Citrate and 0.2 M Sodium Phosphate	5.5
0.15 M Sodium Citrate	5.0
0.2 M Sodium Citrate	5.5
HEPES	6.2-8.2

Table 4.3 The specificity of α -fucosidases and neuraminidase

Fucosidase	Substrate					
	Le ^Y	Le ^X	H type II	Le ^b	Le ^a	H type I
Almond meal pH 5.5	+ .13 h	+ .52 h	- .52 h	+ .52 h remove most of it	+ .52 h	- .37 h
CHO-derived cell line pH 5.5	+ .95 h. 23 % removed	- .95 h.	+ .25 h. small amount left	- .95 h 4 % removed	+ .95 h 50 % removed	- .95 h
Bovine Kidney pH 5.5			- .46 h			- .65 h
Human Placenta pH 5.5			+ .46 h		+ .46 h	+ .72 h. 42 % removed
Bovine Epididymis pH 6.5			+ .46 h			+ .48 h 12 % removed

Substrate	Neuraminidase
2.3-Sialyl Le ^c	+ .24 h 89 % + .65 h
2.3-Sialyl Le ^c -borate complex	+ .16.8 % in 65 h and 19 % in 165 h
H type I	+ .25 h 40 %
Le ^a	+ .25 h 75 %
GlcNAc	+ .25 h

+ . h — indicates complete removal within the indicated hours.

+ . h and % — indicate a percentage of substrate removed at a certain incubation time.

- . h — can not be removed within the indicated hours.

The assay was done by incubation 1 μ L of 1 mM synthetic standard, 1 μ L enzyme (Table 4.1), and 5 μ L buffer (listed in Table 4.2). Then the reaction mixture was loaded on C-18 Sep Pak cartridge and washed with water and eluted in 3.5 mL HPLC MeOH for CE analysis.

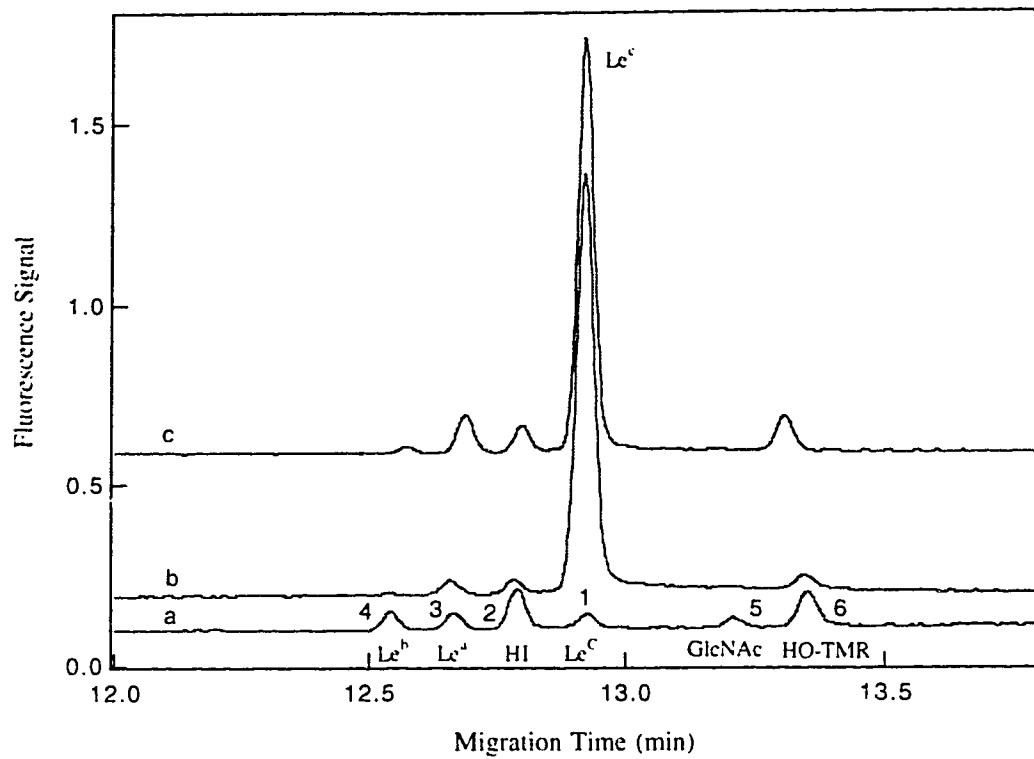


Figure 4.1 Electropherograms of A431 crude cell extracts incubated with substrate Le^c-O-TMR and donor GDP fucose (50 μ M each). (a) The baseline separation of five standards of tetramethylrhodamine labeled oligosaccharides: Le^b, Le^a, H type I, Le^c, GlcNAc, and the linker arm (5 $\times 10^{-10}$ M each except 1 $\times 10^{-9}$ M for H I) from left to right, the standard mixture was dissolved in a 1:1 of MeOH:PBpBS buffer. (b) 17 and (c) 41 h incubation, total concentrations of labeled compounds injected were 2.8 $\times 10^{-8}$ M TMR.

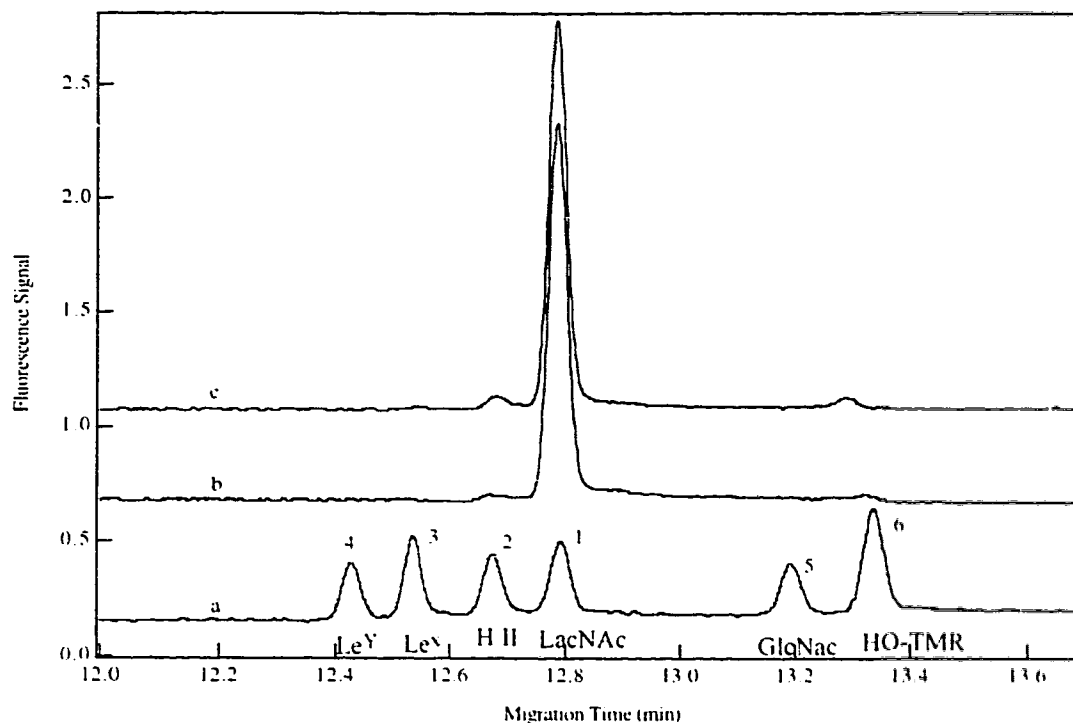
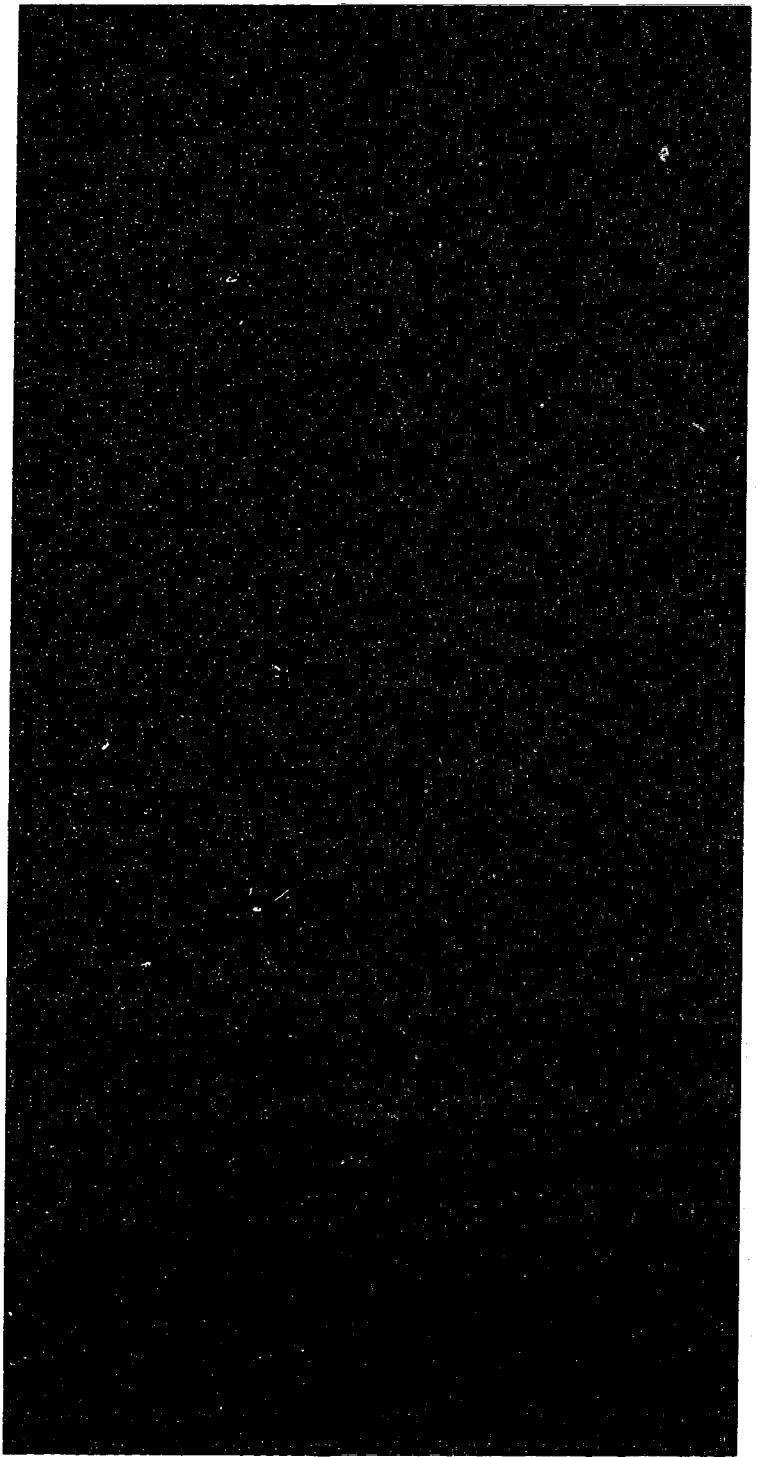


Figure 4.2 Electropherograms of LacNAc-TMR incubated with A431 cell extracts and GDP fucose (50 μ M each). (a) The baseline separation of LacNAc standard series (5×10^{-10} M for each). From left to right, the corresponding peaks are Le^Y, Le^X, H type II, LacNAc, GlcNAc and the linker arm H-O-TMR. After (b) 17 and (c) 41 h incubation, samples were diluted in running buffer to obtain 2.8×10^{-8} M total TMR labeled compounds prior to CE analysis.

Figure 4.3 Photography of laser scanning confocal microscopy of 25 μ M Le^C uptake by A431 cells for 18 h. The photo picture is in next page.



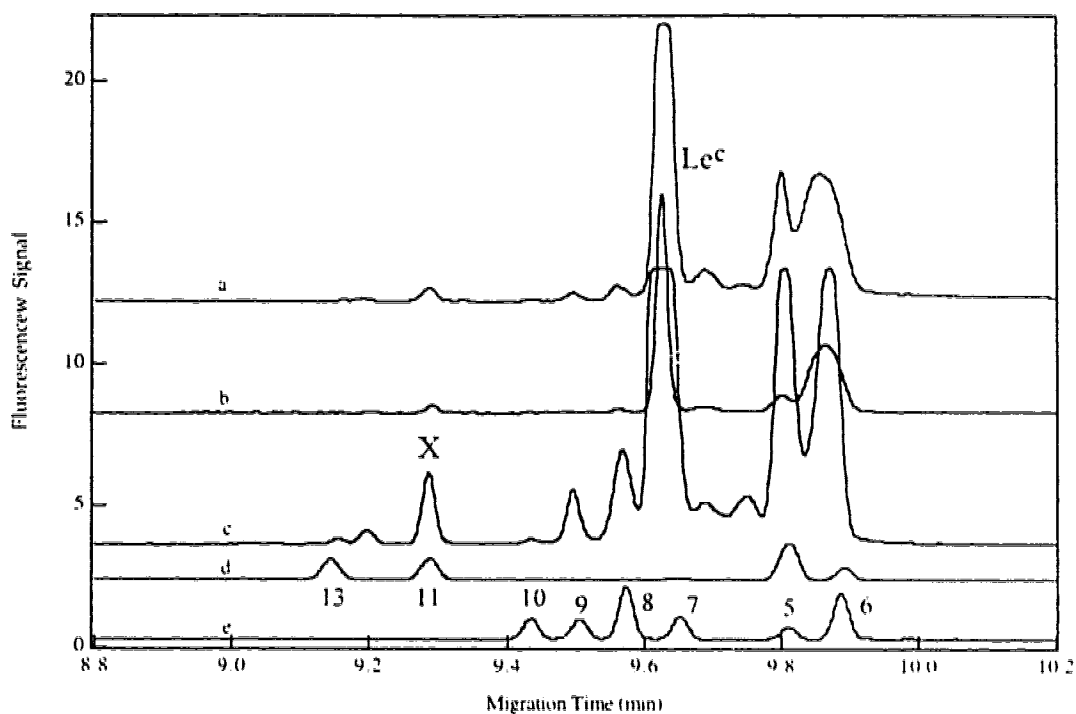


Figure 4.4 Electropherograms of A431 cells grown in culture medium containing 25 μM Le^c for 20 h. (a) lysed cell pellet after Le^c incubated with 6×10^6 cells for 20 h, (b) post trypsin PBS wash, and (c) pretrypsin PBS wash. (d) Sialyl Le^c series standards, and (e) Separation of six Le^c series standards.

- 5 GlcNAc, $\beta\text{GlcNAc-O-TMR}$.
- 6 HO-TMR, $\text{H-O}(\text{CH}_2)_8\text{CONHCH}_2\text{CH}_2\text{NH-tetramethylrhodamine}$, the linker arm
- 7 Le^c , $\beta\text{Gal}(1 \rightarrow 3) \beta\text{GlcNAc-O-TMR}$, Lewis C
- 8 H I, $\alpha\text{Fuc}(1 \rightarrow 2) \beta\text{Gal}(1 \rightarrow 3) \beta\text{GlcNAc-O-TMR}$, H type I
- 9 Le^a , $\beta\text{Gal}(1 \rightarrow 3)[\alpha\text{Fuc}(1 \rightarrow 4)] \beta\text{GlcNAc-O-TMR}$, Lewis A
- 10 Le^b , $\alpha\text{Fuc}(1 \rightarrow 2)\beta\text{Gal}(1 \rightarrow 3)[\alpha\text{Fuc}(1 \rightarrow 4)]\beta\text{GlcNAc-O-TMR}$
- 11 2,3-sialyl Le^c , $\alpha\text{NeuAc}2 \rightarrow 3\beta\text{Gal}(\rightarrow 3)\beta\text{GlcNAc-O-TMR}$,
- 13 2,3-sialyl LacNAc, $\alpha\text{NeuAc}2 \rightarrow 3\beta\text{Gal}(1 \rightarrow 3)\beta\text{GlcNAc-O-TMR}$
- X unknown sugar

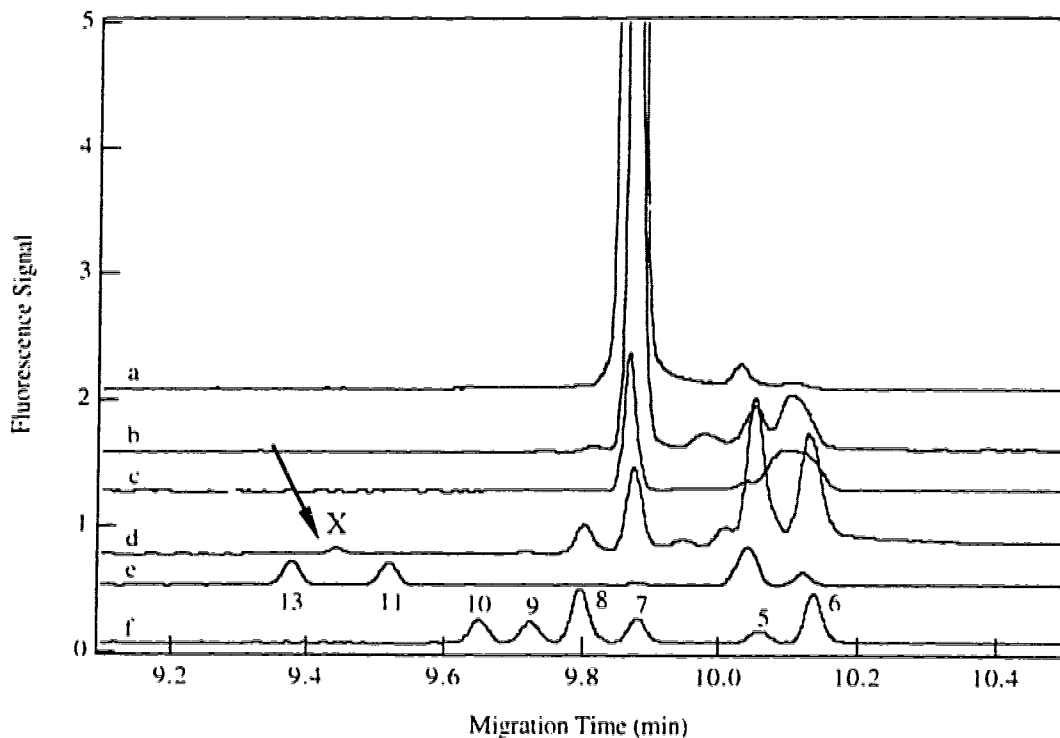


Figure 4.5 Electropherograms of Le^c uptaken by 3×10^6 A431 cells for 18 h. (a) culture medium (CM). (b) post-trypsin wash. (c) pre-trypsin wash. and (d) cell pellet. (e) A mixture containing 2,3 sialylLacNAc, 2,3sialyl Le^c, GlcNAc, and the linker arm (1×10^{-9} M). (f) Le^c standard series.

- 5 GlcNAc. β GlcNAc-OTMR.
- 6 HO-TMR. H-O(CH₂)₈CONHCH₂CH₂NH-tetramethylrhodamine. the Linker arm
- 7 Le^c. β Gal(1→3) β GlcNAc-O-TMR. Lewis C
- 8 H I. α Fuc(1→2) β Gal(1→3) β GlcNAc-O-TMR. H type I
- 9 Le^a. β Gal(1→3)[α Fuc(1→4)] β GlcNAc-O-TMR. Lewis A
- 10 Le^b. α Fuc(1→2) β Gal(1→3)[α Fuc(1→4)] β GlcNAc-O-TMR
- 11 2,3-sialyl Le^c. α NeuAc2→3 β Gal(→3) β GlcNAc-O-TMR,
- 13 2,3-sialyl LacNAc. α NeuAc2→3 β Gal(1→3) β GlcNAc-O-TMR
- X unknown sugar

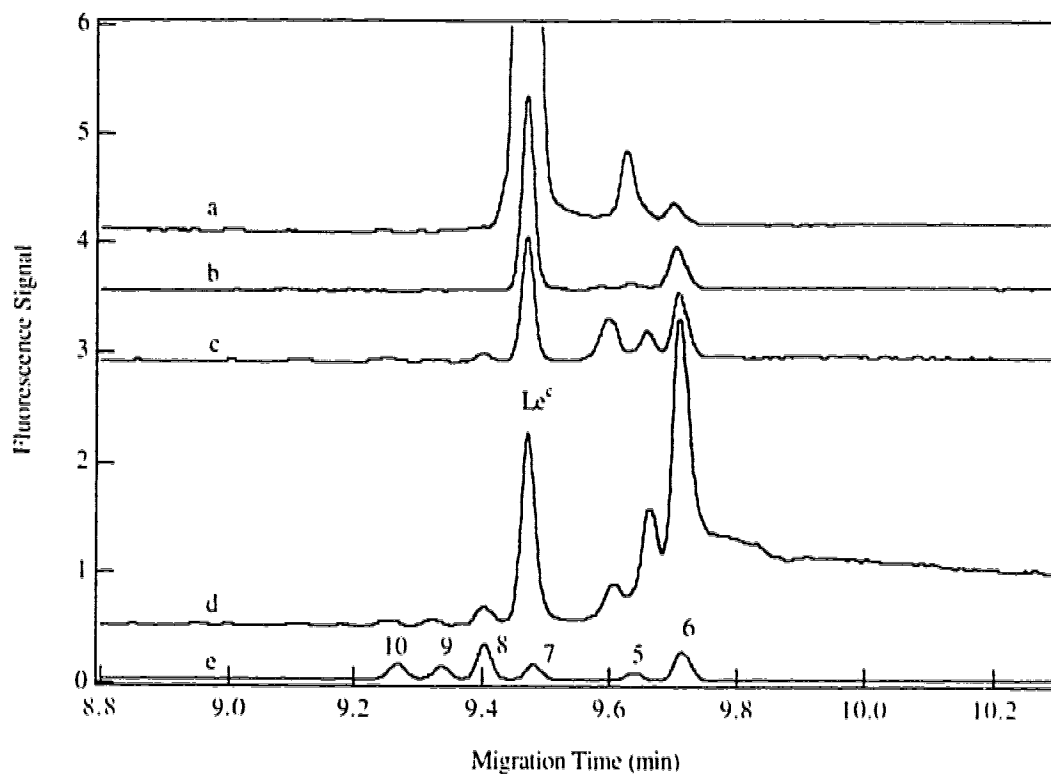


Figure 4.6 Electropherograms of A431 (3×10^6) cells incubated with substrate Le^c ($15 \mu\text{M}$) for 19 h. (a) culture medium containing substrate Le^c , (b) pre-trypsin wash, (c) post-trypsin wash, (d) lysed cell pellet, and (e) Le^c series standards.

- 5** GlcNAc. β GlcNAc-OTMR.
- 6** HO-TMR. $\text{H-O}(\text{CH}_2)_8\text{CONHCH}_2\text{CH}_2\text{NH-tetramethylrhodamine}$, the Linker arm
- 7** Le^c . β Gal(1 \rightarrow 3) β GlcNAc-O-TMR. Lewis C
- 8** H I, α Fuc(1 \rightarrow 2) β Gal(1 \rightarrow 3) β GlcNAc-O-TMR. H type I
- 9** Le^a , β Gal(1 \rightarrow 3)[α Fuc(1 \rightarrow 4)] β GlcNAc-O-TMR. Lewis A
- 10** Le^b , α Fuc(1 \rightarrow 2) β Gal(1 \rightarrow 3)[α Fuc(1 \rightarrow 4)] β GlcNAc-O-TMR

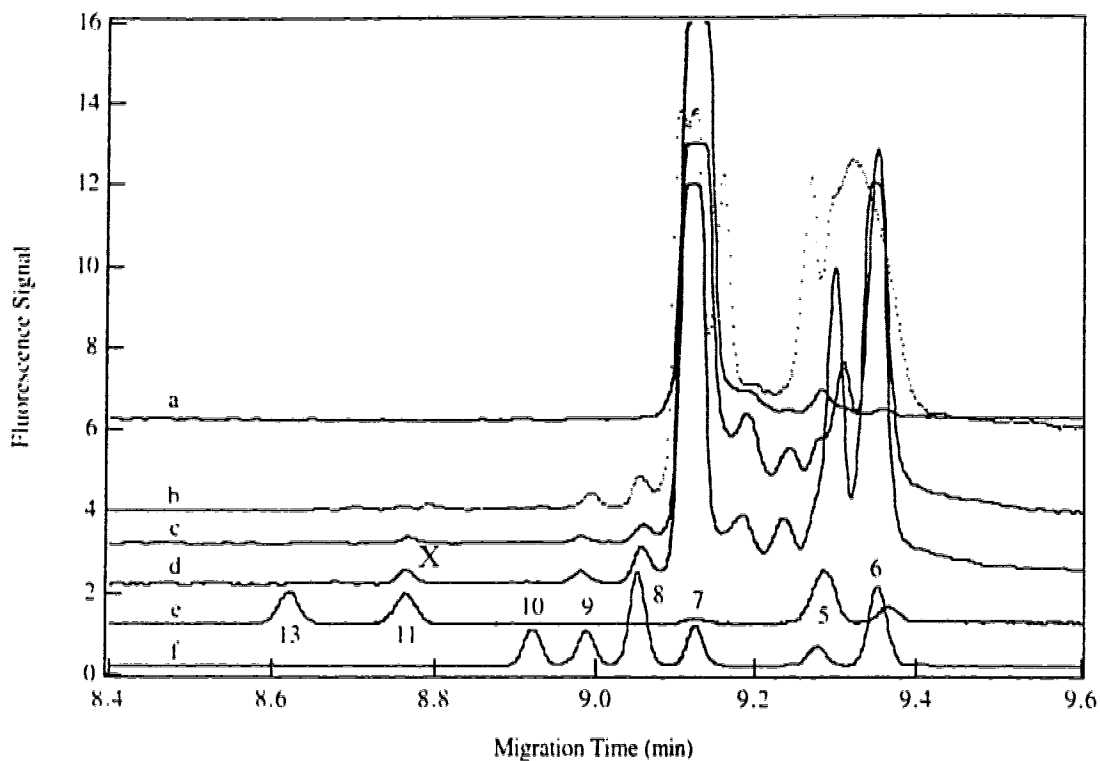


Figure 4.7 Electropherograms of (a) culture medium, (b) pretrypsin PBS wash, (c) post-trypsin PBS wash, (d) 25 μM Le^c of 19 h cell uptake pellet (6×10^6 cells), (e) sialyl series standards, and (f) Le^c series standards.

- 5 GlcNAc. $\beta\text{GlcNAc-O-TMR}$.
- 6 HO-TMR. $\text{H-O}(\text{CH}_2)_8\text{CONHCH}_2\text{CH}_2\text{NH-tetramethylrhodamine}$, the Linker arm
- 7 Le^c , $\beta\text{Gal}(1 \rightarrow 3) \beta\text{GlcNAc-O-TMR}$, Lewis C
- 8 H I, $\alpha\text{Fuc}(1 \rightarrow 2) \beta\text{Gal}(1 \rightarrow 3) \beta\text{GlcNAc-O-TMR}$, H type I
- 9 Le^a , $\beta\text{Gal}(1 \rightarrow 3)[\alpha\text{Fuc}(1 \rightarrow 4)] \beta\text{GlcNAc-O-TMR}$, Lewis A
- 10 Le^b , $\alpha\text{Fuc}(1 \rightarrow 2)\beta\text{Gal}(1 \rightarrow 3)[\alpha\text{Fuc}(1 \rightarrow 4)]\beta\text{GlcNAc-O-TMR}$
- 11 2,3-sialyl Le^c , $\alpha\text{NeuAc}2 \rightarrow 3\beta\text{Gal}(\rightarrow 3)\beta\text{GlcNAc-O-TMR}$,
- 13 2,3-sialyl LacNAc, $\alpha\text{NeuAc}2 \rightarrow 3\beta\text{Gal}(1 \rightarrow 3)\beta\text{GlcNAc-O-TMR}$
- X unknown sugar

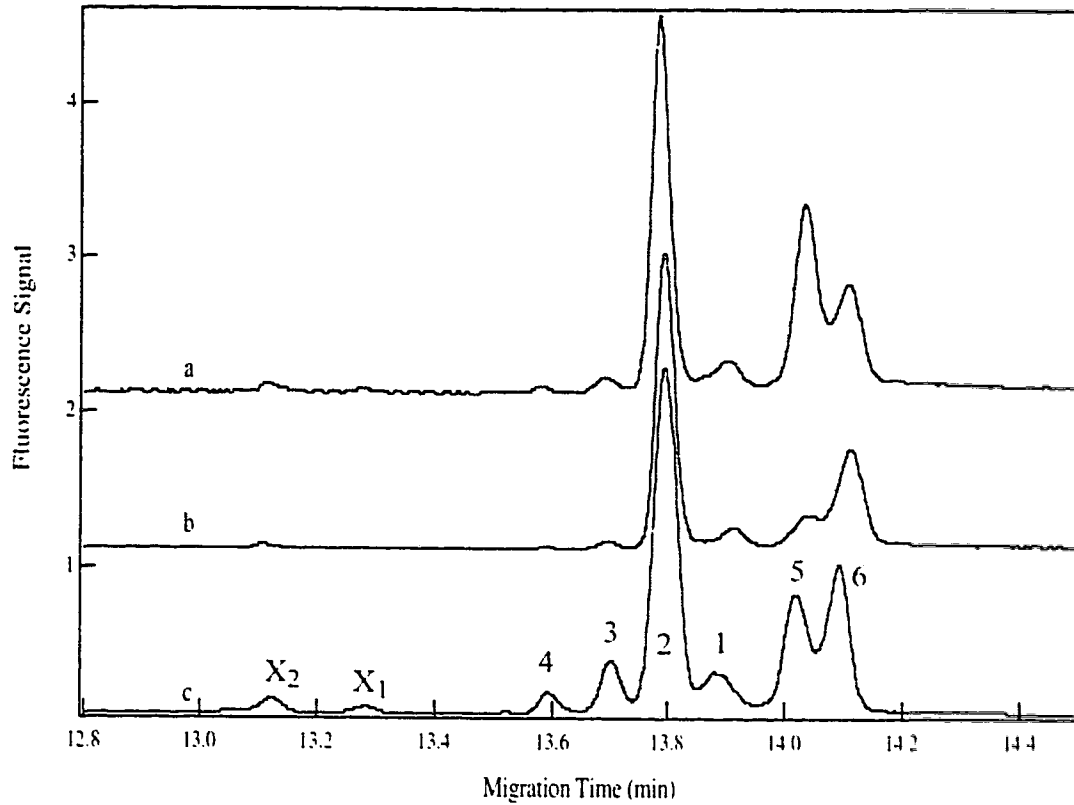


Figure 4.8 Electropherograms of the 19.5 h of 25 μM Le^c uptake by A431 cells (6×10^6). (a) pre-trypsin PBS wash. (b) post-trypsin PBS wash. and (c) cell uptake pellet.

- 5 GlcNAc. $\beta\text{GlcNAc-O-TMR}$.
- 6 HO-TMR. $\text{H-O}(\text{CH}_2)_8\text{CONHCH}_2\text{CH}_2\text{NH-tetramethylrhodamine}$. the linker arm
- 7 Le^c. $\beta\text{Gal}(1\rightarrow3) \beta\text{GlcNAc-O-TMR}$. Lewis C
- 8 H I. $\alpha\text{Fuc}(1\rightarrow2) \beta\text{Gal}(1\rightarrow3) \beta\text{GlcNAc-O-TMR}$. H type I
- 9 Le^a. $\beta\text{Gal}(1\rightarrow3)[\alpha\text{Fuc}(1\rightarrow4)] \beta\text{GlcNAc-O-TMR}$, Lewis A
- X₁ unknown sugar
- X₂ unknown sugar

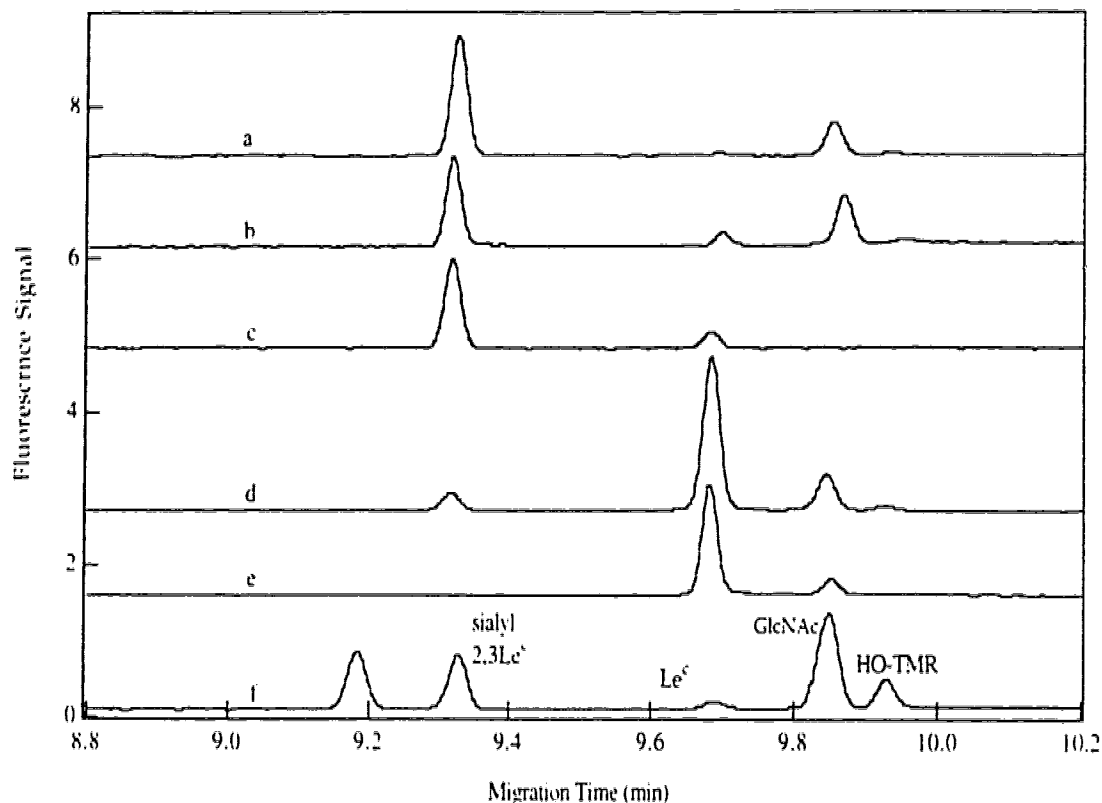


Figure 4.9 Electropherograms of hydrolysis of 2,3 sialyl Le^c by neuraminidase. (a) to (c) 2,3sialyl Le^c (initially dissolved in PBpBS buffer) was desalted by Sep Pak cartridge, lyophilized, and incubated with neuraminidase for 24, 65, and 165 h. (d) and (e) 2,3 Sialyl Le^c (initially dissolved in H₂O) was dried and incubated with neuraminidase for 24 and 65 h. (f) Separation of a standard mixture containing 2,3 sialyl LacNAc, 2,3 sialyl Le^c, Le^c, GlcNAc and the linker arm (peaks from left to right).

Standard 2,3sialyl Le^c (dissolved in different solvents) digested by neuraminidase:

For (b) and (c): 0.5 μ L 1 mM sialylLe^c (in H₂O) dried, 5 μ L 150 mM citrate (pH 5.0) and 0.5 μ L neuraminidase (9 μ U/ μ L) were added and the mixture was incubated at 37 $^{\circ}$ C. After 21 and 65 h incubation, 1 μ L of each incubation mixture was removed.

For (d) to (f): 0.5 μ L of 1 mM sialylLe^c (dissolved in 10 μ L of 10 mM PBpBS) was desalted by Sep Pak cartridge and dried out. 5 μ L of 150 mM citrate (pH 5.0) and 0.5 μ L neuraminidase (9 μ U/ μ L) were added to the dried sample and incubated up to 165 h at 37 $^{\circ}$ C.

A removal of 1 μ L aliquot of mixtures at each time point were loaded on Sep Pak cartridge and the TMR labeled substrate and products were finally eluted with 3.5 mL MeOH. Each mixture was diluted in PBpBS (about $1.2\text{-}2.4 \times 10^{-8}$ M total TMR labeled compounds) prior to CE analysis.

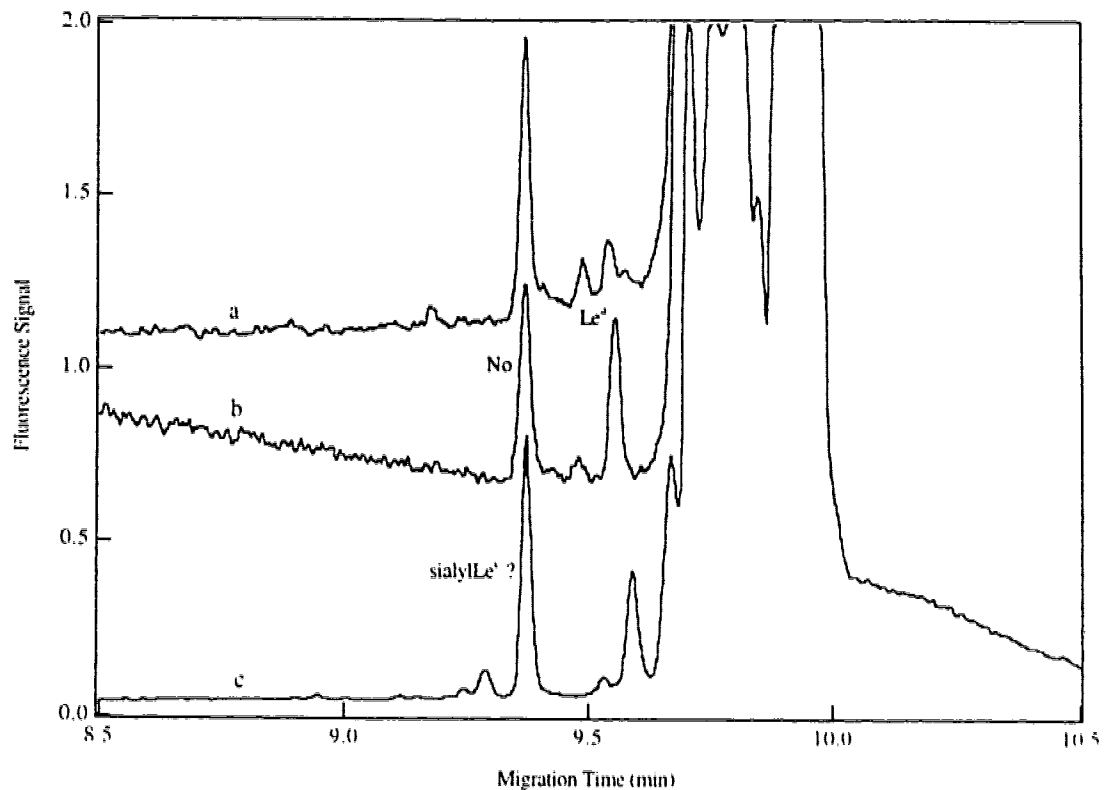


Figure 4.10 Electropherogram of an α -fucosidase (a) and a neuraminidase (b) digestion of post-trypsin PBS wash (same sample as in Figure 4.4), respectively. (c) the cell pellet of Le^c uptake by A431 cells for 20 h.

Neuraminidase treatment: A 5 μ L mixture in MeOH (same sample as Figure 4.4 post-trypsin PBS wash) was dried, 4 μ L of 150 mM citrate (pH 5) buffer and 1 μ L of 9 μ U/ μ L neuraminidase was added, and the mixture was incubated at 37 $^{\circ}$ C for 46 h. 1 μ L of mixture was removed, purified by Sep Pak cartridge and dried. The dried sample was redissolved in 5 μ L of MeOH prior to CE analysis.

α -Fucosidase treatment: The sample after neuraminidase treatment was dried, 1 μ L α -fucosidase (15.6 μ U/ μ L) from human placenta and 4 μ L H₂O was added (pH 5) and the mixture was incubated at 37 $^{\circ}$ C for 67 h. No buffer was added prior to CE analysis.

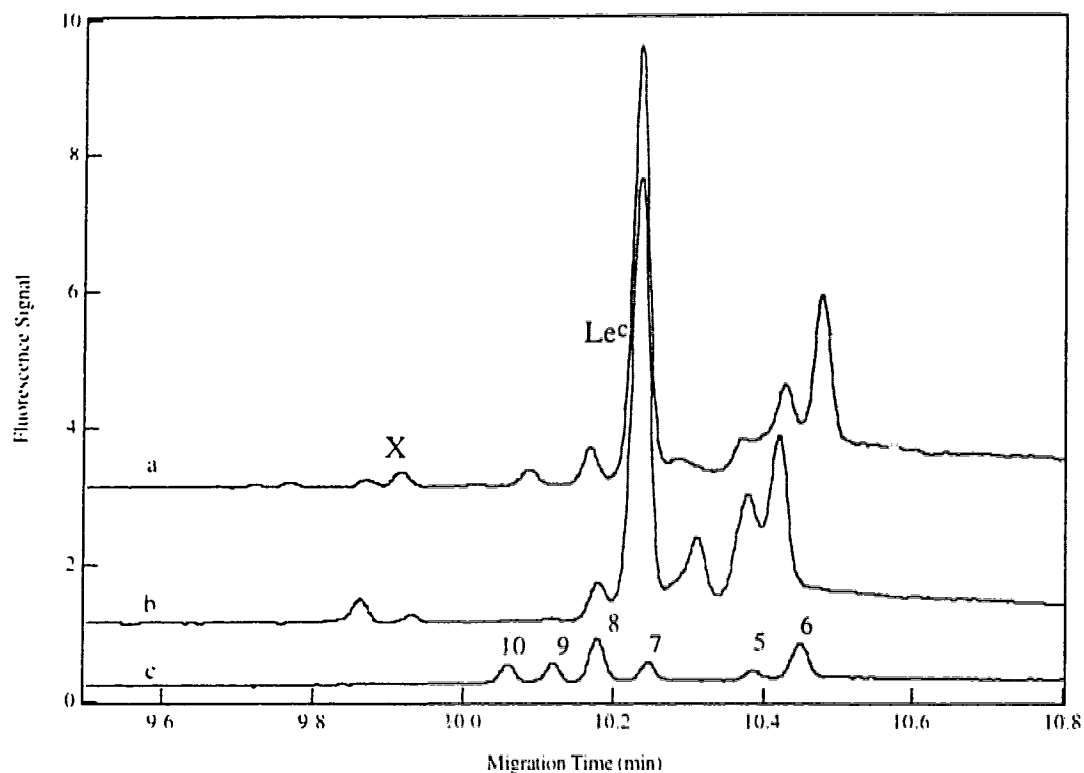


Figure 4.11 Electropherograms of α -fucosidase treatment of the pellet from $25 \mu\text{M}$ Le^c uptake by A431 cells for 20 h. (a) the A431 cell pellet after uptake Le^c for 20 h (also see Figure 4.4 a). (b) Sample from (a) was treated by α -fucosidase from human placenta for 36 h. (c) the Le^c series standard.

Fucosidase treatment: A431 cell pellet in $4 \mu\text{L}$ MeOH was dried. A $4 \mu\text{L}$ of buffer (pH 5.5) and $0.5 \mu\text{L}$ α -fucosidase from human placenta ($15.6 \mu\text{U}/\mu\text{L}$) were added to the dried sample and incubated at 37°C for 36 h. This mixture was diluted by adding $10 \mu\text{L}$ MeOH and $6 \mu\text{L}$ PBpBS running buffer prior to CE analysis.

- 5 GlcNAc, $\beta\text{GlcNAc-O-TMR}$.
- 6 HO-TMR. $\text{H-O}(\text{CH}_2)_8\text{CONHCH}_2\text{CH}_2\text{NH-tetramethylrhodamine}$. the Linker arm
- 7 Le^c , $\beta\text{Gal}(1\rightarrow3) \beta\text{GlcNAc-O-TMR}$, Lewis C
- 8 H I, $\alpha\text{Fuc}(1\rightarrow2) \beta\text{Gal}(1\rightarrow3) \beta\text{GlcNAc-O-TMR}$, H type I
- 9 Le^a , $\beta\text{Gal}(1\rightarrow3)[\alpha\text{Fuc}(1\rightarrow4)] \beta\text{GlcNAc-O-TMR}$, Lewis A
- 10 Le^b , $\alpha\text{Fuc}(1\rightarrow2)\beta\text{Gal}(1\rightarrow3)[\alpha\text{Fuc}(1\rightarrow4)]\beta\text{GlcNAc-O-TMR}$
- X unknown sugar

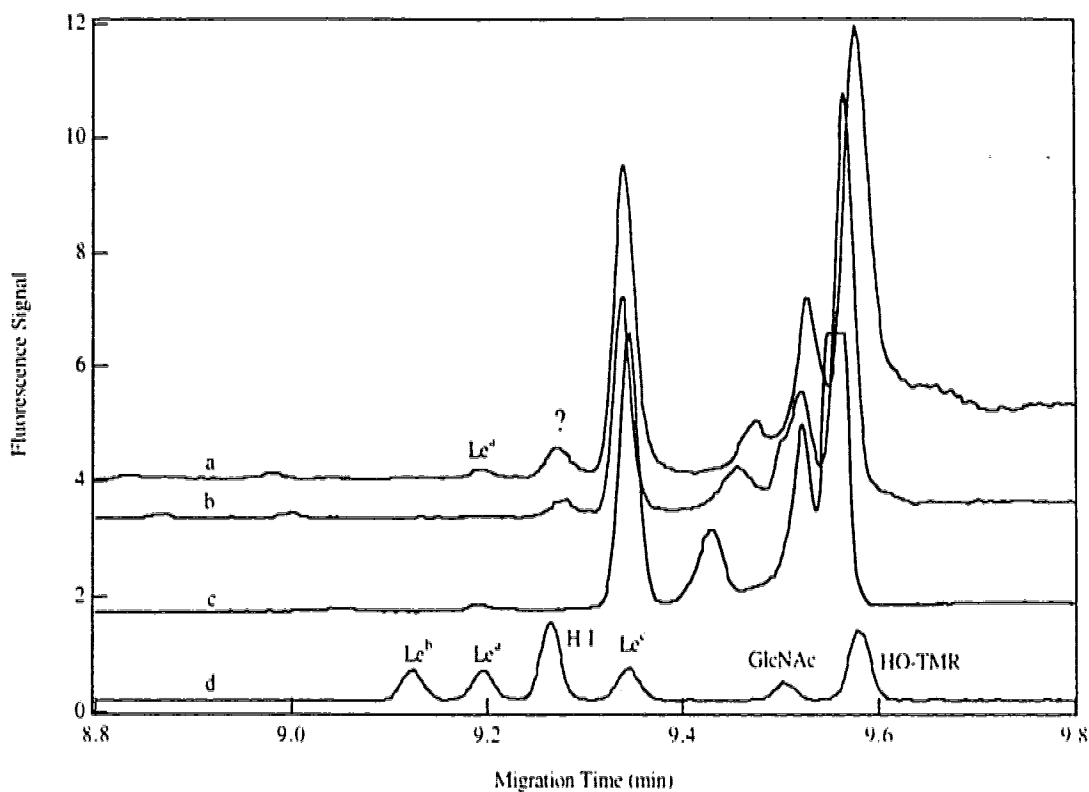


Figure 4.12 The electropherograms of α -fucosidase and neuraminidase treated pellet of 15 μ M Le^c uptake by A431 cells for 19 h.
 (a) The cell pellet from 15 μ M Le^c uptake by A431 cells for 19 h (see Figure 4.6d)
 (b) The human placenta α -fucosidase hydrolyzed the pellet for 94 h.
 (c) Sample after fucosidase treatment from above was further hydrolyzed by a neuraminidase for 67 h.
 (d) The separation of six standard mixtures.

α -Fucosidase treatment: An aliquot of 5 μ L pellet (15 μ M Le^c uptake by A431 cells) saved in MeOH was dried. 4 μ L pH 5.5 (150 mM citrate) buffer and 1 μ L 15.6 μ U/ μ L α -fucosidase from human placenta were added. The mixture was incubated for 94 h at 37 $^\circ$ C. 4 μ L MeOH was added prior to an CE injection.

Neuraminidase treatment: The sample after α -fucosidase treatment from above was dried. Then 1 μ L neuraminidase and 4 μ L H_2O were added and incubated for 67 h at 37 $^\circ$ C.

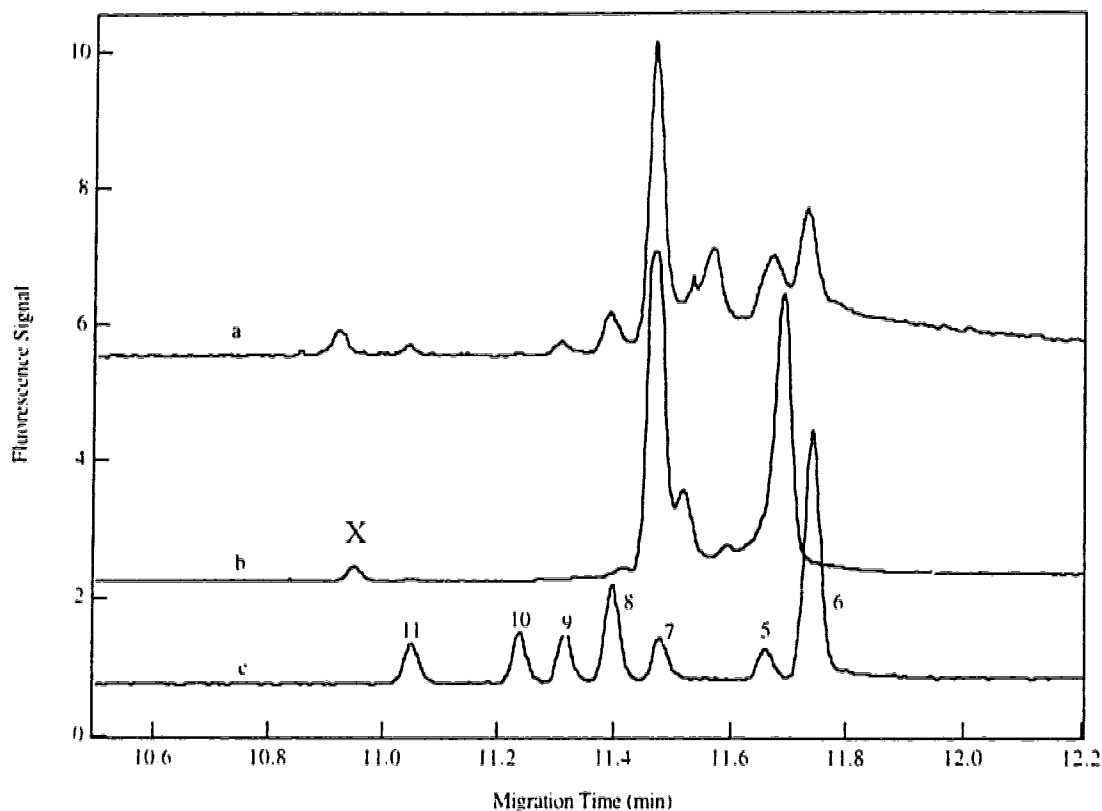


Figure 4.13 Electropherograms of neuraminidase treatment of 25 μM Le^c for uptake 19.5 h by A431 cell pellet. (a) Pellet of Le^c uptake by A431 cells for 19.5 h. (b) Sample from (a) was digested by neuraminidase for 68 h. (c) Separation of seven standards.

- 5 GlcNAc, $\beta\text{GlcNAc-O-TMR}$.
- 6 HO-TMR. H-O(CH₂)₈CONHCH₂CH₂NH-tetramethylrhodamine. the Linker arm
- 7 Le^c, $\beta\text{Gal}(1\rightarrow3)\beta\text{GlcNAc-O-TMR}$. Lewis C
- 8 H I, $\alpha\text{Fuc}(1\rightarrow2)\beta\text{Gal}(1\rightarrow3)\beta\text{GlcNAc-O-TMR}$. H type I
- 9 Le^a, $\beta\text{Gal}(1\rightarrow3)[\alpha\text{Fuc}(1\rightarrow4)]\beta\text{GlcNAc-O-TMR}$. Lewis A
- 10 Le^b, $\alpha\text{Fuc}(1\rightarrow2)\beta\text{Gal}(1\rightarrow3)[\alpha\text{Fuc}(1\rightarrow4)]\beta\text{GlcNAc-O-TMR}$
- 11 2,3-sialyl Le^c, $\alpha\text{NeuAc}2\rightarrow3\beta\text{Gal}(\rightarrow3)\beta\text{GlcNAc-O-TMR}$,
- X unknown sugar

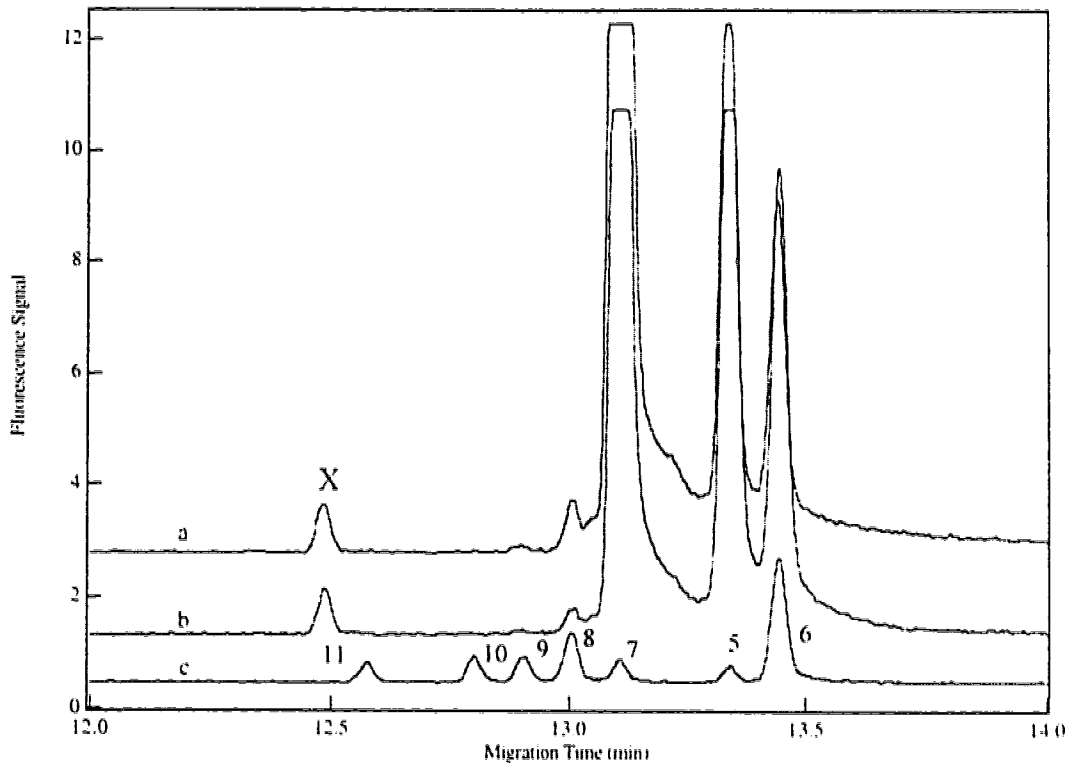


Figure 4.14 Electropherograms of A431 cell extract incubated with Le^c without adding donor GDP fucose (Mixture A). (a) 21 h . (b) 65 h incubation, and (c) Le^c standard series.

- 5 GlcNAc. β GlcNAc-OTMR.
- 6 HO-TMR. H-O(CH₂)₈CONHCH₂CH₂NH-tetramethylrhodamine, the linker arm
- 7 Le^c. β Gal(1→3) β GlcNAc-O-TMR, Lewis C
- 8 H I, α Fuc(1→2) β Gal(1→3) β GlcNAc-O-TMR, H type I
- 9 Le^a. β Gal(1→3)[α Fuc(1→4)] β GlcNAc-O-TMR, Lewis A
- 10 Le^b. α Fuc(1→2) β Gal(1→3)[α Fuc(1→4)] β GlcNAc-O-TMR
- 11 2,3-sialyl Le^c. α NeuAc2→3 β Gal(→3) β GlcNAc-O-TMR,
- X unknown sugar

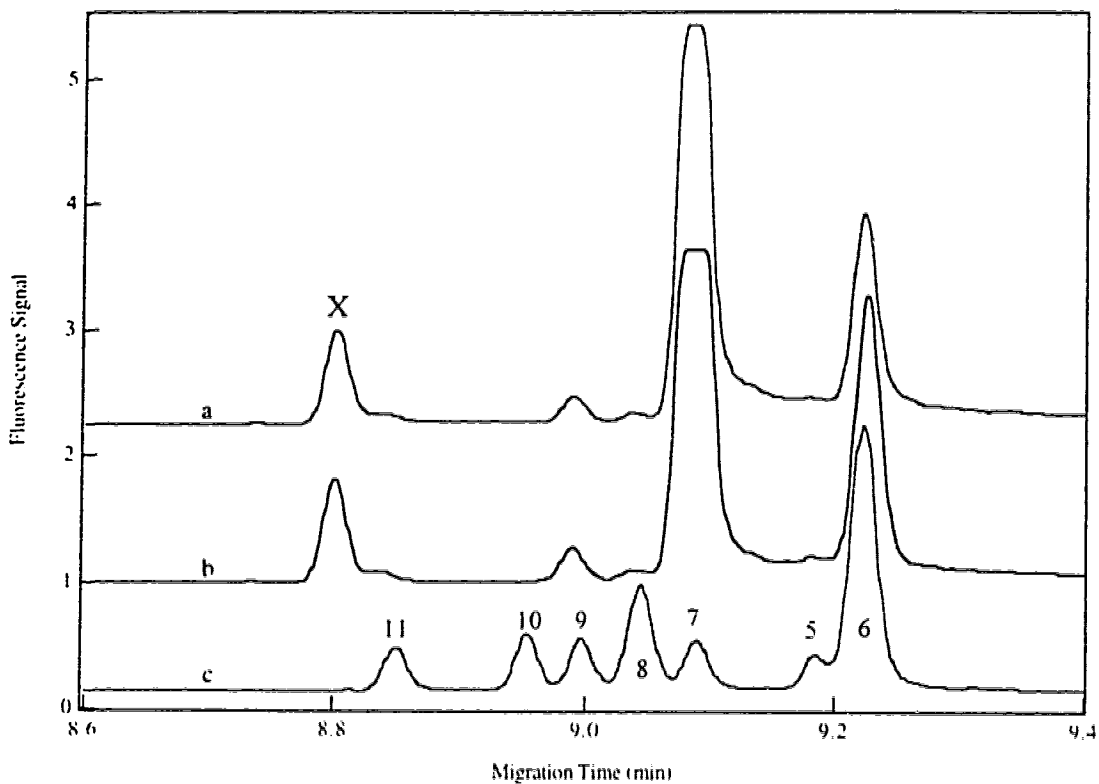


Figure 4.15 Electropherograms of A431 cell extract and Le^c incubated with PAPS (a sulfate donor) or without a PAPS. (a) A431 cell extract incubated with Le^c without adding a donor PAPS. (b) A431 cell extract incubated with Le^c and a donor of PAPS. (c) Le^c series standards.

- 5 GlcNAc, β GlcNAc-OTMR.
- 6 HO-TMR, H-O(CH₂)₈CONHCH₂CH₂NH-tetramethylrhodamine, the Linker arm
- 7 Le^c, β Gal(1→3) β GlcNAc-O-TMR, Lewis C
- 8 H I, α Fuc(1→2) β Gal(1→3) β GlcNAc-O-TMR, H type I
- 9 Le^a, β Gal(1→3)[α Fuc(1→4)] β GlcNAc-O-TMR, Lewis A
- 10 Le^b, α Fuc(1→2) β Gal(1→3)[α Fuc(1→4)] β GlcNAc-O-TMR
- 11 2,3-sialyl Le^c, α NeuAc2→3 β Gal(→3) β GlcNAc-O-TMR,
- X unknown sugar

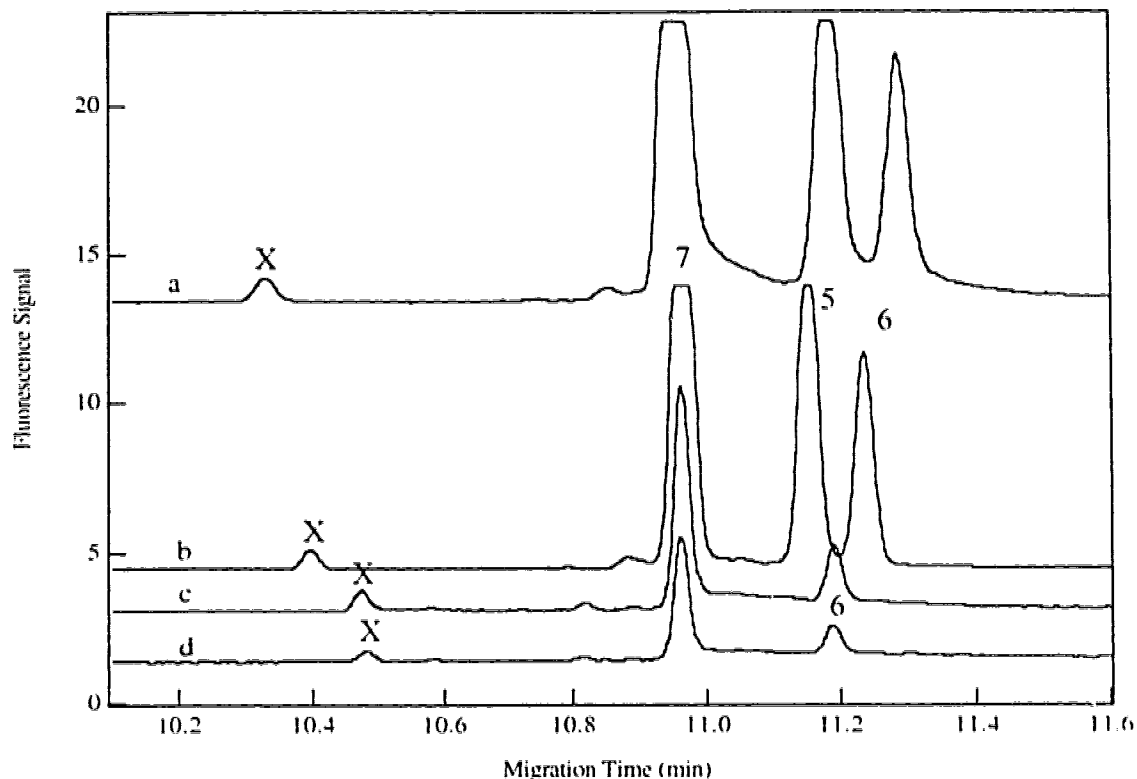


Figure 4.16 Electropherograms of Mixture A hydrolyzed by phosphatases. (a) A431 cell extract was incubated with Le^c for 65 h. The total TMR concentration was 1×10^{-7} M. (b) Sample prepared in the same way as in (a) was digested by alkaline phosphatase for 68 h at pH 8.5 (50 mM Tris buffer) and at 37 °C. 1×10^{-7} M total TMR was injected. Samples from (a) were digested with phospholipase A2 at pH 8.6 (c) and pH 9.5 (d) at room temperature for 66 h. 100 \times 5 sec in (c) and 200 \times 5 sec in (d) with 1×10^{-7} M total TMR were injected. Capillary is 42.6 cm long and 10 μ m i.d..

- 5 GlcNAc. β GlcNAc-OTMR.
- 6 HO-TMR. H-O(CH₂)₈CONHCH₂CH₂NH-tetramethylrhodamine. the Linker arm
- 7 Le^c, β Gal(1 \rightarrow 3) β GlcNAc-O-TMR. Lewis C
- 8 H I, α Fuc(1 \rightarrow 2) β Gal(1 \rightarrow 3) β GlcNAc-O-TMR. H type I
- 9 Le^a, β Gal(1 \rightarrow 3)[α Fuc(1 \rightarrow 4)] β GlcNAc-O-TMR. Lewis A
- X unknown sugar

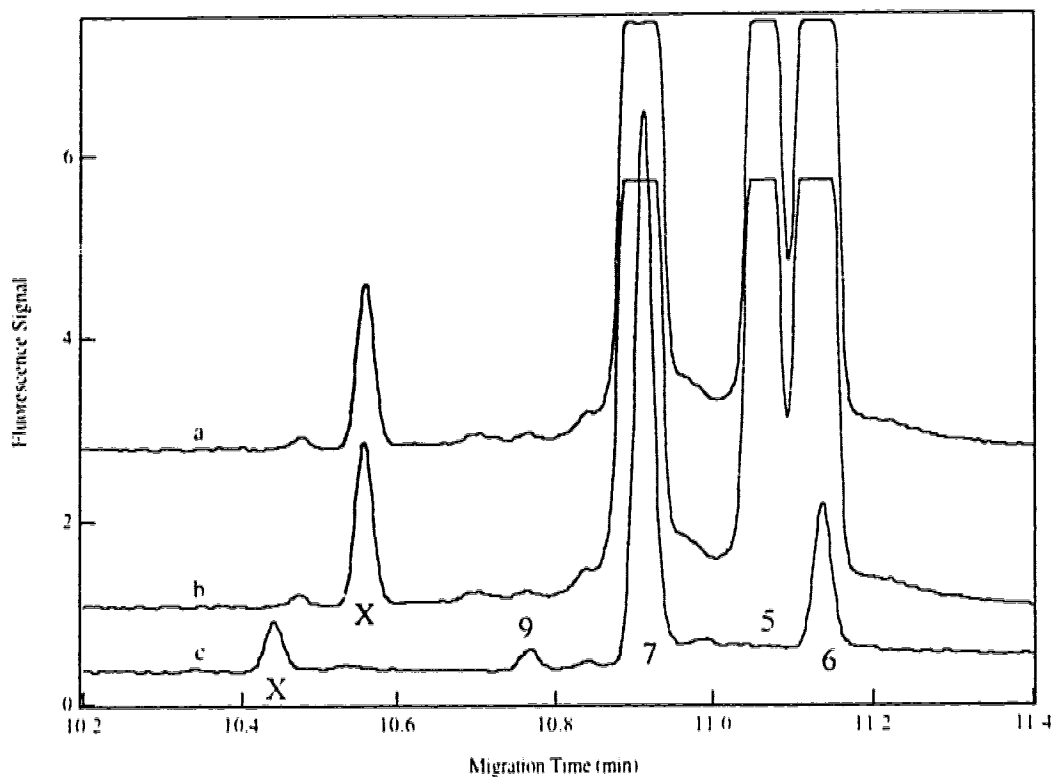


Figure 4.17 Electropherograms of mixture A digested by three sulfatases. (a) the sulfatase from *Aerobacter aerogenes* (compared to Figure 4.14a). (b) the sulfatase from Abalone Entrails (compare to Figure 4.14a). (c) the sulfatase from limpet (compare to Figure 4.15a).

- 5 GlcNAc. β GlcNAc-OTMR.
- 6 HO-TMR. H-O(CH₂)₈CONHCH₂CH₂NH-tetramethylrhodamine. the Linker arm
- 7 Le^c. β Gal(1→3) β GlcNAc-O-TMR. Lewis C
- 8 H I. α Fuc(1→2) β Gal(1→3) β GlcNAc-O-TMR. H type I
- 9 Le^a. β Gal(1→3)[α Fuc(1→4)] β GlcNAc-O-TMR. Lewis A
- X unknown sugar

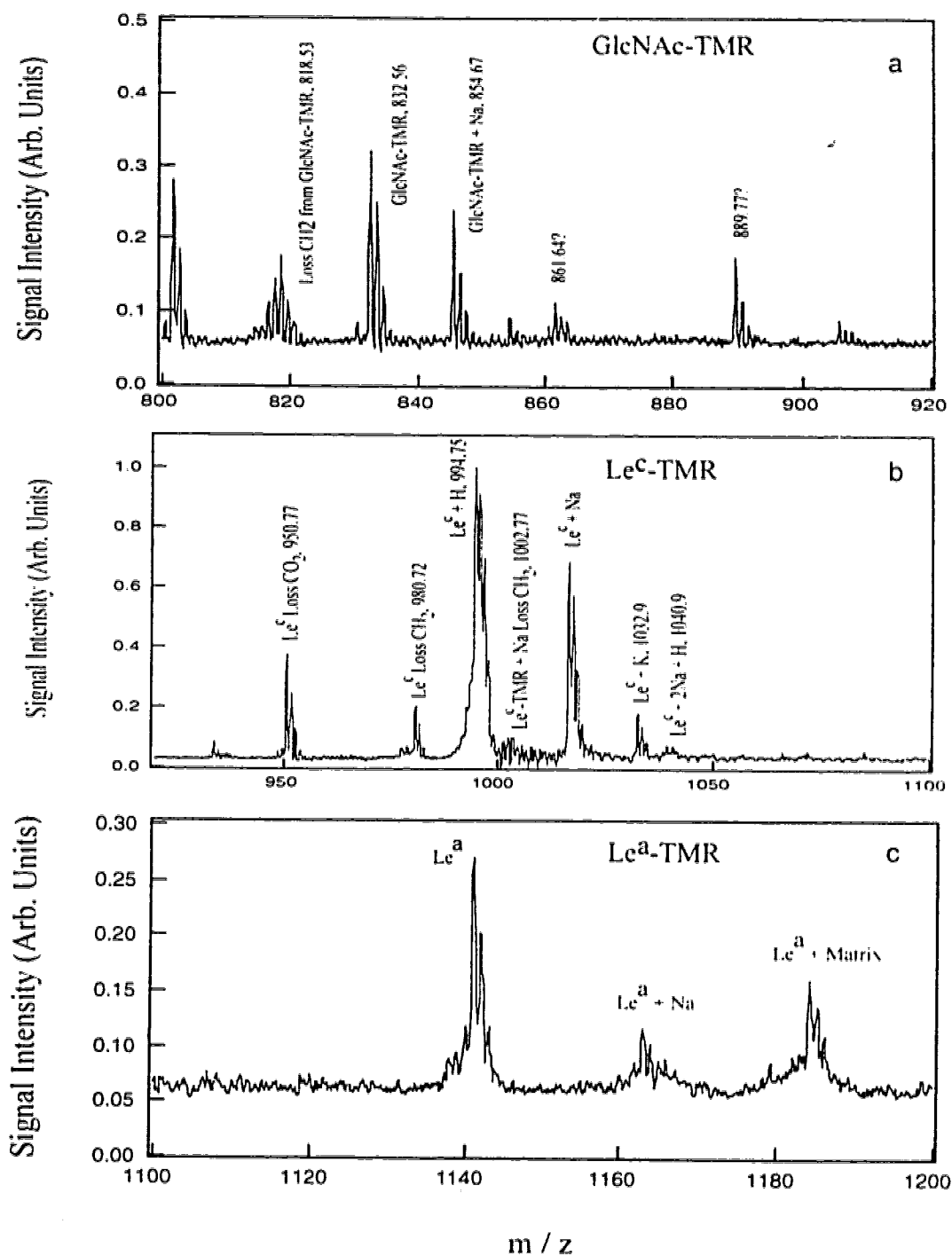


Figure 4.18 Mass Spectrum of A431 cell extract incubated with Le^c for 65 h. About 0.7 pmole total TMR labeled compounds were analyzed using 4-HCCA as the matrix. The capillary electropherogram is in Figure 4.15a. (a) m/z 800-920, (b) 920-1100, and (c) m/z 1100-1200.

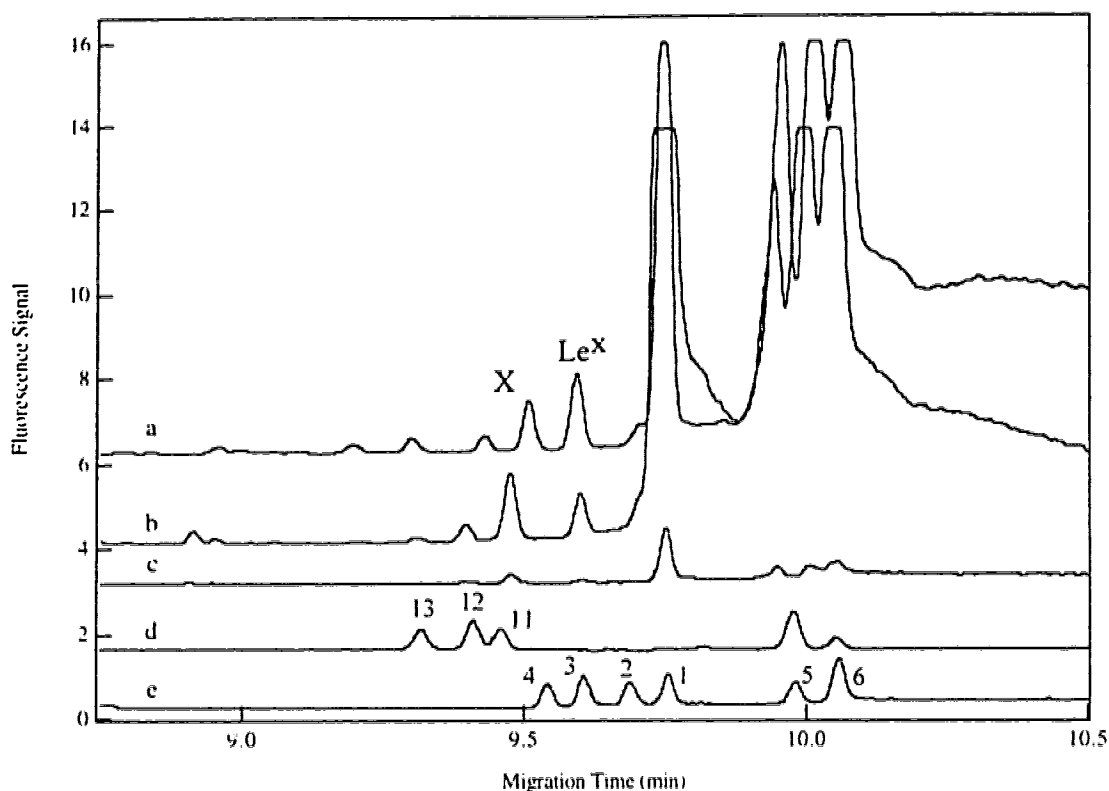


Figure 4.19 Electropherograms of 25 μM LacNAc uptake by HT-29 cells (6×10^6) for 20 h. (a) cell uptake pellet. (b) PBS wash after trypsin. (c) PBS wash before trypsin. (d) separation of 2.3Sialyl LacNAc (13), 2.6sialyl LacNAc (12) and 2.3sialyl Le^c (11) and GlcNAc (5) and the linker arm (6). (e) Separation of LacNAc series standards.

- | | |
|-----------|--|
| 1 | LacNAc, $\beta\text{Gal}(1 \rightarrow 4) \beta\text{GlcNAc-O-TMR}$ |
| 2 | H II, $\alpha\text{Fuc}(1 \rightarrow 2) \beta\text{Gal}(1 \rightarrow 4) \beta\text{GlcNAc-O-TMR}$. H type II |
| 3 | Le ^x , $\beta\text{Gal}(1 \rightarrow 4)[\alpha\text{Fuc}(1 \rightarrow 3)] \beta\text{GlcNAc-O-TMR}$. Lewis X |
| 4 | Le ^y , $\alpha\text{Fuc}(1 \rightarrow 2)\beta\text{Gal}(1 \rightarrow 4)[\alpha\text{Fuc}(1 \rightarrow 3)]\beta\text{GlcNAc-O-TMR}$. Lewis Y |
| 5 | $\beta\text{GlcNAc-O-TMR}$. GlcNAc |
| 6 | H-O(CH ₂) ₈ CONHCH ₂ CH ₂ NH-tetramethylrhodamine. the Linker arm |
| 11 | 2,3-sialyl Le ^c , $\alpha\text{NeuAc}2 \rightarrow 3\beta\text{Gal}(\rightarrow 3)\beta\text{GlcNAc-O-TMR}$, |
| 12 | 2,6-sialyl LacNAc, $\alpha\text{NeuAc}2 \rightarrow 6\beta\text{Gal}(1 \rightarrow 4)\beta\text{GlcNAc-O-TMR}$ |
| 13 | 2,3-sialyl LacNAc, $\alpha\text{NeuAc}2 \rightarrow 3\beta\text{Gal}(1 \rightarrow 3)\beta\text{GlcNAc-O-TMR}$ |
| X | unknown sugar |

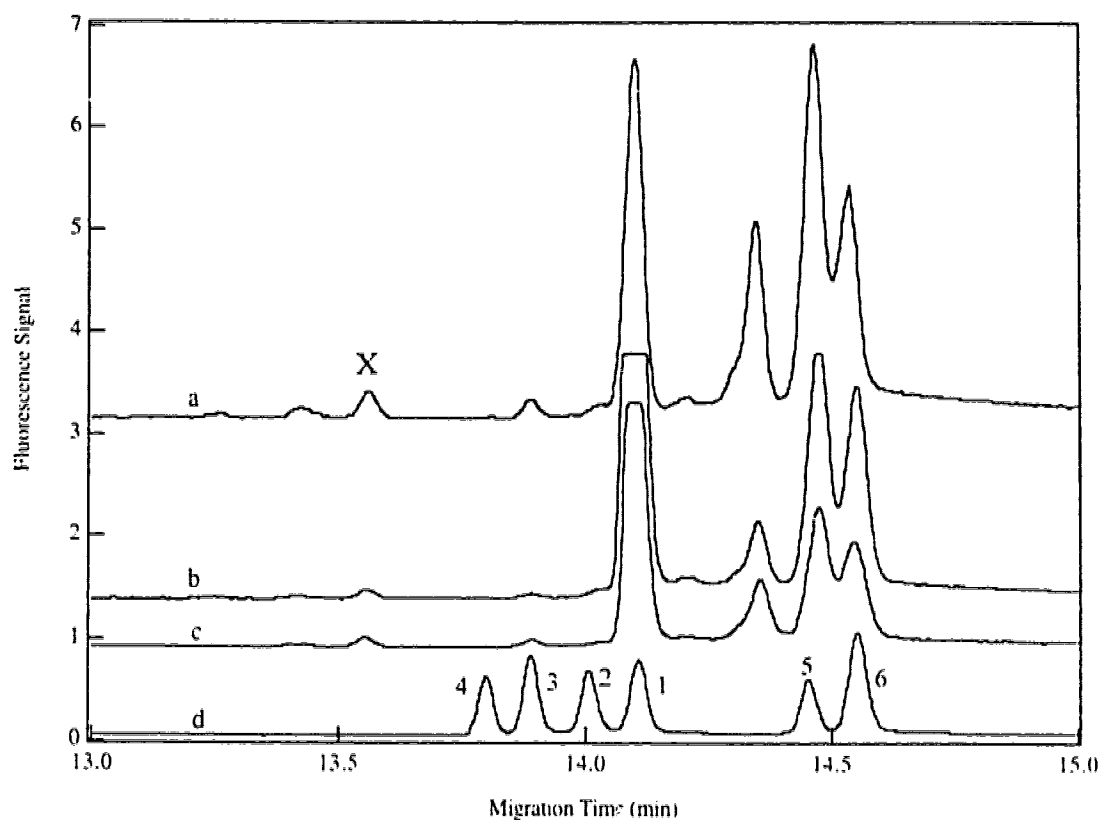


Figure 4.20 Electropherograms of 25 μ M LacNAc uptake by HT-29 cells for 22 h. (a) Cell pellet. (b) Post-trypsin PBS wash. (c) Pre-trypsin PBS wash. (d) LacNAc standard series.

- 1 LacNAc. β Gal(1 \rightarrow 4) β GlcNAc-O-TMR
- 2 H I, α Fuc(1 \rightarrow 2) β Gal(1 \rightarrow 4) β GlcNAc-O-TMR, H type II
- 3 Le^X, β Gal(1 \rightarrow 4)[α Fuc(1 \rightarrow 3)] β GlcNAc-O-TMR, Lewis X
- 4 Le^Y, α Fuc(1 \rightarrow 2) β Gal(1 \rightarrow 4)[α Fuc(1 \rightarrow 3)] β GlcNAc-O-TMR, Lewis Y
- 5 β GlcNAc-O-TMR, GlcNAc
- 6 H-O(CH₂)₈CONHCH₂CH₂NH-tetramethylrhodamine, the Linker arm
- X unknown sugar

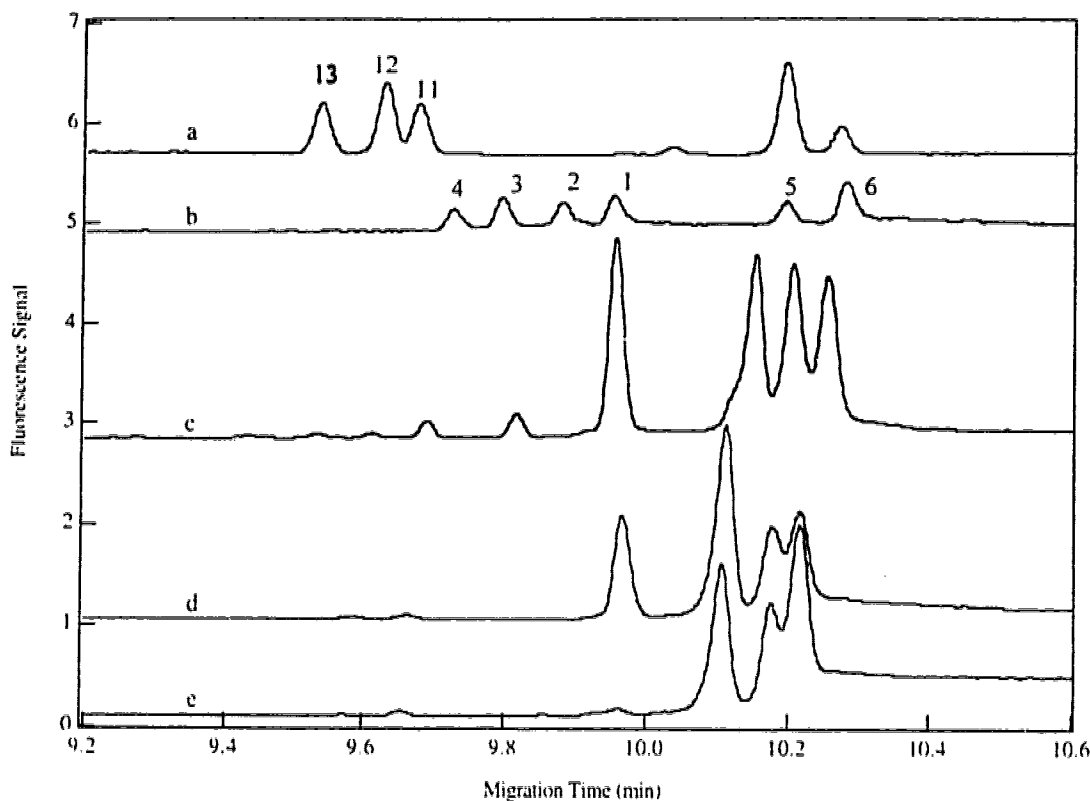


Figure 4.21 Electropherograms of pellet from 25 μM LacNAc uptake by A431 cells (Figure 4.19) for 20 h with the treatment of a fucosidase and a neuraminidase.

(a) sialyl standards, (b) LacNAc series standards, (c) cell uptake pellet, (d) α -fucosidase 36 h digestion, and (e) neuraminidase 36 h treatment.

Fucosidase treatment: A 2 μL aliquot of the LacNAc uptake HT-29 pellet dissolved in MeOH was dried. α -fucosidase (2 $\mu\text{U}/\mu\text{L}$, almond meal) and buffer (pH 5.5) were added. After 36 h incubation, the sample was diluted by adding 10 mL MeOH and 6 mL PBpBS buffer prior to CE injection.

Neuraminidase treatment: The sample, same as above, was treated with 4 μL of 150 mM citrate buffer (pH 5) and 0.5 μL neuraminidase (9 $\mu\text{U}/\mu\text{L}$). The mixture was incubated at 37 $^{\circ}\text{C}$ for 36 h.

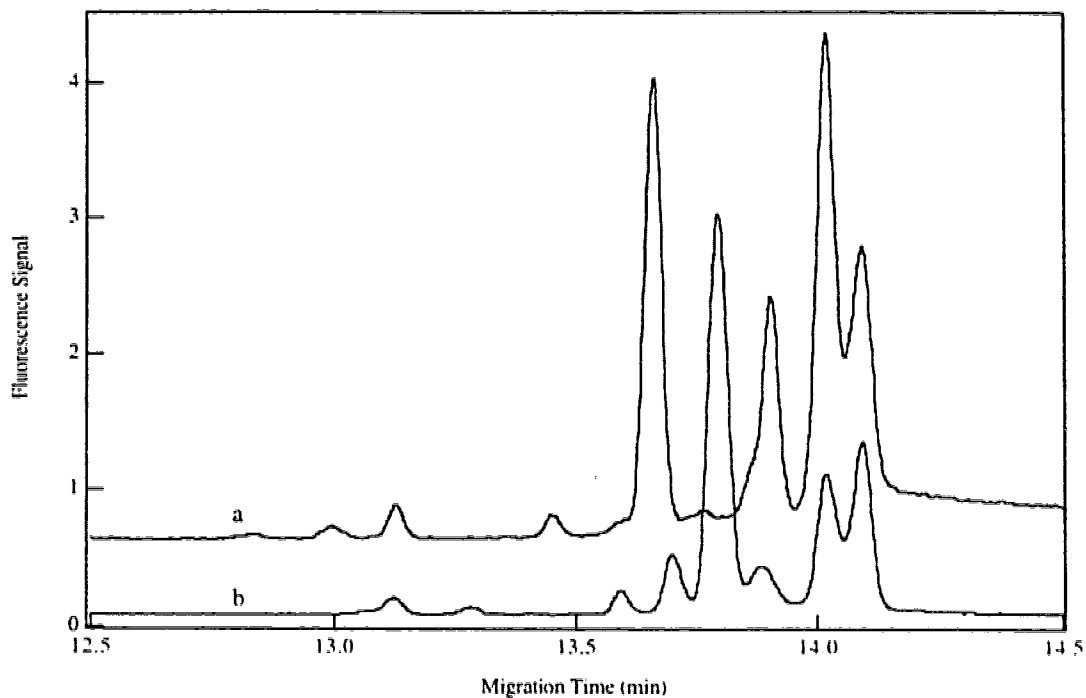


Figure 4.22 Electropherograms of LacNAc uptake by HT-29 cells (a) and Le^c uptake by A431 cells (b).

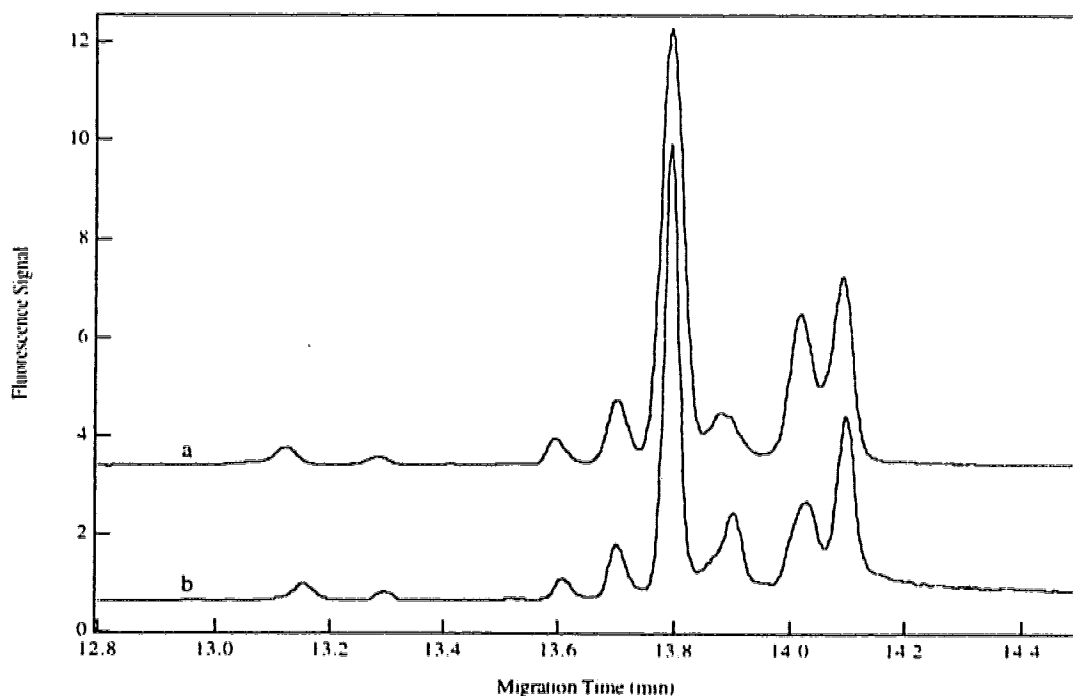


Figure 4.23 Electropherograms of the same A431 cell uptake sample run in different time (b) was two months later than the (a). Capillary 45.5 cm long in (a) and 42.6 cm long in (b). All other conditions were the same.

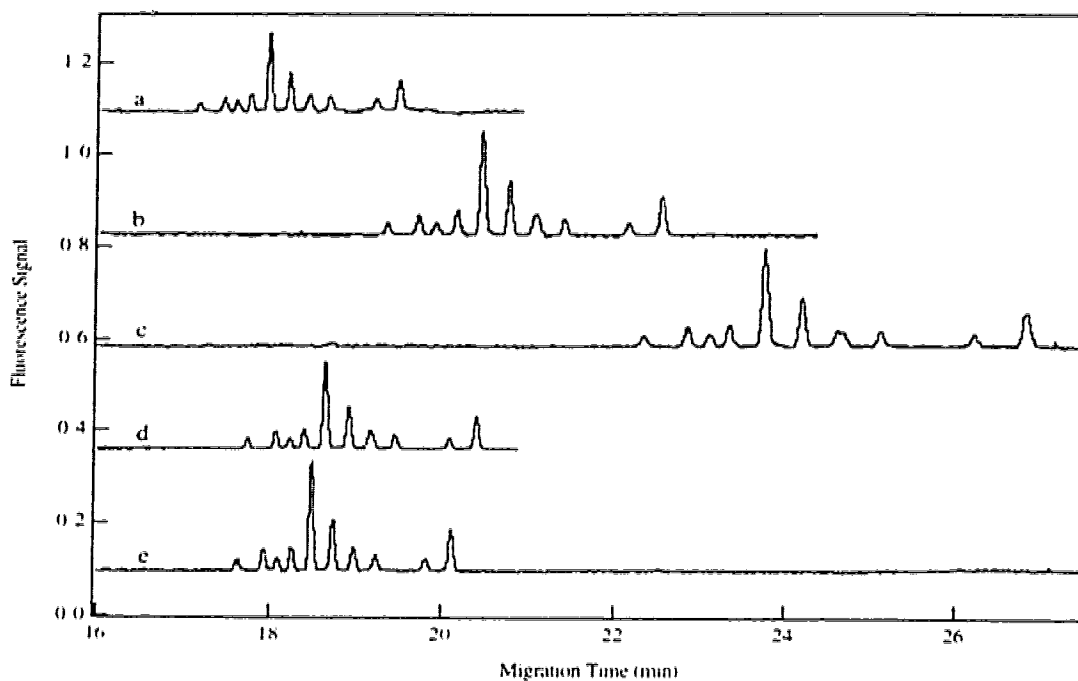


Figure 4.24 Electropherograms of the separation of 1-13 TMR labeled compounds by different buffer compositions.

Separation buffers: (a) $P_2Bp_2B_2S_2$. (b) $P_2Bp_3B_2S_2$. (c) $P_2Bp_4B_2S_2$. (d) $P_2Bp_2BS_2$. (e)

$P_{1.9}Bp_{1.9}B_{2.9}S_{1.9}$. The mixture containing 12 synthetic sugars labeled with TMR and one linker arm. Each TMR labeled compound is 1×10^{-8} M in 80 μ L BS and 123 μ L PBpBS (pH 9) buffer mixture.

P: phosphate. B: borate. Bp: phenyl boronic acid and S: SDS. .

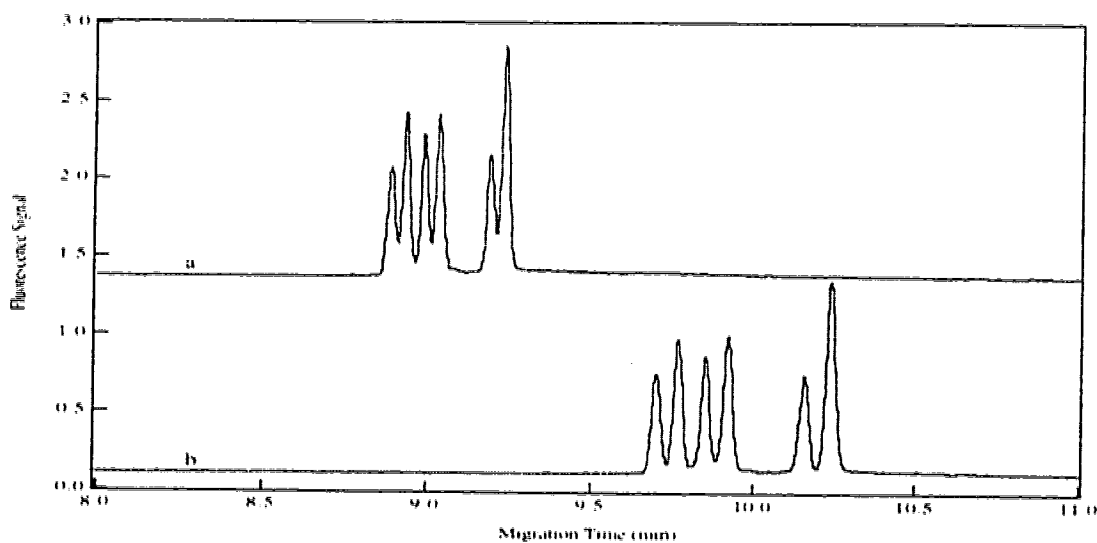


Figure 4.25 Electropherograms of the separations of six LacNAc series standards by 10 mM PBsBS (a) and 10 mM PBpBS (b). Bs: 3-amino phenyl borate.

CHAPTER 5

THE BIOSYNTHESIS OF Le^x IN *HELICOBACTER PYLORI*

* A portion of this chapter has been published.

Chan, N.W.C., Stangier, K., Sherburne, R., Taylor, D. E., Zhang, Y., Dovichi, N. J., and Palcic, M.M.

Glycobiology (1995), 5, 683-688.

Acknowledgment: We would like to thank Dr. S. Forsbers for methylation analysis (Complex Carbohydrate Research Center, University of Georgia).

5.1 INTRODUCTION

Oligosaccharides not only are found in mammalian cells but also on bacteria cell surfaces. In 1961 (1), A, B and H blood group structures were found on the gram-negative bacteria, and recently the H type I determinant (α Fuc(1 \rightarrow 2) β Gal(1 \rightarrow 3)GlcNAc-) (2) and Lewis X (Le^X) structures have been reported (3). While the mammalian glycosyltransferases that synthesize these structures are well characterized (4, 5), little is known about the corresponding bacterial enzymes. The recent report of the Le^X structure, β Gal(1 \rightarrow 4) α Fuc(1 \rightarrow 3) β GlcNAc- on O antigens of *Helicobacter pylori* (*H. pylori*) (3), a human pathogen and a microaerophilic bacterium thought to cause several diseases in the gastrointestinal tract of humans worldwide, including chronic active gastritis, gastric and duodenal ulcers, and gastric adenocarcinoma (6), prompted our investigation into its biosynthesis. In mammals, this structure is found on glycoproteins and glycolipids where it is a stage-specific embryonic antigen and a tumor associated marker (7-9). The Le^X structure has also been found in a lower eukaryote, in the surface antigen from the eggs of the parasitic worm *Schistosoma mansoni*, where it has been shown to play a signaling role in the interaction of the parasite with its human host (10).

Chemical analysis, the alditol acetate method together with ¹H NMR data, was used to characterize the O antigen composition from *H. pylori*. The detection limit is in the micromole range (3). TLC-immunostaining assay has been used to identify glycolipid receptors from *H. pylori* isolated from the antral mucosal biopsy specimen (11). The main steps in this assay are: a silica gel-coated plate was treated by a blocking buffer (polyvinylpyrrolidone), followed by incubation with *H. pylori* (10⁸ cells/ml), then it was treated by blocking buffer again, followed by antibody treatment, and detection by a TLC densitometer. The sensitivity is in the upper nanomole range. Other general methods including SDS-PAGE, methylation and mass spectrometry have been used to characterize and identify an antigenic polysaccharide from *Campylobacter coli* Penner serotype 0:30 bacteria cells (12). All these methods have been utilized to detect and characterize the

bacteria cell surface carbohydrates or antigens. However, the enzymes that participate in the process to generate those antigens have not been explored. A radiochemical method has been applied to assay glycosyltransferases. It required both a donor and a substrate, and the sensitivity for the product detection can reach the femtomole range. The method cannot differentiate more than two products. From chapter 4, capillary electrophoresis with laser-induced fluorescence detection has been used to monitor Le^c uptake by A431 cells. The minor products from 10 cells can be detected. With this sensitive technique and since synthetic sugar substrates are available, the glycosyltransferases in *H. pylori* have also been investigated.

In mammals, the Le^x structure is synthesized by the strictly sequential addition of galactose from UDP-Gal to GlcNAc catalyzed by a β (1 \rightarrow 4) galactosyltransferase, followed by the transfer of fucose from GDP-Fuc to the disaccharide β Gal(1 \rightarrow 4) β GlcNAc (LacNAc) by an α 1 \rightarrow 3fucosyltransferase. In this chapter, both GlcNAc and LacNAc were chosen as substrates to monitor the galactosyltransferase and fucosyltransferase activities from the *H. Pylori* bacteria cell extract, respectively. The biosynthesis of Le^x occurs in an analogous fashion in *H. pylori* and was detected with CE-LIF.

5.2 EXPERIMENTAL SECTION

5.2.1 Materials

β GlcNAc-O-TMR(GlcNAc-O-TMR), β Gal(1 \rightarrow 4) β GlcNAc-O-TMR (LacNAc-O-TMR), β Gal(1 \rightarrow 4)[α Fuc(1 \rightarrow 3)] β GlcNAc-O-TMR (Le^x-O-TMR) and H-O-(CH₂)₈CO(CH₂)₈CONHCH₂CH₂NH-tetramethylrhodamine (a linker arm called H-O-TMR) and corresponding unlabeled substrates R-O-(CH₂)₈COOMe (R including GlcNAc, LacNAc and Le^x), were synthesized by Dr. Ole Hindsgaul (Department of Chemistry, University of Alberta). GDP-fucose was synthesized by the method of Golhale et al (13). The antibodies used were mouse isotype IgM anti-human CD15MAB

(Cederlane Laboratories) which have documented specificity for (β Gal(1 \rightarrow 4)[α Fuc(1 \rightarrow 3)] β GlcNAc(1 \rightarrow 3) β Gal(1 \rightarrow 4)Glc)Lacto-N-fucopetaose III (LNFP III) also called hapten X and Le^x (14) Anti-Le^a MAB (Synaff-Chembiomed) was specific for (β Gal(1 \rightarrow 3)[α Fuc(1 \rightarrow 4)]GlcNAc and anti-Le^b MAB was specific for α Fuc(1 \rightarrow 2) β Gal(1 \rightarrow 3)[α Fuc(1 \rightarrow 4)]GlcNAc. Sep-Pak plus C-18 reverse phase cartridges were obtained from Waters (Mississauga, Ont.), and conditioned before use by washing with 1 mL of methanol and 20 mL of water. Protein concentrations were estimated with a Bio-Rad protein assay kit which was based on the method described by Bradford (15) using bovine serum albumin as a standard. All other chemicals were of reagent grade.

5.2.2 Cell Growth (Dr. Diane E. Taylor and Dr. Richard Sherburne)

Helicobacter pylori strains UA 861, UA 802 and UA 1182 were isolated from endoscopic biopsy specimens obtained from patients attending the University of Alberta Hospital using methods described previously by Taylor et al (16, 17). *H. pylori* strains were grown on brain heart infusion agar (Oxoid Basingstoke, U.K.) containing 5% yeast extract, 5% bovine serum with 15 μ g/mL vancomycin and 15 μ L amphotercin. Cultures were incubated with 5% carbon dioxide, 5% hydrogen and the balance nitrogen at 37 °C. Control cultures of *Escherichia coli* (*E. Coli*), *Campylobacter fetus* (*C. fetus*) and *Campylobacter jejuni* (*C. jejuni*) were grown on Mueller Hinton agar (Oxoid Basingstoke U.K.) and incubated in 5% carbon dioxide at 37 °C. Each petri dish contained 2.5×10^9 colony forming units (c.f.u.).

E. Coli, *C. fetus*, *C. jejuni* and *H. pylori* whole cells were removed from agar plates and suspended in phosphate buffered saline (PBS; pH 7.3). The whole-cell suspensions were then centrifuged using a Clinical Centrifuge (International Equipment Co. model CL) and washed twice with PBS.

5.2.3 Enzyme Extract Preparation and Activity Screening (by Nora W. C. Chan in Dr. Monica M. Palcic's group)

Cells were collected from the Petri dishes by washing with 2 mL of 20 mM HEPES buffer (pH 7.0) and centrifuging at 3,000 g for 10 min at 4 °C. The supernant (2 mL) was removed and saved for assays of secreted enzymes. The cell pellet was resuspended in 4 mL of 20 mM HEPES buffer (pH 7.0) and disrupted by sonication for 5 × 15 sec using a microprobe tip. The cells were spun at 3,000 × g for 10 min. and the supernant (4 mL) was retained for analysis of soluble enzymes. The pellet was resuspended in 1 mL of 20 mM HEPES (pH 7.0), containing 20 mM MnCl₂, 0.2% BSA and 0.2% Triton X-100. the suspension was vortexed for 5 min., centrifuged for 10 min. at 3,000 x g and the supernatant (1 mL) set aside for assays for membrane-bound enzymes. Enzyme activity was stable in all the extracts for 7 days when stored at 4 °C.

$\alpha(1\rightarrow3)$ and $\alpha(1\rightarrow4)$ fucosyltransferase activities were assayed by incubating 24 μ L of extract at 37 °C for 90 min with 450 μ M acceptor, 50 μ M GDP-fucose, 45,000 d.p.m. GDP-[³H] fucose, 20 mM HEPES buffer at pH 7.0, 20 mM MnCl₂ and 0.2% BSA in a total volume of 40 μ L. For $\alpha(1\rightarrow3)$ fucosyltransferase activity, Gal $\beta(1\rightarrow4)$ GlcNAc β -O-(CH₂)₈-COOMe was used as an acceptor. for $\alpha(1\rightarrow4)$ fucosyltransferase activity Gal $\beta(1\rightarrow3)$ GlcNAc β -O-(CH₂)₈COOMe was used as an acceptor. After incubation, the reaction mixtures were loaded onto Sep-Pak Plus C-18 cartridges, the cartridges were washed with 50 mL of water to remove unreacted donor and then products were eluted with 5 mL of methanol and quantitated by counting in 10 mL of Ecolite (+) cocktail in a Beckman LS 1801 scintillation counter (18).

$\beta(1\rightarrow4)$ Galactosyltransferase activity was estimated by incubating 10 μ L of the various extracts at 37 °C for 90 min. with 372 μ M GlcNAc β -O-(CH₂)₈COOMe, 182 μ M UDP-galactose, 80,000 d.p.m. UDP-[³H]Gal, 77 mM sodium cacodylate buffer (pH 7.4), 8 mM MnCl₂ and 0.25 M NaCl in a total volume of 55 μ l. Radiolabeled product was isolated and quantitated as described previously for the fucosyltransferase assays. A

milliunit of enzyme activity is the amount that catalyzes the conversion of one nanomole of acceptor to product per minute under the standard screening conditions. Negative control assays for both activities that utilized uninoculated plates. *Escherichia coli* cells, *Campylobacter fetus*, and *Campylobacter jejuni* were carried out in an analogous fashion.

5.2.4 Capillary Electrophoresis

For fucosyltransferase reactions, the incubation mixtures contained 33 μL of the membrane associated extract from UA 802 or UA 861, 28 μM LacNAc-O-TMR and 50 μM GDP-fucose in a total volume of 40 μL of 20 mM Hepes buffer (pH 7.0), containing 20 mM MnCl_2 and 0.2% BSA. After incubation at 37 °C for 3 h, the samples were applied to Sep-Pak Plus C-18 cartridges which were washed with 30 mL of water, then the product was eluted in 3.5 mL of HPLC grade methanol. Samples were diluted (1:2) with running buffer (10 mM phosphate, 10 mM borate, 10 mM SDS and 10 mM phenylboronic acid) and analyzed by capillary electrophoresis by injecting 13 μL onto the electrophoresis column (42 cm long) at 1 kv for 5 sec (19, 20). For the galactosyltransferase reactions, 15 μL of the Triton X-100 extract was incubated for 3 h at 37 °C with 182 μM GlcNAc-O-TMR, 182 μM UDP-Gal in 245 mM NaCl, 8 mM MnCl_2 and 77 mM sodium cacodylate buffer, pH 7.4, all in a total volume of 55 μL . Products were isolated by Sep Pak, eluted in 3.5 mL methanol and analyzed by capillary electrophoresis at 400 V/cm as described previously for the fucosyltransferases. The peak identifications were accomplished by adding internal standard (either adding GlcNAc or the linker arm) and compared with a electropherogram of standard sugar mixture performed at the closest time possible.

5.2.5 Preparative Synthesis and Methylation Analysis

All preparative syntheses were carried out for 48 h at room temperature in 1.5 mL microfuge tubes. Mixtures contained 0.5 mg of acceptor (Gal β (1 \rightarrow 4)GlcNAc β -O-

(CH₂)₈COOMe or GlcNAcβ-O-(CH₂)₈COOMe), 1.5 equivalents of GDP-fucose or UDP-Gal and between 0.25 to 1.0 mL of the Triton X-100 extract from all three strains (0.4 munits).

The methylation analysis (21, 22) utilized the Hakomori procedure (23). In this sequence, the permethylated oligosaccharide obtained during the Hakomori methylation was subjected to sequential hydrolysis (2 M trifluoroacetic acid (TFA), 100 °C, 2h), N-acetylation (methanol, pyridine/acetic anhydride), hydrolysis (2 M TFA, 121 °C, 2h), and reduction with sodium borodeuteride. The resulting partially methylated alditols were then acetylated and analyzed by gas chromatography (electron impact) using a 50 meter methyl silicone capillary column (Quadrex Corporation) equipped with a mass selective detector. Scans were compiled at a rate of 1 scan /s over a m/z range of 40-500 a.m.u.

5.3 RESULTS AND DISCUSSION

5.3.1 Fucosyltransferase and Galactosyltransferase Activities

α1.3 fucosyltransferase activity was quantitated using Galβ(1→4)GlcNAcβ-O-(CH₂)₈COOMe as an acceptor and GDP-fucose as the donor. For strain UA 861 most of the activity was detected in the Triton X-100 extracts, while activity was found in all fractions for UA 802 and UA 1182 extracts (Table 5.1). UA 802 and 1182 had comparable levels in all fractions that was consistently higher than that found membrane bound in UA 861 cells. No α1.4 fucosyltransferase activity was found in any of the strains using βGal(1→3)βGlcNAc-O-(CH₂)₈COOMe as an acceptor. While the levels of activity were comparable in different extracts of UA 802 and UA 1182, they were highly variable and occasionally undetectable in extracts from UA 861 cells. Neither α1.3 nor α1.4 fucosyltransferase activity was present in *Escherichia coli*, *Campylobacter fetus*, and *Campylobacter jejuni* cells grown on the same media.

Table 5.1 Cellular distribution of galactosyltransferase and fucosyltransferase activities in *H. pylori* extracts

Strain	Fucosyltransferase (mU) ^a			Galactosyltransferase (mU)		
	Secreted	Soluble	Membrane bound	Secreted	Soluble	Membrane bound
UA 861	8 x 10 ⁻⁴	1.7 x 10 ⁻³	0.01 (1.4 x 10 ⁻³) ^b	0.026	0.014	1.0 ^c (0.2)
UA 802	1.4	1.6	0.41 (0.41)	0.073	0.053	4.0 (4.0)
UA 1182	0.93	2.3	0.57 (1.9)	0.47	1.5	10.0 (31.3)

^aAll activities were from the extraction of one Petri dish containing 2.5 x 10⁹ c.f.u. The volumes of the extracts were 2 mL for secreted, 4 mL for soluble and 1 mL for membrane bound.

^bSpecific activities (mU/mg protein) determined for membrane-bound enzymes only were given in parentheses.

^cα1→6 Galactosyltransferase activity characterized and detected by CE and determined by methylation analysis.

The $\beta 1 \rightarrow 4$ galactosyltransferase activity was the highest in the Triton X-100 extracts in all of the strains, suggesting that it is a membrane-bound enzyme (Table 5.1). The highest level of activity was found in *H. pylori* strain UA 1182 (10 millimits), and no activity was observed in control *Campylobacter fetus*, *Campylobacter jejuni* or *Escherichia coli*.

5.3.2 Detection Le^x and a New Product by CE-LIF

The characterization of the reaction products was achieved by capillary electrophoresis with laser induced fluorescence detection using acceptors labeled with tetramethylrhodamine (TRSE) (19, 20). The electropherograms from these mixtures are shown in Figure 5.1. For UA 861 and UA 802, incubation mixtures containing GDP-fucose and LacNAc-O-TMR both gave a new peak in the electropherogram with the same elution time as a synthetic reference sample of Le^x-O-TMR (Figure 5.1b and 5.1c). The extract from UA 802 incubated with UDP-Gal and GlcNAc-O-TMR gave a new peak with the same elution time as a LacNAc-O-TMR standard (Figure 5.1d). For UA 861 incubation with GlcNAc only new peak had a longer elution time than LacNAc which was shown (vide infra) to be the $\alpha(1 \rightarrow 6)$ isomer (Figure 5.1e) proved by methylation methods.

5.3.3 Identification of the New Product

The results from capillary electropherogram suggested that di- and trisaccharides had been produced by galactosyltransferases and fucosyltransferases in the extracts. Structural characterization of the products of these reactions was achieved by preparative incubation, isolation and analysis by ¹H-NMR spectroscopy. A spectrum was obtained from the UA 802 incubations although only 52% of the acceptor was converted to product (data not shown). The product from UA 861 incubations was shown by methylation (24) analysis to be $\alpha\text{Gal}(1 \rightarrow 6)\text{GlcNAc}$ -, the α anomeric configuration being

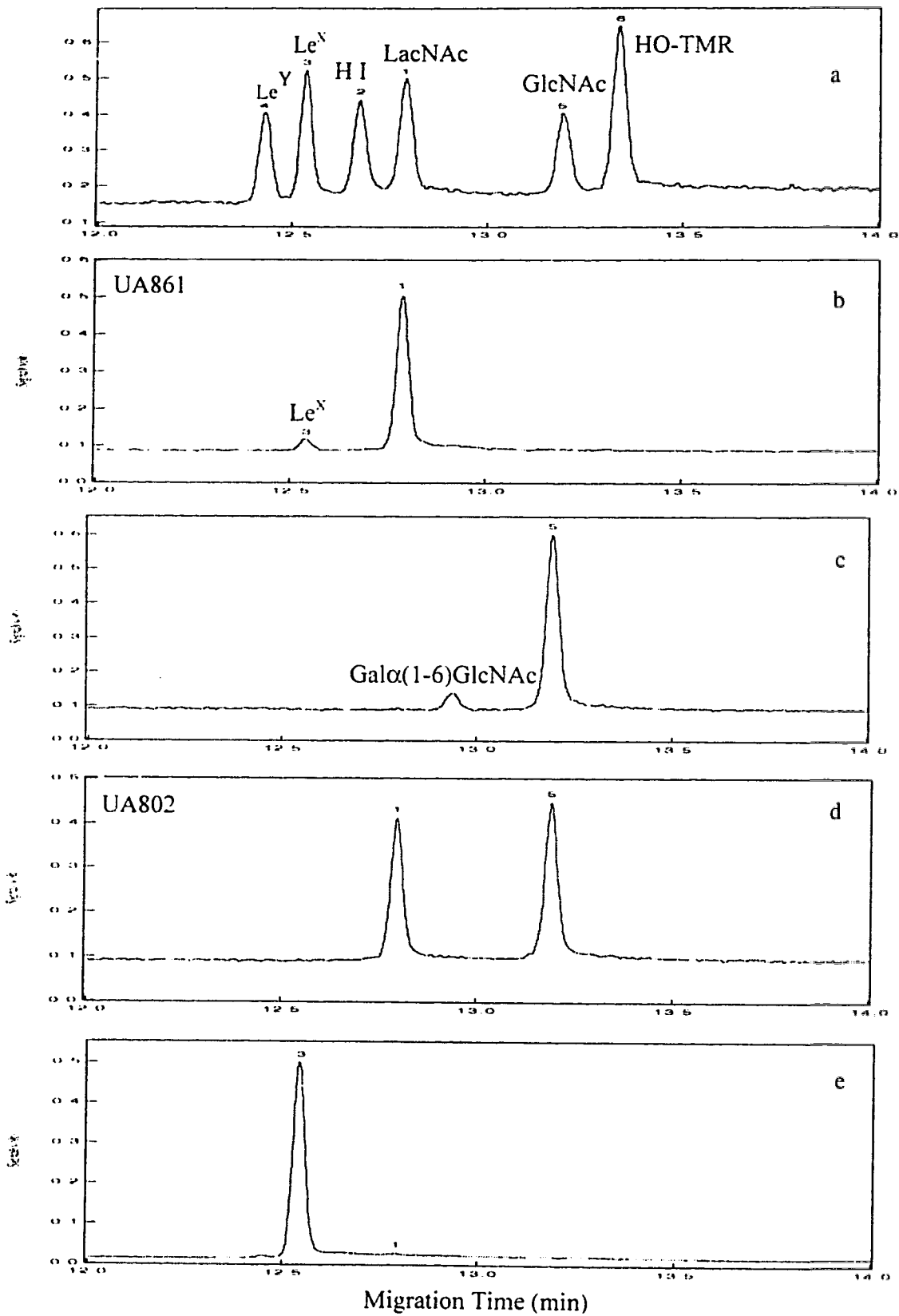


Figure 5.1 Analysis of reaction mixture from *Helicobacter pylori* UA861 and UA802 incubations by capillary zone electrophoresis with laser induced fluorescence detection.

(a). Baseline separation of five standard tetramethylrhodamine oligosaccharides found in mammalian metabolism (7, 26) (LacNAc-(1), α Fuc(1→2) β Gal(1→4)GlcNAc β - (2), β Gal(1→4)[α Fuc(1→3)]GlcNAc- (3), α Fuc(1→2) β Gal(1→4)[α Fuc(1→3)]GlcNAc β - (4), GlcNAc β - (5) and the linker arm-H-O-TMR (6). The capillary was 42 cm long (10 μ m i.d.) and the samples were injected onto the electrophoresis column at 1 kv for 5 s. The running buffer was 10 mM of each phosphate, borate, phenylboronic acid and SDS, the separation voltage was 400V/cm.

(b). Electropherogram showing the reaction product from incubations containing LacNAc-O-TMR (peak 1) and GDP-fucose with Triton X-100 extract from *H. pylori* strain UA 861. Peak 3 corresponds to Le^x β Gal(1→4)[α Fuc(1→3)] β GlcNAc-O-TMR.

(c). Electropherogram showing the product obtained from incubations containing GlcNAc-TMR (peak 5) and UDP-Gal with an extract of *H. pylori* strain UA 861. Subsequent methylation analysis confirmed the unidentified peak to be α Gal(1→6) β GlcNAc-O-TMR.

(d). LacNAc-O-TMR product (peak 1) formed in incubations of GlcNAc-O-TMR (peak 5) and the donor UDP-Gal with an extract from *H. pylori* strain UA 802.

(e). Quantitative formation of Le^x (peak 3) by an extract of *H. pylori* strain UA 802 utilizing LacNAc-O-TMR as the acceptor and the donor GDP-fucose.

(samples around 0.4-0.74 attomoles were injected, capillary is 41.9 cm long).

evident from a doublet ($J_{1,2} = 3.7$ Hz) at 5.02 p.p.m. in the $^1\text{H-NMR}$ spectrum (data not shown).

In the methylation analysis (21, 22), a portion of the product from UA 861 incubations was subjected to the technique using the Hakomori procedure (23). The resulting partially methylated alditol acetates were then analyzed by gas liquid chromatography-mass spectrometry (GC-MS). Two derivatives were observed as 2,3,4,6-tetra-*O*-methyl-1,5-di-*O*-acetyl galactitol and *N*-acetyl-*N*-methyl-1,5,6-tri-*O*-acetyl-3,4-di-*O*-methylglucosaminitol in 1:1 ratio. The first derivative derived from terminal (unsubstituted) galactose, and the second was from 6-*O*-substituted *N*-acetylglucosamine. The only possible oligosaccharide yielding these derivatives in the observed ratio would be Gal(1→6)GlcNAc. No other derivatives were observed.

5.3.4 Biosynthesis Pathway of Le^x in *Helicobacter Pylori*

The biosynthesis of Le^x in *Helicobacter pylori* is thereby shown to proceed outlined in Figure 5.2. GlcNAc-O-TMR is converted to LacNAc-O-TMR by α (1→4) galactosyltransferase in UA 802 utilizing UDP-Gal as a donor. For UA 861 no β (1→4) galactosyltransferases activity is present, and only the α (1→6) galactosyltransferase product has been isolated. Both UA 861 and UA 802 convert LacNAc to Le^x with fucosyltransferases utilizing synthesized GDP-fucose as a donor substrate. Insufficient activity was present to confirm this structure by NMR in UA 861 extracts. However, capillary electropherograms of reaction mixtures are consistent with Le^x formation. The extract from UA 802 does not transfer fucose from GDP-fucose to the monosaccharide GlcNAc-OR, confirming that the biosynthesis of Le^x in *Helicobacter pylori* is strictly ordered, i.e. galactosylation is followed by fucosylation, as in mammalian biosynthesis. The acceptors used in this study are synthetic, therefore, although it could not be shown here, *in vitro*, that GDP-Fuc is transferred to GlcNAc-OR, it may still be possible, *in vivo*,

5.4 CONCLUSIONS

Radiochemical assays can be used to screen for glycosyltransferase activities from *H. pylori* extracts. The trace amount of Le^x from fucosyltransferase reaction of UA 861 with LacNAc can be identified as compared with the chemical synthetic Le^x. It is very hard to get enough sample to do other structural analysis. For the further characterization of one of the unknown peaks from UA 861 incubated with GlcNAc and donor UDP-Gal, the preparative method can be used to get a relatively large amount of product for a methylation analysis.

The biochemical basis for the different cellular distribution and levels of activity of the enzymes in the two strains of *Helicobacter pylori* are unclear. Different protein sequences or post-translationally modified proteins might be involved. Diversity at the genome level has been demonstrated for different strains of *H. pylori* (17). One recent publication (25) shows different results. They hypothesize that the human Le^b blood group antigen functions as a receptor for the bacteria's adhesins and mediates its attachment to gastric pit and surface mucous cells, in which a human α 1,3/4-fucosyltransferase is expressed in FVB/N transgenic mice. The isolation of homogeneous enzymes, sequencing and cloning of the galactosyltransferases and fucosyltransferases will provide insights into their differential properties. A comparison with the sequences of mammalian glycosyltransferases will be of particular interest. It is important to know carbohydrate ligand and synthesize appropriate inhibitors for specific adhesion.

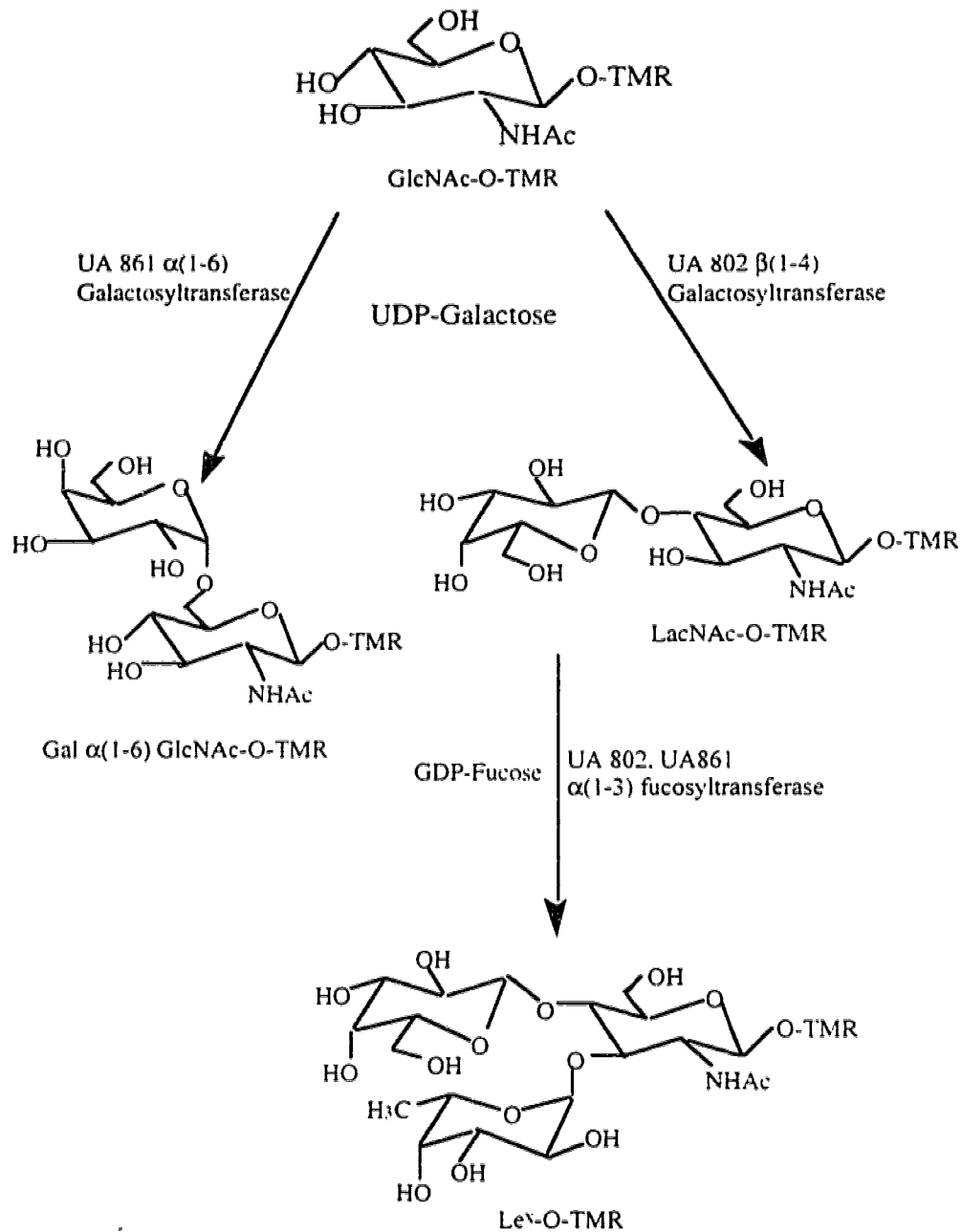


Figure 5.2 Schematic diagram of biosynthesis of Le^x in *Helicobacter pylori*. Galactosylation of GlcNAc is catalyzed by α 1,4 galactosyltransferase in strains UA 802 and UA 1182 *H. pylori* utilizing the donor UDP-Gal. Insufficient β 1,4 activity is found in UA 861 where major product detected is Gal $\alpha(1\rightarrow6)$ GlcNAc. In both strains, fucosylation of disaccharide LacNAc is catalyzed by α 1,3 fucosyltransferases which transfer a fucose from GDP-Fuc giving Le^x.

5.5 REFERENCES

- (1) Springer, G. F.; Williamson, P.; Brandes, W. C. *J. Exp. Med.* **1961**, *113*, 1077-1093.
- (2) Sashkov, A. S.; Vinogradov, E. V.; Knirel, Y. A.; Nifant'ev, N. E.; Kochetkov, N. K.; Dabrowski, J.; Kholodkova, E. V.; Stanislavsky, E. S. *Carbohydr. Res.* **1993**, *241*, 177-188.
- (3) Aspinall, G. O.; Monteiro, M. A.; Pang, H.; Walsh, E. J.; P., M. A. *Carbohydr. Lett.* **1994**, *1*, 151-156.
- (4) Schachter, H. *Current Biology* **1991**, *1*, 755-765.
- (5) Kleene, R.; Berger, E. G. *Biochim. Biophys. Acta* **1993**, *1154*, 283-325.
- (6) Moran, A. P.; Helander, I. M.; Kosunen, T. U. *J. Bacteriol.* **1992**, *174*, 1370-1377.
- (7) Hakomori, S. *Adv. Cancer Res.* **1989**, *52*, 257-331.
- (8) Muramatsu, T. *Biochimie* **1988**, *70*, 1587-1596.
- (9) Feizi, T. *Nature* **1985**, *314*, 53-57.
- (10) Velupillai, P.; Harn, D. A. *Proc. Natl. Acad. Sci. USA* **1994**, *91*, 18-22.
- (11) Saitoh, T.; Natomi, H.; Zhao, W.; Okuzumi, K.; Sugano, K.; Iwamori, M.; Nagai, Y. *FEBS* **1991**, *282*, 385-387.
- (12) Aspinall, G. O.; MacDonald, A. G.; Pang, H.; Kurjanczyk, L. A.; Penner, J. L. *The J. Biol. Chem.* **1993**, *268*, 18321-18329.
- (13) Gokhale, U. B.; Hindsgaul, O.; and Palcic, M. M. *Can. J. Chem.* **1990**, *68*, 1063-1071.
- (14) Larsen, E.; Palabrica, T.; Sajer, S.; Gilbert, G. E.; Wagner, D. D.; Furie, B. C.; Furie, B. *cell* **1990**, *63*, 467-474.
- (15) Bradford, M. *Anal. Biochem.* **1976**, *72*, 248-254.
- (16) Taylor, D. E.; Hargreaves, J. A.; Ng, L. K.; Sherbaniuk, R. W.; Jewell, L. D. *Am. J. Clin. Pathol.* **1987**, *87*, 49-54.

- (17) Taylor, D. E.; Eaton, M.; Chang, N.; Salama, S. M. *J. Bacteriol* **1992**, *174*, 6800-6806.
- (18) Palcic, M. M.; Heerze, L. D.; Pierce, M., and Hindsgaul, O. *Glycoconjugate J.* **1988**, *5*, 49-63.
- (19) Zhao, J. Y.; Dovichi, N. J.; Hindsgaul, O.; Gosselin, S.; Palcic, M. M. *Glycobiology* **1994**, *4*, 239-242.
- (20) Zhang, Y.; Le, X.; Dovichi, N. J.; Compston, C. S.; Palcic, M. M.; Diedrich, P. a. H., O. *Anal. Biochem.* **1995**, *227*, 368-376.
- (21) York, W. S.; Darvill, A. G.; McNeil, M.; Stevenson, T. T.; Albeasheimo, P. *Methods in Enzymology* **1985**, *118*, 3-40.
- (22) Stellner, K.; Saito, H.; Hakomori, S. I. *Arch. Biochem. and Biophys.* **1973**, *155*, 464-472
- (23) Hakomori, S. *J. Biochem.*, **1964**, *55*, 205-208.
- (24) Lindberg, B.; Lonngren, J. *Methods Enzymol.* **1978**, *50*, 3-33.
- (25) Falk, P. G.; Bry, L.; Holgersson, J.; Gordon, J. I. *Proc. Natl. Acad. Sci* **1995**, *92*, 1515-1519.
- (26) Hindsgaul, O.; Norberg, T.; Lependu, J.; Lemieux, R. U. *Carbohydr. Res.*, **1982**, *109*, 109-142.

CHAPTER 6

ENZYMATIC HYDROLYSIS STUDY OF A TETRAMETHYLRHODAMINE LABELED TRISACCHARIDE IN YEAST CELLS

6.1 INTRODUCTION

Carbohydrates expressed on the cell surface are related to the activities of glycosyltransferases and glycosidases (1, 2). Determinations of the activities of these enzymes and analysis of the oligosaccharide are essential to the understanding of their roles in cell biology. The characterization of glycosyltransferase activities generally can be done by radiochemical assay with a sugar nucleotide donor, a substrate and a cell extract as the enzyme source as described in previous chapters. However, several products cannot be identified at the same time by this method.

CE-LIF can separate the products and substrate from several enzymatic reactions (3, 4). This technique is particularly useful in enzyme mixture analysis, for example, for analysis of enzymes that produce different products from the same substrate: the product of one enzymatic reaction is the substrate of another enzyme.

In this chapter, CE-LIF was extended for the application of enzyme activity detection in *Saccharomyces cerevisiae* (baker's yeast) cells. It has been reported that glucosidase I is responsible for trimming the terminal α 1, 2-linked glucose from a newly transferred $\text{Glc}_3\text{Man}_9\text{GlcNAc}_2$ oligosaccharide (5, 6). Glucosidase II is an enzyme involved in glycoprotein biosynthesis, releasing both α -1,3-linked glucose residues from the protein-linked oligosaccharide $\text{Glc}_2\text{Man}_9\text{GlcNAc}_2\text{-R}$ in the processing of *N*-glycan (7).

There is no reported CE-LIF method to study glucosidase I and II in yeast cells. To validate the use of CE-LIF for these enzyme assays, isolated as well as crude glucosidase I and II activities from yeast cells were selected for this study. In our experiment, a fluorescently-labeled trisaccharide was chosen as a substrate for the glucosidase I activity study. A fluorescently-labeled disaccharide was chosen as a substrate for glucosidase II. Activities in intact yeast cells were also monitored directly from the cell uptake of the trisaccharide, and the hydrolytic products and substrate were separated and detected by a CE-LIF system.

6.2 EXPERIMENTAL SECTION

6.2.1 Materials

Fluorescently-labeled oligosaccharides and separation buffer were prepared as described in Chapter 3. Trisaccharide [α -D-Glc(1 \rightarrow 2) α -D-Glc(1 \rightarrow 3) α -D-Glc-TMR, **14**], disaccharide [α -D-Glc(1 \rightarrow 3) α -D-Glc-TMR, **15**], monosaccharide [α -D-Glc-TMR, **16**] and the linker arm [H-O-TMR = H-O(CH₂)₈CONHCH₂CH₂NHCO-tetramethylrhodamine, **6**] were dissolved in HPLC water (OmniSolv, BDH), stored in a 1.5 ml plastic vial, wrapped in aluminum foil at 4 °C. All reagents for CE analysis are analytical grade. Isolated glucosidase I and II were the ones used in previous experiments (8). They were stored at 4 °C.

6.2.2 Incubation of Isolated Glucosidase I and II with Trisaccharide and Disaccharide (Dr. Christine Scaman in Dr. Monica Palcic' group)

Samples were obtained by incubating isolated glucosidase I 10 μ L (0.014 munits/L for soluble and 0.0049 munits/L for Brij extracted enzyme) with final concentration of 0.5, 1, or 2.6 mM trisaccharide [α -D-Glc(1 \rightarrow 2) α -D-Glc(1 \rightarrow 3) α -D-Glc-TMR], at 37 °C for 3 h. The buffer was 10 mM sodium phosphate (**buffer A**, pH 6.8) and 0.1 M NaCl. Each reaction mixture was loaded on a C-18 Sep Pak cartridge, washed with 30 mL of water and eluted with 3.5 mL of HPLC pure methanol. The recovered methanol fraction was then lyophilized.

For the isolated glucosidase II there was not enough synthetic disaccharide to carry out a similar procedure as above: instead the mixtures containing trisaccharide, α -D-Glc(1 \rightarrow 2) α -D-Glc(1 \rightarrow 3) α -D-Glc-TMR and disaccharide, α -D-Glc(1 \rightarrow 3) α -D-Glc-TMR from above were incubated further with isolated glucosidase II. 100 μ L (4.78×10^{-11} mole/ μ L. min) aliquot of glucosidase II, about 5 milliunits, was added to each reaction mixture.

One milliunit of enzyme activity is the amount that catalyzes the conversion of

one nmol of acceptor to product per minute under standard screening conditions. eg. p-nitrophenol α -D-glucopyranoside is a substrate for glucosidase II, while glucosidase I does not act on such simple substrate (9, 10).

6.2.3 Incubation of Yeast Cells (Dr. Christine Scaman in Dr. Monica Palešić' group).

Saccharomyces cerevisiae (bakers yeast, Fleischman, Ltd.) was grown on Sabauraud dextrose agar plates (Difco, Ltd.) at 37 °C, and then stored at 4 °C. A typical colony was inoculated into 1 mL sterile Sabauraud dextrose media and grown at room temperature with shaking over night (approximately 17 h) (11).

A subsample of 200 μ L was transferred to a sterile microfuge tube and pelleted. The old medium was removed and the fresh medium was added to the pelleted cells along with sterile filtered trisaccharide, α -D-Glc(1 \rightarrow 2) α -D-Glc(1 \rightarrow 3) α -D-Glc-TMR, from 5 or 10 mM stock solution. The final concentration of the trisaccharide substrate in the culture was 700 to 833 μ M. Tubes were covered with aluminum foil and incubated at 37 °C for 24, 48 h, and 5 days with shaking. At the end of the incubation period, cells were pelleted, and the supernatant was removed. A subsample of the supernatant was saved for analysis by capillary electrophoresis. Cells were then washed with phosphate buffered saline (PBS).

Washed cells were lysed by vortexing for 5 min. with methanol and an equal volume of acid washed glass beads (0.4-0.5 cm diameter) in a Bead Beater (Biospec Products) for 20 min. Cell debris was pelleted. After the supernatant was removed, the cell pellet was washed three more times with methanol. The combined supernatants were lyophilized, redissolved in water and applied to a C18 Sep-Pak cartridge. The Sep Pak was washed with 30 mL Milli-Q water and eluted with 10 mL methanol. The methanol elute, containing the rhodamine labeled substrate and products, was lyophilized and analyzed by capillary electrophoresis.

6.2.4 Time Course of Trisaccharide Hydrolysis by Glucosidase I

A 5 μL aliquot of 5 mM Tri-O-TMR was lyophilized, and 7.5 μL Glucosidase I was added. The reaction started in a 500 μL microfuge tube at 37 $^{\circ}\text{C}$. TLC sampling was done by removing a 0.25 μL aliquot from the reaction mixture at 0, 0.3, 1.0, 1.3, 2.0, 3.0, and 6.0 h (50% conversion time) time point. TLC reagent is composed of 7:2:1 (isoprop:H₂O:NH₄OH in volume). At the same time, a 0.25 μL aliquot mixture was also removed at each time point, quenched into 100 μL 1.25 mM tris-HCl for Sep Pak work-up, and quantitated by CE.

6.2.5 Absorption Measurement for the Tetramethylrhodamine Labeled Compounds

Absorption measurements were performed on a Cary 219 spectrophotometer with maximum wavelength at 550 nm. The concentrations of both trisaccharide-O-TMR and monosaccharide-O-TMR were 2×10^{-6} M in 10 mM borate and SDS buffer. The extinction coefficients were determined as 8×10^4 and 7×10^4 $\text{cm}^{-1} \text{M}^{-1}$ for the trisaccharide and monosaccharide, respectively.

6.2.6 Capillary Electrophoresis

The CE-LIF instrumentation and the separation conditions have been described in chapter 4. Samples were electrokinetically injected onto a 10 μm I.D. capillary. The injection voltage typically is 500-1000 v for 5s. The separation was performed at ambient temperature in an unthermostated control room. To reduce contamination, the capillary tip was rinsed before and after sample injection. The running buffer was replaced every two injections. Peak identity in the electropherogram was obtained by comparing the migration time or relative position of the analyte in the sample with those of the standards. The substrate peak can be used as a internal standard.

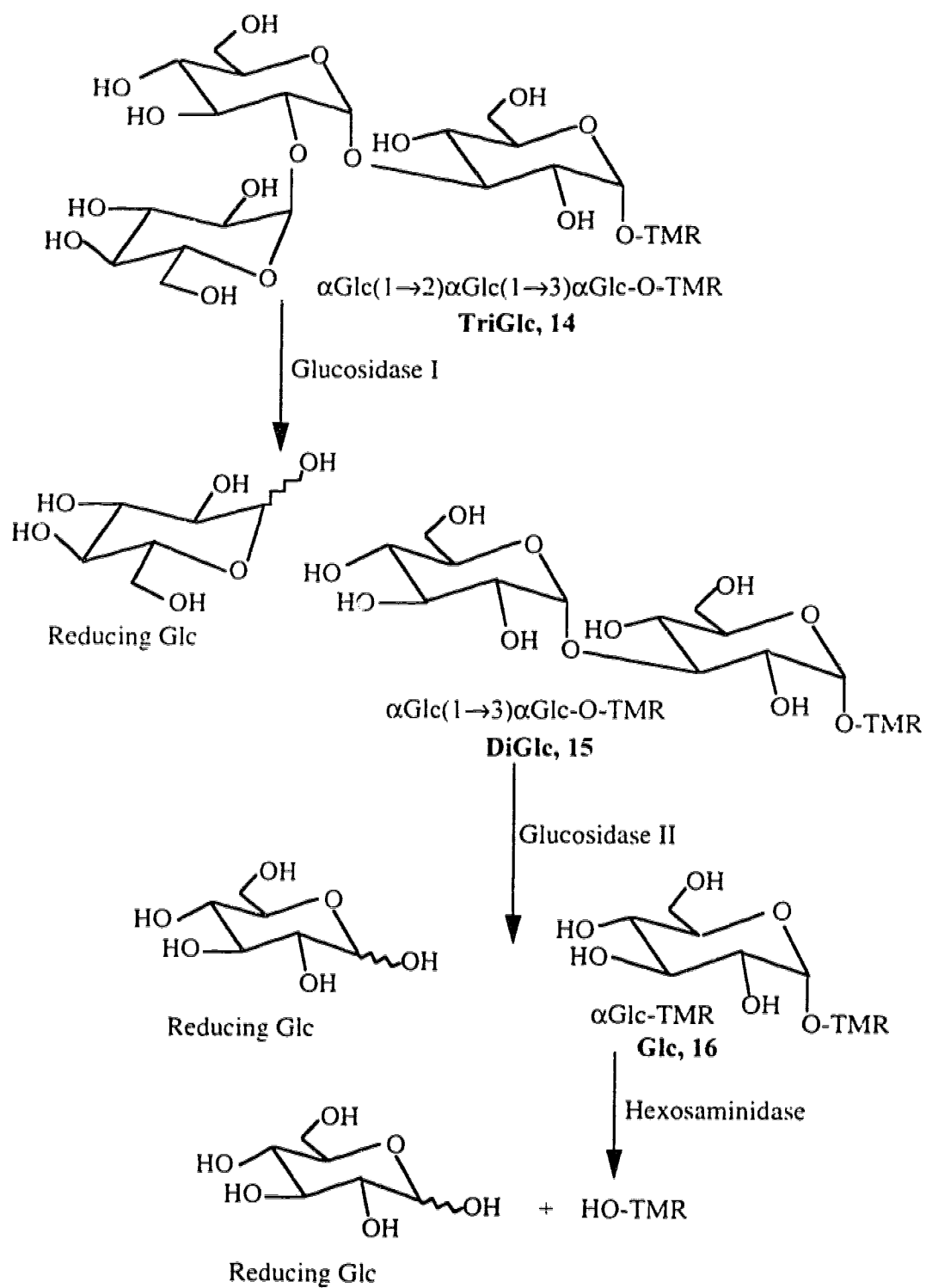
6.3 RESULTS AND DISCUSSION

Scheme 6.1 is the summary of the potential hydrolytic transformations for which standards were prepared and analyzed in the yeast cell study. Degradation of trisaccharide (α -D-Glc(1 \rightarrow 2) α -D-Glc(1 \rightarrow 3) α -D-Glc-TMR, **14**) by glucosidase I would produce disaccharide (α -D-Glc(1 \rightarrow 3) α -D-Glc-TMR, **15**) that, on further degradation by glucosidase II, would generate monosaccharide (α -D-Glc-TMR, **16**). Then hexosaminidase can remove the six member ring from the monosaccharide and the final hydrolytic product is the fluorescently tagged linking arm (HO-TMR, **6**).

Capillary electrophoresis is able to separate the substrates and the potential hydrolytic products mentioned above. The electropherogram in Figure 6.1 is the baseline separation of a synthetic oligosaccharide mixture containing T (**14**), D (**15**), M (**16**), and the linker arm (**6**) using 10 mM each of borate, phosphate, phenyl borate and SDS (pH 9) in the running buffer. The trisaccharide elutes first, followed by the disaccharide, then the monosaccharide and the linker arm. The injection volume was in the 20 picoliter range and the detection limit was in the zeptomole (10^{-21}) range.

The isolated glucosidase I was incubated with the fluorescently labeled trisaccharide substrate (**14**). Results from the electropherogram of Figure 6.2 showed the peaks of the substrate trisaccharide and a product disaccharide. Since trisaccharide, α -D-Glc(1 \rightarrow 2) α -D-Glc(1 \rightarrow 3) α -D-Glc-TMR, is a specific synthetic substrate for glucosidase I, disaccharide α -D-Glc(1 \rightarrow 3) α -D-Glc-O-TMR can not be degraded by this glucosidase. The disaccharide tends to accumulate during this incubation.

The CE-LIF can be used for a time course study. Figure 6.3 shows a series of electropherograms of the products from the isolated glucosidase I study. The trisaccharide concentration is 3.3 mM and incubated with 7.5 μ L of isolated glucosidase I. Figure 6.4 shows the percentage conversion of trisaccharide to the disaccharide. A six hour incubation gave approximately 50% percent conversion of trisaccharide to disaccharide.



Scheme 6.1 Schematic diagram of hydrolytic pathways in yeast cells.

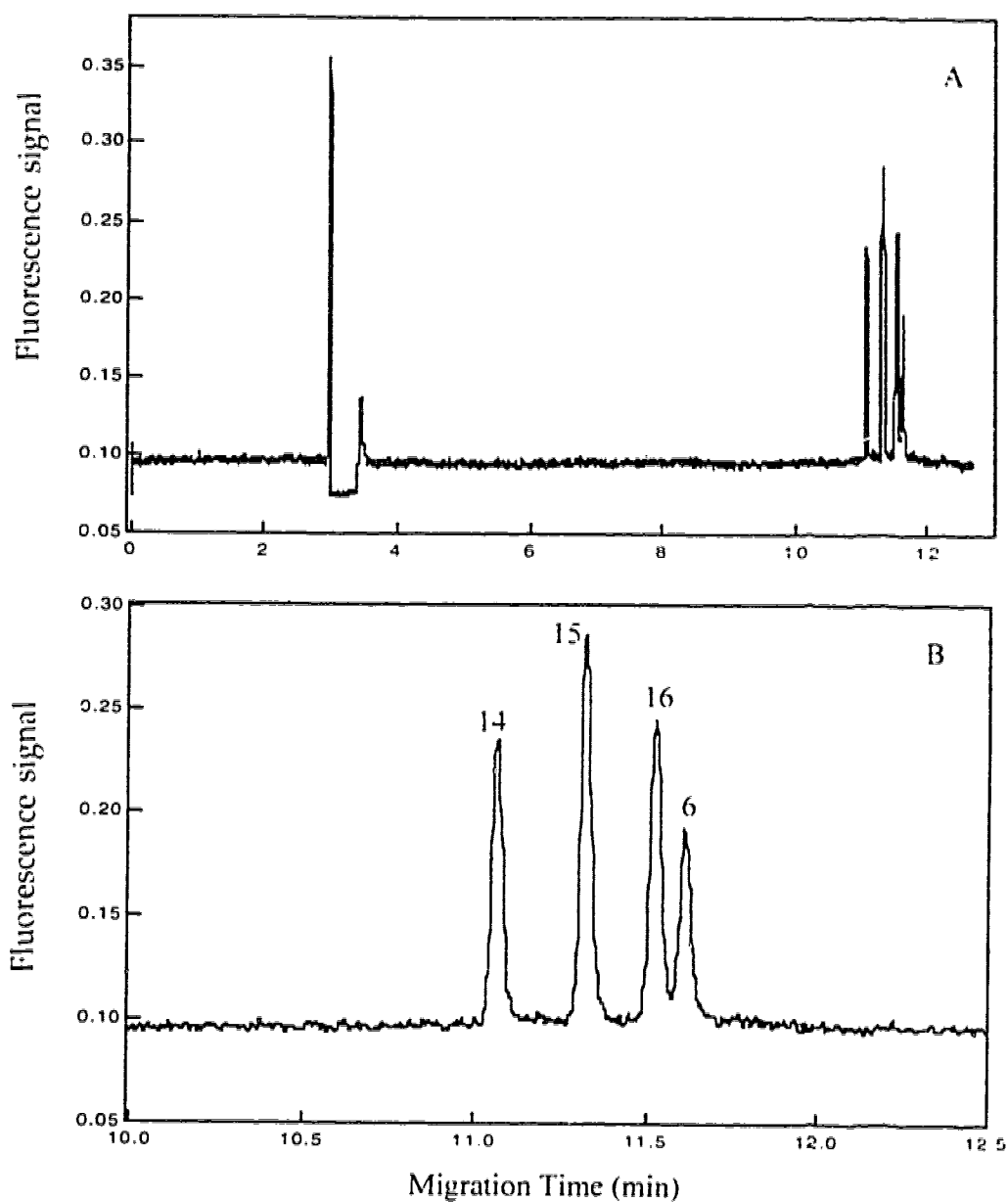


Figure 6.1 Electropherogram of three fluorescently labeled saccharide and one linker arm. Capillary 46 cm x 10 μm I.D. x 144 μm O.D.; running buffer, 10 mM phosphate-borate-phenylborate-SDS, running voltage, 400 v/cm, injection time 5s, injection volume 17 μl , concentration of each compound, 2.5×10^{-9} M. Peaks: T = 14 = α -D-Glc(1 \rightarrow 2) α -D-Glc(1 \rightarrow 3) α -D-Gl-cTMR, D = 15 = α -D-Glc(1 \rightarrow 3)-D-Glc-TMR, M = 16 = α -D-Glc-TMR, and the linker arm L = 6 = H-O-TMR = H-O(CH₂)₈CON-CH₂CH₂NHCO-tetramethylrhodamine. Data were smoothed five times using binomial filter.

Table 6.1 Trisaccharides incubation with glucosidase I

[Trisaccharide], mM	Ratio of D/ (D + T), %	[Disaccharide], mM
0.5	28	0.14
1.0	17	0.17
2.6	10	0.26

The isolated glucosidase II enzyme has been incubated with the mixture after glucosidase I was incubated with trisaccharide. The peaks in order of elution are identified as trisaccharide, disaccharide, monosaccharide and the linker arm (HO-TMR) in electropherogram of Figure 6.5, respectively. From the measurement of peak heights in the electropherograms and the known initial concentration of the trisaccharide, we can calculate the percentage and the concentration of each compound. Each peak height is divided by the addition of the total peak heights in each electropherogram to give the percentage. When the initial trisaccharide concentration was 0.5 mM, the formation of disaccharide percentage is increased from 28 % (Table 6.1) to 42 % (Table 6.3) after incubation with glucosidase I and II, respectively. This result proved that the isolated glucosidase II contained some activity of glucosidase I because more trisaccharide was hydrolyzed to disaccharide and also contained hexominidase activity because the linker arm was formed.

As expected, the comparison of the ratio increase of disaccharide in Table 6.1 and 6.2 reveals that the isolated glucosidase II still contained glucosidase I because more disaccharide was generated at the same time when glucosidase II hydrolyzed disaccharide.

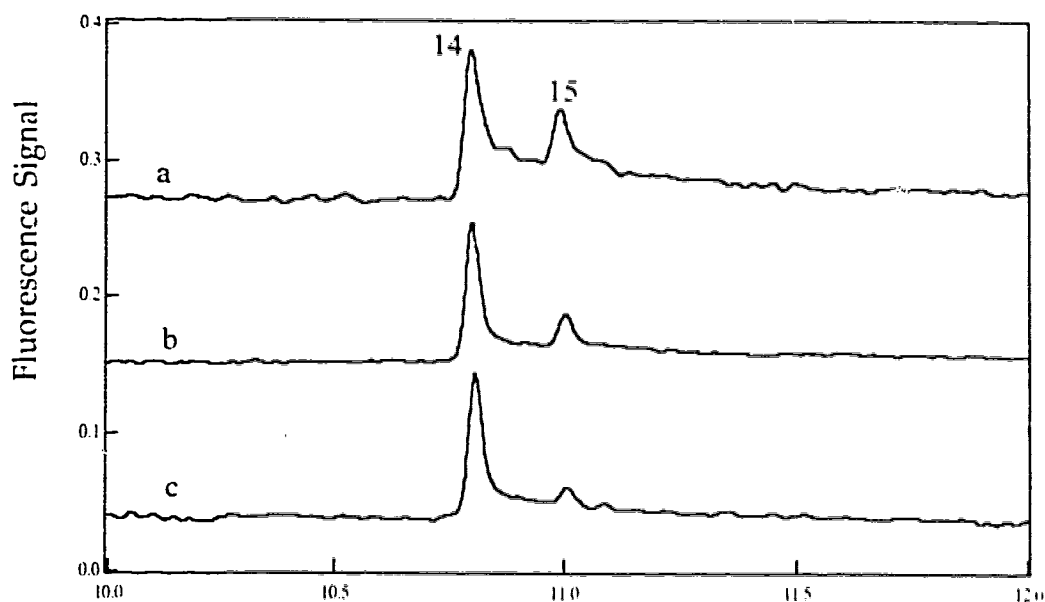


Figure 6.2 Capillary electropherograms of trisaccharide hydrolyzed by glucosidase I. Trisaccharide concentrations were (a) 0.5 mM, (b) 1.0 mM and (c) 2.6 mM. All other CE conditions are the same as in Figure 6.1.

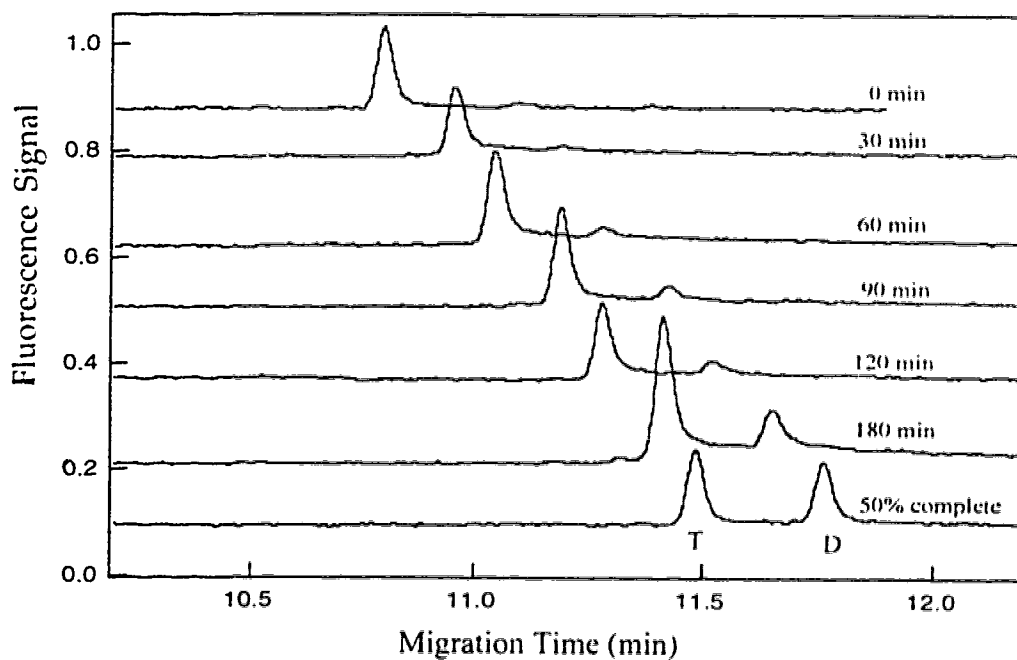


Figure 6.3 Electropherograms of the time course study of glucosidase I incubated with trisaccharide. The diagrams were offset. Only trisaccharide and disaccharide were presented in each electropherogram. CE separation conditions were the same as Figure 6.1 except that the capillary was 43.6 cm long.

Table 6.2 Trisaccharide and Disaccharide incubated with glucosidase II

[I + D]. mM	[T]. mM	[D]. mM	[M]. mM	[TMR]. mM
0.5	0.1	0.2		0.2
1.0	0.2	0.5	0.1	0.2
2.6	1.7	0.5		0.4

Table 6.3 Percentage of tri and disaccharide incubation with glucosidase II

[T + D]. mM	T %	D %	M %	TMR %
0.5	27	42		31
1.0	16	50	12	22
2.6	64	20		16

Glucosidase I specifically removes the terminal glucose from $\alpha 1.2$ position in trisaccharide (Table 6.1), while glucosidase II removes an $\alpha 1.3$ glucose from disaccharide. The last glucose residues on monosaccharide-TMR can be removed by a hexosaminidase similar to the degradation of Le^c by A431 cells in Chapter 4.

The CE enzyme assay was applicable to whole yeast cells incubated with the trisaccharide. The electropherogram in Figure 6.6 is from the yeast cells incubated with the trisaccharide-TMR for 48 h. The disaccharide is formed and nearly no monosaccharide was found. The hexosaminidase in the yeast cell can rapidly hydrolyze monosaccharides formed by glucosidase II degradation of disaccharide. The hydrolytic pathway is limited by the glucosidase I. The hydrolytic products observed are the results from the sequential enzyme actions of α -glucosidase I, II and hexosaminidase.

6.4 CONCLUSION

A hydrolytic enzyme assay has been developed using CE-LIF. The capillary

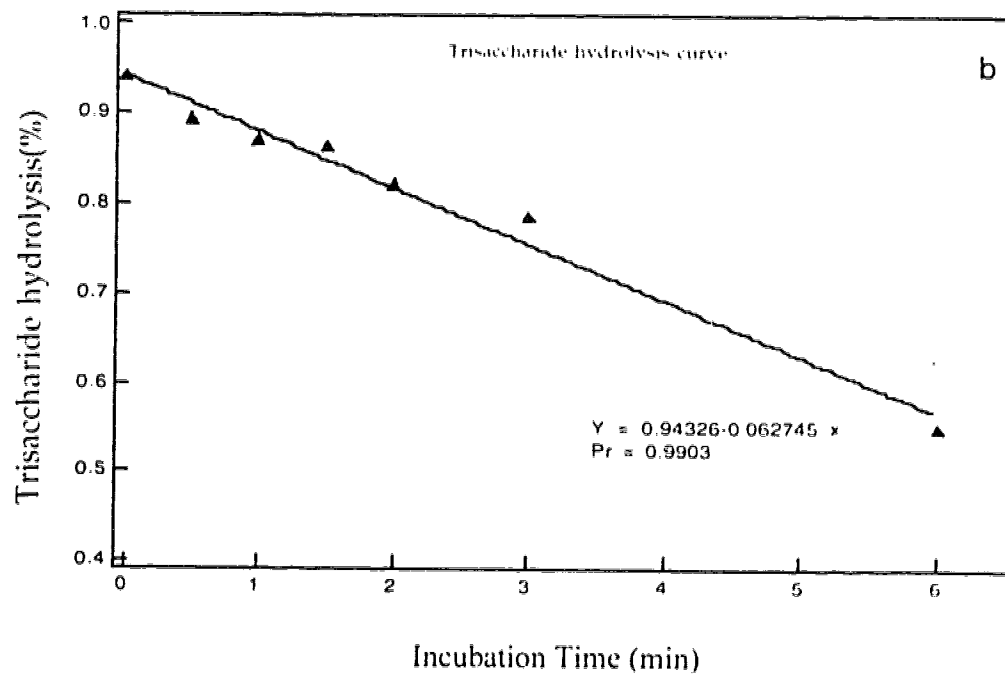
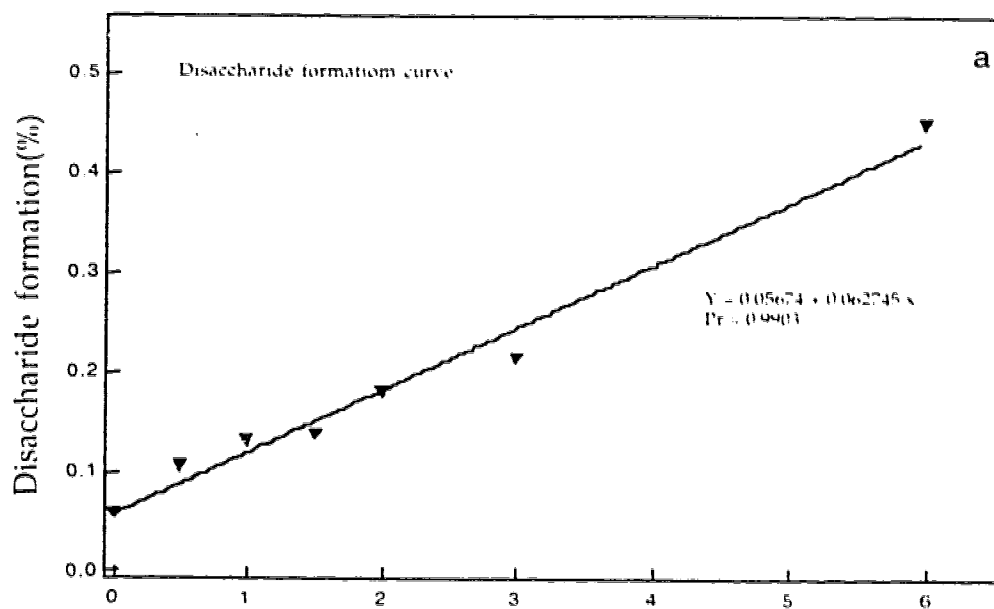


Figure 6.4 Time course study of glucosidase I hydrolysis of trisaccharide (a) and the formation of disaccharide (b) with incubation time.

electrophoresis with laser-induced fluorescence detection is an effective separation and detection technique combined with a pure synthetic fluorescently labeled substrate. This technique is proven to be applicable for low volume (picoliter) sample injection and low detection limit (10^{-21} mole) for monitoring of major substrate and minor enzymatic reaction products. It can be extend to other enzyme assays using a fluorescently labeled substrate or donor. Since the yeast cell wall is thick, it is easy to handle and isolate one yeast cell from other yeast cells. This make yeast cells more attractive than other eukaryotic cells for a single cell studies.

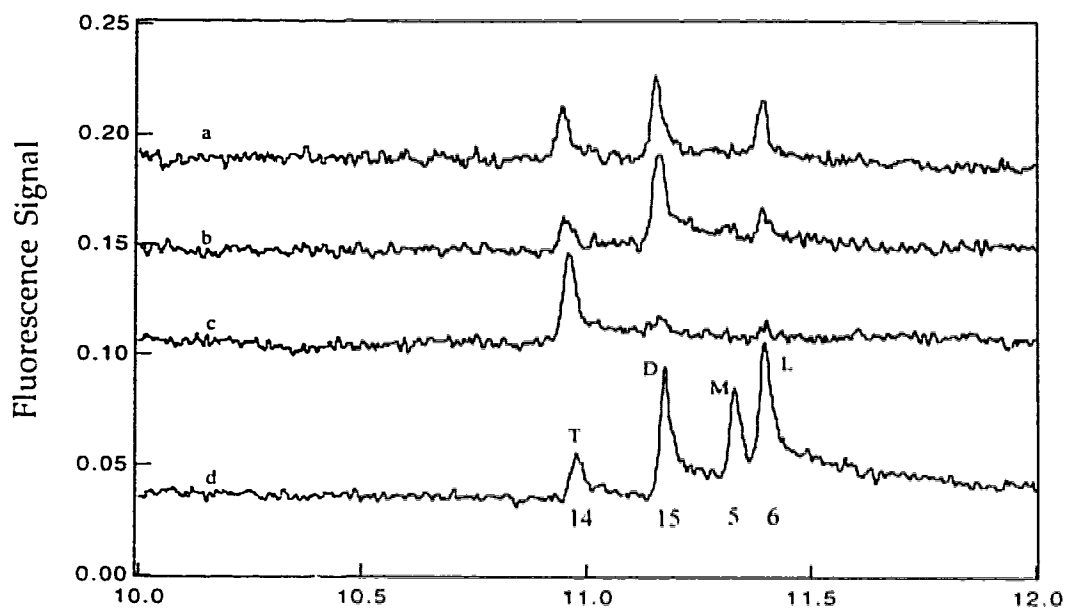


Figure 6.5 Capillary electropherograms of mixtures after glucosidase I hydrolysis was further incubated with glucosidase II. The total fluorescently labeled compounds were (a) 0.5 mM, (b) 1.0 mM and (c) 2.6 mM. (d) is the separation of four standards. All other CE conditions were the same as Figure 6.1

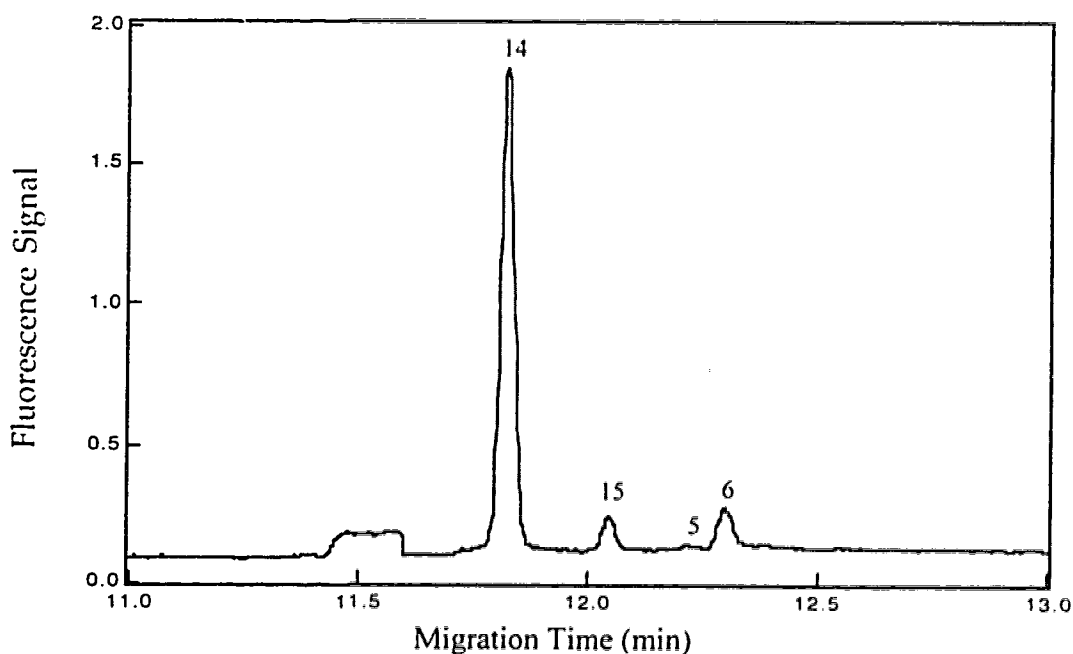


Figure 6.6 Electropherogram of trisaccharide (14) incubated with yeast cells for 48 h. The mixture after Sep Pak was lyophilized and redissolved in running buffer prior to CE analysis. Capillary is 43.5 cm long. Other CE conditions were the same as Figure 6.1.

6.5 REFERENCES

- (1) Kobata, A. and Takasaki, S. in *Cell Surface Carbohydrates and Cell Development* (M. Fukuda, Eds.), **1992**, pp. 1-24.
- (2) MacGregor, G. R.; Nolan, G. P.; Fiering, S.; Roederer, M. and Herzenberg, L. A. in *Gene Expression in Vivo* (E. J. Murray and J. M. Walker, Eds.), Humana Press, Clifton, NJ, **1990**, pp.217-236.
- (3) Zhao, J. Y.; Dovichi, N. J.; Hindsgaul, O.; Gosselin, S. and Palcic, M. M. *Glycobiology* **1994**, 4, 239-242.
- (4) Zhang, Y.; Le, X.; Dovichi, N. J.; Compston, C.A.; Palcic, M. M.; Diedrich, P. and Hindsgaul, O. *Anal. Biochem.* **1995**, 227, 368-376.
- (5) Verostek, M. F.; Atkinson, P. H. and Trimble, R. *J. Biolog. Chem.*, **1993**, 268 (16), 12095-103.
- (6) Pukazhenthil, B. S.; Varma, G. M.; Vijay, I. K.; *Indian J. Biochem. & Biophys.* **1993**, 30, 333-340.
- (7) Alonso, J. M.; Santa-Cecilia, A. and Calvo, P. *Biochem. J.* **1992**, 278(pt3), 721-7.
- (8) Neverova, I.; Scaman, C. H.; Srivastava, O. P.; Szweda, R.; Vijay, I. K. and Palcic, M. M. *Anal. Biochem.* **1994**, 222, 190-195.
- (9) Bause, E.; Erkens, R.; Schweden, J. and Janenicke, L. *FEBS Lett.* **1986**, 206, 208-212.
- (10) Shailubhai, K.; Pratta, M. and Vijay, I.K. *Biochem. J.* **1987**, 247, 555-562.
- (11) Lohr, D. in *Yeast: a Practical Approach*, (Campbell, I. and Duffus, J. H. Eds), IRL Press Washington, DC, **1988**, pp.125-145, pp.255-275.

CHAPTER 7
CONCLUSION

The involvement of carbohydrates analysis in biological processes has attracted much interest. The enzymes catalyzing oligosaccharide biosynthesis are associated with malignant transformation and tumor progression (1). Their development can provide essential information on diseases diagnostic (2, 3) and play a role in the drug discovery process (4).

A major problem associated with carbohydrate analysis in biological samples are that only extremely small amounts of sample are available and that biological active oligosaccharides have similar structures. Capillary electrophoresis with laser-induced fluorescence detection (CE-LIF) provides high sensitivity and excellent resolution for fluorescently labeled oligosaccharides (5, 6).

In Chapter 2, aminated monosaccharides were assayed at nanomolar concentrations by derivitizing them with the fluorogenic reagent 3-(*p*-carboxybenzoyl)-quinoline-2-carboxyaldehyde (CBQCA) to produce a fluorescent derivative. Labeling conditions were optimized to favor the formation of the CBQCA-aminated sugar derivatives over secondary fluorescent products. Samples as dilute as 1.0×10^{-9} M of 1-glucosamine were labeled by CBQCA and detected in the electropherogram. Five labeled aminated sugars were separated by capillary electrophoresis using a running buffer containing a mixture of phenyl borate and borate buffer. The detection scheme was based on a low-scattering sheath flow cuvette as a post column detector and two photomultiplier tubes that have mutually excluded wavelength ranges to prevent the water Raman band from contributing to the background signal. The system has a detection limit of 75 zeptomole of fluorescently labeled 1-glucosamine. Therefore, the CE-LIF can be used to analysis and detection oligosaccharides with high resolution and great sensitivity.

Chapters 3 to 6 focused on the *in vitro* and *in vivo* glycosyltransferases and glycosidases studies in cancer cells and bacteria cells.

In Chapter 3, the biosynthetic transformations of a labeled derivative of N-acetyllactosamine (β Gal(1 \rightarrow 4) β GlcNac, LacNAc) in crude microsomal extracts were separated and monitored by the CE-LIF. Six authentic standards were baseline separated in a single run within 11 minutes. These standards included LacNAc-O-TMR, the tri- and tetrasaccharides that would be formed either by α (1 \rightarrow 2) or α (1 \rightarrow 3) fucosylation of LacNAc, or both (i.e. H type II, Le^X and Le^Y sequences), and two potential degradation products (GlcNAc and the linker arm) produced by galactosidase and hexosaminidase. All of the standards were kinetically competent substrates for the enzymes present in HT-29 cells. The action of competing enzymes acting on the common LacNAc sequence could thus be monitored in a single run from a few thousand molecules. After substrate LacNAc was incubated with microsomal cell extract for 24 h, the formation of Le^X was detected and confirmed by α fucosidase hydrolysis. Therefore, CE-LIF can be used for the study of glycosyltransferases in microsomal extract (*in vitro*).

Chapter 4 focused on the *in vivo* cell uptake study by A431 cells. A better substrate Le^c (compared to LacNAc) was used for the characterization of the fucosyltransferases in the crude cell extract of A431 cells. Tetramethylrhodamine labeled substrates were applied for cell uptake studies. The endogenous enzymatic Golgi reaction products were resolved and monitored using CE-LIF after the cell uptake of Le^c. Laser scanning confocal microscopy proved that the fluorescently labeled Le^c localized in the Golgi apparatus of A431 cells. The biosynthesis of Le^a and H type I was monitored as well as several unknown products in electropherograms. The identification of Le^a and H type I was further confirmed by α fucosidase hydrolysis from human placenta. The specificity of substrates was also characterized by hydrolysis enzymes, such as neuraminidase and fucosidases. Phosphatases and sulfatases were also tested for the peak identifications. Hence, the CE-LIF and methodology to study *in vivo* cell uptake can be applied to the assay of other enzymes in cancer cells with fluorescent substrates available.

The biosynthesis of the Le^x determinant in two strains of *Helicobacter pylori* was studied in Chapter 5. In strain UA 861, the biosynthesis of a new disaccharide (Gal β (1 \rightarrow 6)GlcNAc) was monitored by CE-LIF and confirmed by the methylation method. Less Le^x was synthesized in strain UA 861 than in UA 802. The biosynthesis of carbohydrates in bacteria was also monitored using this separation and detection technique.

In chapter 6, the CE-LIF was utilized to monitor enzyme products formed during the incubation of trisaccharides with glucosidase I, and the incubation of a disaccharide with glucosidase II. Glucosidases were isolated from the yeast cell. Glucosidase I only cleaves α 1,2 glucose from the trisaccharide terminal. The sequential activity of α -glucosidase I, II, as well as hexaminidase inside the yeast cell, act specifically on α -D-Glc(1 \rightarrow 2) and α -D-Glc(1 \rightarrow 3) and Glc-TMR, respectively.

CE-LIF was proven to be an effective method to determine both the major and minor enzyme products in a single analysis. It can be used to detect both biosynthesis and hydrolysis products.

Our work had several objectives. Firstly, to label monosaccharides in a very diluted solution and separate these labeled isomers. Secondly, to develop a method to detect the products from enzyme reactions in microsomal and crude cell extracts without isolating each enzyme. And thirdly, to detect glycosyltransferase activities in cancer cells (*in vivo*) by incubating A431 cells and HT-29 cells with synthetic substrates, respectively.

In the past few years, there have been several studies on the purification and isolation of glycosyltransferases using ELISA, TLC and radiochemical methods (7-9). A few groups have studied carbohydrate related enzymatic reaction products by capillary electrophoresis (10-14). Our work demonstrates the successful application of CE-LIF to the study of enzymes either *in vitro* or *in vivo*.

The methods developed in Chapter 2 might be used effectively to label carbohydrates found in some biological fluids (15). The assay developed in Chapter 3 could be used to characterize many other enzyme activities in crude cell extracts and

could be used to characterize many other enzyme activities in crude cell extracts and discover new enzyme activities. The availability of pure sugar standards or substrates are essential in characterizing biosynthetic products.

Several groups have worked on the detection of enzymatic products in single cells using on-column CE-LIF detection (16, 17). This methodology should be readily adaptable for other glycosyltransferase studies in cancer cells and bacteria cells. The assay developed in Chapter 4 could be applied to study enzymatic reactions in cancer cells, tissue, and other enzymatic activities in a single cell with zeptomole detection sensitivity. With the improvement of mass detection limit in MALDI mass spectrometry (18), the coupling of CE-MS can increase the power of separation and identification for new enzymatic products. The methodology developed here can also be used for metabolism studies in drug industry.

7.2 References

- (1) Dennis, J. W. in *Cell Surface Carbohydrates and Cell Development* (Fukuda, M. Eds.), CRC press, Boca Raton, Florida, **1992**, pp 161-194.
- (2) Orntoft, T. F. *Apmis. Supplementum* **1992**, 27:181-7.
- (3) Stanley, P and Ioffe, E. *FASEB J.* **1995**, 9(14):1436-44.
- (4) Wen, D. X.; Livingston, B. D.; Medzihradzky, K. F., Kelm, S.; Burlingame, A. L.; Paulson, J. C. *J. Biol. Chem.* **1992**, 267, 21011-9.
- (5) Liu, J., Shirota, O and Novotny, M. *Anal. Chem.* **1991**, 63, 413-417.
- (6) Zhao, J. Y.; Diedrich, P.; Zhang, Y.; Hindsgaul, O.; Dovichi, N. J. *J. Chromatogr. B.* **1994**, 657, 307-313.
- (7) Stults, C. L.; Wilbur, B. J.; Macher, B. A. *Anal. Biochem.* **1988**, 174, 151-6.
- (8) Stults, C. L.; Sullivan, M. T.; Macher, B. A.; Johnston, R. F. and Stack, R. J. *Anal. Biochem.* **1994**, 219 (1): 61-70.
- (9) Palcic, M. M.; Heerze, L. D.; Pierce, M. and Hindsgaul, O. *Glycoconjugate J.* **1988**, 5, 49-63.
- (10) Lee, K. B.; Desai, U. R.; Palcic, M. M.; Hindsgaul, O. and Linhardt, R. J. *Anal. Biochem.* **1992**, 205, 108-114
- (11) Zhao, J. Y.; Dovichi, N. J.; Hindsgaul, O.; Gosselin, S. and Palcic, M. M. *Glycobiology.* **1994**, 4, 239-242.
- (12) Zhang, Y.; Le, X.; Dovichi, N. J.; Compston, C. A.; Palcic, M. M., Diedrich P. and Hindsgaul, O. *Anal. Biochem.*, **1995**, 227, 368-376.
- (13) Le, X.; Scaman, C.; Zhang, Y.; Zhang, J.; Dovichi, N. J.; Hindsgaul, O.; Palcic, M. M. *J. Chromatogr. A.* **1995**, 716, 215-220.
- (14) Karamanos, N. K.; Axelsson, S.; Vanky, P.; Tzanakakis, G. N.; Hjerpe, A. *J Chromatogr. A.* **1995**, 696, 295-305.

- (15) Zhang, Y.; Arriaga, E.; Diedrich, P.; Hindsgaul, O.; Dovichi, N. *J. Chromatogr. A*. **1995**, 716, 221-229.
- (16) Xue, Q. and Yeung, E. S. *Anal. Chem.*, **1994**, 66, 1175-1178.
- (17) Gilman, S. D. and Ewing, A. G. *Anal. Chem.* **1995**, 67, 58-64.
- (18) Whittal, R. M.; Palcic, M. M.; Hindsgaul, O. and Li, L. *Anal. Chem.* **1995**, 67, 3509-3514.